SYNTHETIC MICROBIAL COMMUNITIES FOR SYNGAS-DRIVEN ODD-CHAIN ELONGATION

IVETTE PARERA OLM

Propositions

1. Syngas-driven chain-elongating microbial communities operate somewhere in the middle of an acidogenic–solventogenic dichotomy.
   (this thesis)

2. Genome-scale metabolic modelling is a double-edged sword in the study of microbial metabolism.
   (this thesis)

3. Realising the full potential of syngas fermentation requires an interdisciplinary approach.

4. Relying solely on hypothesis-based research introduces bias and impedes the discovery of observational findings.

5. Social media companies' need for profit is too toxic for mental health.

6. Quality friendships are as important to health as a good diet or physical activity.

Propositions belonging to the thesis, entitled

Synthetic Microbial Communities
for Syngas-driven Odd-Chain Elongation

Ivette Parera Olm
Wageningen, 27th October 2023

Synthetic microbial communities for syngas-driven odd-chain elongation

Ivette Parera Olm

Thesis committee

Promotor
Prof. Dr D.Z. Machado de Sousa
Personal Chair at the Laboratory of Microbiology
Wageningen University & Research

Co-promotor
Prof. Dr M. Suarez Diez
Professor of Systems and Synthetic Biology
Wageningen University & Research

Other members
Prof. Dr A. ter Heijne, Wageningen University & Research
Dr J. Alves, Universidade do Minho, Braga, Portugal
Dr B. Molitor, Eberhard Karls Universität Tübingen, Germany
Dr D. Bajić, Delft University of Technology

Synthetic Microbial Communities
for Syngas-driven Odd-Chain Elongation

Ivette Parera Olm

Thesis

TABLE OF CONTENTS

General introduction and Thesis outline

—

1.1   A call for sustainability

The last century has seen an unprecedented rise in carbon dioxide (CO_2) emissions into the atmosphere, causing average global temperatures to rise to levels never seen before (Intergovernmental Panel on Climate Change [IPCC], 2018, 2023). Human activities with a large environmental footprint such as burning fossil fuels, deforestation, and industrial processes have contributed to this increase. The rise in CO_2 emissions is recognized as a major driver of climate change, which has already resulted in profound societal and environmental impacts. Among others, these include rising sea levels, intensified heatwaves, diminished rainforests, heightened risks of species extinction, and compromised food security. Unfortunately, current projections indicate that the emission reduction commitments outlined by countries under the 2015 Paris Climate Agreement (United Nations Framework Convention on Climate Change, 2015) are unlikely to be fulfilled (Climate Action Tracker).

Considering the projected growth of the human population in the next decades (United Nations Department of Economic and Social Affairs, Population Division, 2022), it is expected that, if no actions are taken, the future scenario regarding climate change will worsen, although it is important to note that anthropogenic emissions alone are not the sole contributor (IPCC, 2018, 2023). Natural climate fluctuations and geological events also play a role in climate change. Nevertheless, population growth is a factor that strongly influences the demand for resources and energy consumption, making anthropogenic emissions a key factor in the equation. It is widely recognized that humanity is exceeding the planet's ecological limits (Global Footprint Network). This concept is often referred to as ecological overshoot, where human demand for resources and ecological services exceeds the regenerative capacity of Earth.

It is therefore crucial to implement sustainable practices across all sectors (IPCC, 2023). These include transitioning to cleaner energy sources, improving forest- and crop-land management, and reducing food waste, all attainable strategies that should be incentivised and supported with effective policies. In this thesis, we address one of these necessary practices: the sustainable production of chemicals.

1.2   The three biorefineries

The largest contributor to CO_2 emissions is the exploitation of fossil fuels for energy generation and industrial processes (International Energy Agency [IEA], 2023). The chemical industry is the third largest industry subsector of direct CO_2 emissions. Production of ammonia, a key constituent of fertilisers, is the largest contributor from primary chemical production (45%), followed by methanol synthesis (28%) and high-value chemicals (27%). Due to rising demand of products, direct CO_2 emissions from the chemical industry are predicted to increase by 20% in 2030 and by 30% in 2050 (IEA, 2018).

The strong dependency of the chemical sector on fossil fuels poses environmental concerns and raises issues regarding resource availability, thereby emphasizing the urgent need to search for alternative, renewable solutions. Moreover, society is grappling with the accumulation of municipal and industrial wastes (Hoornweg et al., 2013). An opportunity exists to exploit these waste

materials and use them as feedstocks for the sustainable production of biochemicals, in what has been framed as the biorefinery concept (Calvo-Flores & Martin-Martinez, 2022; Fernando et al., 2006; Takkellapati et al., 2018). Although different classifications are encountered in literature (Cherubini et al., 2009), three major distinct strategies have emerged within this framework, categorized based on the intermediate chemical they generate: the sugar platform, the syngas platform, and the carboxylate platform (Holtzapple & Granda, 2009) (Fig. 1.1).

The sugar platform, also known as the "biochemical platform", traditionally involves the breakdown of carbohydrate-rich feedstocks like crops or lignocellulosic materials into simple sugars through enzymatic hydrolysis (Fernando et al., 2006). These sugars can then be converted via microbial fermentation into a diverse range of biochemicals. The sugar platform has a long record and it has been well-established in industry to produce biofuels (bioethanol and biodiesel). However, the economic viability of this platform heavily relies on the feedstock's composition. The presence of recalcitrant lignin in woody biomass —which can account for 15–25% of the total dry matter— is problematic, necessitating additional pre-treatment steps to facilitate enzymatic hydrolysis (Cherubini, 2010).
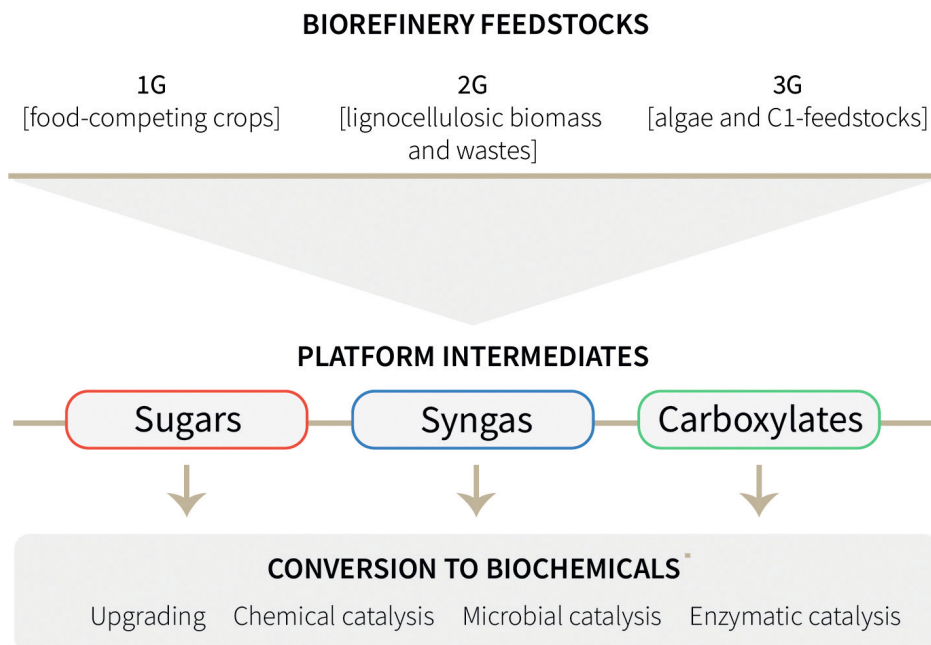
The syngas platform (or thermochemical platform) bypasses this limitation by gasifying carbonaceous materials to produce synthesis gas (syngas), a mixture primarily composed of carbon monoxide, hydrogen, and carbon dioxide (CO, H_2, and CO_2) (Fernando et al., 2006). Feedstocks for gasification include not only lignocellulosic biomass but also solid wastes such as agricultural or municipal organic waste streams. The syngas platform offers the advantage of accessing all carbon within an organic material regardless of its characteristics, making it an ideal and versatile technology to exploit recalcitrant biomass. Despite its high versatility, a negative aspect of the syngas platform is the high energy input (>700°C) that is required for gasification. In addition, the composition of the resulting syngas varies depending on the biomass and gasifier used, which can be a disadvantage depending on the subsequent application of the gas (Chandolias et al., 2018).

Syngas serves as a versatile feedstock itself. Traditionally, it has been used in Fischer-Tropsch synthesis to produce hydrocarbons, such as diesel and jet fuels (Fernando et al., 2006). Syngas is also utilised in the synthesis of methanol and in the production of ammonia through the Haber-Bosch process. These traditional applications of syngas have been deployed in large-scale industrial operations for decades. However, syngas has been also demonstrated to be a suitable feedstock for microbial conversion, giving rise to what is known as syngas fermentation (Liew et al., 2016; Redl et al., 2017; Sun et al., 2019). Syngas fermentation is the topic of this thesis and is addressed later in the text (§ 1.3 and § 2.1).

The third biorefinery, the carboxylate platform, relies on the use of anaerobic microbial consortia (also termed open mixed cultures or undefined cultures) to efficiently convert organic wet waste streams into short-chain carboxylic acids (SCCAs: acetate, propionate, and butyrate) as valuable intermediates for further conversion (Agler et al., 2011; Moscoviz et al., 2018). Typical feedstocks are wastes from municipal, agricultural, or industrial processes. Open mixed cultures are particularly suited to treat such heterogeneous feedstocks due to their high microbial diversity, robustness, and adaptability.

In essence, the three biorefinery platforms differ in their feedstock conversion methods and the nature of the key intermediates (platforms) generated —sugar, syngas, and carboxylates, re-

spectively. However, the subsequent conversion methods for these intermediates are theoretically platform-independent and interchangeable (Fig. 1.1). Moreover, these platforms can be combined or integrated with other conversion processes, offering significant potential for diversification in the sustainable production of chemicals and fuels (Fernando et al., 2006; Richter et al., 2013). The choice of biorefinery will depend on factors such as feedstock availability (e.g., gasification is suitable for lignocellulosic biomass) and the required intermediate for subsequent conversion (e.g., sugars are often used in fermentation processes).

BIOREFINERY FEEDSTOCKS

1G	2G	3G
[food-competing crops]	[lignocellulosic biomass and wastes]	[algae and C1-feedstocks]

PLATFORM INTERMEDIATES

Sugars — Syngas — Carboxylates

CONVERSION TO BIOCHEMICALS

Upgrading   Chemical catalysis   Microbial catalysis   Enzymatic catalysis

Figure 1.1 A simplified scheme of the biorefinery concept. The platform intermediates —sugars, syngas, and carboxylates — can be produced from first-, second- and third-generation feedstocks (1G, 2G, and 3G, respectively) and be converted to a plethora of biochemicals via chemical and biological methods.

On a final note, it is pertinent to refer the terminology of first-, second-, and third-generation feedstocks in the context of biorefineries (Cherubini, 2010; R.A. Lee & Lavoie, 2013). First-generation feedstocks include food crops such as corn, sugarcane, and vegetable oils. Second-generation feedstocks encompass non-food biomass like agricultural residues (e.g., straw, corn stover) and dedicated crops (e.g., switchgrass, miscanthus). Third-generation feedstocks, also known as advanced feedstocks, comprise algal biomass and, more recently, C1 feedstocks (Liu et al., 2020a). In the pursuit of sustainable production, there is a growing focus on second- and third-generation feedstocks due to their abundance, reduced competition with food and feed production, and potential for lower environmental impact. Combining biorefinery platforms and utilizing different feedstocks offers opportunities for flexibility and diversification in sustainable chemical and fuel production (Fig. 1.1).

1.3   The syngas fermentation era and the rise of acetogens

Recent years have witnessed a growing interest on C1 feedstocks (i.e., syngas, methanol, formate) for microbial conversion to biochemicals. This approach holds promise in reducing reliance on fossil fuels and minimizing carbon emissions. Furthermore, advancements in biotechnology and microbial engineering have expanded our understanding of C1 utilization pathways, paving the way for innovative approaches in converting these feedstocks into valuable chemicals (Bae et al., 2022; Humphreys & Minton, 2018; Katsyv & Müller, 2020; H. Lee et al., 2022; Z. Liu et al., 2020). Syngas stands out among C1 feedstocks due to its inherent versatility. Besides gasification-derived syngas, CO-rich gas streams that are generated by the steel and iron industries can be utilised in the same ways, thereby reutilising a carbon-rich source that is otherwise combusted (Molitor et al., 2016).

Syngas fermentation employs microorganisms as catalysts to convert CO, CO_2, and H_2 into desired products. Various microbial groups can use these gaseous compounds as carbon and/or energy sources (Diender et al., 2015; Sipma et al., 2006). Among them, acetogens are promising biocatalysts in syngas fermentation, since they can fix CO_2 into acetyl-CoA, a biochemical platform from which a variety of chemicals can be derived. Acetogens are widely distributed in nature: over 100 acetogens from 23 genera have been isolated from diverse environments, including a wide range of temperatures and pH (H. Lee et al., 2022). Most studied strains belong to the *Clostridium*, *Acetobacterium* and *Moorella* genera, with representative species being *Clostridium autoethanogenum*, *Acetobacterium woodii* and *Moorella thermoacetica*. The diverse nature of acetogens is reflected in their differing genomic features and metabolic capabilities (Bengelsdorf et al., 2016; Diender et al., 2015; Drake et al., 1997; Laura & Jo, 2023; Schuchmann & Müller, 2014).

Acetogens are strict anaerobes that fix two molecules of CO_2 into one molecule of acetyl-CoA through the reductive acetyl-CoA or Wood-Ljungdahl pathway (WLP) (Fig. 1.2) (Schuchmann & Müller, 2014; Schuchmann & Müller, 2016). The WLP is thought to be the most ancient pathway for CO_2 fixation. It consists of two branches, one for each molecule of CO_2: the methyl and the carbonyl branch. In the methyl branch, CO_2 is first reduced to formate (via formate dehydrogenase) that is ultimately converted to methyl-tetrahydrofolate (methyl-THF) through a series of conversions and reductive steps that involve six reducing equivalents. Methyl-THF is then transferred via a methyltransferase and a corrinoid iron-sulphur protein (ergo, methyl-CoFeSP) to the bifunctional CO dehydrogenase/acetyl-CoA synthase (CODH/ACS). In the carboxylate branch, CO_2 is reduced to CO via the CODH/ACS with two reducing equivalents. The CODH/ACS also catalyses the subsequent synthesis of acetyl-CoA from the methyl and carbonyl groups formed in the methyl and carbonyl branches, respectively. Acetyl-CoA is further converted into acetate via phosphotransacetylase and acetate kinase, generating one molecule of ATP via substrate-level phosphorylation. Acetate production via the WLP results in zero net ATP synthesis, sine ATP required for formate activation with THF is regenerated in the acetate kinase reaction (Fig. 1.2).
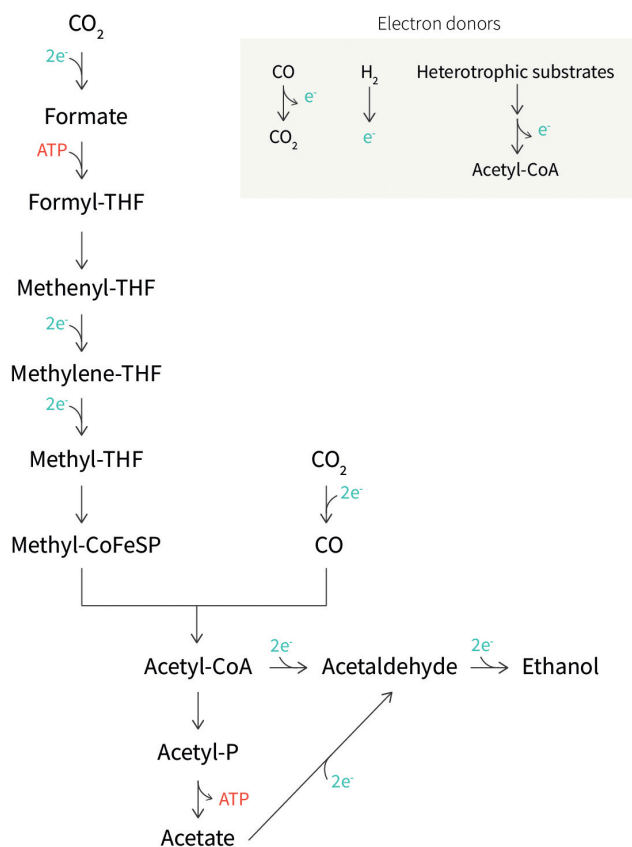
Figure 1.2 The reductive acetyl-CoA or Wood-Ljungdahl pathway (WLP) used by acetogens to fix two molecules of CO_2 into one molecule of acetyl-CoA, and subsequent conversion steps to acetate and ethanol. Acetogens may retrieve electrons from CO, H_2 or heterotrophic substrates. ATP: adenosine triphosphate; CoFeSP: corrinoid iron-sulphur protein; e-: electrons; THF: tetrahydrofolate.

To gain energy, acetogens employ either of two described membrane-bound protein complexes that couple the transfer of electrons between electron carriers with the translocation of cations across the membrane (Schuchmann & Müller, 2014; Schuchmann & Müller, 2016). These are the reduced ferredoxin:NAD+ oxidoreductase (Rnf) complex and the energy-converting hydrogenase (Ech) complex. The proton gradient generated by Rnf or Ech is used by an APTase to synthetise ATP. The Rnf complex is found in many industrially-relevant acetogens, including *C. autoethanogenum*, *A. woodii* and *Acetobacterium wieringae*. The Rnf couples the reversible reduction of NAD+ with reduced ferredoxin (Fd^{2-}) with the translocation of Na+ or H+ across the membrane. The reduction of NAD+ (E_0' = -320 mV) with Fd^{2-} (E_0' = -400 to -500 mV) is an exergonic reaction that can drive the transport of cations against gradient across the cell membrane to create a proton motive force and, ultimately, ATP synthesis via ATP synthase. The Ech complex, present in *M. thermoacetica*, operates in a similar manner as the Rnf, yet coupling the oxidation of ferredoxin to H_2 generation.

Therefore, the availability of ferredoxin has a strong impact on the energetics of acetogens. While the conversion steps of the WLP are the same for all acetogens, the electron carriers and some of the enzymes involved (which includes electron-bifurcating enzymes) vary across strains, with implications in the energetic and general metabolism (Schuchmann & Müller, 2014).

Acetogens can retrieve electrons to fix CO_2 from a variety of autotrophic (CO, H_2) and heterotrophic substrates (sugars, ethanol, etc.), which confers them with a unique versatility in the anaerobic realm (Drake et al., 1997; Schuchmann & Müller, 2016). Most heterotrophic substrates are degraded to the level of acetyl-CoA (subsequently forming acetate) through the conventional pathways (e.g., glycolysis). Utilisation of H_2 (E_0'= -400 mV) involves the activity of electron-bifurcating hydrogenases that couple the exergonic reduction of NAD^+ (E_0' = -320 mV) to the endergonic reduction of ferredoxin (E_0'= -400 to -500 mV) (Diender et al., 2015). Hydrogenases are known to be competitively inhibited by CO (Ceccaldi et al., 2017; Schuchmann & Müller, 2013). That said, CO-tolerant hydrogenases have been described, allowing some species to use H_2 also in the presence of CO (Fox et al., 1996; Soboh et al., 2002). Utilisation of CO involves the monofunctional CODH, an enzyme specialised in the oxidation of CO to CO_2. Contrary to H_2, the redox potential of the CO/CO_2 pair (E_0'= -520 mV) is sufficiently low to drive the reduction of ferredoxin (E_0'= -400 to -500 mV) (Schuchmann & Müller, 2014). During growth on CO as sole substrate, part of the Fd^{2-} is used to generate NADH for some of the reductive reactions of the WLP. Since more Fd^{2-} is obtained than is required in reductive reactions, the rest can be funnelled to the Rnf complex to drive ATP synthesis. Therefore, growth on CO is more energetically-favourable than growth on CO_2/H_2.

Ethanol is an overflow product of acetogens that is produced when there is an excess of reducing equivalents (Allaart et al., 2023; Diender et al., 2015). Two routes have been described for the production of ethanol from acetyl-CoA in acetogens (Fig. 1.2). In the first pathway, acetyl-CoA is converted to ethanol via acetaldehyde using a bifunctional aldehyde/alcohol dehydrogenase (AdhE). The second pathway involves the conversion of acetate to acetaldehyde through the acetaldehyde:ferredoxin oxidoreductase (AOR), followed by the reduction of acetaldehyde to ethanol by an alcohol dehydrogenase (Bengelsdorf et al., 2016). Other than acetate and ethanol, a handful of products can be formed by acetogens due to their restricted energy metabolism. In the last decade, significant progress has been made in the engineering of acetogens to synthetise non-native products from syngas (Köpke & Simpson, 2020; Lee et al., 2022), including acetone (Arslan et al., 2022; Liew et al., 2022) and 3-hydroxybutyrate (Woolston et al., 2018). However, efficient genome manipulation techniques of these non-model microorganisms are still limited, and overcoming the energetic limitations is a challenging task (Cherubini, 2010; Lee, 2021). An alternative is to rely on the native networks that sustain microbial communities, the core topic of this thesis and that is introduced next.

1.4 Harnessing the power of microbial networks: the case of chain elongation

The use of microbial communities in bioprocesses has several advantages, among them division of labour, metabolic redundancy and robustness (De Vrieze et al., 2017; Diender et al., 2021). Microbial communities can be classified in two types: open mixed cultures (undefined), and synthetic co-cultures (defined), the latter being the focus of this thesis. The features, advantages and disadvantages, and the application potential in syngas fermentation of these two types of microbial cultures are extensively described in Chapter 2 (for a summary of studies up to 2021, see Table 2.1 and Table 2.2).

A common denominator of microbial communities applied in syngas fermentation is the presence of chain-elongating microorganisms that consume the ethanol and acetate that are produced by acetogens (Diender et al., 2016b; Ganigué et al., 2016). This way, butyrate (C4) and caproate (C6) can be produced, increasing the value of end products of the syngas fermentation process. Chain elongation is regarded as a secondary fermentation in the carboxylate platform (described in § 1.2), as it involves the conversion of SCCAs to medium-chain carboxylic acids (MCCAs; e.g., butyrate, caproate) provided that an electron donor is available. Chain elongation is the result of the reverse β-oxidation pathway, a cycle that adds an acetyl-CoA derived from the electron donor (e.g., ethanol) to a carboxylic acid, elongating its carbon chain length with two carbons at a time (e.g., acetate to butyrate) (Angenent et al., 2016; Cavalcante et al., 2017). The best characterised microorganism performing chain elongation is *Clostridium kluyveri* (Barker & Taha, 1942; Weimer & Stevenson, 2012); its genome is fully sequenced (Seedorf et al., 2008), and it has been extensively characterised through physiology and modelling studies (Bornstein & Barker, 1948; Candry et al., 2018; Candry et al., 2020b; Kenealy & Waselefsky, 1985; Parera Olm & Sousa, 2023; Yin et al., 2017; Zou et al., 2018).
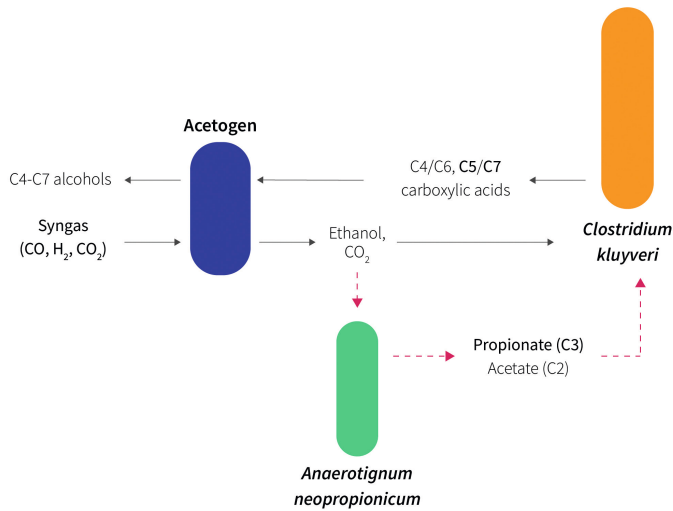
Figure 1.3 Synthetic co-cultivation can drive the production of odd-chain products from syngas by incorporating an ethanol-consuming, propionigenic strain —for example, *Anaerotignum neopropionicum*. Medium-chain carboxylates of odd-numbered carbon length (e.g., valerate) can theoretically be formed in this system via ethanol-based chain elongation of propionate by *Clostridium kluyveri*.

Because acetogens produce compounds of even-numbered carbon chain (ethanol and acetate), syngas-driven chain elongation has so far heavily focused on the production of even-chain products (i.e., butyrate, caproate) (Baleeiro et al., 2019; Table 2.1; Table 2.2). Synthetic co-cultures can aid in shifting the product spectrum towards odd-chain products by selecting the right strains for the desired metabolic network (Fig. 1.3).

Ideally, such a candidate should be able to use the substrates or intermediates produced in syngas fermentation. To date, no carboxydotrophic microorganism has been described with the ability to produce propionate. However, a few propionigenic bacteria have been isolated that can grow on ethanol (Schink et al., 1987; Stams et al., 1985). One of these species is the ethanol-consuming, propionigenic bacterium *Anaerotignum neopropionicum* (Benito-Vaquerizo et al., 2022b; Tholozan et al., 1992), which is subject of this thesis. The metabolism of this microorganism, which proceeds via the acrylate pathway, is described further on (Chapter 4). Propionate is a SCCA that can be used by *C. kluyveri* analogously to acetate, resulting in the production of odd-chain MCCAs in the system (i.e., valerate, heptanoate) (Bornstein & Barker, 1948). Thus, the integration of the three processes —syngas fermentation, propionigenesis and chain elongation— should be able to generate odd-chain products (C5/C7) from syngas (Fig. 1.3). Investigating the feasibility and potential of synthetic co-cultures in achieving this goal is the core objective of this thesis.

THESIS OUTLINE

This thesis aims to explore the feasibility and potential of synthetic microbial co-cultures as biocatalysts for the conversion of C1 gaseous feedstocks (CO, CO_2(+H_2)) into chemical building blocks. Specifically, I focused on realising the production of odd-chain carboxylic acids and alcohols, an area that has received significantly less attention than the production of the even-chain counterparts. While the primary approach is experimental, computational methods have proven to be valuable research tools in the development of this thesis. At the same time, the experimental work was essential in assessing the feasibility of the computational models developed. Ultimately, with this work I also intend to contribute to a deeper understanding of the physiology and metabolism of some of the bacterial species relevant to the field of C1 gas fermentation.

In **Chapter 2**, we provide an extensive review on the conversion of carbon monoxide into chemicals using microbial communities. A distinction is made between the use of open mixed cultures (undefined) and synthetic co-cultures (defined), and we expose the benefits and disadvantages of each. The review incorporates data from research conducted until 2021 that successfully demonstrated the production of methane, carboxylic acids, alcohols, as well as higher-value chemicals (e.g., 3-HB), by syngas-fermenting microbial communities, either in one-pot or two-stage processes. We place emphasis on the strengths of synthetic co-cultures, and discuss the challenges and opportunities they present.

Chapter 3 describes a novel synthetic co-culture composed of *Clostridium kluyveri*, well-known for its chain elongation metabolism, and *Anaerotignum neopropionicum*, a propionigenic bacterium able to grow on ethanol. We show that the co-culture converts ethanol and CO_2 —products of syngas fermentation— into even- and odd-chain carboxylates (up to C7). Propionate produced by *A. neopropionicum* is a key intermediary in the system. We envision that this co-culture has the potential to be used for the upgrading of ethanol from syngas fermentation. Alternatively, it could be integrated with the syngas fermentation platform by combining a carboxydotrophic acetogen with *A. neopropionicum* and *C. kluyveri*, as we later tested (**Chapter 5**). **Chapter 3** also provides novel insights into the physiology of ethanol fermentation by *A. neopropionicum*, and investigates the metabolism of odd-chain elongation by *C. kluyveri*. Our findings suggest that consumption of propionate by *C. kluyveri* proceeds at the cost of excessive ethanol oxidation to acetate, resulting in a decrease of the theoretical odd/even end-product ratio in the system.

Genome-scale metabolic modelling was employed to assess the metabolic capabilities of syngas-fermenting co-cultures and to gain insights into the underlying metabolic conversions and interactions. In **Chapter 4**, we constructed the first genome-scale metabolic model (GEM) of *A. neopropionicum*, the ethanol-consuming, propionigenic strain used in **Chapter 3**. By integrating *in silico* analysis with experimental data, we gained new knowledge on the metabolism of this bacterium, with focus on the acrylate pathway, responsible for the fermentation of ethanol to propionate, and its implications for energy conservation. Later, we incorporated this model in the multi-species GEM of a syngas-fermenting synthetic tri-culture comprising this strain together with *Acetobacterium wieringae* strain JM and *C. kluyveri* (**Chapter 5**).

Building up on the work done so far, **Chapter 5** presents a proof-of-concept for the synthetic tri-culture composed of the acetogen *A. wieringae* strain JM, *A. neopropionicum* and *C. kluyveri*

and that is able to produce C4–C7 carboxylic acids and higher alcohols from CO at neutral pH. Chemostat experiments showed that the acetogen switches from an entirely acetogenic metabolism in monoculture to partial ethanol production when co-cultivated with either of the ethanol-consuming species. This observed behaviour is consistent with the thermodynamic regulation observed in other acetogens when an ethanol sink is present. Due to technical and time constraints, a steady-state of the tri-culture in chemostat cultivation was not attained. Instead, the feasibility of the tri-culture was evaluated through community flux balance analysis (cFBA) using a multi-species GEM that combined the models of the three species involved. For that purpose, we previously constructed and validated the GEM of the acetogen *A. wieringae* JM. Model simulations indicate that a balanced presence of the three strains would promote the viability of the tri-culture in steady-state CO fermentation. Furthermore, the impact of incorporating H_2 as an additional energy source alongside CO on the product spectrum of the culture was simulated.

In the last few years, numerous *Clostridium* co-cultures used in syngas fermentation have been documented in the literature. These cultures involve various acetogens that exhibit a wide range of optimal pH values for growth. The study in **Chapter 6** aims to consolidate this knowledge by comparing the functionality and productivity of co-cultures of a selection of acetogens with *C. kluyveri* fermenting CO, at different pH values. Our findings show the metabolic variations and environmental adaptations of different acetogens, and emphasise its importance in selecting suitable co-culture combinations that can enhance CO/H_2 utilisation and product formation.

Finally, in **Chapter 7**, I conclude the thesis with a general discussion that summarises the key findings, contributions to existing knowledge, and implications of the research conducted. I also highlight the limitations and challenges encountered throughout the study, and propose directions for future research in the field of microbial communities applied to syngas fermentation.

Conversion of carbon monoxide to chemicals using microbial consortia

—

Ivette Parera Olm & Diana Z. Sousa

Abstract

Syngas, a gaseous mixture of CO, H_2 and CO_2, can be produced by gasification of carbon-containing materials, including organic waste materials or lignocellulosic biomass. The conversion of bio-based syngas to chemicals is foreseen as an important process in circular bioeconomy. Carbon monoxide is also produced as a waste gas in many industrial sectors (e.g., chemical, energy, steel). Often, the purity level of bio-based syngas and waste gases is low and/or the ratios of syngas components is not adequate for chemical conversion (e.g., by Fischer-Tropsch). Microbes are robust catalysts to transform impure syngas into a broad spectrum of products. Fermentation of CO-rich waste gases to ethanol has reached commercial scale (by axenic cultures of *Clostridium* species), but production of other chemical building blocks is underexplored. Currently, genetic engineering of carboxydotrophic acetogens is applied to increase the portfolio of products from syngas/CO, but the limited energy metabolism of these microbes limits product yields and applications (for example, only products requiring low levels of ATP for synthesis can be produced). An alternative approach is to explore microbial consortia, including open mixed cultures and synthetic co-cultures, to create a metabolic network based on CO-conversion that can yield products such as medium-chain carboxylic acids, higher alcohols and other added-value chemicals.

2.1 Introduction

2.1.1 Syngas fermentation for a circular economy

As the worldwide population grows and the consumption of fossil resources increases, there is the need to develop new technologies to produce commodity chemicals from renewable resources. By 2050, chemicals may no longer be synthesised from fossil fuels, according to targets established after the Paris agreement and the European Green Deal (European Commission, 2018; European Commission, 2019). Lignocellulosic biomass and wastes (agricultural, industrial and municipal) have been identified as priority feedstocks for a biobased industry (Cherubini, 2010; Popp et al., 2014). These are inedible materials, and their use does not compete with human or animal nutrition or with the utilization of arable land, therefore circumventing ethical concerns. Wastes in particular are heavily under-utilised materials, especially in developing countries (Tripathi et al., 2019). The conversion of biomass and wastes through hydrolysis-fermentation is very attractive, but bottlenecks of the process are the low biodegradability of lignin (which represents 10–25% of plant biomass) and the costly pre-treatment steps (Kawaguchi et al., 2016; Sims et al., 2010). An alternative that gets increasing attention is the gasification of biomass and wastes followed by the chemical or biological conversion of the generated synthesis gas (also known as syngas) (Daniell et al., 2012; Griffin & Schultz, 2012).

Syngas is a gas mixture of mainly carbon monoxide (CO), hydrogen (H_2) and carbon dioxide (CO_2) that can be generated from solid carbonaceous feedstocks (e.g., coal, lignocellulosic biomass) and carbon-containing wastes (e.g., agricultural waste). Chemical conversion of syngas by, e.g., Fischer-Tropsch (FT) process, is a mature technology used for the conversion of mainly coal-generated syngas into hydrocarbons, alcohols and organic acids (Wood et al., 2012). FT processes use metal catalysts under high temperature and pressures, and require high H_2:CO molar ratios. Chemical catalysts are highly sensitive to syngas impurities such as ammonia (Christensen et al., 2011), sulphur species (Bambal et al., 2014), alkali ions (Balonek et al., 2010) or water (Christensen et al., 2011), which makes them less suitable for the treatment of biomass/waste-generated syngas. Gas clean-up treatments can reduce the concentration of most impurities, but complete removal is hindered by the cost of these technologies and the inherent variability of the feedstock (Abdoul-moumine et al., 2015).

Biological conversion of syngas involves its fermentation by microorganisms, which are in general more resistant to impurities in the gas and, in addition, do not require a fix H_2:CO molar ratio (Abubackar et al., 2011; Daniell et al., 2012; Liew et al., 2016; Redl et al., 2017). The biological route operates under mild temperature and pressure conditions, and overall has higher mass and energy conversion efficiencies compared to chemical catalysis (Griffin & Schultz, 2012; Wei et al., 2009). Furthermore, microbial processes result in higher product selectivity with the formation of fewer by-products. Syngas fermentation technology can also be applied for the treatment of CO-containing waste gases from heavy industry such as steelmaking. Often, CO-rich off-gases gases from steel mills are burned leading to CO_2 emissions; in 2019, on average 1.85 tonnes of CO_2 were emitted per every ton of steel produced (World Steel Association, 2022), contributing to approximately 8% of global emissions. This is a serious environmental problem with impact on climate change. Other opportunities are emerging to use gas fermentation technology associated

to CO_2 capture technology. For example, the production of CO by electrochemical reduction of CO_2 has been proved feasible and with high Faraday efficiencies (>80%) (Ma et al., 2016; Messias et al., 2019; Verma et al., 2018).

2.1.2 Microbes using carbon monoxide for growth

Microbes have exploited CO as sustenance for much of their evolutionary history. Proof of that are the different ways in which CO may be involved in microbial metabolism, which makes it necessary to define some terms. Microorganisms that can use CO as carbon and energy source are denominated *carboxydotrophs*, to be distinguished from *carboxydovores*, which may use electrons from CO but require organic carbon for growth (King & Weber, 2007). At the same time, CO metabolism can take two forms: respiratory and fermentative (Diender et al., 2015). The former relies either on O_2 (aerobic) or other external electron acceptors (anaerobic). In this review, the focus is on the latter: fermentative CO metabolism, which is, by definition, anaerobic. Microorganisms that ferment CO are carboxydotrophic. Therefore, the term *carboxydotroph* is used in this text to refer to the ability to use CO anaerobically but, in another context, it may refer to both aerobic and anaerobic microorganisms.

The fermentation of CO/syngas is carried out by acetogens, a specialised group of anaerobic bacteria able to use CO and H_2/CO_2 as sole carbon and energy sources via the reductive acetyl-CoA pathway, also known as the Wood-Ljungdahl pathway (WLP) (Daniell et al., 2012). Acetogenesis is not a phylogenetic trait; it is widely represented in at least 23 bacterial genera (Drake et al., 2008; Schuchmann & Müller, 2014). Most known acetogens belong to the genera *Clostridium* and *Acetobacterium*, within the Clostridia class. The WLP results in acetyl-CoA as end-product of CO and H_2/CO_2 fermentation. Since autotrophy via the WLP is energetically limited, most acetyl-CoA is directed towards acetate production to generate ATP. Thus, the majority of acetogens produce acetic acid as sole metabolic end-product. Some microorganisms can derive other chemicals from acetyl-CoA as intermediate. For example, *Clostridium autoethanogenum*, *Clostridium ljungdahlii*, *Clostridium ragsdalei* and *Alkalibaculum bacchi* are able to produce ethanol; *C. autoethanogenum*, *C. ljungdahlii* and *C. ragsdalei* can also produce 2,3-butanediol (2,3-BDO); *Eubacterium limosum* and *Butyribacterium methylotrophicum* are able to produce butyrate; and *Clostridium carboxidivorans* can produce butyrate, butanol, caproate and hexanol (Bengelsdorf et al., 2018).

The key enzyme of CO oxidation to CO_2, carbon monoxide dehydrogenase, is present in other anaerobic microorganisms that harbour variations of the WLP. Besides acetogenic bacteria, CO can be used as electron donor and/or carbon source by some methanogenic archaea and sulfate-reducing bacteria (Sipma et al., 2006). However, compared to acetogens, methanogens and sulfate-reducing bacteria are more sensitive to elevated levels of CO.

Syngas fermentation processes can be implemented with pure cultures of acetogens or with microbial communities. This chapter focuses on the latter: undefined and defined consortia of microorganisms that convert syngas to biochemicals of interest. For an overview of monoculture-based processes, we refer to recent reviews (Redl et al., 2017; Sun et al., 2019; Wainaina et al., 2018).

### 2.1.3 The microbial consortia approach for syngas fermentation

The fermentation of syngas has been most studied and implemented in industry using pure cultures of acetogens (Daniell et al., 2012; Liew et al., 2016). From a process perspective, monocultures are easy to control and predict, since optimal conditions for growth are well-defined. Process conditions can be tuned to target a product of interest with high selectivity and yields. As an example, the highest ethanol concentration (48 g L^{-1}) and volumetric productivity (369 g L^{-1} d^{-1}) from syngas were achieved with pure cultures of *C. ljungdahlii* (Gaddy, 2007, p. 200; Phillips et al., 1993). However, a major limitation of the use of monocultures for syngas conversion is the energetic constraint in the formation of products other than acetate and ethanol (Katsyv & Müller, 2020). Genetic and metabolic engineering of Clostridia strains has advanced remarkably in the last decade, paving the way towards the expression of heterologous products and enhanced yields (Humphreys & Minton, 2018; Joseph et al., 2018). For instance, industrially relevant titres have recently been achieved for acetone, iso-propanol and 2,3-BDO (Köpke & Simpson, 2020). Yet, important hurdles remain to be addressed in genetic engineering of Clostridia to further expand the product portfolio of syngas fermentation, such as low DNA transformation efficiencies, insufficient high-throughput recombineering tools and, in general, the need for a better understanding of acetogenic platforms at the molecular level (Charubin et al., 2018). Another disadvantage of monoculture-based strategies is the lack of robustness against process fluctuations. This is of particular relevance in the case of syngas fermentation, since the gas composition varies depending on the source or gasification method (Couto et al., 2013). Mixed cultures are less affected than monocultures of carboxydotrophs by changes in the syngas composition (Esquivel-Elizondo et al., 2017b), and are also expected to be more robust against syngas impurities (e.g., nitrogen oxides, tars), which have been shown to inhibit cell growth or interfere with product distribution in monocultures of acetogens (Xu et al., 2011) .

Microbial consortia are emerging as a promising strategy aimed at overcoming the limitations of monocultures and taking syngas fermentation a step forward (Cui et al., 2020; Diender et al., 2021; Wainaina et al., 2018). In nature, microbes rarely thrive alone; instead, cooperation and communication with other microorganisms are extremely important for survival (West et al., 2007; Zengler & Zaramela, 2018). Communities can perform complicated functions that individual populations cannot, for instance the production of energy-demanding products. Compared to monocultures, microbial consortia can convert much more complex substrates and have better robustness, both because of a highly diverse community structure and a capacity to evolve. The capabilities of microbial consortia have long been exploited in bioremediation, wastewater treatment and the production of fermented foods (Bader et al., 2010). In the last decade, advances in -omics approaches and a greater understanding of microbial interactions have driven forward the fields of microbiome engineering and synthetic ecology, aimed at unlocking the full potential of microbial communities for biotechnological applications (Brenner et al., 2008; Johns et al., 2016; Lawson et al., 2019; McCarty & Ledesma-Amaro, 2019; Strous & Sharp, 2018).

The use of microbial consortia in syngas fermentation has specific advantages. For one thing, communities composed of multiple carboxydotrophic microbes with different CO tolerance can handle syngas streams with variable composition. This functional redundancy may enhance gas consumption and mitigate the detrimental effect of syngas contaminants on individual populations. Moreover, provided that carboxydotrophic populations keep CO levels low, CO-sensitive

microbes can thrive in an environment that would otherwise be hostile. In addition, the co-culture capabilities can be extended by syntrophic interactions between species in the consortia, such as cross-feeding of intermediates (e.g., acetate, ethanol) or exchange of essential nutrients (e.g., amino acids, vitamins). An example of this is the co-culture of *Citrobacter malonates* Y19 and the acetogen *Sporomusa ovata*. The latter has been reported to produce acetate from CO, but at rather low rates (Balk et al., 2010; Lee et al., 2018). On the other hand, *C. amalonaticus* Y19 is unable to use autotrophic substrates but it can oxidise CO to H_2 and CO_2 (Yeol Jung et al., 1999), which may be used as substrates by the acetogen. A study found that co-cultures of *S. ovata* and *C. amalonaticus* Y19 produced almost double the amount of acetate than monocultures of *S. ovata*, from the same amount of CO (Lee et al., 2018). In addition, growth of both microorganisms and CO consumption was higher in the co-culture than in monocultures. This example is just one of many that demonstrates the relevance of mutualistic interactions in microbial consortia (Diender et al., 2021; Morris et al., 2012). There are, on the other hand, potential downsides when using consortia of microorganisms compared to monocultures. Some examples are the occurrence of competing or inhibiting pathways, the generation of side-products that reduce product selectivity or incompatible cultivation conditions (i.e., pH, temperature, etc.) between species in the community. These issues can be tackled through rational microbial consortia engineering, multi-species metabolic modelling and bioreactor/bioprocess design (Ben Said & Or, 2017; De Vrieze et al., 2017; Johns et al., 2016).

Two types of microbial consortia can be distinguished: open mixed cultures (also referred to as 'open cultures', 'mixed cultures' or 'microbiomes') and synthetic co-cultures (Fig. 2.1). The former consist of self-assembled, highly diverse microbial communities naturally occurring in defined habitats, in which the populations are mostly unspecified. Synthetic co-cultures are consortia of specified microbial strains that engage in interaction under aseptic and controlled conditions. Most synthetic co-cultures reported in literature are composed of two or three microbial species, with a few including up to five (Goers et al., 2014). The following sections summarise the main developments regarding the implementation of open mixed cultures (§ 2.2) and synthetic co-cultures (§ 2.3) in syngas fermentation processes.
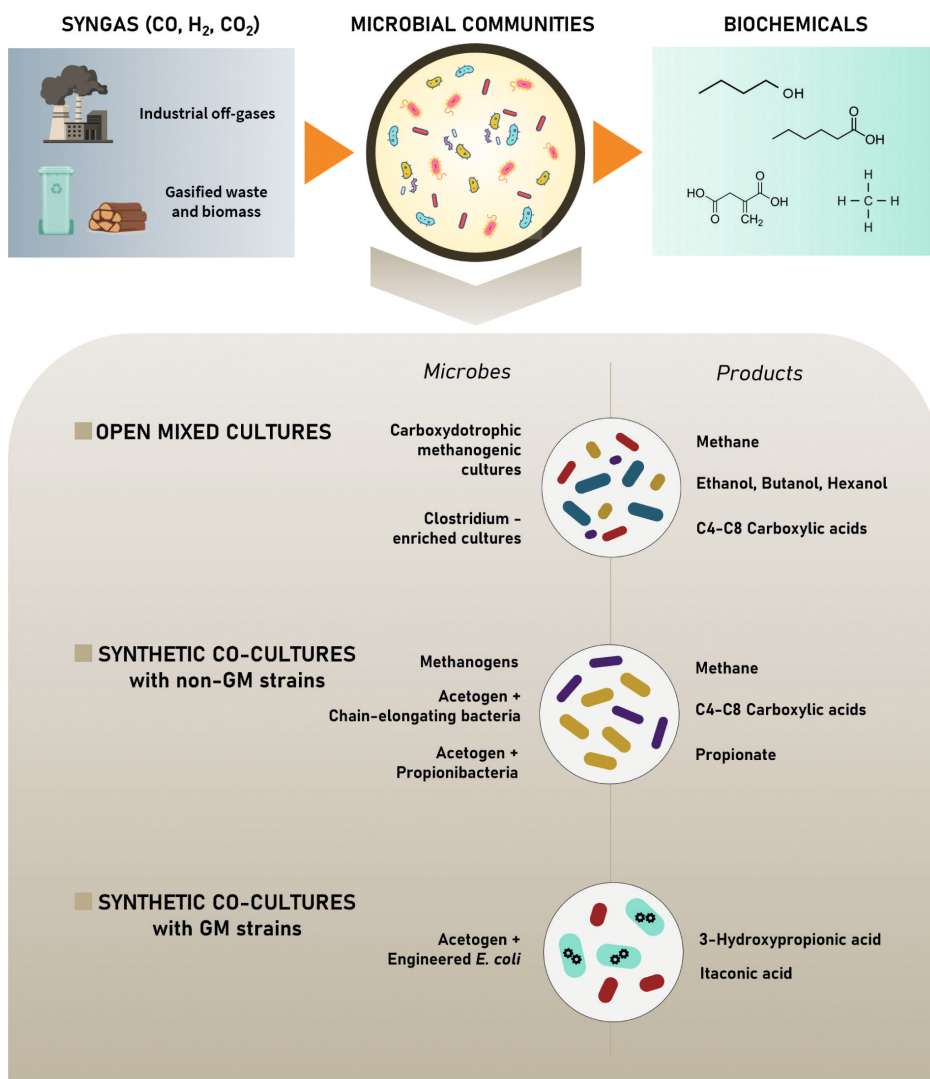
Figure 2.1 Overview of the types of microbial communities that can be applied in syngas fermentation to produce biochemicals. Syngas (CO, H_2 and CO_2) can be obtained via the gasification of organic wastes or lignocellulosic residues. Off-gases from the steel and iron industries are also sources of CO-rich gas. Open mixed cultures (from, e.g., sludges) enriched in carboxydotrophic, methanogenic and/or Clostridia species can be used to produce methane, alcohols, or medium-chain carboxylic acids from syngas. Alternatively, synthetic co-cultures can be used, composed of non-engineered microorganisms alone or in combination with genetically modified (GM) platform organisms such as Escherichia coli. The latter option allows to expand the range of products that can be obtained from syngas to compounds of added-value, such as 3-hydroxypropionic acid or itaconic acid.

2.2   CO conversion by open mixed cultures

2.2.1   Anaerobic sludges as biocatalysts for syngas fermentation

The main components of syngas (CO, H_2 and CO_2) can sustain anaerobic growth of a number of microbial groups: acetogens and hydrogenogenic bacteria, carboxydotrophic and hydrogenotrophic methanogens and sulfate-reducing microorganisms (Diender et al., 2015). In turn, the products of CO/syngas fermentation (mainly H_2, CO_2, acetate and ethanol) can support growth of acetoclastic methanogens, chain-elongating bacteria, ethanol oxidisers, syntrophic acetate-oxidizing bacteria and propionibacteria, among others (Baleeiro et al., 2019; Liew et al., 2016). The range of final products that can be obtained via syngas fermentation by open mixed cultures (in the absence of external electron acceptors) therefore includes short- and medium-chain carboxylic acids, simple and higher alcohols and methane. When sulfate is available and sulfate-reducing microorganisms are present, sulphide is also produced. An overview of some of the works on syngas/CO conversion by mixed cultures is shown in Table 2.1.

Open mixed cultures for syngas fermentation are based on inocula from anaerobic natural or engineered environments that harbour a high microbial diversity. Typical inocula include anaerobic digester sludges (Alves et al., 2013; Arantes et al., 2018; Chakraborty et al., 2019; Esquivel-Elizondo et al., 2017a; Ganigué et al., 2015; Ganigué et al., 2016; Sipma et al., 2003; Wang et al., 2018a), wastewater treatment granules (Guiot et al., 2011; Sipma et al., 2003) and faeces of herbivores (Li et al., 2020; Park et al., 2013; Singla et al., 2014; Tang et al., 2021; Xu et al., 2015). Sludges from anaerobic digesters employed in traditional wastewater treatment processes have been proposed as most suitable syngas biocatalysts (Alves et al., 2013; Guiot et al., 2011; Sipma et al., 2003). These cultures have a high adaptation capacity, essential to treat a vast range of organic and inorganic substrates. Most importantly for syngas fermentation, the ability to oxidise CO seems to be a ubiquitous property across anaerobic sludges (Sipma et al., 2003).

An acclimation period is generally required to obtain a microbiome capable of efficiently converting CO. The inoculum largely determines the duration of this acclimation period, which can be as short as a few days (Guiot et al., 2011; Park et al., 2013; Sipma et al., 2003; Tang et al., 2021) or weeks (Ganigué et al., 2016; Sipma et al., 2003; Wang et al., 2018b), and in some cases lasts several months (Alves et al., 2013; Esquivel-Elizondo et al., 2017a; He et al., 2018). Because different microbes have different optimal conditions for growth, the outcome of the process depends not only on the inoculum source but also on the environmental conditions applied to enrich and maintain the culture. Acetogenic bacteria are more tolerant to CO than other microorganisms present in anaerobic sludges, therefore dominating enriched cultures exposed to moderate or high levels of CO (Duan et al., 2021; Esquivel-Elizondo et al., 2017a; Grimalt-Alemany et al., 2018a; Grimalt-Alemany et al., 2018b; Shen et al., 2018; Wang et al., 2018a; Wang et al., 2018b). For example, during the CO-enrichment process of an anaerobic sludge, the relative abundance of members from the Clostridiales order, which includes many acetogenic species, increased from 5% in the inoculum to 66–95% in enriched cultures (pCO = 20–61 kPa) (Esquivel-Elizondo et al., 2017a). Similarly, a recent study showed that mixed cultures exposed to high pCO (96 kPa) were dominated by members of the Firmicutes phylum, to which many acetogens belong, while low pCO (35 kPa) shifted the community towards Proteobacteria, a phylum that includes hydrogenogenic carboxy-

dotrophs (Duan et al., 2021). Methanogens, on the other hand, are generally inhibited at moderate CO pressures starting from 30 - 80 kPa (Alves et al., 2013; Esquivel-Elizondo et al., 2017a; Guiot et al., 2011). In a recent study, Duan et al. (2021) revealed the crucial role of under-characterised taxa in CO-enriched communities. Authors identified novel bacterial genera and species which may participate in CO-oxidation to end-products and maintain fundamental metabolism (e.g., citric cycle, amino acid biosynthesis), extending the functional redundancy of the communities and overall increasing their stability. Besides CO, the presence of other gases in the mixture has an impact on the performance of syngas-converting communities. With few exceptions, pure cultures of carboxydotrophs can rarely consume H_2 and CO simultaneously, since almost all hydrogenases are inhibited by CO (Adams, 1990; Chen & Blanchard, 1978; Fox et al., 1996; Hess et al., 2015; Kim et al., 1984; Oswald et al., 2016). In contrast, mixed cultures can metabolise H_2 along with CO, since H_2 can be used by hydrogenotrophic microorganisms that might be present in the community (Esquivel-Elizondo et al., 2017b). Overall, the addition of CO_2 and H_2 has been shown to increase the microbial diversity of CO-enriched cultures and promote a higher acetate/ethanol ratio (Esquivel-Elizondo et al., 2017b; Esquivel-Elizondo et al., 2017a).

Temperature and pH are two operational parameters with a major influence on the evolution of CO enrichments. Grimalt-Alemany et al. (2019) showed that mesophilic syngas-enrichments (37 °C) are characterised by a higher microbial diversity and a more intricate metabolic network compared to thermophilic syngas-enrichments (60 °C). Another finding of that study was that the maximum specific growth rates of microbes were significantly higher (twofold) in thermophilic conditions. Similar findings were reported by Alves et al. (2013), who observed a rapid decrease in microbial diversity in long-term CO/syngas enrichments of anaerobic sludges at 55 °C. The pH is perhaps the most crucial parameter determining the structure and product composition of syngas-converting communities. Several authors have emphasised its critical effect on the regulation between acetogenesis and solventogenesis, requiring a tight control of acidic conditions (Chakraborty et al., 2019; Ganigué et al., 2016; Grimalt-Alemany et al., 2018a; Grimalt-Alemany et al., 2018b), while, for methanogenesis, neutral or slightly alkaline conditions are required (Grimalt-Alemany et al., 2018a; Grimalt-Alemany et al., 2018b).

Finally, the addition of medium supplements (e.g., yeast extract, reducing agents) and inhibitors of specific types of metabolism is also common practice to alter the structure of microbial communities and stimulate the production of target products (Chakraborty et al., 2019; Grimalt-Alemany et al., 2019; Sancho Navarro et al., 2016). In this regard, the addition of methanogenic inhibitors is an extended practice in syngas fermentation processes using open mixed cultures to supress methane production. Inocula from anaerobic sludges are likely to harbour an active methanogenic population. This can be a hurdle when products other than methane are targeted. Three approaches are commonly used to inhibit methane production by open mixed cultures used in bioprocesses, namely i) operation in (mildly) acidic conditions (Pereira, 2014; Steinbusch et al., 2009), ii) heat-shock treatment of the inoculum (Nam et al., 2016; Steinbusch et al., 2009) and iii) the addition of methanogenic inhibitors such as 2-bromoethanesulfonate (2-BES) (Ganigué et al., 2015; Ganigué et al., 2016; Luo et al., 2018; Steinbusch et al., 2009; Zinder et al., 1984). The latter, in concentrations ranging 10–50 mM, has proven very efficient and is therefore a popular choice; however, it can certainly contribute to increasing process costs at industrial scale since periodical addition is

necessary in continuous operation. Moreover, 2-BES can lose efficacy during long-term operation (He et al., 2018) and can be metabolised by dehalogenating and sulfate-reducing bacteria present in microbial communities (Chiu & Lee, 2001; Steinbusch et al., 2009). Eventually, moderate to high concentrations of CO should inhibit most methanogenic activity and avoid the addition of specific inhibitors.

One of the big advantages of using open cultures in bioprocesses is that these do not require operation under aseptic conditions. In addition, long-term reproducibility of mixed cultures can be ensured by using suitable cryopreservation methods (Grimalt-Alemany et al., 2020). On the other hand, these systems are highly dependent on microbial interactions, which are very difficult to predict and, to a great extent, unknown. Other drawbacks are the long times required to achieve steady-state conditions and the challenging product recovery due to the presence of many by-products at low concentrations. Large-scale continuous processes using open mixed cultures are well-established in industry (e.g., in wastewater treatment and food fermentation), but not yet applied for syngas fermentation. Decades of research have shed light on the structure of anaerobic sludges, their governing microbial interactions and the influence of operational parameters, although mainly in the context of conversion of organic compounds (Amani et al., 2010; Leng et al., 2018; Novaes, 1986; Wang et al., 2018c). However, developments in the last decade are driving forward the syngas fermentation platform for mixed cultures at a rapid pace. The next sections relate these advances, centred on the production of methane, carboxylic acids and alcohols.

2.2.2 Syngas biomethanation

Conversion of CO-rich waste gases by open mixed cultures is a popular method to produce methane (Gavala et al., 2021; Grimalt-Alemany et al., 2018b). Traditional wastewater treatment processes rely on microbial communities that perform methanogenesis as ultimate step of anaerobic digestion. These cultures are suited to produce methane from syngas, provided they have or acquire a sufficient carboxydotrophic potential (Guiot et al., 2011). Biomethanation of syngas presents several advantages over its analogous catalytic process (Diender et al., 2018; Grimalt-Alemany et al., 2018b; Grimalt-Alemany et al., 2019). Microbes are less sensitive than metal catalysts to impurities and to the ratio C/H in syngas. Biocatalysts are cheap, self-replicating, and can yield high methane contents in a single step. Using microbes, higher methane selectivity can be obtained, in contrast to the use of metal catalysts that result in the production of higher hydrocarbons as by-products. However, production rates of biomethanation are lower compared to the chemical process. Recent years have witnessed increased efforts to improve the efficiency of syngas biomethanation; these include the development of novel reactor configurations, insights on the impact of operational parameters and improved knowledge on the microbial community structure and interactions.

Methanogenesis from CO can take place via three routes: i) direct conversion by carboxydotrophic methanogens, ii) via acetate as intermediate by acetoclastic methanogens, and iii) via H_2/CO_2 as intermediates by hydrogenotrophic methanogens. Direct methanation of CO is rather infrequent due to complete inactivation of methanogens in the presence of moderate concentrations of CO (Guiot et al., 2011; Sipma et al., 2003). Four methanogenic species have been demonstrated to use CO for growth: *Methanothermobacter thermoautotrophicus* (Daniels et al., 1977), *Methanosarcina barkeri* (O'Brien et al., 1984), *Methanosarcina acetivorans* (Kliefoth et al., 2012; Rother

& Metcalf, 2004) and *Methanobacter marburgensis* (Diender et al., 2016a). However, all of them require rather long periods of adaptation to CO and growth is significantly slower than on their typical substrates. Consequently, CO conversion to methane in microbial communities is highly dependent on bacterial-archaeal interactions. Several studies have demonstrated the preferential use of certain pathways in anaerobic sludges used for syngas biomethanation. In this regard, the incubation temperature plays a determining role. Experiments with vancomycin, an inhibitor of acetogenic activity, have shown that, under mesophilic conditions, methanogenesis occurs primarily via acetate as intermediate (Arantes et al., 2018; Sancho Navarro et al., 2016). Mesophilic conditions are favourable to acetogenic bacteria, which provide acetate to acetoclastic methanogens; in contrast, higher temperatures generally shift the microbial community towards H_2-producing carboxydotrophs, which favour the hydrogenotrophic methanogenic route (Grimalt-Alemany et al., 2019; Guiot et al., 2011; Sipma et al., 2003). In both environments, when the H_2 pressure is kept sufficiently low, acetate can be converted to H_2/CO_2 by syntrophic acetate-oxidizing bacteria, which can compete with acetoclastic methanogens and create a niche for hydrogenotrophic methanogens (Li et al., 2020; Sancho Navarro et al., 2016, p. 2020). The effect of temperature on the microbial composition of communities performing syngas biomethanation extends to the process performance. Several studies have reported the positive impact of thermophilic over mesophilic conditions on conversion rates (Asimakopoulos et al., 2020; Asimakopoulos et al., 2021a; Grimalt-Alemany et al., 2019; Guiot et al., 2011; Sipma et al., 2003). For example, Grimalt-Alemany et al. (2019) observed an 18-fold higher methane productivity from enrichments incubated at 60 °C compared to enrichments incubated at 37 °C. Thermophilic conditions are therefore the preferred mode of operation for syngas biomethanation processes (Grimalt-Alemany et al., 2018b).

Two other operational conditions, the pH and the pCO, also influence the performance of methanogenic communities using syngas. Since most methanogens grow optimally around neutrality, syngas biomethanation processes are generally operated at pH values between 7 and 7.6 (Grimalt-Alemany et al., 2018b). Carboxydotrophic bacteria can also proliferate in this pH range (Bengelsdorf et al., 2018), thus providing intermediates for methanogenesis. The effect of CO levels has been extensively studied. Alves et al. (2013) reported no methane production in thermophilic enrichments from anaerobic sludge incubated with solely CO as substrate (35 kPa). Methane was detected in enrichments incubated with $CO/H_2/CO_2$ (pCO = 18 kPa), but production ceased in subsequent transfers. Instead, both syngas- and CO-enriched cultures produced acetate. Elimination of methanogens in the enrichments could be due to the low growth rate of methanogens or their higher susceptibility to CO (Diender et al., 2016a; Guiot et al., 2011; Rother & Metcalf, 2004). Similarly, Luo et al. (2013) reported 50% lower methanogenic activity by an anaerobic sewage sludge exposed to a pCO of 51 kPa, compared to the control in the absence of CO. These observations are in line with those of Guiot et al. (2011), who reported inhibition of methanogenesis in enriched granular sludge at pCO between 30 and 83 kPa. Nevertheless, some archaeal genus, such as *Methanobacterium*, have been shown to tolerate CO levels up to 96 kPa in microbial communities (Duan et al., 2021). In addition, strategies are in place to enhance CO utilisation by methanogenic cultures. For instance, a system with gas recirculation enabled a CO conversion efficiency of 75% and a methane yield of 95% under a pCO of 60 kPa (Guiot et al., 2011). In some cases, an acclimation phase has enabled methane production by anaerobic sludges exposed to 100 kPa CO (Arantes et al., 2020; Sancho Navarro et al., 2016).

Table 2.1 Overview of syngas fermentation processes using open mixed cultures.

Cultivation system	T (°C)	pH	Enriched microbial taxa (relative abundance)	Syngas composition (%)	Product titre or productivity	Ref.
Bench scale TBR	60	7	Biofilm: *Methanothermobacter* (30%), *Therminicola* (16%), *Coprothermobacter* (23%) Liquid: undefined (30%), *Therminicola* (23%), *Methanothermobacter* (15%)	$CO/H_2/CO_2/N_2$ (20:45:25:10)	Methane 8.49 mmol L_{bed}^{-1} h^{-1}	Asimakopoulos et al., 2020
TBR (7.5 L)	60	7	Derived from Asimakopoulos et al., 2020	$CO/H_2/CO_2/N_2$ (20:45:25:10)	Methane 17.6 mmol L_{bed}-1 h^{-1}	Asimakopoulos et al., 2021b
TBR + FBG	60	7	Derived from Asimakopoulos et al., 2020	$CO/H_2/CO_2/N_2$ (11:35:44:10)	Methane 14.4 mmol L_{bed}-1 h^{-1}	Asimakopoulos et al., 2021b
Floating MBR	55	8.2	ND	$CO/H2/CO2$ (55:20:10)	Methane 1.43 mmol L^{-1} h^{-1}	Chandolias et al., 2019
MOBB	35 - 37	5.8 - 6.7	ND	$CO/H_2/CO_2$ (60:30:10)	Methane 3.04 mmol L^{-1} h^{-1}	Pereira, 2014
HfMBR	55	6.5	Biofilm: *Thermoanaerobacterium* (92.8%)	CO/H_2 (40:60)	Acetate 24.6 g L^{-1} 16.4 g L^{-1} d^{-1}	Shen et al., 2018
HfMBR	35	6	Biofilm: *Clostridium* (41.6%), undefined (42%)	CO/H_2 (40:60)	Butyrate 1.4 g L^{-1} Caproate 0.88 g L^{-1} Caprylate 0.53 g L^{-1}	Shen et al., 2018
Column reactor filled with porous pad	35	7 to 5.8 - 6.5[a]	*Acinetobacter, Alcaligenes, Rhodobacter, Methanobacterium, Methanoseaeta*	CO/N_2 (60:40)[b]	Caproate 0.22 g L^{-1} Heptanoate 0.21 g L^{-1} Caprylate 0.15 g L^{-1}	He et al., 2018
HfMBR	35	4.5	Biofilm: *Clostridium* (86.3%)	CO/H_2 (60:40)	Ethanol 16.9 g L^{-1}	Wang et al., 2018b

Cultivation system	T (°C)	pH	Enriched microbial taxa (relative abundance)	Syngas composition (%)	Product titre or productivity	Ref.
CSTR with cell-recycle	37	7	*Alkalibaculum bacchi* (56%), *Anaerotignum propionicum* (34%), *Clostridium sp.* (10%)	$CO/H_2/N_2$ (28:60:12)	Ethanol 8 g L^{-1}; Propanol 6 g L^{-1} Butanol 1 g L^{-1}	Liu et al., 2014a
STR	37	7 to 4.3[a]	ND	$CO/H_2/CO_2/N_2$ (32:32:8:28)	Butyrate 2.17 g L^{-1} Butanol 0.43 g L^{-1}	Ganigué et al., 2015
STR	37	6 to 4.8[a]	*Clostridium ljungdahlii, Clostridium carboxidivorans, Clostridium kluyveri*	$CO/H_2/CO_2/N_2$ (32:32:8:28)	Butanol 1.1 g L^{-1} Hexanol 0.6 g L^{-1}	Ganigué et al., 2016
STR	33	4.9	ND	CO (100)	Ethanol 11.1 g L^{-1} Butanol 1.8 g L^{-1} Hexanol 1.5 g L^{-1}	Chakraborty et al., 2019

TBR = trickle-bed reactor; FBG = fluidized bed gasifier; MBR = membrane bioreactor; MOBB = multi-orifice baffled bioreactor; HfMBR = hollow-fiber membrane bioreactor; (C)STR = (continuous) stirred tank reactor; ND = no data. [a]The pH was initially set and not controlled afterwards. [b]Percentage at the end of the process, with a gas inflow of 60 kPa CO plus N_2 as make-up gas, assuming a total pressure of 101 kPa.

2

Syngas biomethanation has been investigated in a variety of process configurations with the aim to improve gas-to-liquid transfer and cell concentrations. Besides the use of traditional stirred-tank reactors (CSTRs), tested designs include bubble columns, gas-lift reactors, trickle-bed reactors (TBRs) and multi-orifice baffled bioreactors (MOBBs) (Grimalt-Alemany et al., 2018b). The most promising results so far have been obtained with the use of TBRs. Recently, Asimakopoulos et al. (2020) reported a CH_4 productivity from syngas of 8.49 mmol·L_{bed}^{-1}·h^{-1} in a lab-scale TBR operated in continuous mode at 60 °C. The inoculum used was an enriched mixture of two anaerobic sludges, intended to increase microbial diversity. Interestingly, the methanogenic population was more abundant in the biofilm of the TBR, while carboxydotrophic bacteria were mostly found in the liquid phase. In a follow-up study, the process was scaled-up; a 7.5 L TBR, that used the same enrichment and syngas mixture and was operated in the same conditions as the lab-scale reactor, achieved a maximum CH_4 productivity of 17.6 mmol·L_{bed}^{-1}·h^{-1}, the highest reported so far for syngas biomethanation Asimakopoulos et al. (2021b). At this rate, H_2 and CO conversion efficiencies were 97% and 76%, respectively, and CH_4 selectivity was 99%. The higher performance of the scaled-up system was attributed to an improved gas-liquid mass transfer due to a more efficient sparging component and a much higher height/diameter ratio, in addition to a more accurate pH control. To further test the process, the TBR was coupled to a gasifier that generated syngas from wood pellets; the generated gas contained 11–27% CO and was fed into the reactor at atmospheric pressure. The microbial consortium produced CH_4 at a maximum rate of 14.4 mmol·L_{bed}^{-1}·h^{-1} without any inhibitory effects. Few other studies have demonstrated continuous operation of bioreactors for syngas biomethanation by open cultures with syngas (CO/H_2/CO_2) as sole substrate (Asimakopoulos et al., 2021b; Grimalt-Alemany et al., 2018b). Pereira (2014) studied syngas conversion to methane by a mesophilic sludge in a 10.6 L MOBB operated in continuous mode. The system produced CH_4 at a maximum rate of 73 mmol·L^{-1}·d^{-1} with negligible amounts of by-products in the liquid and a $Y_{CH4/CO}$ of 0.6–0.8 (mol/mol), higher than reported in similar works (Grimalt-Alemany et al., 2018b; Grimalt-Alemany et al., 2018a). Yet, the conversion efficiency eventually dropped due to the prolonged high flow rates applied (Pereira, 2014). In a recent study, Chandolias et al. (2019) tested a novel configuration consisting of a floating membrane in a membrane bioreactor and achieved a maximum CH_4 productivity of 34 mmol·L^{-1}·d^{-1}, in this case, using a thermophilic digester sludge.

Overall, CH_4 productivity in syngas biomethanation processes is very dependent on the process configuration and specific process conditions, which affect gas-to-liquid mass transfer and cell concentrations. Considerable progress over the last years and successful examples of scale-up cases such as that of Asimakopoulos et al. (2021b) offer good perspectives for syngas biomethanation in the future. A key aspect to bring this technology to commercial application will be to ensure its economic feasibility by, e.g., combining syngas biomethanation with existing gasification plants and improving reactor design to increase productivities (Grimalt-Alemany et al., 2018b).

2.2.3   Production of ethanol by mixed cultures

Ethanol is undoubtedly the most common target product of syngas fermentation due to its commercial use as biofuel (Gavala et al., 2021; Liew et al., 2016; Teixeira et al., 2018). Despite high productivities have been achieved with pure cultures of acetogens, the robustness of open mixed culture operation has driven an interest for its production in these systems. Singla et al. (2014)

were the first to demonstrate ethanol production by microbial communities using syngas. In their study, a mesophilic enriched consortium obtained from faeces produced up to 2.2 g L^{-1} ethanol in semi-continuous mode (adding fresh syngas to serum bottles every 24 hours). Liu et al. (2014a) tested continuous fermentation of syngas to ethanol by mixed culture in a CSTR including a cell recirculation unit. Authors reported the production of up to 8 g L^{-1} ethanol from syngas at 37 °C and pH 7. Consumption of ethanol was followed by the accumulation of propanol and butanol, with peak concentrations of 6 g L^{-1} and 1 g L^{-1}, respectively. The microbial community was composed of the alkaliphilic acetogen *Alkalibaculum bacchi* (56%), the propionibacterium *Anaerotignum propionicum* (formerly, *Clostridium propionicum*; (Ueki et al., 2017)) (34%) and other Clostridia species (10%). A follow-up study concluded that the mixed culture could convert 50% more carboxylic acids into their respective alcohols compared to monocultures of *A. bacchi* (Liu et al., 2014b), evidencing the positive effect of synergistic microbial interactions in syngas-fermenting communities.

A limitation of the fermentation process of Liu et al. (2014a) was the rather low CO and H$_2$ utilisation (20–60%), a common problem due to the low solubility of these gases and low gas mass transfer rates in CSTRs. Novel reactor configurations can help overcome this issue (Asimakopoulos et al., 2018). In a recent study, Wang et al. (2018b) reported a relatively high ethanol production from syngas by mixed culture in a hollow-fibre membrane biofilm reactor (HfMBR). HfMBRs, most popular in the field of gas and wastewater treatment, have recently attracted the attention of researchers in the field of syngas fermentation (Asimakopoulos et al., 2018; Shen et al., 2018; Shen et al., 2014; Wang et al., 2018b). In a HfMBR, a gaseous substrate flows through the lumen of a hollow-fibre membrane and is consumed by the biofilm formed on the outer surface of the membrane. The high surface area allows a high volumetric gas transfer rate which, in turn, translates into high production rates (Martin & Nerenberg, 2012). A non-acclimated sludge used by Wang et al. (2018b) produced up to 16.9 g L^{-1} ethanol from CO/H$_2$ (60:40) in a HfMBR operated in consecutive batch at pH 4.5 and 35 °C. Ethanol was the only soluble product of CO/H$_2$ fermentation. Interestingly, a similar HfMBR-based process operating at pH 6.5 and 55 °C converted CO/H$_2$ (40:60) to mostly acetate (98.6%) (Shen et al., 2018). While the different temperature, gas composition and sludge characteristics could have contributed to the divergent product profile observed in these two studies, pH is most likely the determining factor. Several studies have reported that an acidic pH is key to promote ethanol production in syngas fermentation cultures (Chakraborty et al., 2019; Ganigué et al., 2016; Grimalt-Alemany et al., 2018a). Yet, no ethanol (but acetate) was produced by a sludge-derived culture in a HfMBR operated at pH 4.5 using H$_2$/CO$_2$ as substrates (Zhang et al., 2013), highlighting that CO, which is a stronger reductant than H$_2$, is also essential to promote alcohol production by acetogens.

2.2.4   Production of carboxylic acids and higher alcohols by mixed cultures

Acetate is the simplest carboxylic acid that can be produced from syngas. Titres in the range of 20 - 30 g L^{-1} have been obtained for sludge-derived consortia utilising syngas in continuous fermentation (Nam et al., 2016; Shen et al., 2018). Continuous operation of a thermophilic HfMBR reached a maximum acetate production rate of 16.4 g L^{-1}d^{-1} with high product selectivity (Shen et al., 2018). However, acetate production by mixed cultures has not received much attention due to

the significantly higher production rates that can be obtained by pure cultures and the rather low economic value of this product.

Instead, over the last decade, increased attention has been given to the production of medium-chain carboxylic acids (MCCAs) via anaerobic fermentation processes, a type of biorefinery referred to as the carboxylate platform (Agler et al., 2011; Angenent et al., 2016; Moscoviz et al., 2018; Spirito et al., 2014). The carboxylate platform relies mostly on sludges used in classical anaerobic digestion and aims at revalorising wastewater streams. Recently, several studies have extended this platform to the revalorisation of CO-rich gases. The products of syngas fermentation, acetate and ethanol, can be used by microorganisms that perform ethanol-based chain-elongation, producing MCCAs such as butyrate and caproate as end-products. Different processes are devised to convert syngas into MCCAs by microbial communities, including the use of synthetic co-cultures, discussed in section 2.3.4, and multiple-step processes, summarised elsewhere (Baleeiro et al., 2019). Here, the focus is on one-step conversions by open mixed cultures.

Ethanol chain-elongating communities are present in both natural and engineered environments, and are dominated by relatives of *Clostridium kluyveri*, the best-studied ethanol chain-elongating microorganism and only isolate to date (Angenent et al., 2016; Candry et al., 2020a; Spirito et al., 2014). Mesophilic conditions are preferred to *C. kluyveri* and most acetogens. However, the two isolated strains of *C. kluyveri* grow optimally at a pH of 6.8 and 7.6 (Barker & Taha, 1942; Weimer & Stevenson, 2012), while acetogenic bacteria generally thrive in mildly acidic conditions (Bengelsdorf et al., 2018; Martin et al., 2016). Therefore, pH is critical in determining the outcome of syngas-fermenting chain-elongating communities (Ganigué et al., 2015; Ganigué et al., 2016; Richter et al., 2016a).

Ganigué et al. (2015) used a carboxydotrophic enrichment from sludge in a syngas fermentation process without pH control. Acetogenesis was dominant at the initial pH of 7, while production of C4–C6 compounds prevailed at the mid/end of the fermentation, when the pH dropped to ~ 4.3. At the end of the process, the C4–C6 products represented 75–90% of the total, with butyrate (2.17 g L^{-1}) as main product. In a follow-up study, it was determined that pH values around 4.8 favoured a sustained production of higher alcohols (Ganigué et al., 2016). In a semi-continuous process without pH control (initial pH 6), the mixed culture converted syngas to a maximum of 1.1 g L^{-1} butanol and 0.6 g L^{-1} hexanol. To favour the synthesis of C6 compounds, attributable to *C. kluyveri*, it was critical to prevent pH to decrease below 4.5–5.

In a recent study, He et al. (2018) used a novel reactor configuration to promote gas transfer in a chain-elongating process. The system consisted of a reactor filled with a porous sponge pad and with a gas recirculation line. CO was used as sole carbon and energy source, and the partial pressure was gradually increased thorough the fermentation, from 15 to 61 kPa CO. Similar to the studies of Ganigué et al. (2015, 2016), operation was done at mesophilic conditions and the pH, initially set at 7, was not controlled. In contrast to those studies, though, the culture did not produce alcohols but a mixture of odd- and even-chain carboxylic acids including caprylate (C8), detected for the first time in a syngas-fermentation process by a mixed culture. Production of C6–C8 carboxylates only began at the end of the fermentation, when CO pressure was 61 kPa. Maximum concentrations of caproate, heptanoate and caprylate were 0.22 g L^{-1}, 0.21 g L^{-1} and 0.15 g L^{-1}, respectively. The production of C5-C8 carboxylates halted in the last phase, likely due to product inhibition. The

different product profile compared to the studies of Ganigué and co-workers could be explained by the different inoculum source and enrichment process, which resulted in quite different microbial compositions of the enriched cultures. The consortium used by Ganigué et al. (2016) was mainly composed of *C. ljughdalii*, *C. carboxidivorans* and *C. kluyveri*, while He et al. (2018) enriched a microbial community dominated by species of *Acinetobacter*, *Alcaligenes*, *Rhodobacteraceae* and a low abundance of *Clostridium spp.* On the other hand, product concentrations and production rates achieved by He et al. (2018) were not higher than those reported in similar studies. This could be due to i) the use of a non-acclimated inoculum, ii) the use of CO (not syngas) as sole carbon and energy source and iii) CO provided (≤ 60 kPa CO) being insufficient. Regardless, this work demonstrated that up to C8 carboxylic acids can be produced from CO in one-pot cultivation.

Similar to ethanol production, the use of HfMBR has proven very promising for the production of carboxylic acids from syngas. Shen et al. (2018) demonstrated production of MCCAs from CO/H_2 for the first time in a HfMBR. Cultivation of the sludge-derived culture was studied at pH 6 under mesophilic (35 °C) and thermophilic (55 °C) conditions. In both scenarios, utilisation of CO and H_2 exceeded 95%. Mesophilic cultivation in sequential batch mode produced caproate (0.88 g L^{-1}) and up to 0.53 g L^{-1} caprylate, the highest caprylate concentration reported for a CO-fermenting system using mixed cultures. In contrast, thermophilic batch cultivation yielded a high acetate concentration (27.9 g L^{-1}) and product specificity (96.7%), with butyrate (< 1 g L^{-1}) as only elongated carboxylate. Microbial community analysis revealed that the mesophilic enrichment was abundant in *Clostridium spp.* (41.6%), while the thermophilic microbial community comprised a large proportion of close relatives to *Thermoanaerobacterium* (92.8%). Overall, the work of Shen et al. (2018) highlighted the great potential of HfMBR in syngas/CO fermentation processes and its functionality with open mixed cultures.

In a recent study, Chakraborty et al. (2019) applied a cycle of high and low pH cycle to produce MCCAs in a stirred-tank reactor using a CO-acclimatized sludge. CO was used as sole substrate. The system produced acetate (6.2 g L^{-1}), butyrate (1.2 g L^{-1}) and caproate (0.42 g L^{-1}) at pH 6.2, which were subsequently converted to ethanol (11.1 g L^{-1}), butanol (1.8 g L^{-1}) and hexanol (1.5 g L^{-1}) at pH 4.9. The concentrations of butanol and hexanol obtained in this study are the highest reported so far for mixed cultures growing on syngas. However, CO utilisation remained below 59%, very far from the high conversion efficiencies obtained in HfMBR systems (Shen et al., 2018; Zhang et al., 2013).

2.3 CO conversion by synthetic co-cultures

2.3.1 Synthetic co-cultures: a win-win

A fundamental principle of bioprocess design is that a microorganism should be selected that fits the right process, not the other way around (Straathof et al., 2019). Synthetic co-cultures offer the possibility to select and combine microbial strains harbouring the required pathways for a specific process without renouncing some of the benefits of mixed cultures, such as robustness or division of labour (Cui et al., 2020; Diender et al., 2021). Contrary to open mixed cultures, microbial species that contribute negatively to the consortium (e.g., by generating undesired by-products, "stealing" intermediates or hampering growth of other partners) can be left out of the consortia. This cultiva-

tion approach has a big potential in the field of syngas fermentation. By using synthetic co-cultures, metabolic networks can be constructed that yield a broader range of end-products compared to monocultures of acetogens. In addition, such networks can be translated into multi-compartment kinetic and genome-scale metabolic models, contributing to a further understanding of the microbial interactions and to optimization of the system (Benito-Vaquerizo et al., 2020; Foster et al., 2021; Li & Henson, 2019). Computational modelling can also be used to predict novel co-culture interactions (Li & Henson, 2021).

Yet what makes synthetic co-cultures stand out over other cultivation approaches is their unique feature: modularity (Diender et al., 2021). Microbial strains can be incorporated or removed from an established consortium to fit a different process. In principle, there is only one imperative when designing co-cultures for syngas fermentation: at least one of the partners must be able to grow on CO. The choice of the other partner(s) will largely determine the product spectrum of the co-culture. To date, synthetic co-cultures have been established to convert CO/syngas into a range of products including methane, carboxylic acids, higher alcohols and other added-value chemicals. The following sections relate such developments, which are summarised in Table 2.2.

2.3.2   Production of methane by synthetic co-cultures

Methane can be produced from syngas by mixed cultures, as discussed earlier (§ 2.2.3). A drawback of using these cultures is that competing pathways result in the production of side products such as acetate, propionate, ethanol or methanol, overall lowering methane specificities and production rates (Grimalt-Alemany et al., 2018b; Guiot et al., 2011). An alternative is to employ defined consortia that selectively combine efficient carboxydotrophic strains with CO-tolerant methanogens that can use the products of syngas fermentation at high rates. The conversion of CO to methane via H_2/CO_2 is preferred to the acetate route, as it results in higher conversion rates (Guiot et al., 2011). Several hydrogenogenic carboxydotrophs have been isolated (Diender et al., 2015); among them, the thermophile *Carboxydothermus hydrogenoformans* and the photosynthetic mesophile *Rhodospirillum rubrum* are well-studied and have been employed in synthetic co-cultures for syngas conversion to methane.

Klasson et al. (1990) established a methanogenic co-culture composed of *Rodhospirillum rubrum* and two methanogens, *Methanosarcina barkeri* and *Methanobacterium formicicum*. *R. rubrum* grows anaerobically on CO in the presence of light, producing H_2 and CO_2. The methanogens are both capable of H_2/CO_2 conversion to methane, with some differences. *M. formicicum* displays a high rate of H_2 uptake but is inhibited in the presence of CO. On the other hand, *M. barkeri* has higher tolerance to CO but converts H_2 at a lower rate. To compensate for each other's weaknesses, both methanogens were co-cultivated with *R. rubrum* to increase conversion of syngas to methane. The performance of the tri-culture was studied in two reactor configurations: a packed bubble column (PBC) and a TBR. Both reactors were operated under mesophilic conditions and included a light source to facilitate growth of *R. rubrum*. A 100% CO conversion was obtained in the TBE, while performance of the PBC was poorer, with a 79% CO conversion. Methane productivities reached 3.4 mmol·L$_{liquid}$$^{-1}$·h^{-1} and 0.4 mmol·L$_{liquid}$$^{-1}$·h^{-1} for the TBR and the PBC, respectively. These are inferior to those reported for biological processes developed in later studies (Asimakopoulos et al., 2021b; Grimalt-Alemany et al., 2018b). In addition, methane content in the outflow gas was

rather low, 18–32%. Nevertheless, the work of Klasson et al. (1990) demonstrated the functionality of synthetic co-cultures combining carboxydotrophic bacteria with methanogenic archaea for syngas biomethanation, establishing a precedent for later studies.

A more successful case is the thermophilic co-culture consisting of *Carboxydothermus hydrogenoformans* and the methanogen *Methanothermobacter thermoautotrophicus* (Diender et al., 2018). *C. hydrogenoformans* grows on CO producing H_2 and CO_2 as main products. *M. thermoautotrophicus* uses CO very poorly; however, it can tolerate its presence while growing on H_2/CO_2. Both strains grow optimally at around 65°C, with the advantage that such thermophilic conditions increase reaction kinetics and gas transfer rates (Guiot et al., 2011). Batch co-cultures of *C. hydrogenoformans* and *M. thermoautotrophicus* incubated at 65°C converted syngas to methane reasonably fast: 60 kPa CO were used in 24 h, while monocultures of the methanogen required 500 h to consume less CO. This suggests that removal of H_2/CO_2 by the methanogen favour thermodynamics of CO consumption by the carboxydotroph. Pressures up to 150 kPa CO could be used by the co-culture, which converted CO to CH_4 with $Y_{CH4/CO}$ close to theoretical values. In a CSTR, the co-culture of *C. hydrogenoformans* and M. thermoautotrophicus generated a headspace with methane peaks of 77% and a maximum production rate of 6 mmol·L_{liquid}^{-1}·h^1. This is significantly higher than rates reported for similar processes with biomass retention (Grimalt-Alemany et al., 2018b; Westman et al., 2016), but still lower than the highest rate obtained in TBRs by Asimakopoulos et al. (2021b). The genus *Carboxydocella* is another group of thermophilic bacteria comprising strains with a carboxydotrophic hydrogenogenic metabolism (Slepova et al., 2006; Sokolova, 2002). Kohlmayer et al. (2018) established a synthetic consortium of five microbial species: *Carboxydocella thermautotrophica*, *Carboxydocella sporoproducens* and three methanogens isolated from an anaerobic digester sludge (taxonomy of the archaea was not specified in the study). The co-culture was used to produce methane from syngas in thermophilic conditions. By including several strains with the same type of metabolism, functional redundancy and robustness were improve in the consortium. The two *Carboxydocella* strains can grow on CO, but *C. sporoproducens* exhibits slower growth compared to *C. thermautotrophica*. *C. sporoproducens*, though, can better withstand conditions of CO deprivation due to the formation of spores. On the other hand, methanogenesis was strengthened by the combined activity of three archaeal strains. In serum bottles, the mixed culture consumed 99% of the CO and 100% of the H_2 and produced an outflow gas with a 55% CH_4 content, which was 100% of the theoretical maximum for the used syngas. Interestingly, the co-culture proliferated well without added vitamins or yeast extract, suggesting that the five microbes might benefit each other from nutrient exchange (Kohlmayer et al., 2018). Despite this was a rather small-scale study, is showed the positive effect of functional redundancy in syngas-fermenting microbial communities and demonstrated the viability of a five-partner consortia, which is rather uncommon (Goers et al., 2014).

Table 2.2 Overview of syngas fermentation processes using synthetic co-cultures.

Microorganisms	Cultivation system	T (°C)	pH	Syngas composition (%)	Product titre or productivity	Ref.
Rhodospirillum rubrum, *Methanosarcina barkeri* and *Methanobacterium formicicum*	PBC	34	6.8 - 7.2	$CO/H_2/CO_2/Ar$ (55:20:10:15)	Methane 3.4 mmol L^{-1} h^{-1}	Klasson et al., 1990
Clostridium hydrogenoformans and *Methanothermobacter thermoautotrophicus*	CSTR	65	7.2	CO/H_2 (33:66)	Methane 6 mmol L^{-1} h^{-1}	Diender et al., 2018
Carboxydocella thermautotrophica, *Carboxydocella sporoproducens* and three methanogens	serum tubes	63	6.5	$CO/H_2/CO_2/CH_4$ (20:50:20:10)	Methane 0.72 mmol L^{-1} h^{-1}	Kohlmayer et al., 2018
Clostridium autoethanogenum and *Clostridium kluyveri*	serum bottles	37	6	CO/H_2	Butyrate 0.75 g L^{-1} day^{-1} Caproate 0.29 g L^{-1} day^{-1}	Diender et al., 2016b
C. autoethanogenum and *C. kluyveri*	CSTR	37	6.2	CO/H_2 (47:53)	Butyrate 1.1 g L^{-1}, 0.55 g L^{-1} day^{-1} Caproate 0.82 g L^{-1}, 0.41 g L^{-1} day^{-1}	Diender et al., 2019
Clostridium ljungdahlii and *C. kluyveri*	CSTR	37	6	$CO/H_2/CO_2$ (60:35:5)	Butyrate[a] 2.8 g L^{-1}, 2.7 g L^{-1} day^{-1} Caproate[a] 1.4 g L^{-1}, 1.3 g L^{-1} day^{-1} Hexanol[a] 4.7 g L^{-1}, 0.54 g L^{-1} day^{-1}	Richter et al., 2016a
C. ljungdahlii and *C. kluyveri*	CSTR	37	6.3	$CO/H_2/CO_2$ (60:35:5)	Octanol[b] 0.78 g L^{-1}, 2 mg L^{-1} day^{-1}	Richter et al., 2016a
Acetobacterium wieringae JM and *Anaerotignum neopropionicum*	serum bottles	30	7 - 7.2	$CO/CO_2/N_2$ (50:20:30)	Propionate 1.8 g L^{-1} Isovalerate 0.41 g L^{-1}	Moreira et al., 2021
Eubacterium limosum and *E. coli* GM	serum bottles	37	7	CO/N_2 (50:50)	3-HP 45.7 mg L^{-1} Itaconic acid 25.8 mg L^{-1}	Cha et al., 2021

PBC = packed bubble column; CSTR = continuous stirred tank reactor; GM = genetically modified; 3-HP = 3-hydroxypropionic acid. [a]Production rates are calculated as combined net rates in the reactor and in the gas stripping system. Butyrate and caproate concentrations refer to amounts dissolved in the reactor. Hexanol concentration refers to the condensate of the gas stripping system. [b]Octanol concentration and production rate refer to the condensate of the gas stripping system.

2.3.3 Production of carboxylic acids and alcohols by synthetic co-cultures

Synthetic co-cultures are promising systems for the production of MCCAs from syngas. Microbial MCCA production using monocultures of wild-type acetogens is challenging. A few acetogenic strains have been reported to produce C4 and C6 compounds from $CO/H_2/CO_2$, among them *C. carboxidivorans* (Phillips et al., 2015) and *E. limosum* (Chang et al., 2001), yet in rather low concentrations. A popular alternative is the co-cultivation of an acetogen with *C. kluyveri*, whose unique metabolism is based on the elongation of short-chain carboxylic acids with ethanol or other electron donors (Angenent et al., 2016; Spirito et al., 2014).

Diender et al. (2016b) established a synthetic co-culture of *C. kluyveri* and the well-known acetogen *C. autoethanogenum* that produced butyrate and caproate as end products from solely CO as carbon and energy source. In this system, *C. autoethanogenum* converts CO into acetate and ethanol, which are taken up by *C. kluyveri* to produce butyrate and caproate. Butanol and hexanol were also detected, resulting from the reduction of the respective carboxylates by *C. autoethanogenum*. Experiments showed that, while growth of *C. kluyveri* was inhibited in the presence of > 50 kPa CO in monocultures, it was sustained under a headspace of 130 kPa CO in co-cultivation with *C. autoethanogenum*. This co-culture illustrated how mutualistic interactions can be exploited to establish robust synthetic co-cultures. *C. autoethanogenum* produces the substrates for *C. kluyveri* (acetate and ethanol), at the same time that keeps dissolved CO levels low enough to allow growth of its partner. In addition, it was observed that ethanol production in monocultures of *C. autoethanogenum* would not have been sufficient to support growth of *C. kluyveri*. A follow-up study suggested that *C. kluyveri* enhanced solventogenic metabolism of *C. autoethanogenum* by removing ethanol from the environment (Diender et al., 2019). Gene transcription of the central metabolism of *C. autoethanogenum* did not change in co-culture compared to monoculture conditions, indicating that the metabolic shift in the presence of *C. kluyveri* was thermodynamically driven. This is in line with related studies supporting that acetogenesis/solventogenesis in gas-fermenting microorganisms is controlled at the thermodynamic level (Richter et al., 2016b; Valgepea et al., 2018). In continuous fermentation, the co-culture of *C. autoethanogenum* and *C. kluyveri* produced butyrate and caproate at rates of 0.55 g L^{-1} day^{-1} and 0.41 g L^{-1} day^{-1}, respectively. This work, established as proof-of-concept, was recently picked up by industry in a joint project of the corporations Evonik and Siemens, demonstrating the great potential of syngas-fermenting synthetic co-cultures in industry (Haas et al., 2018).

Richter and colleagues upgraded the synthetic co-culture approach of Diender et al. (2016b) with a continuous bioprocess that included cell-recycling and in-line product extraction (Richter et al., 2016a). The co-culture was established with *C. kluyveri* and *C. ljungdahlii*, a close relative of *C. autoethanogenum* with excellent ethanol productivities from syngas (Martin et al., 2016). Similar to the co-culture of Diender et al. (2016b), in this consortium *C. ljungdahlii* produced acetate and ethanol from syngas, which were used by *C. kluyveri* to produce longer-chain carboxylates via chain-elongation. In addition, at a narrow pH range of 5.7–6.4, the elongated carboxylates were reduced by *C. ljungdahlii* to their respective alcohols, n-butanol, n-hexanol and, for the first time in a syngas-fermenting system, n-octanol was detected (up to 0.78 g L^{-1} in the condensate of the gas stripping system) (Richter et al., 2016a). Operation of their bioreactor at values higher than 6.4 gradually reduced and eventually crashed the population of *C. ljungdahlii*, which requires

2

mildly acidic conditions to support growth. Without the acetogen, ethanol production halts and the co-culture crashes. On the other hand, mildly acidic conditions are detrimental to *C. kluyveri*, which grows in a pH range of 6–7.5 (Barker & Taha, 1942; Weimer & Stevenson, 2012). In addition, acidic pH values result in the accumulation of undissociated acids (pKa ~ 4.7), which are toxic to microorganisms (Kim & Rhee, 2013). This discrepancy between optimum pH for solventogenesis and acid production has been reported in similar studies (Diender et al., 2016b; Ganigué et al., 2016). As Richter and co-workers stated, there is a need to isolate chain-elongating microorganisms with an optimum pH of growth of 5–5.5, a more favourable environment for acetogens to produce ethanol (Richter et al., 2016a).

Alternatively, carboxydotrophic strains could be employed that can thrive at a pH range around neutrality. While the most prominent carboxydotrophic strains thrive in mildly acidic conditions (Martin et al., 2016), acetogens have been isolated with optimal pH values ranging from 5.4 to 9.8 (Bengelsdorf et al., 2018). An example is *Acetobacterium wieringae* strain JM, a novel carboxydotroph that grows optimally at pH 7 (Arantes et al., 2020). The authors of that study speculated that *A. wieringae* strain JM played a crucial role in syngas-enriched communities by providing substrate to ethanol-consuming propionibacteria, which grow optimally at neutral pH (Piwowarek et al., 2018). To test this hypothesis, Moreira et al. (2021) cultivated *A. wieringae* strain JM with *Anaerotignum neopropionicum*, a propionibacterium unique for its ability to grow on ethanol (Tholozan et al., 1992). The synthetic co-culture was capable of converting CO to propionate (1.78 g L^{-1}) via cross-feeding of ethanol at pH 7. In addition, isovalerate was detected in low amounts in the co-culture, while not in monocultures. Isovalerate could be produced by *A. neopropionicum* from amino acids; therefore, authors hypothesised that amino acid transfer took place between *A. wieringae* and *A. neopropionicum* in co-culture. Interestingly, proteomic analysis of the co-culture revealed sign of stress response in both strains, such as increased abundance of sporulation and antibiotic resistance proteins. It remains a question whether this would negatively affect the stability and functionality of the co-culture in the long-term or, on the contrary, the two populations would eventually come to a beneficial deal.

2.3.4 Production of other value-added chemicals by synthetic co-cultures

So far, this chapter has discussed various case studies of synthetic co-cultures and open mixed cultures employed in the conversion of syngas/CO to commodity chemicals such as methane, MCCAs and simple alcohols. The production of biochemicals of higher complexity by syngas-consuming cultures is still challenging, for example due to metabolic limitations of the microorganisms or to the requirement of different environmental conditions. A strategy that has been used to overcome this issue is the introduction of engineered strains of genetically accessible microorganisms.

The majority of studies on the use of synthetic co-cultures applied to syngas fermentation have relied on the abilities of wild-type microbial strains (Diender et al., 2016b; Diender et al., 2018; Kohlmayer et al., 2018; Lee et al., 2018; Richter et al., 2016a). Engineering of Clostridia strains to produce heterologous compounds has advanced rapidly in the last decade, but limitations remain and further understanding of molecular mechanisms is required (Charubin et al., 2018). Model microorganisms such as *Escherichia coli*, in contrast, have been widely engineered for the production of a vast range of biochemicals. If a suitable strategy is in place, such strains could be co-cul-

tivated with acetogens to facilitate the production of valuable biochemicals from syngas. Cha and co-workers (2021) followed this approach with two co-cultures of the acetogen *E. limosum* grown with two genetically-engineered *E. coli* strains. In both co-cultures, *E. limosum* converted CO into acetate, which was used as carbon source by *E. coli*. The two engineered strains of *E. coli* used acetate to produce 3-hydroxypropionic acid (3-HP) and itaconic acid (ITA), respectively. At the end of batch cultivations (72 hours), the co-cultures produced a maximum of 45.7 mg·L^{-1} 3-HP and 25.8 mg·L^{-1} ITA. Consumption of CO increased 10% in co-cultivation compared to monocultures of *E. limosum*, evidencing that the mutualistic interaction enhanced carbon flux. This study demonstrated for the first time the production of value-added chemicals (3-HP and ITA) from syngas using co-cultures. However, several issues need to be addressed, as noted by the authors. First, the concentration of CO dissolved had to be minimized to allow growth of *E. coli*, thus a condition of mass-transfer limitation was sought. This was initially achieved by inoculating *E. limosum* and *E. coli* at high ratios, up to 150:1 (based on OD$_{600}$). Over the course of cultivations, though, CO consumption rates and cell concentrations decreased, pointing to the need to improve process stability. Another major problem is that acetate assimilation by *E. coli* in anaerobic conditions requires the addition of an electron acceptor. Trimethylamine N-oxide (TMAO) was chosen since it yielded the highest acetate assimilation rate and it did not significantly affect CO conversion rates. The fact that TMAO should be supplied proportionally to the desired amount of product would significantly reduce co-culture efficiency and increase process costs, making it unfeasible to implement this strategy at industrial scale. Nevertheless, the work of Cha et al. (2021) is a first step towards modular pathway engineering of synthetic co-cultures to facilitate the production of high-value chemicals from syngas.

2.4   CO conversion via sequential processes

Sequential processes can also be used to produce value-added biochemicals from syngas. While these are not one-pot strategies, they may comply with the feature of modularity, characteristic of synthetic cultures. The greatest advantage of this approach compared to one-pot cultures is that it circumvents cultivation divergences between partners in a consortium, by growing each partner in a separate bioreactor (e.g., combinations aerobic/anaerobic, low/high pH or temperature, etc.). A few proof-of-concept studies have shown the potential of this strategy applied to the conversion of CO-rich gases. Hu et al. (2016) designed a two-stage process to produce microbial oil from syngas. In the first reactor (60 °C, pH 6), the acetogen *Moorella thermoacetica* converted CO/H$_2$/CO$_2$ to acetate. Acetate was then fed into the second reactor (28 °C, pH 7.3) for its aerobic conversion to C16-C18 triacylglycerides by an engineered strain of the yeast *Yarrowia lipolytica*. The integrated process produced 18 g L^{-1} lipids at a rate of 0.19 g L^{-1} h^{-1}. Acetate as intermediate was also used in the two-step process established by Oswald et al. (2016) to produce malic acid. In this case, *C. ljungdahlii* was first grown in a batch reactor converting syngas to acetate. Subsequently, the reactor was adapted for aerobic cultivation of *Aspergillus oryzae*, which was inoculated on top of the existing culture. Malic acid was produced to a maximum concentration of 2.02 g L^{-1}. However, the second-stage process was not reproducible in triplicate reactors. Recently, the production of biopolymers has also been demonstrated using sequential processes (Hwang et al., 2020, p. 2;

2

Lagoa-Costa et al., 2017). In one study, effluent from syngas fermentation by *C. autoethanogenum* (containing acetate, ethanol and 2,3-BDO) was fed in pulses into a second reactor for the production of polyhydroxyalkanoates (PHAs) (Lagoa-Costa et al., 2017). The second reactor contained an enriched mixed culture used in a previous process adapted to PHA production. Only acetate was consumed by the mixed culture, which accumulated a maximum of 24% PHA. Hwang et al. (2020) designed a two-stage process for polyhydroxybutyrate (PHB) production differing from the rest in that formate, instead of acetate, was used as intermediate. In the first stage, the acetogen *Acetobacterium woodii* was used for conversion of syngas under optimised conditions for ≈100% formate selectivity. The formate solution was concentrated and supplied in fed-batch mode into the second reactor, where formate was converted to PHB by genetically modified *Methylbacterium extorquens* AM1. All these studies require further improvements, mostly related to medium optimisation in the second reactor. Inadequate composition of ions and certain (toxic) components in the syngas fermentation effluent can have a detrimental effect on the non-acetogenic partner. Nonetheless, these works show that integrated bioprocesses are a feasible platform to convert gaseous substrates to biochemicals of added-value.

2.5 Challenges and opportunities of syngas-fermenting microbial communities

By discussing syngas fermentation by mixed cultures, it becomes clear that there are many challenges, but also many opportunities, for future developments in the field. Open-mixed cultures are very robust and resilient, offering good prospects for the production of methane and short-chain fatty acids, such as acetate and butyrate. The main challenge with open mixed cultures is product selectivity. A better understanding of microbial compositions and interactions, and the effect of varying process parameters, is necessary. Knowledge on complex microbial communities converting syngas may also source inspiration for the creation of synthetic co-cultures as recently exemplified by Moreira et al. (2021), where a co-culture producing propionate was constructed based on the microbial composition of an enriched culture. Compared to the enriched culture, the co-culture produced higher amounts of propionate, and side products (like methane) were eliminated. Open mixed-cultures and laboratory enrichments may also lead to the isolation of new microorganisms, carboxydotrophs or others, with better characteristics for the construction of synthetic co-cultures. For example, Richter et al. (2016a) observed suboptimal performance of a co-culture of *C. ljungdahlii* and *C. kluyveri* due to a mismatch in the optimal pH of the two species. Isolation of (ethanol-driven) chain-elongators with lower optimal pH for growth would be useful for pairing with solventogenic acetogens during syngas fermentation. Such microorganisms are currently not available in culture collections. Currently, there are also only a limited amount of thermophilic carboxydotrophs isolated, and most of them exhibit a hydrogenogenic metabolism. Studying high-temperature adapted microbiomes (e.g., thermophilic anaerobic sludges, hydrothermal vents, etc.) could lead to discovering novel microbes and metabolisms. Thermophilic organisms could be used to produce volatile compounds, allowing their separation in the gas-phase and reducing

streaming costs. Other environments, such as high salinity sediments, are also not well studied in regard to their potential to convert CO/syngas (Sorokin et al., 2020).

The first steps for co-cultivation of microbes for syngas fermentation are taken. Now, work can be done in two fronts: improvement of current co-cultures for the production of, e.g., MCFA and alcohols (higher titres, higher yields, higher carbon fixation, etc.) or the development of new co-cultures for the diversification of products. The improvement of co-culture systems can be aided by genome-based models (GEMs). These models describe the set of possible reactions by the microbes in the co-culture (based on their genomic content), including extracellular exchange of metabolites (Benito-Vaquerizo et al., 2020; Hanemaaijer et al., 2017; Li & Henson, 2021; Pacheco et al., 2019; Stolyar et al., 2007). The GEM constructed by Benito-Vaquerizo et al. (2020) describes growth of the syngas-converting co-culture comprising *C. autoethanogenum* and *C. kluyveri*, and predicts that succinate addition would improve the production of MCFAs. Experimental testing needs to be conducted to ascertain this, but this is an example of how GEMs can aid in the generation of hypothesis and eventually result in accelerated optimization of co-cultures. Computational models can also be used to predict novel microbial interactions. In a recent study, Li & Henson (2021) performed *in silico* simulations on 170 combinations of acetogen and butyrate-producing bacteria pairings. This led to the discovery of highly performing co-culture designs for syngas fermentation that could guide future experimental studies. Yet, reconstruction of GEMs, and especially their manual curation and experimental validation is still a time-consuming procedure, and applications of GEMs to co-cultivation are so far scarce (Gu et al., 2019).

Co-cultures are also suitable for the introduction of genetic engineered strains, e.g. to supress/overexpress the expression of certain genes (Wen et al., 2017), engineer symbiosis (Wen et al., 2014), create 'artificial' division of labour (Zhang et al., 2015), control populations of different strains (Liao et al., 2019). Regarding syngas fermentations, up to date only wild-type acetogens have been used to establish synthetic co-cultures but this could change soon with the recent developments on genetic engineering of autotrophic Clostridia strains able to convert CO (Humphreys & Minton, 2018; Joseph et al., 2018). Carboxydotrophy can also be engineered in solventogenic Clostridia, as shown by heterologous expression of a carbon monoxide dehydrogenase in *Clostridium acetobutylicum* (Carlson & Papoutsakis, 2017). The urge to produce high-value chemicals from syngas is also putting the focus on engineering pathways for the assimilation of one-carbon compounds (e.g., glycine pathway) in *E. coli* strains that can natively produce value-added chemicals (Gleizer et al., 2019; Kim et al., 2020).

2.6 Conclusions

Microbial communities have a tremendous potential in syngas fermentation processes, broadening the product spectrum beyond acetate and ethanol. Open mixed cultures are sustained by decades of research and industrial experience on the field of anaerobic digestion (of wastes/wastewaters), which can be transferred to the conversion of CO-rich gases to methane, MCCAs and alcohols. Synthetic co-cultures can enhance product selectivity, offer modularity and allow the use of kinetic and genome-scale metabolic models for further optimisation. Recently, genetically engineered strains of model organisms have been co-cultured with acetogens, enabling the production of added-value

chemicals from C1 substrates. Industrial implementation of syngas-fermenting microbial consortia for the production of valuable biochemicals is not yet a reality. However, growing interest on the utilization of C1-gases nurtured by major efforts undertaken over the last few years might certainly drive this platform forward faster than anticipated.

2.7   Acknowledgements

Upgrading dilute ethanol to odd-chain carboxylics acids by a synthetic co-culture of *Anaerotignum neopropionicum* and *Clostridium kluyveri*

———

Ivette Parera Olm & Diana Z. Sousa

Abstract

Dilute ethanol streams generated during fermentation of biomass or syngas can be used as feed-stocks for the production of higher-value products. In this study, we describe a novel synthetic microbial co-culture that can effectively upgrade dilute ethanol streams to odd-chain carboxylic acids (OCCAs), specifically valerate and heptanoate. The co-culture consists of two strict anaerobic microorganisms: *Anaerotignum neopropionicum*, a propionigenic bacterium that ferments ethanol, and *Clostridium kluyveri*, well-known for its chain-elongating metabolism. In this co-culture, *A. neopropionicum* grows on ethanol and CO_2 producing propionate and acetate, which are then utilised by *C. kluyveri* for chain elongation with ethanol as the electron donor. A co-culture of *A. neopropionicum* and *C. kluyveri* was established in serum bottles with 50 mM ethanol, leading to the production of valerate (5.4 ± 0.1 mM) as main product of ethanol-driven chain elongation. In a continuous bioreactor supplied with 3.1 g ethanol L^{-1} d^{-1}, the co-culture exhibited high ethanol conversion (96.6%) and produced 25% (mol/mol) valerate, with a steady-state concentration of 8.5 mM and a rate of 5.7 mmol L^{-1} d^{-1}. Additionally, up to 6.5 mM heptanoate was produced at a rate of 2.9 mmol L^{-1} d^{-1}. Batch experiments were also conducted to study the individual growth of the two strains on ethanol. *A. neopropionicum* showed the highest growth rate when cultured with 50 mM ethanol ($\mu_{max} = 0.103 \pm 0.003$ h^{-1}) and tolerated ethanol concentrations of up to 300 mM. Cultivation experiments with *C. kluyveri* showed that propionate and acetate were used simultaneously for chain elongation. However, growth on propionate alone (50 mM and 100 mM) led to a 1.8-fold reduction in growth rate compared to growth on acetate. Our results also revealed sub-optimal substrate use by *C. kluyveri* during odd-chain elongation, where excessive ethanol was oxidised to acetate. This study highlights the potential of synthetic co-cultivation in chain elongation processes to target the production of OCCAs. Furthermore, our findings shed light on to the metabolism of odd-chain elongation by *C. kluyveri*.

3.1   Introduction

Sustainable chemical production is a key factor in reducing our strong dependency on oil and in the mitigation of climate change (IEA, 2018; McGlade & Ekins, 2015). In the last century, numerous microbial processes have been developed and deployed for the production of biochemicals and biofuels (e.g., lactic acid fermentation, acetone-butanol-ethanol (ABE) fermentation), establishing the grounds for a biobased economy (Cherubini, 2010). Traditionally, these microbial processes rely on the fermentation of sugars, either from crops including corn or sugarcane, or from hydrolysed lignocellulosic biomass. While these are feedstocks available in high quantities, the former pose ethical concerns as they compete with food and feed applications. The latter, on the other hand, require costly pre-treatments and contain a significant fraction of recalcitrant lignin (15–25% of total dry matter). To circumvent these limitations, production platforms based on the use of non-conventional feedstocks (e.g., CO_2, glycerol, organic waste streams) are expected to become more prominent in the chemical industry (Blank et al., 2020; Kätelhön et al., 2019). In the last decade, significant advances have been made on the development of a C1-based biorefinery (Qiao et al., 2022). C1 feedstocks comprise formate, methanol, CO_2 and CO. A mixture of CO, H_2 and CO_2, known as synthesis gas (syngas), can be obtained via gasification of hydrocarbon resources, including organic wastes or lignocellulosic biomass (Liew et al., 2016). In addition, syngas-like streams are generated at energy-intensive industrial sites (e.g., steel mills) (De Ras et al., 2019), and syngas production by CO_2-water electrolysis using renewable energy is becoming increasingly feasible (Moreno-Gonzalez et al., 2021; Sunfire, 2020; Xue et al., 2022). Because syngas composition varies depending on the material and technology used for its generation, this feedstock is particularly suited for microbial fermentation, which is more tolerant than chemical conversion (i.e., Fischer-Tropsch) to varying $CO:H_2$ ratios and gas impurities (Bambal et al., 2014; Christensen et al., 2011; Xu et al., 2011).

Syngas can be metabolised by acetogens: strict anaerobic bacteria that use the Wood-Ljungdahl pathway for CO_2 fixation. Acetogens can use reducing equivalents from H_2, CO or other substrates, and produce acetate and ethanol as main products (Schuchmann & Müller, 2014). So far, syngas fermentation has been industrially deployed almost exclusively for the production of ethanol; yet, to maximise its value as sustainable production platform, it is essential to expand the array of products (Gavala et al., 2021; Köpke & Simpson, 2020). Since syngas fermentation effluent contains a mixture of ethanol and acetate, one logical approach for its upgrading is the integration with the chain-elongation platform. Chain elongation is the anaerobic process in which short-chain carboxylic acids (SCCAs; acetate, propionate, butyrate) are converted to medium-chain carboxylic acids (MCCAs; valerate, caproate) provided that an electron donor (e.g., ethanol, lactate) is supplied (Agler et al., 2012; Angenent et al., 2016; Spirito et al., 2014). This conversion is the result of the reverse beta-oxidation pathway, a cycle that elongates a carboxylic acid two carbons at a time by adding an acetyl-CoA derived from the electron donor. *Clostridium kluyveri* was the first isolated bacterium performing chain elongation, and since then it has been thoroughly characterised (Bornstein & Barker, 1948; Candry et al., 2018; Kenealy & Waselefsky, 1985; Seedorf et al., 2008). In recent years, several studies have demonstrated the feasibility of merging syngas fermentation with chain elongation for the production of MCCAs and higher alcohols (Baleeiro et al., 2019). One adopted strategy is the one-pot conversion of CO/syngas by open mixed cultures traditionally

used in anaerobic digestion, which can be enriched for chain-elongating microorganisms (Baleeiro et al., 2022; Baleeiro et al., 2023; Candry et al., 2020a; Chakraborty et al., 2019; Ganigué et al., 2016; He et al., 2018; Liu et al., 2014a; Shen et al., 2018). Despite their robustness and suitability for waste-fed processes, these cultures require rather long acclimation and fermentation times when applied to syngas fermentation, and the abundance of competing pathways (e.g., methanogenesis) compromises product selectivity. A popular alternative is the use of synthetic co-cultures of acetogens with *C. kluyveri* (Diender et al., 2016b; Diender et al., 2019; Fernández-Blanco et al., 2022; Richter et al., 2016a), which are based on CO scavenging by the acetogen and direct cross-feeding of ethanol and acetate. Two-stage processes, where syngas fermentation and chain elongation take place in separate bioreactors, have also been proposed (Gildemyn et al., 2017; Kucek et al., 2016; Richter et al., 2013; Vasudevan et al., 2014), with the advantage that the operational conditions can be optimised for each conversion.

Even-chain MCCAs have received the most attention as target products, largely because intermediates with even number of carbon (i.e., acetate, ethanol, butyrate) are more commonly found in syngas fermentation effluent and in acidogenic waste streams than odd-numbered carbon constituents (Moscoviz et al., 2018). Caproate (C6) and caprylate (C8) have attracted special interest due to their higher economic value and easiness to extract from the water broth compared to butyrate (C4). However, in order to avert market saturation, interest has grown in diversifying away from the caproate platform towards other products, such as branched carboxylates and odd-chain carboxylic acids (OCCAs) (de Leeuw et al., 2021; Stamatopoulou et al., 2020; Strik et al., 2022). In particular, OCCAs (e.g., valerate (C5) and heptanoate (C7)) are valuable building blocks with growing demand from the chemical and cosmetics industries (Agnihotri et al., 2022). To date, only a few studies have addressed the production of OCCAs in ethanol-based chain elongation systems; in these cases, the most common approach has been the supplementation of propionate in mixed cultures (Coma et al., 2016; Ganigué et al., 2019; Grootscholten et al., 2013; Roghair et al., 2018). In addition, the physiology of odd-chain elongation in *C. kluyveri* has been considerably less well-studied than the even-chain metabolism, with exception of early studies (Bornstein & Barker, 1948; Kenealy & Waselefsky, 1985) and a recent investigation by Candry and co-workers (Candry et al., 2020b).

In this work, we propose an alternative to mixed cultures to target the production of OCCAs via ethanol-based chain elongation: a synthetic co-culture of *C. kluyveri* with the propionigenic bacterium *Anaerotignum neopropionicum* (formerly, *Clostridium neopropionicum* (Ueki et al., 2017)). *A. neopropionicum* is among the few propionigenic bacteria described to date with the ability to ferment ethanol while fixing CO_2 (Benito-Vaquerizo et al., 2022b; Tholozan et al., 1992). Based on the physiology of the microorganisms, it is anticipated that a co-culture of *A. neopropionicum* with *C. kluyveri* supplied with ethanol and CO_2 will produce valerate and heptanoate, with propionate as intermediate. Acetate is produced in this system, therefore even-chain products are also expected. We established the *A. neopropionicum - C. kluyveri* co-culture in serum bottles and tested its productivity in an ethanol-fed chemostat bioreactor at increasing ethanol loading rates (ELRs). We also performed pure culture experiments in serum bottles to gain insight into the metabolism of ethanol fermentation in *A. neopropionicum* and the use of propionate during chain elongation

by *C. kluyveri*. Ultimately, our goal was to evaluate the feasibility of applying this co-culture to upgrade syngas fermentation effluent to OCCAs.

3.2   Materials and Methods

3.2.1   Microbial strains and cultivation medium

C. kluyveri DSM 555[T] and *A. neopropionicum* DSM 3847[T] were obtained from the German Collection of Microorganisms and Cell Cultures (Leibniz Institute DSMZ - German Collection of Microorganisms and Cell Cultures GmbH, Braunschweig, Germany). Both strains were cultivated anaerobically in medium containing (per litre): 0.9 g NH_4Cl, 0.8 KCl, 0.3 g NaCl, 0.2 g KH_2PO_4, 0.4 g K_2HPO_4, 0.2 g $MgSO_4$*7 H_2O, 0.04 g $CaCl_2$*2 H_2O, 3.0 g $NaHCO_3$, 0.5 g yeast extract, 10 mL trace element solution from DSMZ medium 318, 1 mL vitamin solution, 0.5 g L-cysteine-HCl as reducing agent and 0.5 mg resazurin as redox indicator. The vitamin solution contained (per litre): 0.5 g pyridoxine, 0.2 g thiamine, 0.2 g nicotinic acid, 0.1 g p-aminobenzoate, 0.1 g riboflavin, 0.1 g pantothenic acid, 0.1 g cobalamin, 0.05 g folic acid, 0.05 g thioctic acid and 0.02 g biotin. The pH was adjusted to 7. Anaerobic bottles of 120 mL contained 50 mL medium under a N_2/CO_2 headspace (80:20 v/v; 170 kPa). For culture maintenance, *C. kluyveri* was grown on 90 mM ethanol and 75 mM acetate, incubated statically at 37°C. *A. neopropionicum* was grown on 50 mM ethanol, statically at 30°C.

3.2.2   Batch experiments in serum bottles

A series of batch experiments were carried out in serum bottles and medium as described above. Ethanol, acetate and propionate were added in a concentration of 25−1000 mM depending on the experiment, as detailed in the Results section. The headspace of the bottles was filled with N_2/CO_2 (80:20 v/v; 170 kPa). Bottles were inoculated with 2 % (v/v) of exponentially-growing cultures of *C. kluyveri* and/or *A. neopropionicum*. For monoculture experiments of *C. kluyveri* with propionate in the medium, pre-cultures used for inoculation were transferred at least three times in medium containing propionate. Experiments with monocultures of *A. neopropionicum* and of *C. kluyveri* were incubated at 30°C and 37°C, respectively. Co-cultures of *A. neopropionicum* with *C. kluyveri* were incubated at 35°C. All bottle experiments were done in triplicates. Liquid samples (1 mL) were routinely taken for analyses of alcohols and carboxylic acids, cell density and pH. Gas samples (0.2 mL) were routinely taken for analysis of headspace composition (H_2, CO_2). For each experiment, cell dry weight (CDW), yields, carbon and electron balances were determined from an additional, equivalent set of bottles that was only sampled at the start and end of cultivation.

3.2.3   Bioreactor setup

An ethanol-limited chemostat experiment was carried out to test the performance of the co-culture of *A. neopropionicum* and *C. kluyveri* at increasing ethanol loading rates (ELRs). A 1.3 L bioreactor vessel (DASGIP® Bioblock, Eppendorf, Germany) with a working volume of 0.7 L was operated anaerobically in continuous mode. The composition of the medium was as described above, except that $NaHCO_3$ was omitted during continuous operation. The reactor was equipped with pH, redox and temperature sensors. The system was operated at 35°C and pH 7, the latter controlled by the

addition of 3 M KHCO$_3$. Agitation was set at 200 rpm. Mass flow controllers (Dasgip MX4/4, Eppendorf, Germany) regulated the inflow of gas (N$_2$ or N$_2$/CO$_2$), which was supplied aseptically via a 0.2 μm filter. Liquid samples were routinely taken for analyses of ethanol and carboxylic acids, cell density and CDW. Gas samples of the headspace were taken for determination of gas composition. Gas and liquid outflow rates were regularly measured during operation. Phase-contrast microscopy (Axio Scope A1, Zeiss) was used periodically to inspect the co-culture.

3.2.4   Bioreactor operation

The co-culture of *A. neopropionicum* – *C. kluyveri* was cultivated in a continuous stirred-tank reactor (CSTR) operated without interruption for 160 days. The experiment can be divided in seven phases, A–G, preceded by a brief batch phase; the operating conditions of each phase are detailed in Table 3.1.

Table 3.1 Operating conditions of the bioreactor.

Phase	Period (days)			ELR (g L^{-1} d^{-1}) [mmol L^{-1} d^{-1}]	HRT (h)	Ethanol inflow (mM)	Remark
Batch	0	-	2.1	-	-	-	-
A	2.1	-	3	1.7 [35]	36	51	Start continuous operation
B	3	-	17.8	1.7 [35]	36	51	Gas flowrate increased to 0.07 vvm
C	17.8	-	29.7	3.1 [64]	36	95	-
D	29.7	-	32.9	8.0 [171]	42	300	-
E.1	32.9	-	43.7	6.3 [122]	54	300	-
E.2	43.7	-	100.7	6.3 [122]	54	300	Technical issues[a]
F	100.7	-	155.7	6.7 [145]	54	319	Technical issues fixed and new medium tank
G	155.7	-	160	6.7 [145]	54	320	pH to 7.3

ELR: ethanol loading rate. HRT: hydraulic retention time. [a]The outflow line clogged on day 55. In addition, during this period ethanol was slowly being stripped out of the medium tank.

Start-up of the bioreactor was done as follows: the autoclaved reactor vessel, containing only mineral medium, trace elements and resazurin, was connected to the system and flushed with N$_2$ (5 L h^{-1}) for ~ 3 hours to establish anaerobic conditions. Next, the gas inflow was switched to N$_2$/CO$_2$ (80:20 v/v) and the flowrate adjusted to 1.8 L h^{-1} (0.04 vvm). The following supplements were then added aseptically to the medium from anaerobic, sterile stock solutions: yeast extract, vitamins, NaHCO$_3$ and L-cysteine-HCl, in the concentrations given above. 50 mM ethanol was supplemented as substrate. When the redox potential dropped below -300 mV, the bioreactor was inoculated with 40 mL (~ 6 % v/v) of exponentially-growing pure cultures of *A. neopropionicum* and *C. kluyveri*. The co-culture was grown in batch for 50 hours, when ethanol became depleted. At this point, the continuous operation was initiated. Fresh medium containing ethanol (initially, 50 mM) was supplied aseptically from a 20-L tank via a peristaltic pump (Masterflex, Germany). The medium

tank was flushed with N_2 aseptically thorough the whole operation to ensure anaerobic conditions. The hydraulic retention time (HRT) was initially set at 36 hours (dilution rate, D = 0.028 h^{-1}), resulting in an ELR of 1.7 g ethanol L^{-1} d^{-1} (phase A). Each subsequent phase was characterised by an increase of the ELR or by the adjustment of a reactor parameter. Modification of the ELR was done either by changing the medium inflow rate (and, thus, the HRT) or by increasing the ethanol concentration in the medium tank (Table 3.1).

3.2.5   Analytical techniques

Gaseous compounds (CO_2, H_2) were analysed in a gas chromatograph (Compact GC 4.0, Global Analyser Solutions, The Netherlands) equipped with two channels and a thermal conductivity detector. H_2 was detected using a Molsieve 5A column operated at 100°C and coupled to a Carboxen 1010 pre-column. Determination of CO_2 was done in a Rt-Q-BOND column operated at 60°C. In both channels, argon was used as carrier gas. Concentrations of soluble compounds, namely ethanol, propanol, lactate and C2-C7 carboxylic acids, were determined by high-performance liquid chromatography (HPLC; LC-2030C, Shimadzu, Japan). The apparatus was equipped with a Shodex SH1821 column operating at 55°C. 0.01 N H_2SO_4 was used as eluent and the flowrate set at 1 mL min^{-1}. Amounts detected in a concentration < 0.3 mM could not be accurately quantified and are considered traces. The Chromeleon™ data analysis software (Thermo Fisher Scientific), version 7.2.9, was used for both GC and HPLC peak integration and analysis.

Microbial growth was estimated based on the measurement of optical density at 600 nm (OD_{600}) using a spectrophotometer (UV-1800, Shimadzu, Japan). CDW was determined by gravimetric analysis: pellets from a known culture volume (~ 50 mL) were washed twice in deionised water, resuspended and transferred into pre-weighed aluminium trays. These were dried overnight at 103°C and weighed again the day after.

3.2.6   Calculations

Specific growth rates (μ, expressed in h^{-1}) in batch incubations were determined as the slope of the linear regression (three to five points; $R^2 \geq 0.99$) derived from the integrated mass balance of cells:

$$\ln\left(C_{X,t}\right) = \mu \cdot t + \ln(C_{X,t_0})$$

where C_X is the cell concentration as OD_{600} during the exponential phase (t_0 - t).
In batch experiments of *A. neopropionicum*, substrate (ethanol) uptake rates (q_S) and production rates of propionate (q_P) and acetate (q_A) (defined collectively as q-rates) were calculated from the respective integrated mass balances which, resolved in combination with the biomass mass balance, give:

$$N_S(t) - N_S(t_0) = \frac{q_S}{\mu} \cdot (N_X(t) - N_X(t_0))$$

$$N_P(t) - N_P(t_0) = \frac{q_P}{\mu} \cdot (N_X(t) - N_X(t_0))$$

$$N_A(t) - N_A(t_0) = \frac{q_A}{\mu} \cdot (N_X(t) - N_X(t_0))$$

where q-rates are calculated from the slope of the linear regression ($R^2 \geq 0.99$) with μ known (calculated as described in the lines above). N_S, N_P and N_A are measured amounts (mmol) of ethanol, propionate and acetate, respectively, during the exponential phase (t_0 - t). N_X (mg CDW) at corresponding time points were indirectly determined from OD_{600} values using the following relationship, that we determined experimentally for *A. neopropionicum* growing on ethanol:

$$CDW \left(mg\ L^{-1}\right) = \frac{(OD_{600} - 0.016)}{0.0032}$$

q-rates are given in mmol g CDW^{-1} h^{-1}.

In batch cultivations, biomass and product yields were calculated as follows:

$$Biomass\ yield\ (Y_X) = \frac{g\ CDW\ formed}{mol\ ethanol\ consumed}$$

$$Product\ yield\ (Y_i) = \frac{mol\ product\ i\ formed}{mol\ ethanol\ consumed}$$

Product specificity (mol/mol) and selectivity (mol e⁻ eq./mol e⁻ eq.) were calculated as follows:

$$Specificity\ of\ product\ i\ (\%) = \frac{mol\ product\ i\ formed}{mol\ total\ soluble\ products\ formed} \cdot 100$$

$$Selectivity\ of\ product\ i\ (\%) = \frac{mol\ electron\text{-}equivalents\ product\ i\ formed}{mol\ electron\text{-}equivalents\ ethanol\ consumed} \cdot 100$$

3.3   Results

First, we studied ethanol utilization by monocultures of *A. neopropionicum*, and odd-chain elongation by *C. kluyveri*. Next, a co-culture of *A. neopropionicum* and *C. kluyveri* was established in serum bottles, with ethanol and CO_2 as sole substrates. The performance of the co-culture was further tested in a continuous bioreactor at increasing ethanol loading rates (ELRs).

3.3.1   Effect of ethanol concentration on the growth and product profile of *A. neopropionicum*

Ethanol tolerance in *A. neopropionicum* was assessed by determining cell growth in serum bottles (batch growth) containing 25 - 1000 mM ethanol. Cell density and production profiles over time are presented in Suppl. material § 3.7: Fig. S3.1, Fig. S3.2. Specific growth rates (μ) obtained under the different ethanol concentrations are shown in Fig. 3.1.
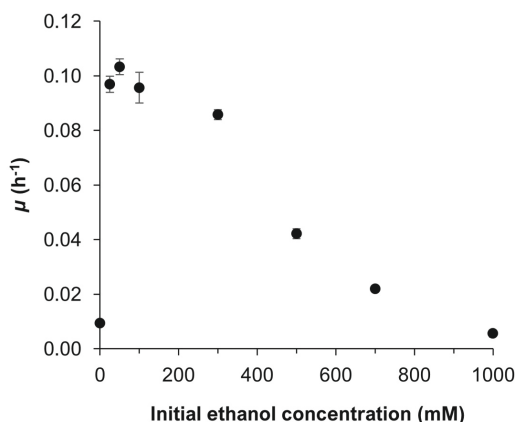
Figure 3.1 Effect of the ethanol concentration on the specific growth rate (μ) of *A. neopropionicum*. Growth rates were obtained from bottles incubated with ethanol (0, 25, 50, 100, 300, 500, 700 mM and 1 M) and CO_2 as substrates. Error bars indicate standard deviations of biological triplicates.

Growth of *A. neopropionicum* was most prominent with 50 mM ethanol, displaying a maximum specific growth rate (μ_{max}) of 0.103 $\pm$ 0.003 h^{-1} (doubling time (t_d) = 6.7 h) (Fig. 3.1). Slightly lower μ were obtained with ethanol concentrations of 25 mM (0.097 $\pm$ 0.003 h^{-1}; t_d = 7.2 h) and 100 mM (0.096 $\pm$ 0.006 h^{-1}; t_d = 7.2 h). Biomass formation was most prominent in this concentration range, with maximum cell densities of 59 $\pm$ 1 mg CDW L^{-1} (both with 50 mM and 100 mM ethanol) and 53 $\pm$ 1 mg CDW L^{-1} (with 25 mM ethanol). The μ declined to 0.086 $\pm$ 0.002 h^{-1} (t_d = 8.1 h) when the initial ethanol concentration was 300 mM; this titre is a threshold above which the growth rate of *A. neopropionicum* dropped sharply (Fig. 3.1). Cultivation in the absence of ethanol resulted in scarce biomass production (16 $\pm$ 2 mg CDW L^{-1}), likely deriving from the utilisation of L-cysteine and yeast extract present in the medium. No significant growth was observed in bottles containing 1 M ethanol.

Product concentrations in the different incubations are shown in Fig. 3.2. Propionate and acetate were the two main products of ethanol fermentation by A. neopropionicum, with minor products being propanol, butyrate and lactate. An initial concentration of 25 mM ethanol yielded the highest propionate:acetate ratio, 1.2 (mol/mol). In this condition, cultures produced 14.2 $\pm$ 0.1 mM propionate and 11.7 $\pm$ 0.2 mM acetate. Incubations with 50 mM and 100 mM ethanol led to similar amounts of propionate (compared to 25 mM ethanol), however acetate concentration doubled (to $\approx$ 21 mM). Higher initial ethanol concentrations ($\geq$ 300 mM) yielded similar production of propionate and acetate, but also promoted the accumulation of secondary products, namely propanol and lactate. Propanol specificity under 25 mM ethanol was 5 % (1.4 $\pm$ 0.1 mM), yet it reached 19 % ($\approx$ 8.5 mM) in the incubations containing 100–700 mM ethanol. Formation of propanol occurred mostly during the stationary phase of growth and, with substrate concentrations > 50 mM ethanol, it coincided with a slight consumption of propionate (Suppl. material § 3.7: Fig. S3.1). Lactate, on the other hand, was not detected with 25 mM initial ethanol, but it reached a specificity of 8 % (1.9 mM $\pm$ 0.2 mM) in the bottles containing 700 mM ethanol. When produced, butyrate concentra-

tions remained low (< 1 mM). It should be noted that ethanol was depleted only in the incubations with 25 mM ethanol (Suppl. material § 3.7: Fig. S3.1). Incomplete conversion in assays with higher initial ethanol concentrations could be due to limitation of CO2/bicarbonate, acidification of the environment (final pH was 6.0 - 6.2, which is suboptimal for A. neopropionicum (Tholozan et al., 1992)) or substrate toxicity. Indeed, a substrate concentration of 1 M ethanol had a detrimental effect not only on growth, as depicted in Fig. 3.1, but
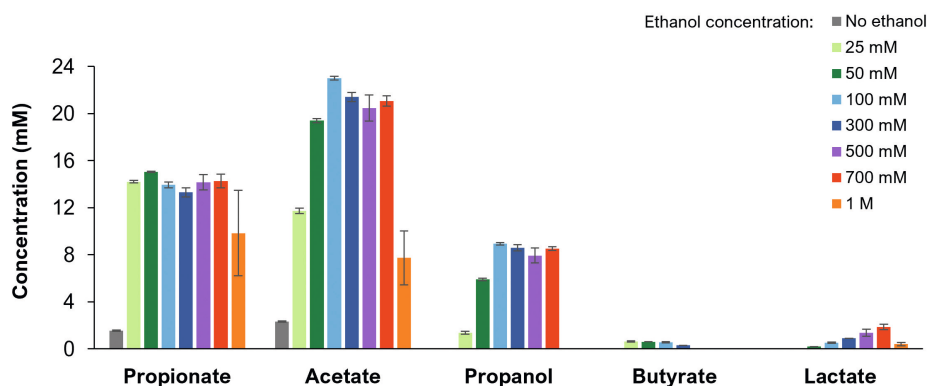
Figure 3.2 Product concentrations at the end of batch incubations of *A. neopropionicum* growing on ethanol (25 – 1000 mM) and CO_2 as substrates. Error bars indicate standard deviations of biological triplicates.

also on the productivity of the cultures (Fig. 3.2). To gain insight into the physiology of *A. neopropionicum*, we determined specific production/consumption rates (q) and product/biomass yields (Y) in the incubations containing 25 - 700 mM ethanol, which are summarised in Table 3.2. In all the incubations, propionate was formed at a faster rate than acetate and propionate yields were higher than acetate yields. The highest specific substrate uptake rate ($q_{S,max}$) was obtained with 100 mM ethanol (64.9 ± 0.2 mmol ethanol g CDW^{-1} h^{-1}). The specific production rates of propionate (q_P) and acetate (q_A) were the highest with 50 mM and 100 mM ethanol (no difference observed within the two conditions). Production rates were slightly lower in the incubations containing 25 and 300 mM ethanol for both propionate and acetate. An initial ethanol concentration of 500 mM or higher had a strong detrimental effect on both production rates.

Biomass and propionate yields (Y_X and Y_P, respectively) were higher with lower initial ethanol concentrations. Thus, the highest Y_X (1.91 ± 0.05 g CDW mol $ethanol^{-1}$) and Y_P (1.21 ± 0.03 mol propionate mol $ethanol^{-1}$) were obtained in the bottles containing 25 mM ethanol. Interestingly, the acetate yield (Y_A) was rather constant across the assays containing 25 to 100 mM ethanol (0.34 - 0.38 mol acetate mol $ethanol^{-1}$). Higher ethanol concentrations led to higher yields of propanol and lactate; from 25 mM to 100 mM initial ethanol, the propanol yield (Y_{PL}) increased from 0.1 to 0.7 (Table 3.2), and that of lactate from 0 to 0.96. In summary, increasing ethanol concentrations led to a reallocation of the substrate from biomass and propionate towards secondary products propanol and lactate.

T able 3.2 q-rates and yields in batch incubations of *A. neopropionicum* growing on ethanol.

Ethanol (mM)	q-rates (mmol i g_{CDW}^{-1} h^{-1})		Biomass yield (g_{CDW} mol ethanol^{-1})		Product yield (mol i mol ethanol^{-1})		
	q_S	q_P	q_A	Y_X	Y_P	Y_A	Y_{PL}
25	42.0 ± 0.6	21.1 ± 0.5	13.9 ± 0.2	1.91 ± 0.05	1.21 ± 0.03	0.38 ± 0.02	0.10 ± 0.01
50	53.0 ± 2.5	23.5 ± 0.8	14.4 ± 0.5	1.27 ± 0.03	0.78 ± 0.01	0.38 ± 0.00	0.40 ± 0.01
100	64.9 ± 0.2	23.7 ± 0.1	13.9 ± 0.1	0.93 ± 0.02	0.60 ± 0.01	0.34 ± 0.00	0.65 ± 0.01
300	ND	18.8 ± 0.8	9.6 ± 0.4	ND	ND	ND	ND
500	ND	10.4 ± 0.8	6.3 ± 0.6	ND	ND	ND	ND
700	ND	8.4 ± 0.5	4.5 ± 0.4	ND	ND	ND	ND

S: substrate (ethanol); P: propionate; A: acetate; X: biomass. PL: propanol. ND: not determined; ethanol partly evaporated in incubations containing ≥ 300 mM ethanol, therefore ethanol consumption could not be reliably quantified in those bottles, and the related parameters could not be calculated.

3.3.2 Comparison of propionate and acetate as electron acceptors during ethanol-driven chain elongation by *C. kluyveri*

Here, we studied the effect of the electron acceptor, acetate or propionate, on the cell growth and product spectrum of *C. kluyveri* during ethanol-based chain elongation. Five conditions were tested in serum bottles (batch). In three of them, the ethanol:carboxylic acid ratio (E/CA; mol/mol) was fixed at 1.2, which corresponds to the theoretical stoichiometry of chain elongation for optimal substrate use (Seedorf et al., 2008). These tests were performed with ethanol (120 mM) and either acetate (100 mM), propionate (100 mM) or both SCCAs (50 mM each) present. To assess the effect of the SCCA concentration, two additional sets were established with ethanol (120 mM) and either acetate or propionate at 50 mM (E/CA = 2.4). Table 3.3 summarises the growth-related parameters obtained in the five conditions tested. Production profiles of all incubations can be found in Suppl. material § 3.7: Fig. S3.3.

Table 3.3 Growth-related parameters of *C. kluyveri* batch growth with ethanol (120 mM) plus the indicated SCCA.

| Electron acceptor (E/CA)	Lag phase (h)	μ (h^{-1})	Y_X (g_{CDW} mol ethanol^{-1})
Acetate 100 Mm (1.2)	17[a]	0.122 ± 0.003	0.59 ± 0.03
Acetate 50 mM (2.4)	17[a]	0.112 ± 0.005	0.83 ± 0.09
Acetate 50 mM + Propionate 50 mM (1.2)	17[a]	0.109 ± 0.007	0.75 ± 0.10
Propionate 100 mM (1.2)	66	0.071 ± 0.002	0.24 ± 0.03
Propionate 50 mM (2.4)	60	0.065 ± 0.006	0.33 ± 0.06

E/CA: ethanol:carboxylic acid ratio (mol/mol). [a]The first sample was taken after 17h, when cells were already exponentially growing (Suppl. material § 3.7: Fig. S3.4). Therefore, the lag phase in these cultures was likely to be < 17h.

Ethanol was depleted in all incubations except for in the bottles with 50 mM propionate, where ~13 mM ethanol remained (Suppl. material § 3.7: Fig. S3.3). The presence of one or another SCCA had a strong impact on the lag phase of the cultures. In all the incubations with acetate, the lag phase was ≤ 17 hours (17 h corresponds to first sampling point after t_0, and at this point cells were already growing exponentially (Suppl. material § 3.7: Fig. S3.4)). In contrast, when cultures were initiated with only propionate (50 mM and 100 mM), the lag phases were 60 h and 66 h, respectively. The presence of acetate or propionate also influenced the growth rate of *C. kluyveri*. Incubations containing 100 mM and 50 mM acetate showed the fastest growth with a μ of 0.122 ± 0.003 h^{-1} ($t_d = 5.7$ hours) and 0.112 ± 0.005 ($t_d = 6.2$ hours), respectively. Growth rates decreased approximately 1.8 times with propionate as sole electron acceptor, with no difference observed within the two propionate concentrations tested (Table 3.3). However, when acetate was supplied next to propionate in equimolar amounts, the growth rate was similar to the cultures containing only acetate. Biomass formation also differed depending on the electron acceptor supplied. Incubations supplied with acetate as sole electron acceptor produced approximately three times more biomass per mol of ethanol consumed than those with only propionate (Table 3.3). In both cases, a higher E/CA ratio of 2.4 resulted in a higher Y_X (1.4-fold increment for both acetate and propionate incubations, compared to an E/CA of 1.2). With acetate only, maximum cell densities were 62 ± 5 mg CDW L^{-1} (100 mM acetate, E/CA = 1.2) and 90 ± 7 mg CDW L^{-1} (50 mM acetate, E/CA = 2.4). Significantly lower cell densities were obtained with only propionate, i.e. 26 ± 3 mg CDW L^{-1} (100 mM propionate, E/CA = 1.2) and 35 ± 4 mg CDW L^{-1} (50 mM propionate, E/CA = 2.4). However, similar to what was observed with the growth rates, when both electron acceptors were present (50 mM each, E/CA = 1.2), biomass production (79 ± 10 mg CDW L^{-1}) was identical to tests with acetate only.

Product specificities (%) at the end of batch cultivations are depicted in Fig. 3.3. As expected, *C. kluyveri* produced only even-chain MCCAs when acetate was the only electron acceptor. With an E/CA ratio of 1.2 (100 mM acetate), butyrate specificity was 55 % (33.8 ± 1.5 mM) and that of caproate, 45 % (27.3 ± 1 mM). Caproate became more abundant with an E/CA ratio of 2.4 (50 mM acetate), reaching a specificity of 73 % (40.6 ± 4.8 mM). Incubations with propionate resulted in the production of valerate as dominant product. With an E/CA of 1.2 (100 mM propionate), valerate specificity was 51 % (54.9 ± 1 mM), and heptanoate represented 7 % of the products (7.4 ± 0.4 mM). Even-chain carboxylic acids (acetate, butyrate and caproate) were also produced; in total, these accounted for 27 % of the products. Propanol was also present (15 %; 15.8 ± 0.4 mM), contributing to an overall odd-chain specificity of 73 % (OCCAs: 58 %). Similar to what was observed in acetate incubations, increasing the E/CA ratio to 2.4 (50 mM propionate) favoured the production of the longer-chain carboxylates, specifically heptanoate (17 %, 14 ± 1 mM) and caproate (17 %, 13.9 ± 1.2 mM) at the expense of their respective precursors (valerate and butyrate). Yet, valerate was the dominant carboxylic acid (40 %, 33.2 ± 2.6 mM). Overall, the specificity of odd-chain products was 70 % (OCCAs: 57 %).

When both propionate and acetate were supplied (50 mM each, E/CA = 1.2), C. kluyveri produced a mixture of odd- and even-chain products. Propionate and acetate were used simultaneously (Suppl. material § 3.7: Fig. S3.3c). The most abundant product was valerate, with a specificity of 42 % (30.4 ± 0.7 mM); however, butyrate and caproate together accounted for a higher proportion

(37.3 mM in total, 51 %). This condition yielded the lowest amount of heptanoate (1.3 ± 0.1 mM, 2 %). There was no difference in H_2 production (~ 50 kPa) across all the conditions tested.
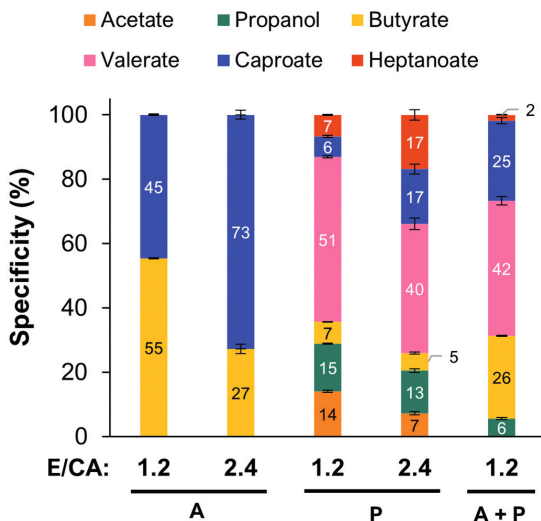
Figure 3.3 Product specificities at the end of batch incubations of *C. kluyveri* grown on ethanol (120 mM) plus the indicated SCCA(s). E/CA: ethanol:carboxylic acid ratio (mol/mol). A: acetate; P: propionate. Error bars indicate standard deviations of biological triplicates.

3.3.3   Synthetic co-culture of *A. neopropionicum* and *C. kluyveri* producing odd- and even-chain MCCAs from ethanol and CO_2

The synthetic co-culture of *A. neopropionicum* and *C. kluyveri* was established with ethanol and CO_2 as sole substrates. A scheme of the co-culture depicting the main conversions and metabolites involved is displayed in Fig. 3.4.
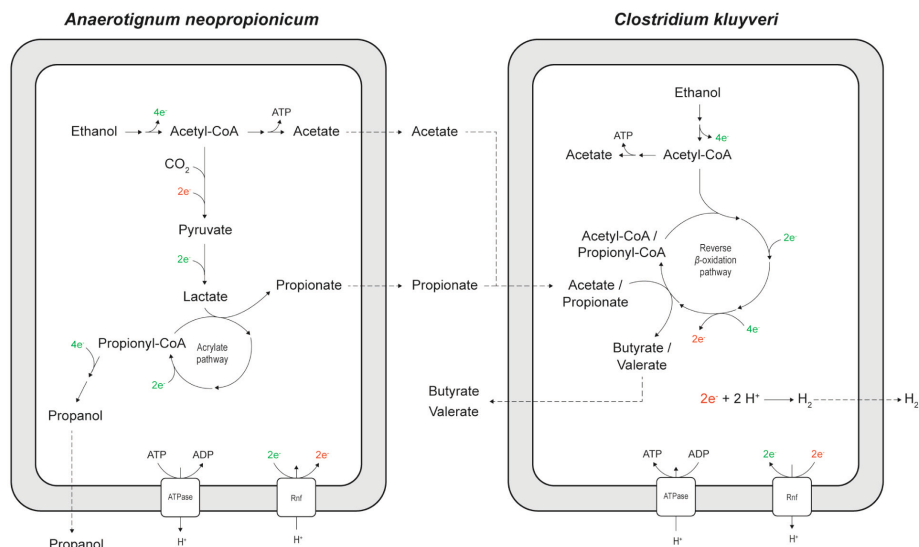
Figure 3.4 Schematic representation of the *A. neopropionicum – C. kluyveri* co-culture. Stoichiometry of the reactions and ATP yield are not shown. Dashed lines indicate metabolite transport or diffusion across the cell. Reducing equivalents in green and in red indicate NADH/NAD(P)H and reduced ferredoxin, respectively. Rnf: ferredoxin:NAD$^+$ oxidoreductase complex.

The co-culture was initiated with 50 mM ethanol. Fig. 3.5 shows substrate consumption and production profile over time. At day 5 of incubation, the co-culture had produced 5.4 ± 0.1 mM valerate, 4.0 ± 0.1 mM butyrate, 1.6 ± 0.1 mM caproate and trace amounts of heptanoate (< 0.5 mM). Ethanol was used by both species, although not simultaneously; two phases could be distinguished in ethanol consumption that are linked to growth of the two microorganisms, as described hereafter. In the first phase, lasting about 55 h, most of the ethanol was consumed (~ 32 mM), and propionate and acetate were produced simultaneously. The almost equimolar amounts of propionate and acetate formed fit with the stoichiometry observed in pure cultures of *A. neopropionicum* (Suppl. material § 3.7: Fig. S3.1b). During this phase no H_2 was produced, an indication that *C. kluyveri* was not yet active. Low amounts of propanol and butyrate (≤ 2 mM) were detected, which could also have been produced by *A. neopropionicum* as this was also observed in pure culture tests (Fig. 3.2). In the second phase (55 h onwards), the remaining ethanol (~ 17 mM) was used for chain elongation by *C. kluyveri*. Acetate and propionate were consumed simultaneously, following the same pattern observed in pure culture incubations of *C. kluyveri* (Suppl. material § 3.7: Fig. S3.3c). The apparent lower consumption of acetate compared to propionate can be explained by endogenous acetogenesis by this strain (1/6th of ethanol, according to theoretical stoichiometry (Seedorf et al., 2008)). Due to limited availability of ethanol in this second phase, only a fraction of the SCCAs was consumed, thus ~ 12 mM propionate and ~ 14 mM acetate remained unused. In this period, H_2 was produced concomitantly with the chain- elongated products to a final partial pressure of 5.5 kPa.Clearly, growth of *A. neopropionicum* was dominant in the co-culture; most of the ethanol was consumed in the first 55 h of incubation by this species (Fig. 3.5). Despite this resulting in acetate and propionate as main final products of the co-culture, and not MCCAs, this experiment

demonstrated the feasibility of C4–C7 carboxylates production by the *A. neopropionicum - C. kluyveri* co-culture from solely ethanol and CO_2 as substrates. Incubation in batch presented two main limitations: i) limited availability of ethanol for chain elongation due to faster consumption by *A. neopropionicum,* and ii) limited buffering capacity (pH at the end of cultivations was 5.9), which could have played an unfavourable role on the growth of both strains. Thus, the co-culture was further on studied in a pH-controlled bioreactor system with continuous ethanol supply.
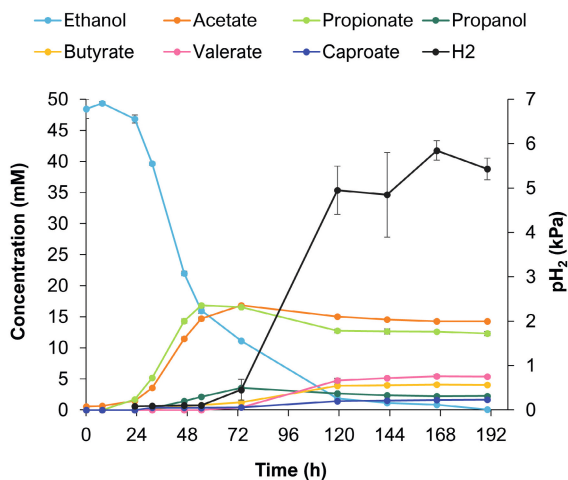
Figure 3.5 Ethanol and product profiles of the *A. neopropionicum - C. kluyveri* co-culture in serum bottles, with ethanol (50 mM) and CO_2 (not shown) as substrates. Error bars indicate standard deviations of biological triplicates.

3.3.4 Continuous production of C4 - C7 carboxylates from ethanol and CO_2 by the *A. neopropionicum - C. kluyveri* co-culture in a chemostat bioreactor

The productivity of the *A. neopropionicum - C. kluyveri* co-culture was tested in a CSTR under a continuous flow of N_2/CO_2 and at increasing ethanol loading rates (ELRs). The bioreactor was operated at 35°C and the pH maintained at 7. Ethanol concentration in the inflow varied from 50 - 300 mM (Table 3.1) to simulate the range of ethanol concentrations in syngas fermentation effluent (Abubackar et al., 2019; Arslan et al., 2019). Microscopic inspection of the culture at different time points during the run confirmed the presence of the two strains and the absence of contamination.
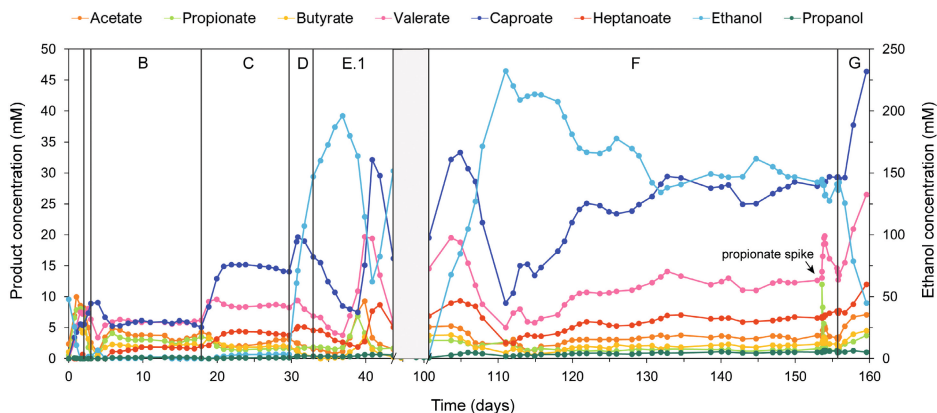
Figure 3.6 Product concentrations (left axis) during continuous fermentation of ethanol (right axis) by the *A. neopropionicum - C. kluyveri* co-culture. The relevant phases B - E.1, F and G are indicated. The shaded area corresponds to a phase (E.2) where several technical issues occurred and is therefore disregarded. The arrow points to the moment we spiked the system with 10 mM propionate.

The bioreactor was started in batch for about two days, after which continuous operation was initiated with an ELR of 1.7 g ethanol L^{-1} d^{-1} and 50 mM ethanol in the inflow (phase A). On day 3, the gas flowrate was increased to 3 L h^{-1} (0.07 vvm; phase B). A steady-state was reached during this phase, with the production of C4–C7 carboxylates (Fig. 3.6). This demonstrated that chain elongation activity by *C. kluyveri* was sustained by cross-feeding of SCCAs (i.e., acetate and propionate) produced by *A. neopropionicum*. Ethanol consumption during phase B was high (99.3 %), indicative that the system was ethanol-limited. Production of C4–C7 carboxylates in this steady-state and subsequent ones is summarised in Table 3.4. Valerate and caproate were equally abundant in phase B, each representing a quarter of the products and with steady-state concentrations of 5.9 ± 0.2 mM and 5.8 ± 0.3 mM, respectively. Their observed production rates were also similar (~ 4 mmol L^{-1} d^{-1}). Heptanoate was also produced, yet at the lowest rate of all the carboxylic acids (1.2 ± 0.1 mmol L^{-1} d^{-1}). As indicated by the product selectivity, most electrons from the substrate (ethanol) ended up in caproate (30.4 ± 1.8 %) and valerate (25.2 ± 0.7 %). Overall, an equal proportion of odd- and even-chain MCCAs were produced during phase B, as indicated by their respective specificities (34.0 ± 1.2 % and 34.9 ± 2.6 %).

To boost chain elongation activity, the concentration of ethanol in the inflow was doubled (95 mM), resulting in an ELR of 3.1 g ethanol L^{-1} d^{-1} (phase C). A new steady-state was reached (Fig. 3.6), in which ethanol consumption remained high (96.6 %) and the biomass density increased from 75 ± 13 mg CDW L^{-1} (O_{600} ~ 0.4) to 106 ± 15 mg CDW L^{-1} (OD_{600} ~ 0.6) (Suppl. material § 3.7: Fig. S3.5). Compared to phase B, steady-state concentrations of caproate and heptanoate more than doubled, and caproate productivity (9.9 ± 0.3 mmol L^{-1} d^{-1}) surpassed valerate productivity (5.7 ± 0.1 mmol L^{-1} d^{-1}) (Table 3.4). The concentration of valerate also increased, while that of butyrate was practically unchanged. The selectivity of the C6 (42.7 ± 1.2 %) and C7 (14.2 ± 0.8 %) carboxylates increased with respect to phase B, indicating a higher allocation of electrons from

ethanol being used for chain elongation. The most abundant product during phase C, based on specificity, was caproate (43.3 ± 1.4 %), followed by valerate (24.8 ± 0.2 %) and heptanoate (12.2 ± 0.7 %). Compared to the previous phase, the specificity of even-chain products (C4+C6) increased to 48.9 ± 1.3 %, a 29 % increment, while that of OCCAs (C5+C7) rose to 37.0 ± 0.7 %, a much lower 8 % increment.

Table 3.4 Averaged production values of C4 - C7 carboxylates in the three steady states (in phases B, C and F) of the bioreactor cultivation.

Steady-state parameter	Phase	ELR (g L⁻¹ d⁻¹)	HRT (h)	Carboxylic acids			
				Butyrate	Valerate	Caproate	Heptanoate
Concentration (mM)	B	1.7	36	2.1±0.2	5.9±0.2	5.8±0.3	1.7±0.2
	C	3.1	36	1.9±0.1	8.5±0.2	14.8±0.5	4.1±0.2
	F	6.7	54	2.1±0.2	12.5±0.8	27.6±1.3	6.5±0.3
Observed prod. rate (mmol L⁻¹ d⁻¹)	B	1.7	36	1.4±0.1	4.0±0.1	3.9±0.2	1.2±0.1
	C	3.1	36	1.3±0.1	5.7±0.1	9.9±0.3	2.8±0.1
	F	6.7	54	0.9±0.1	5.5±0.4	12.2±0.6	2.9±0.1
% Specificity (mol$_i$/mol$_{total\ products}$)	B	1.7	36	9.2±1.1	26.3±0.9	25.8±1.9	7.6±0.8
	C	3.1	36	5.6±0.3	24.8±0.2	43.3±1.4	12.2±0.7
	F	6.7	54	3.4±0.4	20.9±0.6	46.3±0.5	10.9±0.2
% Selectivity (e-mol$_i$/e-mol$_{eth.\ consumed}$)	B	1.7	36	6.7±0.5	25.2±0.7	30.4±1.8	10.7±1.2
	C	3.1	36	3.5±0.2	19.9±0.4	42.7±1.2	14.2±0.8
	F	6.7	54	2.0±0.2	15.7±0.7	42.8±1.5	11.9±0.4

To test the robustness of the co-culture, on day 30, the ELR was set to 8.0 g ethanol L⁻¹ d⁻¹ by increasing the ethanol concentration in the inflow to 300 mM and the HRT to 42 h (phase D). Cell density declined sharply in the following days (Suppl. material § 3.7: Fig. S3.5) and ethanol accumulated up to 147 mM (Fig. 3.6). In an attempt to recover the system, on day 34 the HRT was extended to 54 h, resulting in an ELR of 6.3 g ethanol L⁻¹ d⁻¹ (phase E.1). A few days later, the culture recovered its chain-elongating activity, as denoted by an increase of the concentration of C4 - C7 carboxylic acids, peaking around day 40 (caproate: 32.1 mM; valerate: 19.7 mM; heptanoate: 8.7 mM). Cell density also peaked, at an OD$_{600}$ of 1.2 (Suppl. material § 3.7: Fig. S3.5). However, perhaps due to the fast accumulation of MCCAs, the co-culture performance declined around day 41: at this point, ethanol accumulated and cell density declined sharply, reaching an OD$_{600}$ of ~ 0.5 on day 44. Unfortunately, technical issues occurred in the following weeks (phase E.2): first, on day 55 the outflow line clogged. Second, ethanol in the medium tank (that was placed at room temperature and continuously flushed with N$_2$) was slowly being stripped out. The latter technical fault went undetected for several weeks. These issues altered the culture behaviour and made it not possible to rely on the obtained data. For this reason, phase E.2 is disregarded (shaded area in Fig. 3.6 and in Suppl. material § 3.7: Fig. S3.5). Subsequently, a condenser was connected to the medium tank, which prevented further ethanol loss via gas stripping.

The system was properly functioning again on day 100 at an ELR of 6.7 g ethanol L^1 d^{-1} (phase F), with an ethanol concentration in the inflow of 319 mM. Likely, the higher ethanol loading rate and inflow concentration slowed down growth of both strains - particularly *A. neopropionicum* as seen in pure culture (Fig. 3.1) -, resulting in a rather long acclimation time ($\approx$ 30 days) before the culture stabilised. Initially, ethanol accumulated, reaching 232 mM, accompanied by a biomass drop (from OD_{600} 0.8 to 0.3) and a decline in MCCAs concentrations (Fig. 3.6). However, chain elongation activity recovered on day 111 and, around day 131, the system reached the third steady-state, in phase F. Ethanol consumption during this period was 54.1 %, about half compared to –phases B and C. Nevertheless, MCCA production increased, with the concentrations of valerate (12.5 ± 0.8 mM, 21 %), caproate (27.6 ± 1.3 mM, 47 %) and heptanoate (6.5 ± 0.3 mM, 11 %) being the highest of the three steady-states. Propanol, which can be produced by both strains, became significantly more abundant in this phase, reaching a specificity of 8.4 ± 0.5 % (5.0 ± 0.4 mM), in contrast to $\approx$ 2 % in –phases B and C. Lactate was also detected in this phase ($\sim$ 0.8 mM). The specificity of OCCAs (C5 + C7) in phase F, 31.8 ± 0.7 %, was the lowest of the three periods, while that of even-chain products (C4 + C6), 49.7 ± 0.5 %, was the highest.

   Acetate and propionate concentrations were rather low in phase F (< 4 mM). To test whether shortage of intermediates was limiting chain elongation activity, on day 153 we spiked the system with 10 mM propionate. In the hours following the spike, valerate concentration quickly rose to 19.8 mM before returning to the pre-spike level (Fig. 3.6). This observation led us to increase the pH set point from 7 to 7.3 (phase G), optimum for *A. neopropionicum* (Tholozan et al., 1992) and also favourable to decrease toxicity by accumulation of acids. This change immediately triggered ethanol consumption and a significant increase of the concentration of all carboxylic acids. The bioreactor system had to be shut down shortly after due to logistical reasons, just before the highest concentrations of caproate (46.4 mM), valerate (26.5 mM) and heptanoate (12.0 mM) were recorded.

3.4   Discussion

In this work, we showed that a mixture of C5 - C7 MCCAs can be produced from solely ethanol and CO_2 using a microbial co-cultivation approach. The designed system combines the propionigenic bacterium *A. neopropionicum*, which grows on ethanol producing propionate and acetate, and the chain-elongating microorganism *C. kluyveri* that uses the produced short-chain carboxylates as acceptor molecules for chain elongation (Fig. 3.4). Despite the fact that both strains use ethanol as substrate, during continuous cultivation they established an interaction based on cross-feeding of SCCAs, which allowed the co-culture to sustain over time (Fig. 3.6). We envision that this co-culture could be applied to upgrade dilute ethanol from syngas fermentation effluent to odd-numbered carbon MCCAs.

3.4.1   Effect of ethanol concentration on the co-culture viability

We first investigated ethanol tolerance of *A. neopropionicum*. Syngas fermentation systems yield ethanol titres ranging 0.1 – 0.4 M (5 - 20 g L^{-1}) (Abubackar et al., 2019; Arslan et al., 2019), with the highest reported concentration being 1 M (48 g L^{-1}) (Phillips et al., 1993). Microbial strains used for upgrading of syngas fermentation effluent should tolerate and use ethanol in this range

of concentrations. Ethanol is known for its adverse effects to microorganisms (Cao et al., 2017). While ethanol tolerance of *C. kluyveri* has been extensively investigated (Bornstein & Barker, 1948; Weimer & Stevenson, 2012; Yin et al., 2017; Kenealy & Waselefsky, 1985; Kucek et al., 2016) and demonstrated to support robust growth at concentrations as high as 700 mM ethanol (Weimer & Stevenson, 2012; Yin et al., 2017), the impact of ethanol toxicity on *A. neopropionicum* or other propionibacteria remained unexplored. Our experiments showed that *A. neopropionicum* grows optimally with 25 – 100 mM ethanol (1.2 – 4.6 g L^{-1}) and can tolerate well ethanol concentrations up to 300 mM (13.8 g L^{-1}) (Fig. 3.1). These findings are significant as these ethanol concentrations are within the range typically present in effluents from syngas fermentation. The *A. neopropionicum* - *C. kluyveri* co-culture was functional under substrate loading rates of 1.7 - 6.7 g ethanol L^{-1} d^{-1} and inflow concentrations of up to 300 mM ethanol. While higher ethanol concentrations could have been tolerated by *C. kluyveri*, we did not test those as they would have likely been detrimental to the co-culture due to the inhibitory effect on *A. neopropionicum*.

3.4.2 Continuous production of C5 – C7 carboxylates from ethanol and CO$_2$ by the synthetic co-culture

Most studies so far addressing the conversion of dilute ethanol to MCCAs have targeted the production of even-chain products, either by open mixed cultures or by pure cultures of *C. kluyveri*. Here, we chose an alternative approach, a synthetic co-culture, to target the production of OCCAs. The rationale for this approach was to: i) avoid unwanted reactions, e.g. methanogenesis, which normally take place when using open mixed cultures, ii) incorporate a bacterium able to produce propionate, the key precursor of OCCAs, and iii) cultivate together strains that grow optimally at similar environmental conditions (i.e. temperature, pH).

The *A. neopropionicum* - *C. kluyveri* co-culture produced a maximum of 37.0 ± 0.7 % OCCAs (C5 + C7), achieved with an ELR of 3.1 g ethanol L^{-1} d^{-1} (phase C). Under these conditions, valerate accounted for a significant 25 % of the total products. The maximum steady-state concentrations of valerate (12.5 ± 0.8 mM or 1.3 g L^{-1}) and heptanoate (6.5 ± 0.3 mM or 0.85 g L^{-1}) were obtained under the highest substrate loading rate (6.7 g ethanol L^{-1} d^{-1}; phase F). While these titres were higher than in the previous period where a lower ELR was applied (3.1 g ethanol L^{-1} d^1; phase C), the production rates of the two compounds remained the same. This suggests that the higher valerate and heptanoate concentrations observed in phase F could be due to the longer HRT imposed (54 h, vs. 36 h in phase C). On the contrary, caproate production increased with higher ELRs (Table 3.4). Conversely to phases B and C, ethanol utilisation was not complete (54.1 %) in phase F. Overall, this seems to indicate that such scenario where ethanol was not limiting could have driven excessive ethanol oxidation to acetate by *C. kluyveri*, leading to predominance of even-chain elongation activity. Indeed, caproate was the most dominant product in phase F (46.3 ± 0.5 %) and it was produced at the fastest rate (12.2 ± 0.6 mmol L^{-1} d^{-1}). The specificity of OCCAs decreased in phase F (31.8 ± 0.7 %) with respect to the previous period (phase B) and was actually the lowest within the three steady-states (Table 3.4).

The selectivity of valerate, heptanoate and butyrate also dropped in phase F (Table 3.4), while a substantial fraction of electrons from the substrate was directed to propanol. Propanol production can be attributed to either *A. neopropionicum* (Benito-Vaquerizo et al., 2022b; Tholozan et al., 1992)

and/or *C. kluyveri* (Candry et al., 2020b; Kenealy & Waselefsky, 1985). Propanol can be formed via reduction of propionyl-CoA (Benito-Vaquerizo et al., 2022b; Walther & François, 2016) or via reduction of propionate, as our batch experiments hinted (Fig. 3.5 and Suppl. material § 3.7: Fig. S3.1). The monoculture experiments with *A. neopropionicum* showed that the yield of propanol increased when higher initial ethanol concentrations were used (Table 3.2). This observation was concurrent with high acetate and propionate titres, which accounted for approximately 30 mM on those conditions (Fig. 3.2). In the reactor, the concentration of total carboxylic acids in steady-state F was approximately 54 mM (Table 3.4). Thus, the increased production of propanol by *A. neopropionicum* could have been a mechanism to mitigate undissociated acid toxicity by decreasing the concentration of propionate and preventing further acidification of the environment. Previously, de Leeuw et al. (2021) speculated that *C. kluyveri* reduced carboxylates to alcohols as a way to dispose of excess reducing equivalents under acetate limitation. However, in our reactor, the acetate concentration remained relatively constant at approximately 3 mM during the three steady-states (phases B, C and F), whereas propanol levels increased significantly only during the latter period (Fig. 3.6). Therefore, it appears more plausible that any potential involvement of *C. kluyveri* in propanol formation would have been driven by the accumulation of carboxylic acids in the fermentation broth. Both strains are also able to consume propanol (Kenealy & Waselefsky, 1985; Samain et al., 1982; Tholozan et al., 1992), so it is plausible that the actual propanol formation in the co-culture was higher than we measured. *A. neopropionicum* grows well on propanol in the presence of acetate and CO_2, yielding propionate as end product (Samain et al., 1982; Tholozan et al., 1992). On the other hand, *C. kluyveri* can use propanol for chain elongation analogously to ethanol (Kenealy & Waselefsky, 1985). However, we believe that propanol-driven chain elongation may have contributed very little to MCCA production in our co-culture, as *C. kluyveri* has been reported to favour the utilization of ethanol over propanol when both substrates are present (Kenealy & Waselefsky, 1985). Besides propanol, lactate was detected under the highest ELR tested (6.7 g ethanol L^{-1} d^{-1}). Lactate is an intermediate of the acrylate pathway that *A. neopropionicum* uses to metabolise ethanol (Benito-Vaquerizo et al., 2022b; Tholozan et al., 1992); therefore, its accumulation points to a metabolic bottleneck at high substrate concentrations, as observed in pure culture incubations (Fig. 3.2).

Continuous OCCAs production through ethanol-based chain elongation has also been studied by Grootscholten et al. (2013), who achieved an OCCAs selectivity of 57 %, and by Roghair et al.(2018), who reported similar values. Both studies relied on the use of mixed cultures. The highest valerate concentration (12.5 ± 0.8 mM or 1.3 g L^{-1}) and productivity (5.7 ± 0.1 mmol L^{-1} d^{-1} or 0.58 g L^{-1} d^{-1}) achieved by the *A. neopropionicum - C. kluyveri* co-culture in our study are lower than those achieved by Grootscholten et al., who reported a valerate concentration of 51.9 mM (5.3 g L^{-1}) with at a production rate of 73.3 mmol L^{-1} d^{-1} (7.5 g L^{-1} d^{-1}) (Grootscholten et al., 2013). The authors fed 13 g ethanol L^{-1} d^{-1} into their reactor, a much higher loading rate than applied in our system (1.7 - 6.7 g ethanol L^{-1} d^{-1}). They also continuously supplemented the culture with propionate (10.4 g L^{-1} d^{-1}), which we did not do here as we relied solely on propionate formed by *A. neopropionicum*. By increasing the loading rate to 19.5 g ethanol L^{-1} d^{-1}, Grootscholten et al. also achieved the highest heptanoate productivity in an ethanol-driven chain elongating system, with a titre of 24.6 mM (3.2 g L^{-1}) at a rate of 34.6 mmol L^{-1} d^{-1} (4.5 g L^{-1} d^{-1}) (Grootscholten et al., 2013). Roghair et al. also

supplied high substrate loading rates (32.5 g ethanol L^{-1} and 10.9 g propionate $L^{-1} d^1$, respectively) that led to the formation of 9.2 mM heptanoate (1.2 g L^{-1}) with a productivity of 13.8 mmol $L^{-1} d^{-1}$ (1.8 g $L^{-1} d^{-1}$) (Roghair et al., 2018).

Although the production rates of OCCAs obtained in our study are an order of magnitude lower than the benchmark achieved by Grootscholten et al.(2013), they are superior than reported for a mixed culture in one-pot production from CO (He et al., 2018). In that study, He and co-authors demonstrated the potential of integrating syngas fermentation and chain elongation in a single reactor. However, the titres of OCCAs they obtained were below 2 mM, with maximum valerate and heptanoate production rates of 0.83 mmol $L^{-1} d^{-1}$ and 0.44 mmol $L^{-1} d^{-1}$, respectively (He et al., 2018). In addition, a long acclimation time (~100 days) preceded the production of MCCAs, as observed in similar mixed culture processes (Agler et al., 2012; Ge et al., 2015; He et al., 2018; Kucek et al., 2016). In contrast, the *A. neopropionicum - C. kluyveri* co-culture presented in this work reached steady production of C5 – C7 carboxylates in just a few days when ethanol was fed at 1.7 and 3.1 g $L^{-1} d^{-1}$ (Fig. 3.6). This suggests that, while integration of syngas fermentation and chain elongation in a single step has its advantages (e.g. operation of one bioreactor instead of two), separating the two processes might allow for higher production rates of carboxylic acids.

3.4.3 Insights into the metabolism of odd-chain elongation by *C. kluyveri* and excessive ethanol oxidation

Early studies on *C. kluyveri* showed that propionate is as good electron acceptor as acetate for chain elongation (Bornstein & Barker, 1948; Kenealy & Waselefsky, 1985). The effect of the ethanol:-propionate ratio on the product spectrum has been recently studied (Candry et al., 2020b). Our monoculture experiments with *C. kluyveri* aimed to contribute to the knowledge on odd-chain elongation in this microorganism, focusing on cell growth. The longer lag phase and lower growth rate observed with propionate, compared to growth on acetate (Table 3.3), could be explained by several reasons. On the one hand, it could be due to a higher toxicity of propionate or, more likely, propionyl-CoA, compared to acetate/acetyl-CoA. In *C. kluyveri*, propionate (as well as acetate) is metabolised by the enzyme butyryl-CoA:acetate CoA transferase (Cat3), yielding a propionyl-CoA molecule that is fed into the reverse β-oxidation cycle (Seedorf et al., 2008). Propionyl-CoA is toxic when accumulated inside the cell, retarding growth and inhibiting biosynthetic reactions through inhibition of CoA-dependent enzymes (Deodato et al., 2006; Dolan et al., 2018; Maerker et al., 2005; Maruyama & Kitamura, 1985). Bornstein & Barker (1948) reported some inhibition of *C. kluyveri* grown with propionate concentrations above 68 mM, which are in the range of the levels tested in our study (50 and 100 mM). It could also be hypothesised that the slower growth observed with propionate is due to a lower affinity of the enzymes involved in the reverse β-oxidation pathway for odd-numbered intermediates, compared to even-numbered intermediates. However, in our experiments, acetate and propionate were used simultaneously when they were both initially present (Suppl. material § 3.7: Fig. S3.3c), suggesting no substrate preference. This is in line with observations by Candry et al. (2020b) in their study of odd-chain elongation in *C. kluyveri*. The authors of that study also reported no difference in the specific growth rate of *C. kluyveri* with propionate or acetate as electron acceptors, which contradicts our results (Table 3.3). This discrepancy could be due to the use of different media or, perhaps, the fact that the ethanol concentration (343

mM) and ethanol:carboxylic acid ratio (3.4) in the study of Candry et al. (Candry et al., 2020b) were much higher than in our work; excess ethanol can be oxidised to acetate with concomitant ATP production, supporting growth.

In our study, we also observed that the adverse effects of propionate on cell growth and biomass formation were overcome when acetate was present (Table 3.3). This hints at a shortage of ace-tyl-CoA, key metabolic intermediate derived from acetate and ethanol, as the cause for the lower growth rates and biomass yields observed with propionate. In other words, our results indicate that acetate supplementation improves growth on propionate by *C. kluyveri* during ethanol-driven chain elongation. The latter strategy could therefore be used to enhance production rates in odd-chain elongation processes.

Another relevant finding of our experiments with *C. kluyveri* is that the theoretical ethanol:car-boxylic acid stoichiometry of 1.2 does not result in optimal substrate use, at least during odd-chain elongation. According to theory of chain elongation, $1/6^{th}$ of the substrate (ethanol) is oxidised to acetate for ATP generation and the rest is derived to the reverse β-oxidation pathway (Seedorf et al., 2008). Chain elongation with only acetate does not allow to distinguish between ethanol oxidised to acetate and ethanol used for chain elongation. But, with propionate as electron acceptor, this distinction is possible since only the even-numbered products (acetate, butyrate, caproate) are the result of ethanol oxidation. Thus, with an ethanol:carboxylic acid ratio of 1.2 (theoretical stoichi-ometry), the proportion (specificity) of even-chain products in propionate-fed cultures should be $1/6^{th}$, or 16.7 %. However, in our propionate incubations with this ratio, even-chain carboxylates accounted for 27 % of the products (Fig. 3.3), indicating that more than $1/6^{th}$ of ethanol was oxidised to acetate. This phenomenon, termed excessive ethanol oxidation, has been described in chain-elongating mixed cultures but attributed to the activity of competing, ethanol-oxidising microorganisms that do not perform chain elongation (Grootscholten et al., 2013; Roghair et al., 2018). Our results are in accordance with those of Candry et al. (2020b), who showed that *C. kluyveri* also performs excessive ethanol oxidation during odd-chain elongation and that the stoichiometric product output (16.7 % even-chain and 83.3 % odd-chain) is not achieved with the theoretical E/CA ratio of 1.2. According to that study, the stoichiometric product output is approached with lower ethanol:propionate ratios (e.g., 0.5). It remains a question whether excessive ethanol oxidation also takes place during even-chain elongation or if it is, in fact, a strategy of *C. kluyveri* to deal with propionyl-CoA toxicity and a shortage of acetyl-CoA.

3.4.4 Application of the synthetic co-culture to upgrade syngas fermentation effluent

Synthetic co-cultures are suitable platforms to upgrade syngas fermentation effluent. Co-cultures such as the one presented in this study are less adaptable than open mixed cultures and are there-fore not so suited to treat complex organic waste streams (e.g., food waste). However, gasification of feedstocks followed by syngas fermentation results in a rather "clean" effluent: much simpler in composition (mostly ethanol and acetate) and more consistent than organic waste streams, thus easier to handle by monocultures or synthetic co-cultures. Indeed, syngas fermentation effluent, when supplemented with trace metals and vitamins, has been shown to be as good substrate for *C. kluyveri* as synthetic ethanol/acetate mixtures (Gildemyn et al., 2017).

Contrary to open mixed cultures, synthetic co-cultures can exclude methanogens, which has two advantages when it comes to their use in chain elongation processes. First, the need for methanogenesis inhibitors (e.g. *2*-bromoethanesulfonic acid) is avoided, benefiting both the cost and performance of the process as these chemicals have been shown to lose their effectiveness over time (He et al., 2018; Shrestha et al., 2023). Second, a neutral, instead of acidic pH can be selected for fermentation (most methanogens grow optimally at pH around neutrality [Grimalt-Alemany et al., 2018b]), consequently minimising growth inhibition by accumulation of undissociated carboxylic acids. In addition, multi-species genome-scale metabolic models (GEMs) can be built for synthetic co-cultures to predict phenotypes and find strategies to optimise process performance (Benito-Vaquerizo et al., 2020; Hanemaaijer et al., 2015; Li & Henson, 2019; Stolyar et al., 2007). Recently, we constructed the first GEM of *A. neopropionicum* (Benito-Vaquerizo et al., 2022b); in future research, this GEM could be incorporated into, for example, the existing multi-species GEM of the *Clostridium autoethanogenum - C. kluyveri* co-culture (Benito-Vaquerizo et al., 2020) to evaluate the performance of a synthetic tri-culture applied to syngas fermentation.

An important difference of our study compared to most other works on MCCA production via chain elongation is that we did not provide propionate (or acetate) as electron acceptor, relying only on the endogenous production of SCCAs in the system. In addition, the ethanol loading rates we tested are relatively low compared to those applied in other studies discussed here (Grootscholten et al., 2013; Roghair et al., 2018). Therefore, it is expected that the MCCAs production rates obtained in our study remain relatively low in comparison, but yet prove that the synthetic co-culture has potential to be used as a platform to upgrade dilute ethanol streams to, specifically, OCCAs. Improvement of the *A. neopropionicum - C. kluyveri* co-culture could include determining a more optimal pH of operation that could also support higher substrate loading rates. In our bioreactor experiment, increasing the pH from 7 to 7.3 boosted ethanol consumption and chain-elongating activity of C5 – C7 carboxylates (phase G, Fig. 3.6). A pH of 7.3 is closer to the optimum for *A. neopropionicum* (Tholozan et al., 1992), and it also contributes to alleviating carboxylic acid toxicity. Among the other strategies, in-line product extraction has been shown to significantly enhance production rates by reducing product inhibition (Agler et al., 2012; Ge et al., 2015; Kucek et al., 2016; Vasudevan et al., 2014). Biomass retention, either via anaerobic filter reactors or membrane modules, has also been demonstrated to improve production rates (Gildemyn et al., 2017; Vasudevan et al., 2014). A key finding of our study is that, in line with the work on *C. kluyveri* by Candry and co-authors (Candry et al., 2020b), odd-chain elongation was favoured under ethanol limitation, which can be achieved in controlled chemostat cultivation. Therefore, this approach should be kept in mind when targeting the production of OCCAs via ethanol-driven chain elongation.

3.5   Conclusions

A synthetic co-culture composed of *A. neopropionicum* and *C. kluyveri* was demonstrated to produce valerate and heptanoate from solely ethanol and CO_2 as substrates. In bioreactor cultivation, the co-culture tolerated concentrations of at least 300 mM ethanol (13.8 g L^{-1}) and yielded a maximum of 37 % OCCAs. Our results showed that controlling ethanol use is favourable for OCCA production, and that tuning of pH could further boost chain elongation in this co-culture.

Moreover, experiments with pure cultures of *C. kluyveri* revealed the negative effects of propionate on its growth, which are reversed when acetate is present. Further work is needed to verify the hypothesis that *C. kluyveri* deals with propionate/propionyl-CoA toxicity by performing excessive ethanol oxidation, which would explain the observed shift towards even-chain products during chain elongation of propionate. In view of the results, we propose that the *A. neopropionicum - C. kluyveri* co-culture could be integrated with the syngas fermentation platform to upgrade ethanol to OCCAs. For this, future work should investigate the possibility to establish a tri-culture with an acetogen (one-pot process), or test the co-culture with actual syngas fermentation effluent (two-stage process). In addition, a number of strategies could be explored in order to improve production rates, such as cell retention, in-line product extraction or co-feeding heterotrophic (waste) substrates. Multi-species GEM modelling is a powerful tool that can also aid in the exploration of capabilities of synthetic co-cultures. Altogether, our work shows the potential of synthetic microbial co-cultures to serve as platforms for innovative biotechnological processes.

3.6   Acknowledgements

3.7 Supplementary material
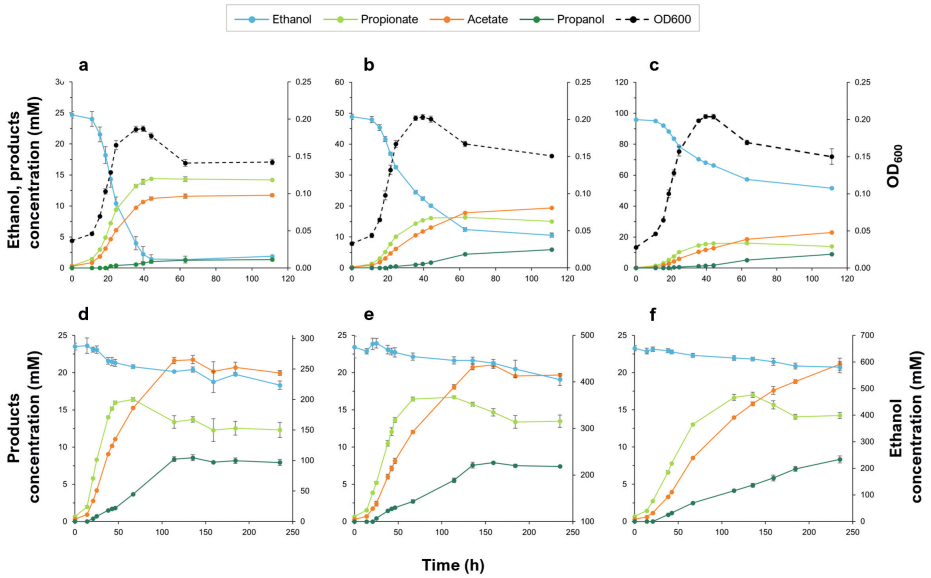
Figure S3.1 Batch cultivations of *A. neopropionicum* grown on ethanol (25 – 700 mM). **a – c**: Substrate and product concentrations, and cell density (OD_{600}) of incubations containing 25 mM (**a**), 50 mM (**b**) and 100 mM (**c**) ethanol. **d – f**: Substrate and product concentrations of incubations containing 300 mM (**d**), 500 mM (**e**) and 700 mM (**f**) ethanol.
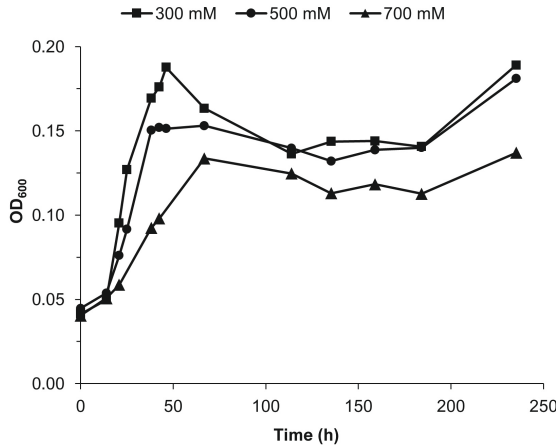
Figure S3.2 Cell density (measured as OD_{600}) of batch cultures of A. neopropionicum grown on 300, 500 and 700 mM ethanol.
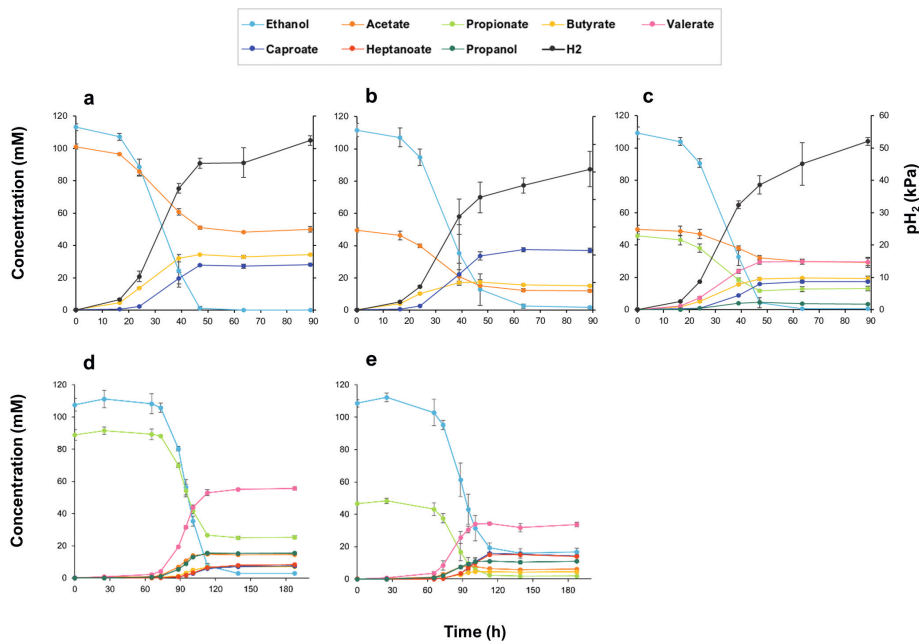
Figure S3.3 Batch cultivations of *C. kluyveri* grown on ethanol (120 mM) plus acetate and/or propionate. Displayed here are substrate and product concentrations of incubations with: **a**) 100 mM acetate (E/CA = 1.2); **b**) 50 mM acetate (E/CA = 2.4); **c**) 50 mM acetate and 50 mM propionate (E/CA = 1.2); **d**) 100 mM propionate (E/CA = 1.2) and **e**) 50 mM propionate (E/CA = 2.4). Evolution of H_2 was only measured in conditions **a** – **c**; in **d** and **e**, final H_2 pressure was the same as in the other incubations ($\approx$ 50 kPa). Heptanoate was also produced in condition **c** (< 2 mM, not shown).
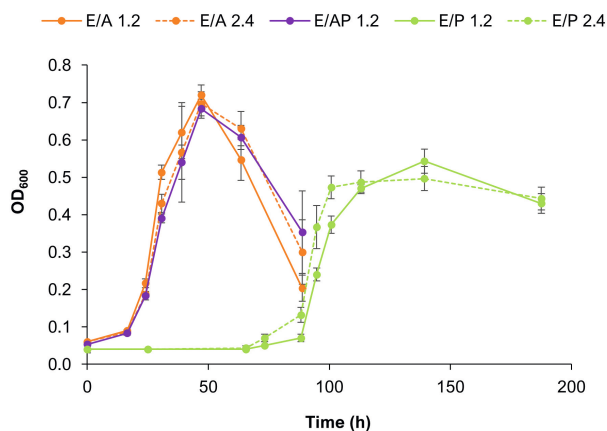
Figure S3.4 Cell density (measured as OD_{600}) of *C. kluyveri* batch cultures incubated with ethanol (120 mM) and either acetate (E/A), propionate (E/P) or both electron acceptors (E/AP) at the indicated ethanol/carboxylic acid ratio.
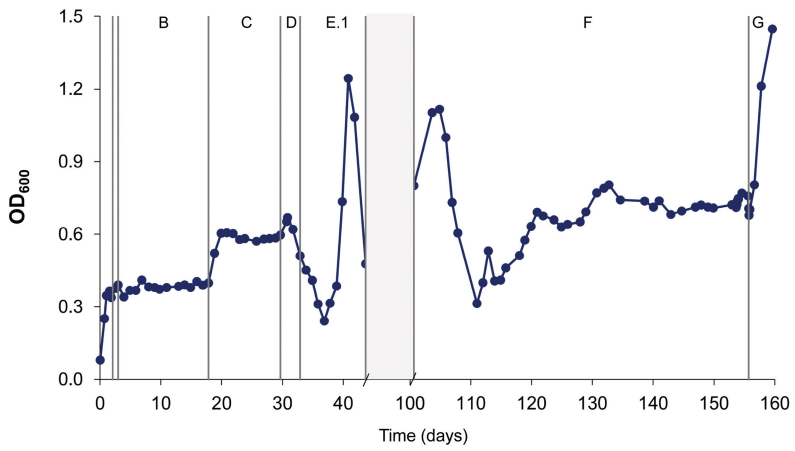
Figure S3.5 Cell density (OD_{600}) of the *A. neopropionicum* – *C. kluyveri* co-culture in ethanol-fed continuous bioreactor. The different phases of operation (A – F) are indicated (see details in Table 3.1). The shaded area corresponds to a period where several technical issues occurred and is therefore disregarded.

Genome-scale metabolic modelling enables deciphering ethanol metabolism via the acrylate pathway in the propionate-producer *Anaerotignum neopropionicum*

—

Sara Benito-Vaquerizo*, Ivette Parera Olm*, Thijs de Vroet, Peter J. Schaap, Diana Z. Sousa, Vitor A.P. Martins dos Santos and Maria Suarez-Diez

Authors contributed equally.

Abstract

Microbial production of propionate from diluted streams of ethanol (e.g., deriving from syngas fermentation) is a sustainable alternative to the petrochemical production route. Yet, few ethanol-fermenting propionigenic bacteria are known, and understanding of their metabolism is limited. *Anaerotignum neopropionicum* is a propionate-producing bacterium that uses the acrylate pathway to ferment ethanol and CO_2 to propionate and acetate. In this work, we used computational and experimental methods to study the metabolism of *A. neopropionicum* and, in particular, the pathway for conversion of ethanol into propionate. Our work describes iANEO_SB607, the first genome-scale metabolic model (GEM) of *A. neopropionicum*. The model was built combining the use of automatic tools with an extensive manual curation process, and it was validated with experimental data from this and published studies. The model predicted growth of *A. neopropionicum* on ethanol, lactate, sugars and amino acids, matching observed phenotypes. In addition, the model was used to implement a dynamic flux balance analysis (dFBA) approach that accurately predicted the fermentation profile of *A. neopropionicum* during batch growth on ethanol. A systematic analysis of the metabolism of *A. neopropionicum* combined with model simulations shed light into the mechanism of ethanol fermentation via the acrylate pathway, and revealed the presence of the electron-transferring complexes NADH-dependent reduced ferredoxin:NADP+ oxidoreductase (Nfn) and acryloyl-CoA reductase-EtfAB, identified for the first time in this bacterium. The realisation of the GEM iANEO_SB607 is a stepping stone towards the understanding of the metabolism of the propionate-producer *A. neopropionicum*. With it, we have gained insight into the functioning of the acrylate pathway and energetic aspects of the cell, with focus on the fermentation of ethanol. Overall, this study provides a basis to further exploit the potential of propionigenic bacteria as microbial cell factories.

4.1 Introduction

Propionic acid is a naturally-occurring carboxylic acid produced by propionigenic bacteria as end-product of their anaerobic metabolism. It is an important intermediate in anaerobic fermentative processes such as those occurring in the human gut, anaerobic digesters and cheese production. It is also an essential platform chemical in the manufacture of cellulose-derived plastics, cosmetics and pharmaceuticals and, due to its antimicrobial properties, it can be used as food preservative (Gonzalez-Garcia et al., 2017; Ranaei et al., 2020). At present, industrial production of propionic acid is based on petrochemical processes, but efforts are being made to develop sustainable production platforms based on the use of propionigenic bacteria as biocatalysts. Microbial production of propionic acid has been researched for over 150 years, however industrial implementation is still limited mainly due to low productivities, which render such processes economically non-competitive (Boyaval & Corre, 1995; Gonzalez-Garcia et al., 2017; Ranaei et al., 2020). So far, most approaches have considered strains of the genus *Propionibacterium* —well-studied due to their involvement in cheese production—, and have focused on the use of sugars as feedstock. However, the chemical industry is increasingly required to rely on the use of non-conventional, inexpensive raw materials to minimize its carbon footprint (Blank et al., 2020). Ethanol, a low-priced common end product of many fermentations, is regarded as one of such feedstocks (Blank et al., 2020; Dagle et al., 2020). Moreover, ethanol can be synthesised from CO, CO_2 and H_2 (syngas) by acetogenic bacteria. Syngas-to-ethanol fermentation technology has been deployed at large scale, and recent advances are expected to accelerate its development in the years to come (Köpke & Simpson, 2020; Molitor et al., 2016; Stoll et al., 2020).

Anaerotignum neopropionicum, formerly *Clostridium neopropionicum* (Ueki et al., 2017), was the first representative of the ethanol-fermenting, propionate-producing bacteria. It was isolated in 1982 from an anaerobic digester treating wastewater from vegetable cannery (Samain et al., 1982). The ability of converting ethanol to propionate is shared with only three other microbial species: the closest relative *Anaerotignum propionicum* (formerly, *Clostridium propionicum* (Ueki et al., 2017), the sulphate-reducing bacterium *Desulfobulbus propionicus* (Laanbroek et al., 1982; Stams et al., 1985), and *Pelobacter propionicus* (Schink et al., 1987). In these four microorganisms, ethanol oxidation to propionate occurs in the presence of CO_2 with concomitant production of acetate, according to the theoretical Eq. 4.1. This ability of propionigenic bacteria could be exploited to upgrade dilute ethanol streams from beer production or syngas fermentation, among others. For example, Moreira et al. (2021) showed that co-cultures of acetogens and ethanol-consuming propionigenic bacteria can convert syngas into propionate. In their study, the acetogen *Acetobacterium wieringae* was co-cultivated with *A. neopropionicum*; *A. wieringae* converted CO to ethanol, which was used by *A. neopropionicum* to produce propionate.

$$3\ CH_3CH_2OH + 2\ CO_2 \rightarrow 2\ CH_3CH_2COO^- + CH_3COO^- + 3H^+ + H_2O \qquad \text{Eq. 4.1}$$

$$\Delta G^0 = -124\ kJ$$
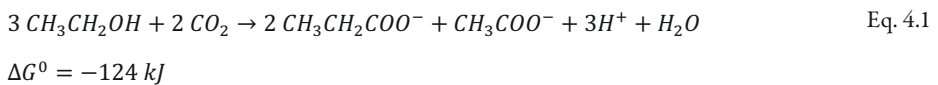
Two main pathways have been described for the fermentative production of propionic acid in bacteria: the methylmalonyl-CoA (also termed succinate pathway or Wood-Werkman cycle) and the acrylate pathway (Gonzalez-Garcia et al., 2017; Reichardt et al., 2014). Most of the known propionigenic bacteria, including strains of the genera *Propionibacterium* and *Cutibacterium*, use the methylmalonyl-CoA pathway for growth. The acrylate pathway is mostly found within members of the phylum Firmicutes (Reichardt et al., 2014). Sugars and lactate are common substrates for these pathways. Ethanol fermenters *D. propionicus* and *P. propionicus* use the methylmalonyl-CoA pathway (Schink et al., 1987; Stams et al., 1985), whereas *A. neopropionicum* and *A. propionicum* use the acrylate pathway (Tholozan et al., 1992).

To fully exploit the potential of microorganisms for biotechnological applications, it is fundamental to understand their metabolism and cellular processes. Genome- scale metabolic models (GEMs) and their analysis with COnstraint-Based Reconstruction and Analysis (COBRA) methods have become indispensable tools in this regard (Ebrahim et al., 2013; Gu et al., 2019; Santos et al., 2011). Flux balance analysis (FBA) is often used as the mathematical approach to explore the intracellular fluxes of GEMs under steady-state conditions (e.g., in chemostat cultivations) (Orth et al., 2010). FBA can be extended to dynamic FBA (dFBA), which simulates the time-step evolution of individual steady-states that take place in time-varying processes, such as batch and fed-batch cultures (Moreno-Paz et al., 2022). A wide range of GEMs have been successfully implemented to unravel novel metabolic features of microorganisms, guide experimental design, or improve bioprocess operation in mono- and co-cultivation. For instance, the reconstruction of the first GEM of *Clostridium ljungdahlii* (iHN637) demonstrated the essential role of flavin-based electron bifurcation in energy conservation during autotrophic growth (Nagarajan et al., 2013). FBA enabled the estimation of intracellular metabolic fluxes in the GEM of the acetogen *Clostridium autoethanogenum* (iCLAU786), helping to understand the effects of CO supplementation on CO_2/H_2-growing cultures (Heffernan et al., 2020). A multi-species GEM was recently developed that described a syngas-fermenting co-culture composed of *C. autoethanogenum* and *Clostridium kluyveri*; the model provided valuable insight into the microbial interactions between the two microorganisms and predicted strategies for enhanced production of the end products butyrate and hexanoate (Benito-Vaquerizo et al., 2020).

Many propionigenic bacteria have been sequenced to date (Butler-Wu et al., 2011; Koskinen et al., 2015; Parizzi et al., 2012), including the ethanol fermenters *D. propionicus* (Pagani et al., 2011), *P. propionicus* (Butler et al., 2009), *A. propionicum* (Poehlein et al., 2016) and *A. neopropionicum* (Beck et al., 2016). This has enabled the reconstruction of GEMs of some of these species. All GEMs of propionigenic bacteria published to date concern strains that harbour the methylmalonyl-CoA pathway. One of these works described the reconstruction of five *Propionibacterium freudenreichii* species using pan-genome guided metabolic analysis [34]. Navone et al. (2018) used the *Propionibacterium* subsp. *shermanii* and the pan-*Propionibacterium* GEMs to guide genetic engineering strategies for increased propionic acid production. Sun et al. (2010) developed a constrained-based GEM of *P. propionicus* and validated fermentative growth of this strain on ethanol.

Here we describe iANEO_SB607, the first GEM of *A. neopropionicum* and the first to model the acrylate pathway in a propionigenic microorganism. The model was reconstructed using automatic tools followed by an extensive manual curation, which led us to the identification of

electron-transferring enzymes involved in the acrylate pathway, cofactor regeneration and energy conservation. In addition, a physiological characterisation of *A. neopropionicum* in batch cultures was performed to validate and complement the reconstruction of the model. FBA was used to assess growth phenotypes on several carbon sources, and dFBA was applied to simulate batch growth of *A. neopropionicum* on ethanol, and ethanol plus acetate. The combination of in-depth modelling and experimentation has enabled us to examine in detail the metabolism of ethanol fermentation in this bacterium and to address pre-existing ambiguities.

4.2   Materials and Methods

4.2.1   Reconstruction of the GEM iANEO_SB607

The genome-scale metabolic network of *A. neopropionicum* was reconstructed in four main steps. First, the genome sequence of *A. neopropionicum* DSM 3847^T (GCA 001571775.1) (Beck et al., 2016) was retrieved from the European Nucleotide Archive in FASTA format and was annotated using RAST (Aziz et al., 2008). An additional re-annotation was carried out using eggNOG-mapper (Huerta-Cepas et al., 2017). The annotation file can be found in the public Gitlab repository: https://gitlab.com/wurssb/Modelling/Anaerotignum_neopropionicum. The second step was the generation of the draft model using ModelSEED (Henry et al., 2010). For this, the RAST annotation file was imported into ModelSEED and a gram-positive template was chosen to reproduce growth on rich medium. The draft model was downloaded in table format and SBML format. The third step consisted on the manual curation and refinement of the draft model. Every reaction entry was analysed individually and modifications were made on the table format file. Specifically, i) unbalanced reactions were corrected based on charged formulas with the corresponding addition/deletion of H$^+$ or H$_2$O molecules; ii) reaction direction was adjusted using eQuilibrator (Flamholz et al., 2012). Reactions were considered reversible if the change in Gibbs free energy was between -30 and 30 KJ mol^{-1} at standard conditions for reactants/products, pH 7.3 and ionic strength 0.1 M. In cases where eQuilibrator did not retrieve information for a specific reaction, reaction direction was adjusted based on information from MetaCyc (Karp et al., 2002) and BIGG (Schellenberger et al., 2010) databases. iii) EC numbers were corrected or inserted for every reaction based on information from KEGG (Ogata et al., 1999) and MetaCyc. iv) The original genes in Patric format (Davis et al., 2019) were replaced by the locus tag format ('CLNEO XXXXX') found in Uniprot (Apweiler et al., 2004) and BRENDA (Schomburg et al., 2002) databases. The re-annotation file was used to identify potential gene(s) associated to reactions that lacked a gene in the original RAST annotation. v) The final step consisted of gap-filling, where reactions were added or removed to reproduce known or observed phenotypes. Gap-filling was done combining a computational and a manual approach: an automatic gap-filling pro- cess was run using the KBase pipeline (Arkin et al., 2018), while the manual curation was based on experimental data obtained in this study and published. The final model, iANEO_SB607, can be found in the git repository in Table format, json and SBML L3V1 (Hucka et al., 2015) standardization. Furthermore, the different versions together with a Memote (Lieven et al., 2020) and FROG report were combined in an OMEX archive file (Bergmann et al., 2014) deposited in BioModels (Chelliah et al., 2015) and assigned the identifier MODEL2201310001.

4.2.2   Generation of the biomass synthesis reaction and sensitivity analysis

The biomass reaction of *A. neopropionicum* was adapted from the biomass reactions of *Clostridium beijerinckii* [GEM iCM925 (Milne et al., 2011)], and *Clostridium autoethanogenum* [GEM iCLAU786 (Valgepea et al., 2017)]. The composition of the main building blocks was maintained but, based on the protocol of Thiele & Palsson (2010), protons were stoichiometrically added to the hydrolysis part of the biomass synthesis reaction. Protons were also added to the reactions of DNA, RNA, proteins, teichoic acids and peptidoglycans synthesis in line with the ATP associated to polimerization. The DNA composition was determined based on the GC content of the genome of *A. neopropionicum* and it was adjusted in the reaction associated to the biosynthesis of DNA. The fatty acids composition was adjusted based on reported experimental data for *A. neopropionicum* (Ueki et al., 2017).

A sensitivity analysis was performed by modifying the content of proteins, phospholipids (plipids) and cell wall components, considering cell wall components as the sum of teichoic acid, peptidoglycans and carbohydrates composition. The rest of components (DNA, RNA and traces) were kept fixed. The composition of proteins and plipids were randomly selected within ±10% of their current value. In this way, the total cell wall components composition was calculated following Eq. 4.2.

$$Cell\ wall\ components = 1 - protein - plipids - (DNA + RNA + trace) \qquad \text{Eq. 4.2}$$

Consecutively, the value of each cell component was distributed within teichoic acid, peptidoglycans and carbohydrates following the same proportion as they had in the original biomass synthesis reaction. For each randomly selected value, a new biomass synthesis reaction was obtained. This new biomass synthesis reaction was maximised as the objective function using FBA in COBRApy (Ebrahim et al., 2013) maintaining fixed ethanol and CO_2 uptake rates. We repeated this process 1000 times, so that we obtained 1000 different biomass synthesis reactions. The composition of the cell wall components, proteins and phospholipids was stored for each biomass synthesis reaction, together with the growth rate, and acetate and propionate production rate. The obtained growth rate, acetate and propionate production rate were normalised with respect the original values and were plotted against each biomass building block (Suppl. material § 4.8: Fig. S4.1).

Additionally, we also studied the effect of varying the growth-associated maintenance (GAM) reaction on the growth rate. In this analysis, the original fractions of the biomass components shown in Eq. 4.2 were maintained, and we randomly selected different GAM values within ±20% of the original value. We repeated this process 1000 times and calculated the growth rate for each GAM value. The obtained growth rate was normalised with respect the original growth rate and was plotted against GAM (Suppl. material § 4.8: Fig. S4.2; gitlab repository).

4.2.3   Model simulations at steady-state

The model was qualitatively validated by assessing growth capabilities and product profile on several carbon sources in steady-state. Model simulations were done using COBRApy, version 0.24.0 (Ebrahim et al., 2013), and Python 3.6.9. The maximum empirical ethanol uptake rate across cultivations was 30 to 40 mmol g_{CDW}^{-1} h^{-1}. Based on this, the lower bound of the substrate uptake

rate per time point was constrained to 30 mmol $g_{CDW}^{-1}h^{-1}$ to assess growth on a single carbon source, and to 30 mmol $g_{CDW}^{-1}h^{-1}$ in total to assess growth on more than one carbon source, unless specified otherwise. The biomass synthesis reaction was used as the objective function. Growth was considered when the growth rate was higher than 0.0001 h^{-1}. To better explore the solution space, the fluxes compatible with the applied constraints were sampled using the sample function with the 'achr' method in the flux_analysis submodule of COBRApy (Herrmann et al., 2019). The lower bound of the biomass synthesis reaction was constrained to be at least 99% of the maximum growth rate calculated by FBA. Presented results are the average and standard deviation of 5000 iterations generated at each condition.

4.2.4   Dynamic flux balance analysis simulations

The reconstructed GEM iANEO_SB607 was subjected to dFBA to simulate batch growth of *A. neopropionicum* on ethanol and ethanol plus acetate. Model simulations were done using COBRApy, version 0.24.0, IBM ILOG CPLEX 128, and Python 3.6.9 (see git repository). The maximum uptake rate, maximum growth rate and initial substrate and biomass concentration, obtained from batch cultivations, were used as model inputs. To constrain the feasible flux space, ethanol uptake was specified to follow a Michaelis-Menten-like kinetics (Eq. 4.3) with parameters $q_{Si,max}$ and $K_{m,i}$:

$$q_{Si} = \frac{q_{Si,max} \cdot S_i}{K_{m,i} + S_i}$$

Eq. 4.3

where q_{Si} is the uptake rate of substrate *i* (mmol $g_{CDW}^{-1}h^{-1}$); $q_{Si,max}$ is the maximum uptake rate of substrate *i* (mmol $g_{CDW}^{-1}h^{-1}$); $K_{m,i}$ is the Michaelis-Menten constant (mM) for substrate *i* and S_i is the concentration of substrate *i* (mM). $K_{m,i}$ was determined based on experimental data and model fitting (Suppl. material § 4.8: Table S4.1). $q_{Si,max}$ was calculated from experimental data of batch fermentations. Concentrations of substrates, products and biomass over time were determined as follows. First, the q_{Si} was calculated using Eq. 4.3 for each given time step and the defined initial concentrations. Then, FBA was applied under those constraints to compute the fluxes at maximum growth rate. After that, the following ordinary differential equations (ODE) were solved:

$$\frac{dX}{dt} = \mu \cdot X$$

Eq. 4.4

$$\frac{dS_i}{dt} = q_{Si} \cdot X$$

Eq. 4.5

$$\frac{dP_j}{dt} = q_{Pj} \cdot X$$

Eq. 4.6

where X is the biomass concentration (g L^{-1}); μ is the specific growth rate (h^{-1}); S_i is the concentration of substrate *i* (mM); q_{Si} is the uptake rate of substrate *i* (mmol $g_{CDW}^{-1}h^{-1}$); q_{Pj} is the production rate of product *j* (mmol $g_{CDW}^{-1}h^{-1}$), and P_j is the concentration of product *j* (mM). Eq. 4.4, 4.5 and 4.6 were used to calculate X, S_i and P_j, respectively. S_i is used as input to calculate the next state following Eq. 4.3. The objective function was changed to maximise the ATP generation ("rxn00062_ c0")

once the model became infeasible due to the low concentration of ethanol. For each time step, the concentration of biomass, substrate and products was computed and the calculated values were stored and plotted.

4.2.5   Experimental batch fermentation data

Cultivation conditions

A. neopropionicum DSM 3847^T was obtained from the German Collection of Microorganisms and Cell Cultures (DSMZ, Braunschweig, Germany). Batch fermentations were done in 117 mL serum bottles containing 50 mL medium with the following composition (per litre): 0.9 g NH_4Cl, 0.3 g NaCl, 0.8 g KCl, 0.2 g KH_2PO_4, 0.4 g K_2HPO_4, 0.2 $MgSO_4 \cdot 7 H_2O$, 0.04 $CaCl_2 \cdot 2 H_2O$, 3.36 g $NaHCO_3$, 10 mL trace element solution from DSM medium 318, 1 mL vitamin solution, 0.5 g yeast extract, 0.3 g $Na_2S \cdot x H_2O$ (x=9-11) as reducing agent and 0.5 mg resazurin as redox indicator. The vitamin solution contained (per litre): 0.5 g pyridoxine, 0.2 g thiamine, 0.2 g nicotinic acid, 0.1 g p-aminobenzoate, 0.1 g riboflavin, 0.1 g pantothenic acid, 0.1 g cobalamin, 0.05 g folic acid, 0.05 g thioctic acid and 0.02 g biotin. The headspace of the bottles was filled with a gas mixture of N_2/ CO_2 (80:20% v/v; 170 kPa). To test growth in the presence of H_2, the headspace of bottles was filled instead with a gas mixture of $H_2/CO_2/N_2$ (10:20:70% and 80:20:0% v/v; 170 kPa). Growth was assessed on the following substrates: ethanol, lactate, glucose and xylose, at an initial concentration of 25 mM. Where indicated, acetate (10 or 25 mM) was added to ethanol-fed cultures. The pH of the medium was 7.1 - 7.2. Cultures were incubated at 30°C statically.

Analytical techniques

Liquid and headspace samples were taken periodically over the course of batch fermentations and analysed for biomass, substrate and product concentrations. Biomass growth was measured by optical density at 600 nm (OD_{600}). Biomass concentration (mg_{CDW} L^{-1}) was estimated from OD_{600} measurements using the correlation: $mg_{CDW}L^{-1} = (OD_{600} - 0.016)/0.0032$, which was experimentally determined from *A. neopropionicum* cultures grown on ethanol. Concentrations of soluble compounds in the supernatant of liquid samples were determined using high-pressure liquid chromatography (HPLC) (LC-2030C Plus, Shimadzu, USA). The HPLC was equipped with a Shodex SH1821 column operated at 65°C. A solution of 0.1 N H_2SO_4 was used as mobile phase, at a flowrate of 1 mL min^1. Detection was done via a refractive index detector. Concentrations below 0.2 mM could not be accurately quantified and are considered traces. Concentrations of gases in headspace samples were determined via gas chromatography (GC) (Compact GC 4.0, Global Analyser Solutions, The Netherlands). To analyse H_2, a Molsieve 5A column operated at 140°C coupled to a Carboxen 1010 column was used. CO_2 was analysed in a RT-Q-BOND column at 60°C.

4.3   Results

4.3.1   Reconstruction of iANEO_SB607, the first GEM of *A. neopropionicum*

A draft model of the metabolism of *A. neopropionicum* was developed by automatic reconstruction using the publicly available genome sequence of the microorganism [DDBJ/EMBL/GenBank

accession number: LRVM00000000; (Beck et al., 2016)]. The draft model comprised 491 genes, 855 metabolites and 907 reactions. This preliminary model predicted growth only on rich medium supplemented with amino acids and biomass precursors, and it did not predict the production of propionate and acetate. We performed an extensive manual curation process that resulted in the deletion, modification or addition of reactions, metabolites and genes (see git repository). The final model, iANEO_SB607, comprises 607 genes, 815 metabolites and 932 reactions (Table 4.1). This is the first GEM of the propionigenic bacterium *A. neopropionicum*.

Table 4.1 Composition of iANEO_SB607.

Features	Abundance
Genes	617
Metabolites	1065
Intracellular metabolites	915
Extracellular metabolites	152
Reactions	1081
Conversion reactions	832
Transport reactions	159
Exchange reactions	76
Reactions associated with genes	775 (71.7%)
Reactions non-associated with genes	306 (28.9%)

Two compartments are recognised in the model: the intracellular compartment (id: 'c0') and the extracellular compartment (id: 'e0'). Metabolites are assigned to either one of the compartments. Reactions are classified as metabolic reactions, transport reactions and exchange reactions. Metabolic reactions describe the biochemical conversion of metabolites within the intracellular compartment. Transport reactions describe the transport of metabolites across the intracellular and extracellular compartments. Exchange reactions simulate the excretion of metabolites outside the cell or the uptake of metabolites into the cell. Reactions are distributed within cell subsystems (Fig. 4.1), except exchange reactions. The model also includes reactions involved in the production of acetate, propionate, butyrate, propanol, isobutyrate and isovalerate. Approximately 80% of reactions could be associated to genes present in the genome of *A. neopropionicum*. The remaining 20% of reactions are not associated with genes. Half of these reactions are mostly exchange reactions and diffusion transport reactions. The other half are spontaneous reactions or gap-filled reactions describing, in a summarised manner, the biosynthesis of biomass building blocks (e.g., lipids, carbohydrates).
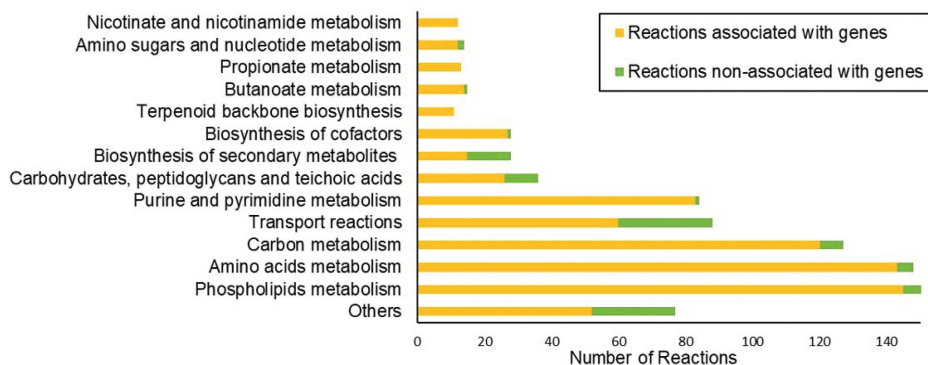
Figure 4.1 Distribution of the reactions of the iANEO_SB607 model within the cellular subsystems.

4.3.2 Sensitivity analysis of the biomass synthesis reaction

The constructed biomass synthesis reaction (BIOMASS_Aneopro_w_GAM) accounts for the production of DNA, RNA, proteins, peptidoglycans, phospholipids, teichoic acids and trace, and it is normalised to 1 gram per mmol. It also includes the growth-associated maintenance (GAM) as an hydrolysis reaction, and the non-growth associated maintenance (NGAM) as a reaction of ATP phosphohydrolase (rxn00062_c0). GAM was assumed to be 40 mmol ATP g_{CDW}^{-1}, as in the GEM of *C. acetobutylicum* (Lee et al., 2008). The lower bound of this reaction was constrained to a rate of 8.4 mmol ATP $g_{CDW}^{-1} h^{-1}$, an estimation based on the models of *C. beijerinckii* (Milne et al., 2011) and *C. autoethanogenum* (Valgepea et al., 2017).

Since the biomass synthesis reaction of *A. neopropionicum* was developed based on these two other species, we performed a sensitivity analysis to test its robustness. The analysis showed the effect of modifying the proportion of the main biomass components from the biomass synthesis reaction on model predictions (i.e., growth and production rates). In all scenarios tested, growth and production rates remained virtually unaffected (Suppl. material § 4.8: Fig. S4.1). The largest deviation of the growth rate, acetate and propionate production rates were ±0.0005 h^{-1}, ±0.005 mmol $g_{CDW}^{-1} h^{-1}$ and ±0.0025 mmol $g_{CDW}^{-1} h^{-1}$, respectively, which are negligible as they only represent 3%, 0.025% and 0.025%, respectively. The effect of varying other biomass components — DNA, RNA and trace — was also considered negligible given that they represent a minor fraction of the biomass (10%). The growth rate was slightly more affected when GAM was changed. The largest deviation was ±0.00175 h^{-1}, which corresponds to 10.8% difference compared to the original growth rate. The biomass synthesis reaction was therefore considered a reliable representation of the biomass composition of *A. neopropionicum*.

4.3.3 Quality of the GEM iANEO_SB607

The quality of the iANEO_SB607 model was evaluated using the SBML validator and the test suite Memote. Additionally, we have run a FROG analysis to verify the reproducibility of the model. The GEM was correctly defined in SBML format, level 3, version 1. The GEM obtained an overall Memote score of 72%. All metabolites, reactions and genes were fully annotated. The annotation per database of reactions and metabolites scored 83%, however the annotation per database of

genes scored a much lower value, 33%. Reactions are mass and charge balanced, except for reactions associated to the synthesis of biomass precursors. The model does not have infeasible cycles and all metabolites are connected. However, the model is only partly consistent (55% scoring); this is due to the creation of metabolites to account for biomass precursors. These metabolites (e.g., RNA) lack a defined formula or a correct charge and, thus, their associated reactions are considered stoichiometrically inconsistent, decreasing the global consistency score. Memote identifies 102 metabolites that can only be consumed or produced, resulting in 422 blocked reactions in the model under the restrictive constraints. When the model does not have constraints, FVA analysis finds 354 blocked reactions, which is in line with the average % of blocked reactions in GEMs (20-40%) (Ravikrishnan & Raman, 2015).

4.3.4 Qualitative assessment of iANEO_SB607 through analysis of growth phenotypes

The iANEO_SB607 model was qualitatively validated by assessing growth of *A. neopropionicum* on several carbon sources and contrasting the results with experimental data. Model predictions matched most of the growth phenotypes observed in cultivation experiments from this and previous studies (Table 4.2; full data is available in the git repository and Suppl. material § 4.8: Table S4.2).

Table 4.2 Growth phenotypes of *A. neopropionicum* on different substrates, predicted by the iANEO_SB607 model and observed in experiments from this and previous studies.

Substrates	iANEO_SB607	This study (exp.)	Tholozan et al. (1992)	Ueki et al. (2017)	Moreira et al. (2021)
Ethanol	+	+	+	+	+
Ethanol and acetate	+	+	+	NA	NA
Ethanol and alanine	+[a]	NA	NA	NA	+
Ethanol and serine	+[b]	NA	NA	NA	+
Pyruvate	+	NA	+	+	NA
D-Lactate	+	+	+	w[c]	NA
D-Glucose	+	+	+	-	NA
Xylose	+	+	+	+	NA
L-Threonine	+	NA	+	+	NA
L-Serine	+	NA	+	+	NA
L-Alanine	+	NA	+	+	NA
D-Alanine	+	NA	+	NA	NA
L-Valine	-	NA	-	w	NA
L-Leucine	-	NA	NA	w	NA
L-Isoleucine	-	NA	NA	w	NA
Lysine	-	NA	-	NA	NA
L-Proline	-	NA	-	-	NA

+ Growth; - No growth; w Weak growth; NA No available data. [a]L-Alanine. [b]L-Serine. [c](LD)-Lactate

The model predicts growth of *A. neopropionicum* on ethanol. Growth on xylose and on glucose is also predicted by the model and supported by experimental evidence, with exception of one study, which reported no growth of *A. neopropionicum* on glucose (Ueki et al., 2017). According to a previous work, *A. neopropionicum* can also grow on D-lactate, but not on L-lactate (Tholozan et al., 1992). In our batch cultivations with DL-lactate as substrate, we repeatedly observed that only ≈50% of the substrate was used. The purity of the L- enantiomer in the racemic mixture solution was, according to the manufacturer, 27 - 33%. This indicates that D-lactate is indeed used by *A. neopropionicum*, but it does not exclude the possibility that L-lactate is also metabolised. Yet, since the latter could not be confirmed, the model considers only the utilisation of D-lactate. The model predicts growth on pyruvate as well as on one pyruvate-derived amino acid, alanine. Serine also supports growth of *A. neopropionicum*, as predicted by the model and observed in cultivation experiments. The model indicates that branched-chain amino acids (valine, leucine and isoleucine) as well as TCA-derived amino acids (lysine and proline), with exception of threonine, are not utilised.
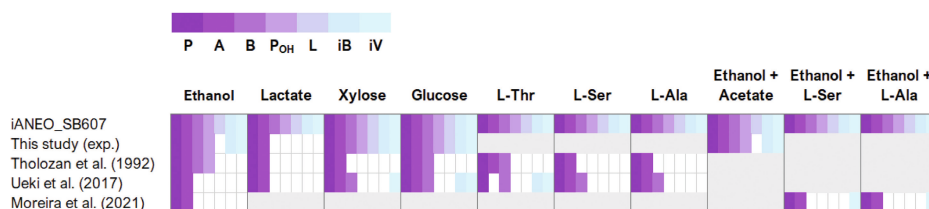
Figure 4.2 Product profile of the fermentation of different substrates by *A. neopropionicum*, predicted by the GEM iANEO_SB607 and observed in experiments from this and previous studies. P: Propionate; A: acetate; B: butyrate; P_{OH}: propanol; L: lactate; iB: isobutyrate and iV: isovalerate. White spaces indicate that the product is not reported produced. Grey areas indicate no available data.

Further model validation was performed by assessing the product profile on a number of substrates from which sufficient experimental data was available, specifically: ethanol, lactate, glucose, xylose, L-threonine, L-serine, L-alanine, ethanol plus acetate, ethanol plus L-serine and ethanol plus L-alanine. For all the substrates tested, the model predicted mixed secretion of propionate and acetate, in accordance with experimental evidence (Fig. 4.2; full data is available in the git repository and Suppl. material § 4.8: Table S4.2). Model analysis shows that secretion of product mixture is a requisite for energy generation and redox cofactor regeneration. The involved pathways and their stoichiometry are described in following sections.

Butyrate, propanol, lactate, isobutyrate and isovalerate are also predicted by the model as fermentation products in all cases, albeit in different proportions. Butyrate appears as a minor product in all the simulations and cultivation experiments, except for in the fermentation of L-threonine; in this case, the model predicts butyrate as a major end product, as previously reported (Ueki et al., 2017). According to model simulations and in agreement with our experimental data, lactate, an intermediate of the acrylate pathway, and propanol are produced in minor amounts. In batch cultivations carried out in this study, isobutyrate and isovalerate were detected as traces with ethanol (plus acetate), glucose or xylose as substrates, but not with lactate. The model predicted both products to be produced as traces with these substrates. Model simulations predicted enhanced

production of isobutyrate and isovalerate with ethanol plus L-valine and ethanol plus L-leucine as substrates, respectively (not shown), as observed in one study (Ueki et al., 2017). The model also predicted the production of isovalerate when L-alanine or L-serine are co-substrates with ethanol, which is in agreement with observations from a recent work (Moreira et al., 2021).

H_2 was not detected as product in any of the fermentations of *A. neopropionicum* carried out in this study (with substrates: ethanol (plus acetate), lactate, glucose, xylose). In addition, H_2 was not utilised nor affected the growth or the product profile of *A. neopropionicum* cultures growing on ethanol (Suppl. material § 4.8: Fig. S4.3). Previous works reported the same observations (Ato et al., 2014; Tholozan et al., 1992). A ferredoxin hydrogenase is annotated in the genome of *A. neopropionicum* (CLNEO_18070; EC 1.12.7.2; model id:'rxn05759_c0'); yet, given the collected evidence, this reaction was blocked in the model.

4.3.5   Quantitative assessment of iANEO_SB607 through dFBA

The iANEO_SB607 model of A. neopropionicum was evaluated quantitatively by simulating the dynamics of batch fermentation using dFBA. Three conditions were considered, with regard to the substrates present: 25 mM ethanol, 25 mM ethanol plus 10 mM acetate, and 25 mM ethanol plus 25 mM acetate. To constrain the model, we used empirical data of ethanol consumption, product formation and cell growth from cultivation experiments. The fermentation profiles obtained by dFBA were contrasted with the experimental data of batch incubations. Across cultivations, carbon balance was 85 - 96%, not completely closed likely due to the difficulty to accurately quantify CO_2 and to slight evaporation of ethanol in the bottles, as reported by others (Candry et al., 2018).

For the condition with only ethanol (and CO_2) as substrate, the time-course data obtained through dFBA accurately reproduced the fermentation profile, with only small deviations (Fig. 4.3). Exponential growth of *A. neopropionicum* began after a relatively short lag phase of ≈13 hours. During the exponential phase, ethanol was uptaken (together with CO_2; not shown) at an empirical maximum consumption rate ($q_{S,max}$) of 36.2±5.5 mmol ethanol g_{CDW}^{-1} h^{-1}. Modelled ethanol consumption fitted the experimental data with a small margin of error. Propionate and acetate were produced simultaneously during the exponential phase, at empirical maximum production rates ($q_{P,max}$ and $q_{A,max}$) of 12.0±0.1 mmol propionate g_{CDW}^{-1} h^{-1} and 8.6±0.5 mmol acetate g_{CDW}^{-1} h^{-1}, respectively. The production profile of propionate was well predicted by dFBA, estimating a final propionate concentration (10.9 mM) close to the experimental value (9.5 mM). However, dFBA predicted a final concentration of acetate (11.5 mM) moderately higher than experimentally observed (8.6 mM). The empirical maximum specific growth rate of A. neopropionicum (μ_{max}) was 0.082±0.006 h^{-1} (duplication time = 8.4 h), which was used to constrain the model. In incubations, the biomass concentration peaked (44.7 ± 1.3 mg_{CDW} L^{-1}) at ≈47 hours, and decreased afterwards. The simulation predicted a slightly deviated pattern of biomass formation during the exponential phase, and it did not predict the observed drop in the stationary phase. Yet, the predicted maximum biomass concentration (44 mg_{CDW} L^{-1}) matched the empirical value. Propanol (1.3 mM) and butyrate (1 mM) were detected as minor products in batch incubations; the evolution of both products was predicted correctly by the dFBA simulations. Traces of isobutyrate and isovalerate were also detected and predicted by dFBA (not shown).
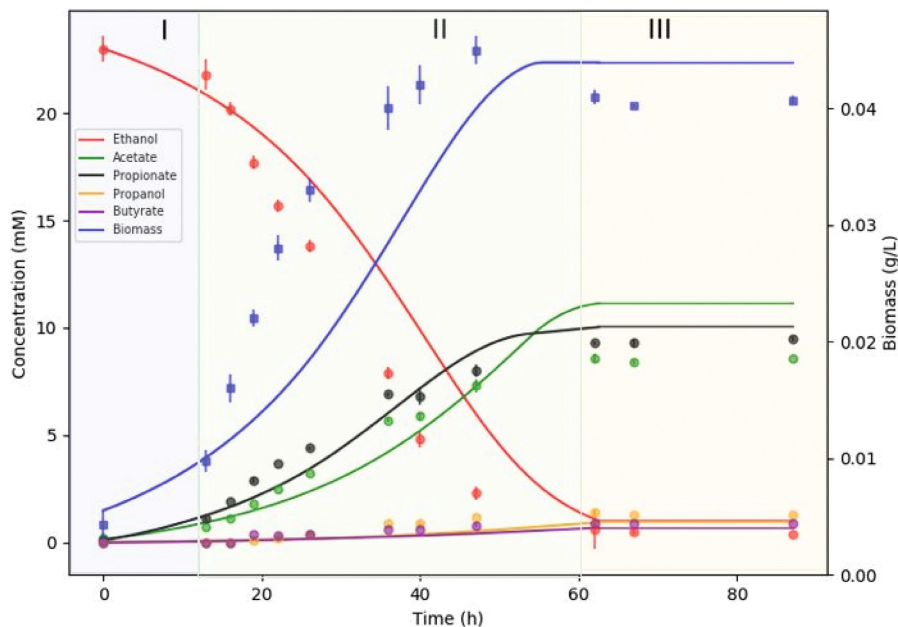
Figure 4.3 Fermentation of ethanol (25 mM) by *A. neopropionicum* in batch cultivation. Dots indicate experimental data, and lines indicate the result of dFBA. Background colours distinguish fermentation phases: lag (blue), exponential (green) and stationary (orange).

To further evaluate the ability of *A. neopropionicum* to upgrade dilute ethanol streams from syngas fermentation, we considered a scenario with ethanol and acetate as co-substrates. Acetate is produced by acetogens as a major product of autotrophic metabolism, and it is therefore found in variable proportions in syngas fermentation effluent. *A. neopropionicum* can utilise acetate in the presence of propanol (Samain et al., 1982) or ethanol (Tholozan et al., 1992) as electron donors. To investigate the effect of acetate as co-substrate on ethanol-fermenting cultures of *A. neopropionicum*, incubations were set up with ethanol (25 mM) and acetate (10 and 25 mM) as substrates, and dFBA was used to simulate the dynamics of these fermentations. dFBA reproduced with high accuracy the fermentation profile of incubations containing ethanol plus 10 mM acetate (Fig. 4.4). In this condition, the observed μ_{max} was 0.098 ± 0.005 h^{-1} (duplication time = 7.1 h); 19% higher than in the incubations without acetate. However, less biomass was formed in comparison; the maximum biomass concentration was 41.1 ± 0.8 mg$_{CDW}$ L^{-1} ($\approx$9% lower), which was also predicted by dFBA. The presence of 10 mM acetate also affected the consumption and production rates; ethanol consumption was faster than in the absence of acetate; the $q_{S,max}$ was 43.3 ± 4.3 mmol ethanol g$_{CDW}$$^{-1}$ h^{-1}, a 20 % increase. The $q_{A,max}$ in this condition dropped to 3.1 ± 0.6 mmol acetate g$_{CDW}$$^{-1}$ h^{-1}. The biggest difference was in the $q_{P,max}$, which was 16.4 ± 0.8 mmol propionate g$_{CDW}$$^{-1}$ h^{-1}, a 37% increase compared to the condition without acetate. The final propionate concentration was also slightly higher, 11.3 mM (vs. 9.5 mM). Here, again, the simulation predicted a similar propionate concentration to

the observed value (12.2 mM), and a higher final acetate concentration (18.3 mM) than observed (16.7 mM). The incubations containing 25 mM acetate at the start followed a different trend than the incubations with 10 mM acetate (fermentation profile not shown). In batch bottles, the biomass concentration reached a similar value to that obtained in the condition with 10 mM acetate, but the μ_{max}, $q_{P,max}$ and $q_{A,max}$ were similar to the condition without acetate (data not shown). The final propionate concentration was 12.5 mM, the highest of the three conditions tested.

The presence of acetate had an effect on the utilisation of ethanol by A. neopropionicum, which is reflected in the fermentation yields. The biomass yield (YX/S) was slightly lower in the presence of both 10 and 25 mM acetate (1.4 gCDW mol ethanol-1 vs. 1.6 gCDW mol ethanol-1 when no acetate was present).
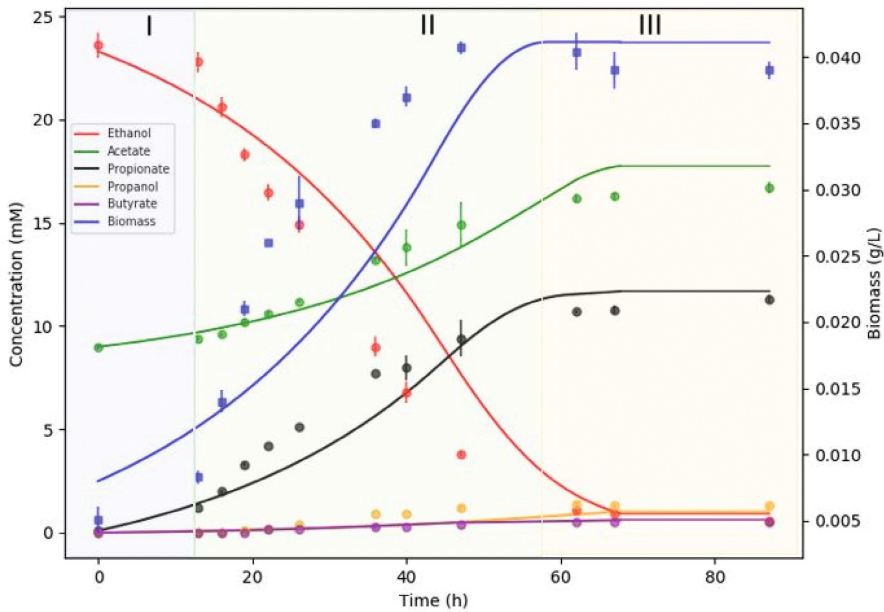

Figure 4.4 Fermentation of ethanol (25 mM) and acetate (10 mM) by *A. neopropionicum* in batch cultivation. Dots indicate experimental data and lines indicate the result of dFBA. Background colours distinguish fermentation phases: lag (blue), exponential (green) and stationary (orange).

With acetate present at the start of incubations, more ethanol was invested in propionate production, as indicated by the propionate yields ($Y_{P/S}$, mol mol-1), which were 0.33, 0.38 and 0.42 for the conditions with no acetate, 10 mM acetate and 25 mM acetate, respectively. The production of acetate followed the inverse trend; acetate yields ($Y_{A/S}$, mol mol-1) were 0.29, 0.18 and 0.06 for the conditions with no acetate, 10 mM acetate and 25 mM acetate, respectively. Similarly, lower yields were obtained for propanol and butyrate when acetate was present (data now shown).

4.3.6   Ethanol fermentation via the acrylate pathway

The reconstructed iANEO_SB607 model describes the metabolism of ethanol fermentation and propionate production via the acrylate pathway in *A. neopropionicum* (Fig. 4.5). Model simulations provided new insights into the enzymatic reactions involved in propionate formation, cofactor regeneration and the energy metabolism of the cell.

Ethanol is oxidised to acetyl-CoA via acetaldehyde through alcohol and acetaldehyde dehydrogenases. The genome of *A. neopropionicum* harbours a bifunctional NAD$^+$-dependent alcohol-aldehyde dehydrogenase (AdhE; CLNEO_13930) that can catalyse this two-step conversion. According to our model, two other alcohol dehydrogenases, encoded by *adh* (CLNEO_16910) and *adhB* (CLNEO_00480), could also drive the oxidation of ethanol to acetaldehyde. Initially, the model also predicted this reaction to be catalysed by NAD(P)H-dependent butanol dehydrogenase (BdhA), encoded by *bdhA* (CLNEO_09740; rxn00536_c0). However, the well-characterised BdhA of *C. acetobutylicum*, which shares 60.7% identity with that of *A. neopropionicum*, is known to contribute primarily to butanol production and it is the alcohol dehydrogenase least involved in ethanol metabolism (Dai et al., 2016). Thus, we reasoned that BdhA would likely not be involved in ethanol oxidation in *A. neopropionicum* and excluded this reaction from model simulations.
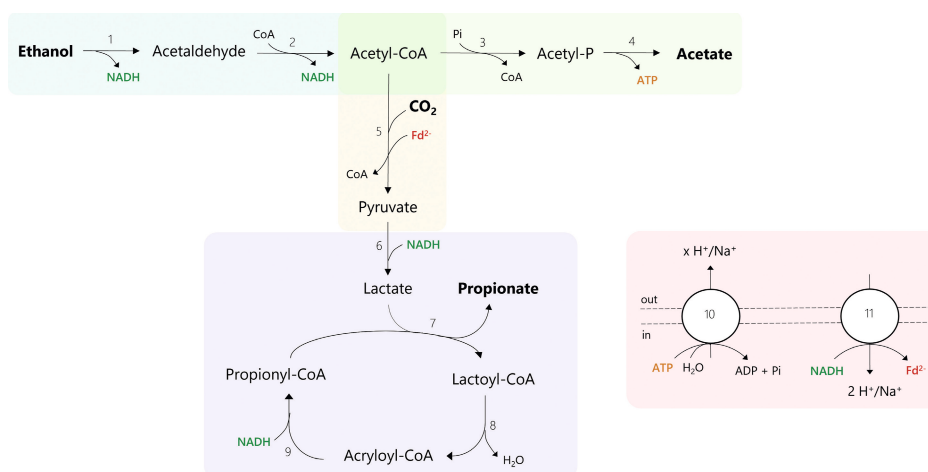
Figure 4.5 Proposed metabolism of ethanol fermentation to propionate via the acrylate pathway in *A. neopropionicum*. Coloured areas designate the following modules: ethanol oxidation (blue), acetate production (green), pyruvate synthesis (yellow), lactate production and acrylate pathway (purple), redox cofactor regeneration and ATPase (red). Numbers in reactions correspond to the following enzymes and reaction ids in the model: 1 and 2, aldehyde-alcohol dehydrogenase (rxn00543_c0 and rxn00171_c0); 3, phosphate acetyltransferase (rxn00173_c0); 4, acetate kinase (rxn00225_c0); 5, pyruvate:ferredoxin oxidoreductase (PFOR; rxn05938_c0); 6, NAD-dependent D-lactate dehydrogenase (rxn00500_c0); 7, propionate-CoA:lactoyl-CoA transferase (rxn01056_c0); 8, lactoyl-CoA dehydratase (rxn02123_c0); 9, acryloyl-CoA reductase (rxn40050_c0); 10, ATPase (rxn10042_c0); 11, Rnf complex (Rnf_c0).

Acetyl-CoA is partly used in the reductive reactions of the metabolism and partly invested in the formation of acetate, an energy-generating step. Acetate is synthesised via phosphate acetyl-

transferase (Pta; CLNEO_28570) and acetate kinase (Ack; CLNEO_28580), yielding ATP via substrate-level phosphorylation (SLP). In the reductive path, acetyl-CoA is converted to pyruvate through the CO_2-fixating reaction catalysed by pyruvate:ferredoxin oxidoreductase (PFOR; CLNEO_15240 or CLNEO_19010 or CLNEO_17780 or CLNEO_03040 or CLNEO_04330 or CLNEO_24550). This conversion requires reduced ferredoxin (Fd^{2-}) as electron carrier. Our hypothesis, supported by model predictions, is that Fd^{2-} is produced in the Na^+-translocating ferredoxin:NAD^+ oxidoreductase (Rnf) complex. The Rnf complex is a membrane-bound respiratory enzyme involved in energy conservation in anaerobic microorganisms (Buckel & Thauer, 2018b). During growth on high-energy substrates, it catalyses the exergonic reduction of NAD^+ with electrons from Fd^{2-} coupled to the translocation of two cations (H^+ or Na^+) across the membrane. The electrochemical potential established by the Rnf complex can then be used by a membrane-bound ATP synthase for energy generation. The Rnf complex can also operate in the reverse direction to produce Fd^{2-} at the expense of ATP (Westphal et al., 2018).

The genome of *A. neopropionicum* harbours a complete *rnf* cluster, composed of the genes *rnfA* (CLNEO_01390), *rnfB* (CLNEO_01400), *rnfC* (CLNEO_01350), *rnfD* (CLNEO_01360), *rnfE* (CLNEO_01380) and *rnfG* (CLNEO_01370). With ethanol as substrate, our assumption is that the Rnf complex of *A. neopropionicum* operates in reverse, generating Fd^{2-}. The endergonic reduction of ferredoxin (E_0'= -500 to -420 mV) with NADH (E_0'= -320 mV) is driven by reverse electron transport across the membrane which, in turn, is an energy-driven process. A membrane-bound V-type ATPase is present in the genome of *A. neopropionicum*, encoded by the genes *atpA/ntpA* (CLNEO_280), *atpB/ntpB* (CLNEO_290), *ntpC*, (CLNEO_260), *atpD/ntpD* (CLNEO_23400), *atpE* (CLNEO_250), *ntpG* (CLNEO_270), *ntpK* (CLNEO_240) and *ntpI* (CLNEO_23330). We theorise that ATP is hydrolysed in the ATPase to create a proton- or sodium motive-force that is used by the Rnf complex to catalyse the reduction of ferredoxin. The production of Fd^{2-} is an energy costly process, the implications of which are addressed later in this section.

Pyruvate produced by the PFOR is subsequently reduced to lactate with NADH via D-lactate dehydrogenase (CLNEO_28010). We assumed NADPH is not used as electron carrier in this reaction, since lactate dehydrogenases have a strict specificity for NAD^+/ NADH (Garvie, 1980; Zhu et al., 2015). Lactate then enters the acrylate pathway, a cyclic chain of reactions involving the intermediates lactoyl-CoA, acryloyl-CoA and propionyl-CoA. The characteristic enzyme of this pathway is propionate-CoA:lactoyl-CoA transferase (Pct, EC 2.8.3.1), which exchanges the CoA moiety between propionyl-CoA and lactate, generating lactoyl-CoA and propionate as end product (Piwowarek et al., 2018; Selmer et al., 2002). Our first annotation of the genome of *A. neopropionicum* did not include Pct. However, an acetate CoA-transferase was present, encoded by the gene *ydiF* (CLNEO_17700), that shared 96% identity with the purified and well-characterised Pct of *A. propionicum* (Selmer et al., 2002). Thus, we deduced that *ydiF* encodes for Pct in *A. neopropionicum* and included this reaction in the model. Lactoyl-CoA dehydratase (CLNEO_17710 and CLNEO_17720) catalyses the dehydration of lactoyl-CoA to acryloyl-CoA, which is subsequently reduced to propionyl-CoA by acryloyl-CoA reductase. Our genome annotation revealed that the acryloyl reductase of *A. neopropionicum* forms an enzymatic complex with an electron-transferring flavoprotein (EtfAB). The complex, hereafter named acryloyl-CoA reductase-EtfAB (Acr-EtfAB), is also present and has been well characterised in *A. propionicum* (Hetzel et al., 2003). Three gene

clusters predicted to encode for acryloyl-CoA reductase (*acrC*) or EtfAB (*acrA*, *acrB*) were found in the genome: (i) CLNEO_21740 (*acrC*), CLNEO_21750 (*acrB_1*) and CLNEO_21760 (*acrA*); (ii) CLNEO_26130 (*acdA_1*) and CLNEO_26120 (*acrB_2*); and (iii) CLNEO_29850 (*acdA_2*) and CLNEO_29840 (*acrB_3*). The *acdA_1* and *acdA_2* genes encode for acyl-CoA dehydrogenases that share low identity (46% and 54%, respectively) with the acryloyl-CoA reductase encoded by *acrC*; thus, we assumed that the former two enzymes are not responsible for acryloyl-CoA reductase activity. The first cluster is the only complete one, composed of acryloyl-CoA reductase (*acrC*) and the A (*acrA*) and B (*acrB_1*) subunits of EtfAB. The proteins encoded by these three genes share an identity of 92.9%, 89.% and 89.1%, respectively, with their homologues from the Acr-EtfAB complex of *A. propionicum*. The Acr-EtfAB of *A. propionicum* is a non-bifurcating soluble enzyme that catalyses the irreversible reduction of acryloyl-CoA to propionyl-CoA with NADH via electron transfer to a flavin moiety and appears not to be involved in energy conservation (Hetzel et al., 2003; Seeliger, 2002). Given their high similarity, we deduced the same features apply to the Acr-EtfAB of *A. neopropionicum*. To our knowledge, this is the first time that the Acr-EtfAB complex is identified in this microorganism.

According to the theoretical stoichiometry, the fermentation of ethanol yields propionate and acetate in a 2:1 ratio (Eq. 1). However, this ratio is not observed in cultures of *A. neopropionicum*; rather, ethanol fermentation resulted in a ≈1.2:1 propionate to acetate ratio (Fig. 4.3 and Suppl. material § 4.8: Table S4.2). We reasoned that the theoretical ratio cannot be achieved in *A. neopropionicum* due to energetic constraints of the cell, specifically, due to the requirement of Fd^{2-}. Model simulations were performed to confirm this. The oxidation of three moles of ethanol generates six moles of NADH and three moles of acetyl-CoA. To fit the theoretical 2:1 propionate to acetate ratio, two moles of acetyl-CoA would have to be used in the reductive part of the metabolism, and one mole of acetyl-CoA should be invested in acetate, with the concomitant production of one mole of ATP via SLP. The synthesis of two moles of pyruvate from acetyl-CoA would require two moles of Fd^{2-}, which is produced at the Rnf complex at the expense of ATP. However, the hydrolysis of one mole of ATP (ΔG^o = -32 kJ mol^{-1}; [Thauer et al., 1977]) could drive the reduction with NADH of no more than ≈1.3 moles of ferredoxin (ΔG^o = -25 kJ mol^{-1}; [Schuchmann & Müller, 2014[). Moreover, two other issues arise: i) even if this one mole of ATP would solely be invested in the reduction of ferredoxin, this would leave no net ATP for growth, and ii) such a scenario would result in excess reducing equivalents from ethanol oxidation that could not be recycled in the production of propionate.

Our model predictions confirmed these inconsistencies and is in agreement with the hypothesis that the propionate to acetate 2:1 ratio cannot be achieved in A. *neopropionicum* during the fermentation of ethanol. Instead, cells must invest more than one mole of acetyl-CoA in acetate production to obtain net ATP to support growth. This leaves less than two moles of acetyl-CoA available for propionate production and, overall, a propionate to acetate ratio lower than the theoretical 2:1. The actual propionate to acetate ratio (close to 1.2:1, based on the fermentation balance) depends on how much Fd^{2-} can be produced per hydrolysed ATP, which in turn depends not only on the Gibbs free energies of ATP hydrolysis and ferredoxin reduction with NADH under physiological conditions but also on the coupling ratio of the ATPase (number of cations translocated per ATP hydrolised). While the Rnf complex can be assumed to translocate two cations per ferredoxin reduced/oxidised,

the coupling ratio of the ATPase remains unknown for *A. neopropionicum*. Our model fitted with a coupling ratio of the ATPase of 3 to 3.5 H$^+$ or Na$^+$ translocated per ATP.

4.3.7   Propanol and butyrate production pathways

A. neopropionicum produces propanol and butyrate as minor products of the fermentation of several substrates (Fig. 4.2). Propanol is formed from propionyl-CoA via propionaldehyde in a two-step reductive conversion catalysed by AdhE (Fig. 4.6). Reduction of propionaldehyde could also be catalysed by NAD$^+$-dependent alcohol dehydrogenases *adh* (CLNEO_16910) and *adhB* (CLNEO_00480).
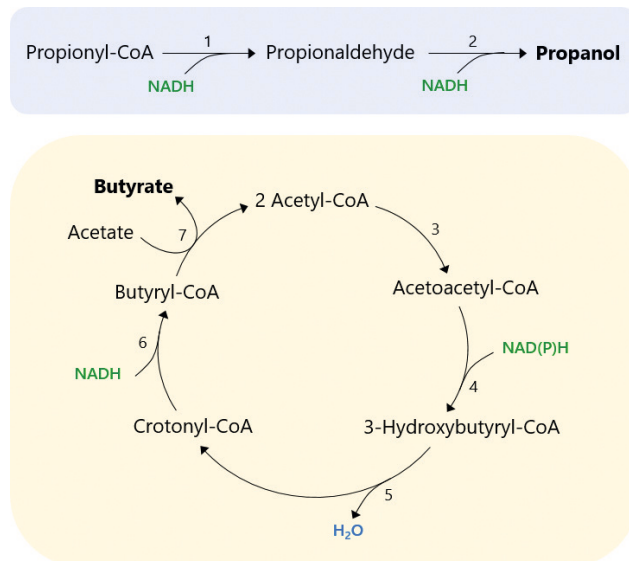
Figure 4.6 Putative pathways for the production of propanol (blue) and butyrate (orange) in *A. neopropionicum*. Numbers in reactions correspond to the following enzymes as annotated in the genome, and reaction ids in the model: 1 and 2, aldehyde-alcohol dehydrogenase (rxn09944_c0 and rxn01710_c0); 3, acetoacetyl-CoA thiolase (rxn00178_c0); 4, 3-oxoacyl reductase (rxn03861_c0); 5, 3-hydroxyacyl dehydratase (rxn03874_c0); 6, acryloyl-CoA reductase-EtfAB (rxn00868_c0) or acyl-CoA dehydrogenase-EtfAB; 7, propionate-CoA:-lactoyl-CoA transferase (rxn00875_c0).

Butyrate production in *A. neopropionicum* takes place via the acetyl-CoA pathway (Fig. 4.6). In this pathway, acetyl-CoA is first converted to butyryl-CoA, which eventually yields butyrate. Most enzymes of the pathway were either present in the genome, were assigned during the re-annotation or were identified through protein sequence alignment. Only one enzyme was not found: acetoace-tyl-CoA thiolase (EC 2.3.1.9), which catalyses the condensation of two molecules of acetyl-CoA to form acetoacetyl-CoA. However, since the rest of genes of the pathway were identified (Suppl. material § 4.7), we added this reaction to the model during the gap-filling process.

A key enzyme of this pathway is the butyryl-CoA dehydrogenase/electron-transferring flavopro-tein complex (Bcd-EtfAB). Bcd-EtfAB is an electron-bifurcating enzyme that couples the reduction

of crotonyl-CoA to butyryl-CoA (E_0'= -10 mV) by NADH to the endergonic reduction of Fd by NADH (Buckel & Thauer, 2018b). Our model predicts that, in *A. neopropionicum*, reduction of crotonyl-CoA could be catalysed by the Acr-EtfAB complex or by either of the two acyl-CoA dehydrogenases that cluster with subunits of the EtfAB complex (*acdA_1-acrB_2* and *acdA_2-acrB_3*). Among the three, the acyl-CoA dehydrogenase encoded by *acdA_2* showed the highest identity with the butyryl-CoA dehydrogenases (Bcd) of *C. acetobutylicum* and of *C. kluyveri* (64% and 63%, respectively). It remains a question whether, in *A. neopropionicum*, the latter two complexes could be involved in the reduction of ferredoxin.

Two distinct routes have been described for the last step of the pathway, the conversion of butyryl-CoA to butyrate. The first route, identified in *C. acetobutylicum* (Walter et al., 1993), involves phosphate butyryltransferase (Ptb; EC 2.3.1.19) and butyrate kinase (Buk; EC 2.7.2.7) and yields ATP via SLP. The second route relies on butyryl-CoA:acetate CoA-transferase (But; EC 2.8.3.8). Co-occurrence of both pathways is rare among butyrate producers (Vital et al., 2014). The genome of *A. neopropionicum* does not encode for Ptb nor Buk, yet our annotation initially assigned these activities to phosphate acetyltransferase (Pta) and acetate kinase (Ack). The Ack of *A. neopropionicum* is significantly similar to the well-characterised Buk (71% identity) of *C. acetobutylicum*. We have considered this similarity to arise from the fact that the two enzymes belong to the same family, yet it has been established that they do not have the same function, since differences in the substrate binding site ultimately determine substrate specificity (Anand et al., 2016; Simanshu et al., 2005; Sullivan et al., 2010). Thus, we assumed that Pta and Ack are not involved in butyrate production in *A. neopropionicum*. Instead, we hypothesise that butyrate production in *A. neopropionicum* takes place via butyryl-CoA:acetate CoA-transferase activity. Our model predicts that the propionate-CoA:lactoyl-CoA transferase (Pct) encoded by the gene ydiF catalyses this reaction. The Pct of *A. propionicum* exhibits broad substrate specificity for monocarboxylic acids, including butyrate, supporting the model prediction (Selmer et al., 2002).

4.3.8 Identification of the NADH-dependent reduced ferredoxin:NADP+ oxidoreductase (Nfn)

During the genome re-annotation and manual curation process, we identified the enzyme NADH-dependent reduced ferredoxin:NADP$^+$ oxidoreductase (Nfn). Nfn is an iron-sulphur flavoprotein complex with electron confurcating/bifurcating activity that reversibly catalyses the endergonic reduction of NADP$^+$ by NADH coupled with the exergonic reduction of NADP$^+$ by Fd^{2-} (Liang et al., 2019). Nfn is composed of two subunits, NfnA and NfnB, whose coding genes were both found in the genome of *A. neopropionicum* under the locus tags CLNEO_00270 and CLNEO_00280, respectively. In the initial automatic annotation, these two genes were assigned to ferredoxin:NADP$^+$ oxidoreductase and glutamate synthase, respectively. It has been reported that NfnA/B share sequence similarities with these two enzymes (Liang et al., 2019). Upon manual inspection, we observed that the protein complex showed a significant identity (60-66 %) with the Nfn complexes of *C. kluyveri* (Wang et al., 2010) and of *C. autoethanogenum* (Wang et al., 2013), which lead us to the re-assignation of the two proteins as NfnA and NfnB.

We used modelling to look into the role of the Nfn complex in the metabolism of *A. neopropionicum* during growth on ethanol. The model shows that the Nfn generates NADPH from NADH

and Fd^{2-} for NADPH-dependent reactions of the cell. For instance, NADPH is required during butyrate production in the reduction of acetoacetyl-CoA to 3-hydroxybutyryl-CoA, a reaction catalysed by a NADPH-dependent 3-oxoacyl reductase. NADPH is also required in the biosynthesis of amino acids and biomass precursors. In our model, the Nfn complex does not function in the reverse direction, the production of Fd^{2-}, during growth on ethanol; this would require NADPH, and ethanol oxidation is assumed to occur only via NAD$^+$-dependent reactions.

4.3.9   Fermentation of other carbon sources: the case of lactate

Besides ethanol, *A. neopropionicum* can grow on lactate, sugars and some pyruvate-derived amino acids (Table 4.2). The fermentation of these carbon sources proceeds with key differences compared to the fermentation of ethanol. To illustrate this with an example, we used the model to describe the case of lactate fermentation, since lactate is a typical substrate of propionate-producing bacteria and, in particular, of species that use the acrylate pathway (Piwowarek et al., 2018; Reichardt et al., 2014). Lactate is metabolised in both oxidative and reductive reactions. In the oxidative branch, lactate is oxidised to pyruvate via lactate dehydrogenase, generating NADH. PFOR then catalyses the decarboxylation of pyruvate to acetyl-CoA and CO$_2$, a reaction that generates Fd^{2-}. The PFOR reaction is reversible; here, it functions in the opposite direction to what occurs with ethanol as substrate. This enables the utilisation of lactate, sugars and pyruvate-derived amino acids. This implies that, contrary to the fermentation of ethanol, the oxidation of these substrates generates directly Fd^{2-}, which can contribute to energy conservation. Acetyl-CoA is used for acetate production via Pta and Ack, yielding ATP via SLP. In the reductive branch, lactate is converted to propionate via the reactions of the acrylate pathway. In this conversion, NADH is needed for the reduction of acryloyl-CoA to propionyl-CoA, but the amount of NADH obtained in the oxidation of lactate is insufficient. Our model predicts that additional NADH is produced in the Rnf complex. Opposite to the scenario with ethanol as substrate, here the Rnf catalyses the exergonic reduction of NAD$^+$ with electrons from Fd^{2-}. This reaction is coupled to the translocation of two cations across the membrane, generating an ion-motive force that can be used by the ATPase to produce ATP. Thus, in the fermentation of carbon sources other than ethanol, ATP is generated both by SLP via acetate production and by chemiosmosis driven by the oxidation of Fd^{2-}.

4.4   Discussion

In this study, we have presented iANEO_SB607, the first GEM of the propionate-producer *A. neopropionicum*. The overall Memote score of 72% indicates the high quality of the model. The low score of gene annotation per database (33%) was expected, since there were almost no available annotations of the genome of *A. neopropionicum* in public databases recognised by Memote. A limitation of the GEM is the lack of an organism-specific biomass composition and GAM/NGAM measurements. Our sensitivity analysis showed a maximum deviation of 10.8% of the growth rate when varying the composition of biomass components or the GAM. NGAM has a more limited impact on growth rate predictions, given that it does not directly relate to the biomass synthesis reaction, still dedicated measurements of these parameters could further improve the predictive

power of the model. Here, our focus has been on gaining insight into the metabolism of ethanol fermentation to propionate, which in this bacterium occurs via the acrylate pathway.

We have also addressed an important issue regarding the energetic metabolism of *A. neopropionicum*. During growth on ethanol, Fd^{2-} is required to reduce acetyl-CoA to pyruvate. In the earliest description of the metabolism of *A. neopropionicum*, authors suggested that the oxidation of acetaldehyde proceeded with ferredoxin as electron carrier, thus fulfilling this demand (Tholozan et al., 1992). However, at the present time it is acknowledged that aldehyde dehydrogenases are NAD(P)-dependent enzymes (Shortall et al., 2021), which invalidates that theory. Theoretically, the Acr-EtfAB complex could drive the reduction of Fd (E_0'= -500 to -420 mV) with NADH (E_0'= -320 mV) via electron bifurcation, given the high reduction potential of the acryloyl-CoA/propionyl-CoA pair (E_0'= +70 mV). Yet, this complex appears not to be involved in the reduction of ferredoxin (Hetzel et al., 2003), most likely to prevent transient accumulation of the very reactive intermediate acryloyl-CoA (Buckel & Thauer, 2013; Buckel & Thauer, 2018a). Instead, our model predicted that Fd^{2-} is produced in the Rnf complex, as previously reported for other anaerobes during growth on low-energy substrates (Westphal et al., 2018). The Rnf complex had been previously identified in the close relative *A. propionicum* (Poehlein et al., 2016). Here, through the re-annotation an a thorough manual curation process, we identified all its subunits (*rnfA-E*, *rnfG*) and via modelling we verified its involvement in the metabolism of the cell.

Our annotation of the genome *of A. neopropionicum* revealed the presence of another key enzyme of the metabolism of anaerobes: the Nfn complex. Our model showed that the Nfn generates NADPH for NADPH-dependent reactions of the metabolism, which is essential during growth. Further investigation is needed to define the instances in which the Nfn operates in the reverse direction, bifurcating electrons from NADPH to produce Fd^{2-} and NADH. The directionality and role of Nfn will depend on the cofactor requirements of the cell.

Butyrate and propanol are produced by *A. neopropionicum* as minor products during the fermentation of several substrates (Fig. 4.2), probably as a means to dispose of excess reducing equivalents generated during substrate oxidation. Our model showed that propanol is produced from propionyl-CoA with propionaldehyde as intermediate via NAD^+-dependent reactions, as Tholozan et al. (1992) suggested. The butyrate production pathway had not been described yet in this microorganism and further research is needed to confirm whether Pct is indeed involved in this pathway as observed in vitro in *A. propionicum* (Selmer et al., 2002) and *Escherichia coli* K-12 (Rangarajan et al., 2005).

Another aspect of the metabolism that we aimed to clarify was the ability of *A. neopropionicum* to produce and consume H_2. In our batch cultivations on different substrates, H_2 was not produced nor consumed, as previously reported (Tholozan et al., 1992). Our results also confirm that neither the product profile nor the growth of ethanol-growing cultures of *A. neopropionicum* are affected by the presence of H_2 (Suppl. material § 4.8: Fig. S4.3). This is an advantageous trait when considering this strain for its application in syngas-fermenting co-cultures, since syngas contains H_2. Interestingly, H_2 tolerance is manifested differently in functionally-related strains. While *P. propionicus* and *D. propionicus* both use the methylmalonyl pathway to metabolise ethanol, the first is not affected by the presence of H_2 while the second is strongly inhibited by it (Schink et al., 1987).

The GEM iANEO_SB607 accurately reproduced observed growth phenotypes on typical sub-strates (ethanol, sugars, lactate and amino acids). For glucose and xylose, model predictions agree with our batch incubations that *A. neopropionicum* can utilize these sugars (Suppl. material § 4.8: Table S4.2). These analyses solve contradictions in literature most likely attributable to differences in media compositions across studies (Choi et al., 2019; Tholozan et al., 1992; Ueki et al., 2017; van der Wielen, 2002). Our results also indicate that D-lactate, and not L-lactate, support growth of *A. neopropionicum*, as previously observed (Tholozan et al., 1992). Yet, the latter authors reported lactate dehydrogenase activity in cell-free extracts with D-, L- and DL-lactate, and hypothesised the presence of a lactate racemase which is absent in our annotated genome. However, *A. neopropionicum* has both L- and D-lactate dehydrogenases, so it cannot be excluded that L-lactate is also metabolised, perhaps at a much slower rate (Moazeni et al., 2010).

dFBA simulations showed good agreement with the dynamics of ethanol (and ethanol plus ace-tate) fermentation by *A. neopropionicum* in batch cultivation (Fig. 4.3 and Fig. 4.4). With ethanol as substrate, the theoretical 2:1 molar ratio of propionate to acetate (Eq. 4.1) was not achieved; instead, this ratio was ≈1.2:1 (Fig. 4.3 and Suppl. material § 4.8: Table S4.2), matching previous observations (Tholozan et al., 1992; Ueki et al., 2017). The model helped clarify this aspect. During growth on ethanol, ATP is solely produced via SLP. Net ATP generation required to sustain growth and to drive ferredoxin reduction needed by PFOR appear as the main cause of the observed propionate to acetate ratio of 1.2:1. In addition, cells might favour acetate over propionate synthesis to prevent accumulation of acryloyl-CoA (Buckel & Thauer, 2018a). Finally, propanol production at the end of the fermentation, likely to halt further acidification of the environment, also contributes to decrease the propionate to acetate ratio observed in batch cultures.

Interestingly, we observed that a low acetate concentration (<25 mM) or low acetate:ethanol ratio (<1) at the start boosted the growth rate and propionate production rate of *A. neopropionicum* during growth on ethanol. However, despite higher rates, final biomass concentrations in batch cultivations were slightly lower in the presence of acetate (10 or 25 mM). Our model showed in-crease flux through acetate:CoA ligase (*acs*; EC 6.2.1.1) in the presence of acetate (10 mM). This reaction assimilates acetate consuming ATP, which would explain the lower biomass concentra-tions observed. Model predictions showed that, in this scenario, more acetyl-CoA is converted to pyruvate through PFOR, which is another energy-consuming step. We also observed a higher flux through butanoyl-CoA:acetate CoA-transferase (catalysed by Pct). Batch cultivation experiments did not show a noticeable increase in butyrate concentration when acetate was present, rather lower. Therefore, we hypothesise that, *in vivo*, most acetate consumed is assimilated via acetate:CoA ligase, as our model predicts, or via reverse direction of PTAr and ACKr, instead of Pct. This deviation to the model is likely due to the fact that biomass synthesis was set as maximization objective in dFBA which would be achieved by a higher flux of acetate towards butyrate instead of assimilating it, saving ATP.

Overall, this work shows the advantages of using a model-driven approach to gain insight into the metabolism of microorganisms. The new findings fill in knowledge gaps and unravel key met-abolic features of *A. neopropionicum*. As a result, this study means a step forward to further exploit this species as a cell factory for propionate production in mono-culture or in co-cultivation from sustainable feedstocks, e.g., syngas, as recently stated by Moreira et al. (2021). Additionally, *A.*

4

neopropionicum can act as an intermediate species to extend the range of products from propionate to longer odd-chain carboxylic acids.

4.5   Conclusions

In this study, we have constructed iANEO_SB607, the first GEM of *A. neopropionicum*. Combining experimental data with a manual curation of the annotated genome and a comprehensive network reconstruction, we have gained insight into the central carbon and energetic metabolism of this microorganism. The model predicted the metabolic capabilities of *A. neopropionicum* with high accuracy, which allowed us to investigate with detail the enzymatic routes involved in the fermentation of ethanol to propionate. Our analysis showed that *A. neopropionicum* produces propionate via propionate-CoA:lactoyl-CoA transferase, the characteristic enzyme of the acrylate pathway. Our in silico analysis revealed, for the first time in this microorganism, the presence of the electron-bifurcating Nfn complex. This model provides the basis to explore the capabilities of *A. neopropionicum* as microbial platform for the production of propionate from dilute ethanol as substrate. While beyond the scope of this study, the construction of this model signifies a step closer towards the development of multi-species models that describe syngas-fermenting co-cultures comprised of acetogens with ethanol-consuming propionigenic bacteria. Follow-up studies that integrate, e.g., omics analyses with data from steady-state fermentations should help improve this GEM.

4.6   Acknowledgements

4.7   Availability of data and materials

All the supplementary information and the data generated in the present study are available in the following Gitlab repository: https://gitlab.com/wurssb/Modelling/ Anaerotignum_neopropionicum.

Supplementary Tables and Figures are presented hereafter (§ 4.8).

The list of genes and homologs of the acrylate and butyrate pathways found in other *Clostridium* species can be found in the Gitlab repository.

4.8   Supplementary material
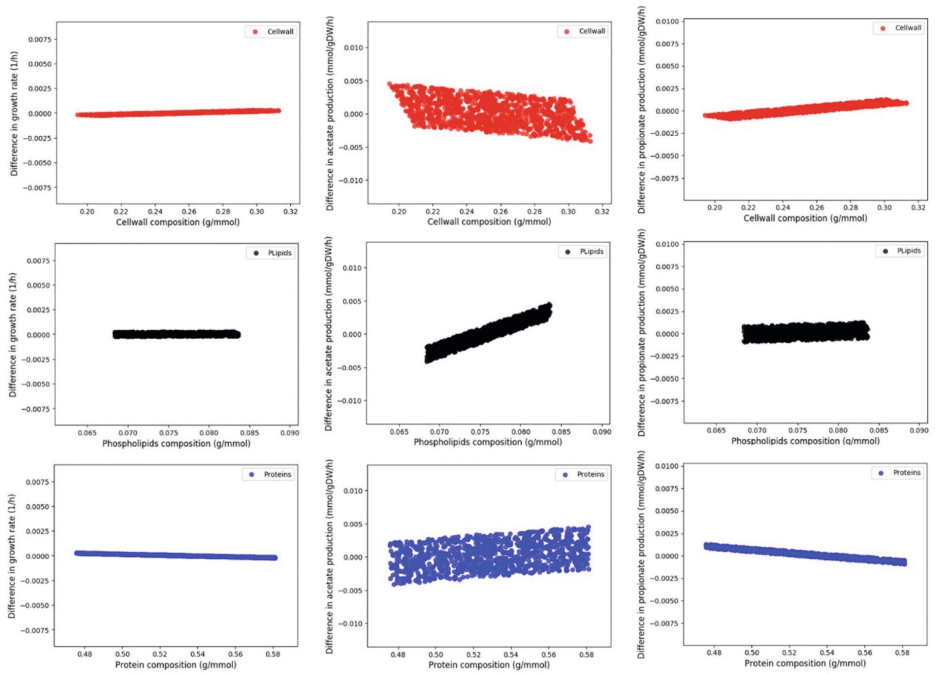
Figure S4.1 Sensitivity analysis of the biomass reaction. Effect of varying the composition of main biomass building blocks on the growth rate and product formation. Growth rate and product formation are represented as the difference between the values obtained when the new biomass reaction is defined as objective function and the values obtained when the original biomass synthesis reaction is defined as objective function.
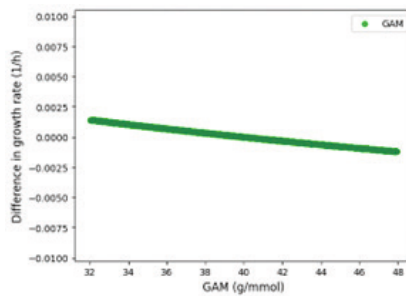
Figure S4.2 Effect of varying the growth-associated maintenance (GAM) of the biomass composition on the growth rate. The effect is represented as the difference between the values obtained when the new biomass reaction is defined as objective function and the values obtained when the original biomass synthesis reaction is defined as objective function.

Table S4.3 Parameters used to simulate batch fermentations through dFBA. Column 'Source' indicates whether the parameter was constrained based on the experimental value (considering standard deviation error) or by model fitting.

Parameter				
Ethanol fermentation (Fig. 4.3)	**Symbol**	**Value**	**Units**	**Source**
Initial biomass concentration	X_0	0.0055	$g\,L^{-1}$	Exp. Value
Initial Ethanol concentration	$S_{eth,0}$	23	mM	Exp. Value
Initial Acetate concentration	$S_{ac,0}$	0.15	mM	Exp. Value
Initial propionate concentration	$S_{prop,0}$	0.09	mM	Exp. Value
Initial butyrate concentration	$S_{but,0}$	0	mM	Exp. Value
Initial propanol concentration	$S_{ppoh,0}$	0	mM	Exp. Value
Maximum growth rate	μ_{max}	0.082	h^{-1}	Exp. Value
Michaelis-Menten constant for ethanol	$Km_{,etoh}$	11	mM	Fitting (≈exp. value)
Maximum ethanol uptake	$q_{etoh,max}$	36.5	mM	Exp. Value
Ethanol + Acetate fermentation (Fig. 4.4)				
Initial biomass concentration	X_0	0.008	$g\,L^{-1}$	Fitting (~ exp. value)
Initial Ethanol concentration	$S_{eth,0}$	23.3	mM	Exp. Value
Initial Acetate concentration	$S_{ac,0}$	9	mM	Exp. Value
Initial propionate concentration	$S_{prop,0}$	0.1	mM	Exp. Value
Initial butyrate concentration	$S_{but,0}$	0	mM	Exp. Value
Initial propanol concentration	$S_{ppoh,0}$	0	mM	Exp. Value
Maximum growth rate	μ_{max}	0.098	h^{-1}	Exp. Value
Michaelis-Menten constant for ethanol	$Km_{,etoh}$	14	mM	Fitting (≈exp. value)
Maximum ethanol uptake	$q_{etoh,max}$	43.6	mM	Exp. Value
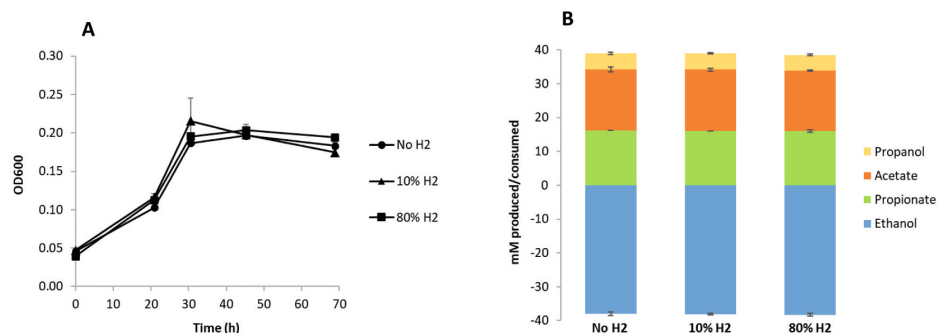
Figure S4.3 Effect of H2 on ethanol-growing cultures of A. neopropionicum. **a)** Cell growth profiles, determined by optical density at 600 nm (OD600). **b)** End products and ethanol consumed at the end of batch fermentations. Error bars indicate the standard deviation of biological triplicates.

Table S4.2 Fermentation balance of batch cultures of *A. neopropionicum* cultivated on different substrates. Note that CO_2, present in the headspace of bottles, is consumed but not included in this table.

Substrate[a]	Substrate consumed (mM)	Products (mM)						
		Propionate	Acetate	Propanol	Butyrate	Lactate	iBut	iVal
Ethanol	22.5±0.6	9.5±0.1	8.6±0.0	1.3±0.0	0.9±0.0	ND	traces	traces
Ethanol + Acetate[b]	23.0±0.5	11.3±0.2	16.7±0.3	1.2±0.1	0.5±0.0	ND	traces	traces
Ethanol + Acetate[c]	23.0±0.3	12.5±0.2	28.7±0.4	0.8±0.1	0.3±0.0	ND	traces	traces
DL-Lactate	13.5±1.2	8.7±0.5	6.2±0.4	ND	ND	ND	ND	ND
Glucose	13.1±1.4	11.3±0.2	8.7±0.1	traces	1.4±0.0	0.9±0.0	traces	traces
Xylose	18.5±0.9	15.0±0.7	11.0±0.3	traces	1.1±0.1	2.9±0.2	traces	traces

iBut: isobutyrate; iVal: isovalerate. ND: not detected. Traces are concentrations <0.2 mM. [a]Except for acetate, all other substrates were added at a concentration of 25 mM. [b]Concentration of acetate was 10 mM. The concentration of substrate consumed corresponds to ethanol. [c]Concentration of acetate was 25 mM. The concentration of substrate consumed corresponds to ethanol.

4

Carbon monoxide conversion to medium-chain carboxylic acids and higher alcohols using a Clostridial tri-culture

—

Ivette Parera Olm*, Sara Benito-Vaquerizo*, Charles Dubaere, Vitor Martins dos Santos, Maria Suarez-Diez, Diana Z. Sousa

*Authors contributed equally.

Abstract

Microbial conversion of biomass-derived C1 feedstocks offers a sustainable approach for the production of chemicals. In this context, synthetic co-cultures of Clostridia species have emerged as promising microbial systems for the production of medium-chain carboxylic acids and alcohols from syngas ($CO/H_2/CO_2$). Here, we investigated the co-cultivation of the acetogenic, carboxydotrophic bacterium *Acetobacterium wieringae* strain JM with *Anaerotignum neopropionicum* and *Clostridium kluyveri* for the production of odd- and even-chain carboxylates from CO. The tri-culture successfully produced C4 to C6 products, including pentanol (C5), an odd-chain higher alcohol that has not been previously reported in a syngas fermentation. Production of alcohols could be attributed to *A. wieringae* JM, which is able of CO-driven reduction of the C3–C6 carboxylic acids produced by *A. neopropionicum* and *C. kluyveri* in the co-culture. Chemostat experiments showed that the activity of the ethanol-consuming species, *i.e.*, *A. neopropionicum* and *C. kluyveri*, stimulates ethanol production by the acetogen *A. weringae* JM. Furthermore, we constructed the first genome-scale metabolic model (GEM) of *A. wieringae* JM (iAWJM_SB617) and integrated the GEMs of all three species to construct a multi-species community model of the tri-culture. Model simulations using community flux balance analysis predicted that maintaining a balanced community in terms of biomass-species ratio, along with low dilution rates (<0.03 h^{-1}, or hydraulic retention times >33.3 h), is essential for the feasibility of the tri-culture in steady-state. Additionally, the addition of H_2 to cocultures was predicted to decrease acetate accumulation and stimulate the production of the longer-chain compounds. Our work contributes to the advancement of synthetic co-cultures as novel platforms for CO/syngas fermentation, and highlights the value of modelling approaches for bioprocess design and optimisation.

5.1 Introduction

The fermentation of CO-rich gases to produce biocommodities, including chemicals, fuels and materials, has gained significant momentum (Köpke & Simpson, 2020; Sun et al., 2019), driven by the growing recognition of the imperative to reduce our reliance on fossil fuels. Innovative technologies enable the revalorisation of organic residues, such as municipal or agricultural waste, through their initial gasification into syngas (a mixture of CO, H_2 and CO_2) and subsequent fermentation of syngas by microorganisms (Liew et al., 2016). Additionally, off-gases from steel mills and other heavy industries can also serve as a feedstock for gas fermentation given their high content (up to 70%) in CO (Molitor et al., 2016). Syngas/CO fermentation relies on acetogenic bacteria as biocatalysts, as these microorganisms can efficiently convert CO, H_2 and CO_2 via the Wood-Ljungdahl pathway. Acetogens belonging to the *Clostridium* and *Acetobacterium* genera, including *Clostridium ljungdahlii, Clostridium carboxidivorans, Acetobacterium woodii* and the industrial workhorse, *Clostridium autoethanogenum*, have been extensively studied for syngas fermentation applications (Bengelsdorf et al., 2016; Heffernan et al., 2022). However, due to the relatively low value of their primary products —ethanol and acetate—, significant efforts are being made to enable the production of non-native compounds in acetogens via metabolic and genetic engineering (Bourgade et al., 2021; Köpke & Simpson, 2020). For example, acetone and isopropanol production have been realised in *C. autoethanogenum* (Liew et al., 2022), and efficient 3-hydroxybutyrate (3-HB) production was accomplished in *C. ljungdahlii* (Lo et al., 2022). However, genomic manipulation of acetogens is still challenging (Charubin et al., 2018; Lee, 2021), and the production of ATP-demanding products remains difficult to achieve due to the energy-limited metabolism of these microorganisms.

More recently, the application of carboxydotrophic microbial communities has been explored as an alternative to broaden the range of products in syngas fermentation (Du et al., 2020; Parera Olm & Sousa, 2021). Synthetic co-cultures, i.e., defined communities of microorganisms, offer a unique advantage in terms of modularity when compared to undefined, open mixed cultures (Diender et al., 2021; Goers et al., 2014). They allow for the choice of strains based on their fitness to meet process demands, such as higher metabolic activity at specific environmental conditions, or resistance to toxic compounds. In addition, synthetic co-cultures enable the modular integration of various microorganisms to construct a desired resource network, allowing to broaden the range of products of fermentations while avoiding unwanted by-products. An example of a promising synthetic co-cultivation approach for syngas fermentation involves the combination of acetogens and chain-elongating bacteria to produce medium-chain carboxylic acids (MCCAs) via ethanol-driven chain elongation. In this process, *Clostridium kluyveri* has been used as a partner strain alongside CO-fermenting acetogens such as *C. autoethanogenum* (Diender et al., 2016b; Haas et al., 2018), *C. carboxidivorans* (Bäumler et al., 2021), and *C. ljungdahlii* (Richter et al., 2016a), among others (Baleeiro et al., 2019). *C. kluyveri* oxidises ethanol produced by acetogens and disposes of the electrons in the reverse β-oxidation pathway, a cyclic set of reactions that enables the elongation of carboxylic acids by two carbons at a time (Angenent et al., 2016; Seedorf et al., 2008). In this way, butyrate (C4) and caproate (C6) can be produced from acetate (C2), increasing the value of end products of the syngas fermentation process.

Besides MCCAs, higher alcohols (>C2) are also valuable products that can be obtained with syngas-fermenting co-cultures, given the solventogenic ability of acetogens. Alcohol formation occurs in the presence of excess reductant (i.e., H_2 or CO), and it is usually triggered by a drop in the extracellular pH caused by the accumulation of carboxylic acids (Arslan et al., 2019; Diender et al., 2016b; Ganigué et al., 2016; Richter et al., 2016b). For example, in a carboxydotrophic co-culture of *C. autoethanogenum* and *C. kluyveri*, it was observed that butyrate and caproate were reduced to butanol and hexanol, respectively (Diender et al., 2016b). CO-driven reduction of carboxylic acids to higher alcohols has also been demonstrated in *C. ljungdahlii* (Perez et al., 2013; Richter et al., 2016a), *Alkalibaculum bacchi* (Liu et al., 2014b) and *Clostridium aceticum* (Fernández-Blanco et al., 2022). On the other hand, very few acetogens are able of direct conversion of syngas to higher alcohols, the most notorious species being *C. carboxidivorans*, with reported butanol titres generally around 1 g L^{-1} (Fernández-Blanco et al., 2023; Fernández-Naveira et al., 2017). For a comprehensive review of the topic, we refer to the publications of Fernández-Naveira et al. (2017) and Fernández-Blanco et al. (2023).

Acetobacterium wieringae strain JM is an acetogen isolated from a carboxydotrophic microbial enrichment (Arantes et al., 2020). Contrary to the type strain —*A. wieringae* DSM 1911[T]—, strain JM is able to grow on 100% CO without formate as co-substrate. Another noteworthy characteristic of strain JM is its capability to efficiently grow at pH 7 (Arantes et al., 2020); this trait differentiates it from the model acetogen *C. autoethanogenum*, a mild acidophile unable to grow at pH above 6.5 (Abrini et al., 1994). The enrichment culture from which strain JM was isolated was found to produce propionate (next to acetate) from CO (Arantes et al., 2020). The authors hypothesised that propionate was formed by propionigenic bacteria, also present in the enrichment, that used the ethanol produced by the acetogen. This hypothesis was further supported by experiments conducted by Moreira et al. (2021), where synthetic co-cultures of *A. wieringae* JM with the propionigenic strain *Anaerotignum neopropionicum* converted CO to propionate. Propionibacteria, including *A. neopropionicum*, exhibit optimal growth at neutral pH (Piwowarek et al., 2018; Tholozan et al., 1992), a property shared by the acetogen *A. wieringae* JM. Thus, strain JM holds promise as an acetogen for coupling with propionibacteria to enable the production of odd-chain products from syngas.

Previously, we demonstrated the production of C5–C7 carboxylic acids from ethanol and CO_2 by a chain-elongating co-culture of *A. neopropionicum* and *C. kluyveri* (Parera Olm & Sousa, 2023). Here, we build up on our previous work by integrating syngas fermentation with odd-chain product formation in a single bioprocess. We show that a tri-culture of *A. wieringae* JM with *A. neopropionicum* and *C. kluyveri* is able to convert CO to carboxylic acids and higher alcohols of odd- and even-carbon chain length during fermentation at pH 7. Additionally, we studied the physiology of *A. wieringae* JM in monoculture vs. in co-culture during carboxydotrophic growth in chemostat bioreactors, revealing a metabolic shift from acetogenesis, in monoculture, to solventogenesis, in co-culture. The experimental data was used to construct and validate the first genome-scale metabolic model (GEM) of *A. wieringae* JM and to build a community model of the tri-culture (using the available GEMs of *C. kluyveri* [Zou et al., 2018] and *A. neopropionicum* [Benito-Vaquerizo et al., 2022b]). Community flux balance analysis (cFBA) was used to explore the feasible combinations of species ratios and growth rates, and to predict the effect of H_2 addition on the product spectrum of the tri-culture.

5.2   Materials and methods

Cultivation experiments

5.2.1   Microbial strains and cultivation

C. kluyveri DSM 555[T] and *A. neopropionicum* DSM 3847[T] were obtained from the German Collection of Microorganisms and Cell Cultures (Leibniz Institute DSMZ - German Collection of Microorganisms and Cell Cultures GmbH, Braunschweig, Germany). *A. wieringae* strain JM is an isolate from our own culture collection (Arantes et al., 2020). Cultivation of *C. kluyveri* and of *A. neopropionicum* was done as described elsewhere (Benito-Vaquerizo et al., 2022b; Parera Olm & Sousa, 2023). In short, both strains were grown anaerobically in bicarbonate-buffered medium (pH 7) containing ethanol (50 mM) for *A. neopropionicum*, or ethanol and acetate (90 mM and 75 mM, respectively) for *C. kluyveri*, as substrates. The medium was supplemented with yeast extract (0.5 g L^{-1}) and vitamins (see composition below). L-Cysteine-HCl (0.5 g L^{-1}) was used as reducing agent, and resazurin (0.5 mg L^{-1}) as redox indicator. Cultures of *C. kluyveri* and of *A. neopropionicum* were incubated statically at 37°C and 30°C, respectively. *A. wieringae* JM was cultivated anaerobically in phosphate-buffered (30 mM) medium containing (per litre): 1 g NH$_4$Cl, 0.7 g NaCl, 2.8 g KH$_2$PO$_4$, 1.3 g Na$_2$HPO$_4$, 0.2 g MgSO$_4$·7H$_2$O, 0.04 g CaCl$_2$·2H$_2$O, 10 mL trace element solution from ATCC medium 1754, 0.5 g yeast extract, 0.75 g L-Cysteine-HCl and 0.5 mg resazurin. Vitamins were added to a final composition of (per litre): 0.5 mg pyridoxine, 0.2 mg thiamine, 0.2 mg nicotinic acid, 0.1 mg p-aminobenzoic acid, 0.1 mg D-Ca-pantothenate, 0.1 mg cobalamin, 0.1 mg riboflavin, 0.05 mg folic acid, 0.05 mg lipoic acid and 0.02 mg biotin. The pH of the medium was adjusted to 7. Cultures of *A. wieringae* JM were grown in serum bottles of 250 mL filled with 50 mL medium and with CO in the headspace (100 % v/v; 170 kPa) as substrate. Bottles were incubated at 30°C, shaking (150 rpm) after 24h statically.

5.2.2   Bioreactors setup and operation

Two cultivation experiments, one in batch and the other in continuous mode, were conducted in BioXplorer 400P' stirred-tank bioreactor vessels (H.E.L Group, Borehamwood, United Kingdom) of 0.5 L (total volume), operated anaerobically. The bioreactor system was equipped with pH, redox and temperature sensors. In both experiments, the system was operated at 30°C and pH 7, the latter controlled by the addition of 3 M KOH. Mass flow controllers regulated the inflow of gases (CO, N$_2$ or N$_2$/CO$_2$) separately. Start-up of bioreactor operation was always done as follows: the autoclaved reactor vessel, containing medium (salts, trace elements and resazurin) as described above for *A. wieringae* JM, was connected to the system and sparged with N$_2$ (3 L h^{-1}) for ≈3 hours to establish anaerobic conditions. The gas inflow was then switched to the desired composition and flowrate for each experiment. Before inoculation, the following supplements were added aseptically to the vessel from anaerobic, sterile stock solutions: yeast extract (0.5 g L^{-1}), vitamins and L-cysteine-HCl (0.75 g L^{-1}). Inoculation using exponentially growing pre-cultures of the pertinent strain(s) was done when the redox potential had dropped and stabilised below -300 mV. Gas and liquid outflow rates were regularly measured during operation. Liquid and headspace samples were taken routinely. Further specific details of each experiment are provided hereunder.

5.2.3   Batch cultivation of the tri-culture with continuous feed of CO

The tri-culture was grown in a bioreactor vessel operated as described above, with a working volume of 350 mL. The fermentation was carried out at 30°C and the pH maintained at 7 for the main part of the cultivation (see results section). The experiment was initiated by inoculating *A. neopropionicum* (5% v/v) and supplying 25 mM ethanol to support growth of this strain, under a headspace of N_2/CO_2 (80:20% v/v, 1 bar, 7 mL min^{-1}). One day later, when cell growth was observed, *A. wieringae* JM and *C. kluyveri* were inoculated (5% and 2.5% v/v, respectively) concurrently with the start of the CO supply. The composition of the headspace was $CO/N_2/CO_2$ (75:25:5% v/v, 1 bar, 7 mL min^{-1}) and it was unchanged for the rest of the fermentation. The agitation was initially set at 300 rpm (days 0 – 4) and later increased to 400 rpm (days 4 – 14).

5.2.4   Chemostat cultivation of *A. wieringae* JM monoculture and bi-culture with *C. kluyveri* and *A. neopropionicum*

The continuous experiment was conducted in two bioreactor vessels (R1 and R2) operated as described above (30°C, pH 7), with a working volume of 400 mL. The medium was amended with 0.005% (v/v) Antifoam 204 to prevent excessive foaming. The gas composition during operation was CO/N_2 (70:30% v/v, 1 bar), and the gas flowrate was set at 4 mL min^{-1} (0.01 vvm). In both bioreactors, the experiment consisted of two consecutive phases, and the respective steady states were compared: i) monoculture of *A. wieringae* JM (in R1 and R2; duplicates), and ii) co-culture of *A. wieringae* JM with *C. kluyveri* (in R1) or with *A. neopropionicum* (in R2) (hereinafter referred to as "bi-cultures"). Inoculation was done when indicated with 5% (v/v) of actively-growing cultures of the pertinent strain. The bioreactors were operated in continuous mode; fresh medium was supplied aseptically from a 20-L tank via a peristaltic pump (Masterflex, Germany). The medium inflow pump was adjusted to give a hydraulic retention time (HRT) of 48 hours (dilution rate, D = 0.021 h^{-1}). The medium tank was flushed with N_2 thorough the whole operation to ensure anaerobic conditions. Continuous operation was preceded by a short batch phase (3.8 days) to grow *A. wieringae* JM. Agitation was set at 350 rpm for the initial batch phase; during continuous operation, it was first increased to 500 rpm (on day 5.8) and, later, to 700 rpm (on day 23.7). Unfortunately, the stirring speed fluctuated at different time points during operation due to system fails; when this occurred, it is indicated in the Results section.

5.2.5   Reduction of carboxylic acids by *A. wieringae* JM in bottles under CO headspace

Batch experiments in serum bottles were conducted to test the ability of *A. wieringae* JM to reduce C3 – C6 carboxylic acids to alcohols in the presence of CO (100% v/v; 170 kPa). Cultivation was done in the medium and conditions described above for this strain (pH 7, 30°C, shaking). *A. wieringae* JM was inoculated in medium containing 20 mM of either carboxylic acid (propionate, butyrate, valerate or caproate) in their sodium salt form. Control incubations were done without the addition of carboxylic acid. Liquid and headspace samples were taken at the start and at the end of incubation.

5.2.6   Analytical techniques

Gaseous compounds (CO, CO_2, and H_2) were analysed in a gas chromatograph (Compact GC 4.0, Global Analyser Solutions, The Netherlands) equipped with two channels and a thermal conductivity detector (TCD). CO and H_2 were detected using a Molsieve 5A column operated at 100°C and coupled to a Carboxen 1010 pre-column. Determination of CO_2 was done in a Rt-Q-BOND column operated at 60°C. In both channels, argon was used as carrier gas. Concentrations of soluble compounds in liquid samples were determined by high-performance liquid chromatography (HPLC; LC-2030C, Shimadzu, Japan). The apparatus was equipped with a Shodex SH1821 column operating at 60°C. 0.01 N H_2SO_4 was used as eluent and the flow rate set at 1 mL min^{-1}. Amounts detected in a concentration < 0.3 mM could not be accurately quantified and are considered traces. The concentration of volatiles (butanol, hexanol, and caproate) was measured on a gas chromatograph (GC-2010, Shimadzu, Japan) equipped with a headspace autosampler (HS-20). The column employed was a DB-WAX Ultra Inert (Agilent, USA), operated at a gradient from 50 to 200 oC, and nitrogen was used as carrier gas. Sample preparation was performed in 10 mL headspace vials with 100 μL of clear liquid sample plus 100 μL 10 mM methanol in 1% (w/v) formic acid to acidify acids in the sample. The vial was transferred to the oven of the autosampler (60 oC) where it was held for five minutes before a headspace sample was taken that was brought on the column. Detection of compounds was done with a FID detector. The Chromeleon™ data analysis software (Thermo Fisher Scientific), version 7.2.9, was used for both GC and HPLC peak analysis. Microbial growth was estimated based on the measurement of optical density at 600 nm (OD_{600}) using a spectrophotometer (UV-1800, Shimadzu, Japan). CDW was determined by gravimetric analysis: pellets from a known culture volume (≈50 mL) were washed twice in deionised water, resuspended and transferred into pre-weighed aluminium trays. These were dried overnight at 105°C and weighed again the day after.

Genome-scale metabolic modelling and simulations

5.2.7   Reconstruction and validation of the GEM of *A. wieringae* JM, iAWJM_SB617

The genome-scale metabolic model (GEM) of *A. wieringae* JM was reconstructed through an orthology based approach using as scaffold the GEM of the acetogen *C. autoethanogenum* — iCLAU786 (Valgepea et al., 2017). The genomic sequence of *A. wieringae* JM (GCA_008107585.1) was retrieved from the National Center for Biotechnology Information (NCBI) under accession number VSLA00000000 (Arantes et al., 2020) and subjected to structural and functional reannotation. Ortholog genes between both species were identified and used to evaluate the reactions in the model. The GEM of the close relative *A. woodii* (Bertsch & Müller, 2015b; Koch et al., 2019) was used to refine the model. A detailed description of the methodology followed for the model reconstruction is given in Suppl. material § 5.6.1. The GEM of *A. wieringae* JM, iAWJM_SB617, can be found in the GitLab repository https://gitlab.com/wurssb/Modelling/triculture_aw_an_ck/-/tree/master/, in Table format, json and SBML L3V1 standardization, together with a MEMOTE report of quality assessment (Lieven et al., 2020).

Details of the qualitative and quantitative validation of the model can be consulted in Suppl. material § 5.6.1. In short, the model was qualitatively validated using flux balance analysis (FBA) to

assess growth phenotypes on several carbon sources. Quantitative validation was done by comparing predicted production rates of acetate and ethanol with those measured in the duplicate chemostat bioreactors of *A. wieringae* JM growing on CO presented in this study. Prediction of production rates of acetate and ethanol under varying CO and H_2 uptake rates were done by constraining the model to the set uptake rates and a growth rate of 0.021 h^{-1}. The solution space and the set of fluxes compatible with the measured rates were explored using flux sampling as detailed in Suppl. material § 5.6.1.

5.2.8 Construction of the community model of *A. wieringae* JM – *C. kluyveri* – *A. neopropionicum* (tri-culture)

The tri-culture model was generated by combining the single species models of each strain: iAWJM_SB617 (this work), iANEO_607 (Benito-Vaquerizo et al., 2022b) and iCKL708 (Zou et al., 2018), for *A. wieringae* JM, *A. neopropionicum* and *C. kluyveri*, respectively. The methodology followed was the same as reported in our previous studies (Benito-Vaquerizo et al., 2020; Benito-Vaquerizo et al., 2022a) and is summarised in Suppl. material § 5.6.1. The tri-culture model was transformed into SBML level 3 version 1 and can be found in the git repository.

5.2.9 Community modelling: framework and simulations

Model simulations of the bi-culture and the tri-culture were done using a steady-state approach that considers balanced growth of the microbial species and that resembles community flux balance analysis (cFBA) (Benito-Vaquerizo et al., 2020; Benito-Vaquerizo et al., 2022a; Khandelwal et al., 2013). Biomass synthesis reactions of each species incorporated the species relative abundance and total biomass. Specific fluxes (mmol g_{CDW}^{-1} h^{-1}) were replaced by environmental fluxes (mmol h^{-1}), taking into account the biomass density of each species (g L^{-1}) and the culture volume (L). An extensive description of community model simulations is given in Suppl. material § 5.6.1. Community growth rate and composition were varied and species growth rates were set to be equal to the community growth rate. Uptake rates were limited by constraining the corresponding exchange reactions. To assess the feasibility of a given scenario, FBA was run to predict the maximal biomass accumulation and only positive non null values were considered indicative of feasible scenarios. Feasible scenarios were further explored by sampling the solution space.

5.3 Results and Discussion

5.3.1 A tri-culture of *A. wieringae* JM, *A. neopropionicum* and *C. kluyveri* produces carboxylic acids and higher alcohols from CO

The proof-of-concept of the synthetic tri-culture of *A. wieringae* JM, *A. neopropionicum* and *C. kluyveri* was tested in batch fermentation with continuous supply of CO. Over the course of the fermentation, the tri-culture produced a mixture of acids (C2 – C7), mostly during exponential phase, and alcohols (C2 – C6), during stationary phase (Fig. 5.1). Cessation of all metabolic activity (day 9) was likely due to nutrient depletion or to the toxicity of accumulated products.
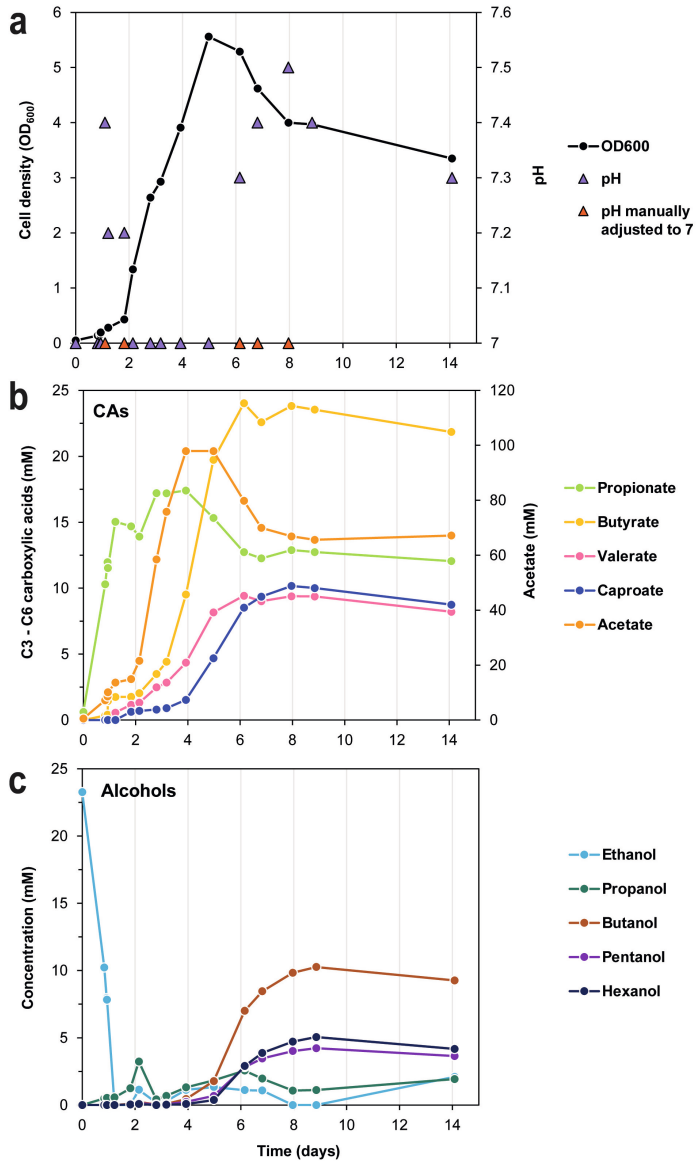
Figure 5.1 Tri-culture of *A. wieringae* JM - *A. neopropionicum* - *C. kluyveri* in a batch bioreactor with continuous supply of CO. **a**) Cell density (OD_{600}) and pH; **b**) production of carboxylic acids (CAs); and **c**) ethanol and higher alcohols.

Cell growth and pH

Prominent growth occurred through days 2 to 5, during which OD_{600} rose exponentially from 0.4 to 5.6 (Fig. 1a). Microscopic inspection of the co-culture confirmed the presence of the three strains and showed predominance of *A. wieringae* JM cells (Suppl. material § 5.6.2: Fig. S5.1). Substantial foaming was formed on top of the liquid layer as cell density increased; therefore, on day 4, antifoam was added (Antifoam 204; 0.005% v/v) and the stirring was increased from 300 to 400 rpm. We chose to keep the agitation at this moderate speed to avoid saturation of the liquid with CO. While *A. neopropionicum* tolerates CO during growth on ethanol, as we observed in batch incubations (data not shown), *C. kluyveri* is inhibited by it, particularly when intense shaking is applied (Diender et al., 2016).

The pH increased at different time points during the fermentation (Fig. 5.1a). Upon the start of the CO feed, the pH rose from 7.0 to 7.4 due to loss of acidity as the CO_2 supplied was lowered from 20% to 5%. Since pH control was based solely on the correction of acidity via the addition of KOH, we manually adjusted the pH to 7 by adding HCl (red data points in Fig. 5.1a). However, a few hours later, the pH had increased to 7.2 (evening measurement), and it remained at this value until manual correction again (at 1.8 days). The pH remained at 7 for the subsequent days, which coincided with exponential growth of the tri-culture. The stationary phase of the culture (day 5 onwards) was characterised by a progressive decline of the cell density and an increase of pH. The latter hinted at the production of alcohols in the system via reduction of accumulated carboxylic acids, as described below.

Acidogenesis

The initially supplied ethanol (25 mM) was depleted after 1.2 days and converted to propionate (15 mM) and acetate (14 mM) by *A. neopropionicum* (Fig. 5.1b-c). Likely, some acetate was also produced from CO by *A. wieringae* JM in this period. Propanol (up to 3 mM) was also formed, as by-product of ethanol fermentation by *A. neopropionicum* (Benito-Vaquerizo et al., 2022b; Tholozan et al., 1992). Acetate continued to accumulate during exponential growth, reaching a maximum concentration on day 4 of 98 mM, while propionate concentration did not increase significantly in the following days. Thus, production of acetate throughout the growth phase can be attributed to the utilisation of CO by the acetogen. The latter is supported by the fact that *A. wieringae* JM was dominant in the co-culture (Suppl. material § 5.6.2: Fig. S5.1). *C. kluyveri* might have also contributed to acetate production, yet to a lesser extent (one molecule of acetate is produced per 1/6th of ethanol consumed, theoretically; Seedorf et al., 2008).

Production of C4 – C6 carboxylates began upon inoculation of *C. kluyveri* and *A. wieringae* JM (day 1). Butyrate was the most abundant product of chain elongation, reaching a concentration of 24 mM at the end of the growth phase, followed by equally high concentrations of valerate and caproate (≈10 mM) (Fig. 5.1b). Traces of heptanoate were detected only from day 5 onwards (<0.3 mM). We also measured isobutyrate (up to 1.7 mM) and isovalerate (up to 2.8 mM) that can be produced by *A. neopropionicum* via the fermentation amino acids present in yeast extract or cross-fed (Benito-Vaquerizo et al., 2022b; Moreira et al., 2021). Chain elongation of even- and odd-chain products took place simultaneously, as seen before in pure culture experiments of *C. kluyveri* (Candry et al., 2020b; Parera Olm & Sousa, 2023). However, the production of butyrate

(from acetate) proceeded at a faster rate than that of valerate (from propionate), and even-chain products (C4+C6) reached a higher concentration. This could indicate that the enzymes involved in chain elongation in *C. kluyveri* have a higher affinity for acetate than for propionate. In addition, previous reports have suggested that *C. kluyveri* oxidises excessive ethanol to acetate in the presence of propionate, increasing the acetate pool and the proportion of even-chain products (Candry et al., 2020b; Parera Olm & Sousa, 2023).

Except for acetate, all the other products could have only been formed from the ethanol produced by the acetogen. Ethanol concentration remained low (≤2 mM) during the fermentation (Fig. 5.1c), indicative of its rapid consumption via cross-feeding. Interestingly, even though the culture was CO-limited, ethanol production was concurrent with that of acetate from initial stages of cultivation. This indicates that consumption of ethanol by *A. neopropionicum* and *C. kluyveri* favoured its production by the acetogen, a phenomenon that we further on studied in chemostat bioreactors (see section below).

Solventogenesis

A maximum of 20.6 mM higher alcohols (C3 – C6) were produced in the stationary phase (day 8.8; Fig. 5.1c), representing 14% (mol/mol) of the products. Butanol accounted for half of them (10.3 mM), followed by hexanol (5.1 mM), pentanol (4.2 mM) and propanol (1 mM). Pentanol is reported here for the first time by a syngas-fermenting community. The production of higher alcohols can be attributed to CO-driven reduction of carboxylic acids by *A. wieringae* JM, as observed in other acetogens (Diender et al., 2016b; Liu et al., 2014b; Perez et al., 2013), while propanol could have also been formed by *C. kluyveri* and *A. neopropionicum* (Candry et al., 2020b; Parera Olm & Sousa, 2023). Alcohol formation was likely driven by the accumulation of carboxylic acids, as these reached 149 mM at the end of the growth phase, on day 5. At that point, the total undissociated fraction of carboxylic acids was ≈0.6%, or a concentration of ≈0.93 mM (at pH 7 and assuming an average pKa of 4.83), which is in the range found to be detrimental to other Clostridia (Diender et al., 2016b; Kucek et al., 2016; Vasudevan et al., 2014; Weimer & Stevenson, 2012). In those studies, growth inhibition was attributed to undissociated caproic acid in a concentration range of 0.5 – 1.5 mM. Here, we calculated a concentration of undissociated caproic acid of 0.035 mM, an order of magnitude lower; therefore, we hypothesise that growth was inhibited by the fraction of undissociated acetic acid (0.56 mM). The reduction of acids to alcohols is assumed to be a mechanism of the cell to avoid further acidification of the environment (Diender et al., 2016b; Ganigué et al., 2015).

Interestingly, the production of higher alcohols occurred simultaneously with the consumption of short-chain carboxylates and with chain elongating activity (days 4 - 8; Fig. 5.1b-c). This contrasts with observations from studies employing mild acidophiles as acetogenic partner, such as *C. autoethanogenum* (Diender et al., 2016b), *C. ljungdahlii* (Richter et al., 2016a) or *C. carboxidivorans* (Bäumler et al., 2023; Ganigué et al., 2016), where alcohol production and chain elongation competed due to the different optimal pH for the viability of the two processes. Here, we hypothesise that the reduction of elongated carboxylates to alcohols (e.g., butyrate to butanol) shifted the equilibrium towards their production from the corresponding precursors via chain elongation (e.g., acetate to butyrate), which was enabled at neutral pH. In addition, our results show that an acidic extracellular pH is not imperative for alcohol production, as generally reported in syngas

fermentation studies (Fernández-Naveira et al., 2017; Ganigué et al., 2016; Richter et al., 2016a). When sufficiently high concentrations of carboxylates were reached, *A. wieringae* JM reduced these to alcohols at pH 7 (Fig. 5.1). Solventogenesis by *A. bacchi* strain CP15, an acetogen that grows optimally at pH 8.0, was also reported to occur at neutral pH (Liu et al., 2014a). Thus, it is more likely that conditions restricting growth (e.g., the accumulation of toxic products or low availability of nutrients) where the availability of reducing equivalents increases are a more important trigger than pH to the production of reduced products such as alcohols (Zahn & Saxena, 2012).

CO consumption, and production of H_2 and CO_2

Consumption of CO by the tri-culture was relatively low; during the growth phase, we measured an average CO partial pressure of ≈ 66 kPa (Suppl. material § 5.6.2: Fig. S5.2), implying a consumption of 15% CO. The headspace of the bioreactor also comprised H_2 and CO_2. H_2 is an expected product as it is produced by *C. kluyveri* during growth; however, the partial pressure of H_2 was very low during the whole fermentation (<1 kPa) (Suppl. material § 5.6.2: Fig. S5.2). This suggests H_2 is consumed by *A. wieringae* JM as complementary energy source to CO, particularly if the availability of the latter was limited (due to gas transfer constraints). *A. neopropionicum* requires CO_2 for propionate formation (Benito-Vaquerizo et al., 2022b; Tholozan et al., 1992). Still, the CO_2 partial pressure increased substantially (from 7 to 20 kPa) during the growth phase (Suppl. material § 5.6.2: Fig. S5.2), indicative that carboxydotrophic metabolism by the acetogen was dominant (as supported by the high acetate production).

5.3.2   Reduction of carboxylic acids to alcohols by *A. wieringae* JM with CO as electron donor

The ability of *A. wieringae* JM to reduce C3 – C6 carboxylic acids to their respective alcohols (i.e., propanol, butanol, pentanol and hexanol) was investigated in batch growth on CO. Each carboxylic acid (20 mM), or none (control), was added separately to cultures of *A. wieringae* JM at the start of incubations. Cell density, CO consumption, products formed and pH at the end of incubations are shown in Table 5.1.

Table 5.1 Parameters of the reduction of C3 – C6 carboxylic acids to alcohols by *A. wieringae* JM in batch cultivation at pH 7 with CO as substrate after 9 days (control, propionate and butyrate) or 28 days (valerate and caproate). Values are the average and standard deviation of biological triplicates.

Carboxylic acid added (20 mM)	Final cell density (g L⁻¹)	CO consumed (mmol) [%]	Carboxylic acid consumed (mM) [%]	Alcohol produced from carboxylic acid (mM)	Final acetic acid (mM)	Final ethanol (mM)	Final pH
None (control)	0.52±0.06	13.9±0.3 [100±0]	-	-	20.8±2.2	17.6±5.4	4.8±0.0
Propionate	0.49±0.10	14.1±0.1 [100±1]	9.1±1.4 [48±12]	8.3±2.4 propanol	31.1±8.9	11.0±2.7	5.1±0.2
Butyrate	0.46±0.06	13.7±0.5 [100±2]	4.9±2.2 [31±13]	4.4±2.2 butanol	28.5±2.0	8.1±5.3	5.0±0.0
Valerate	0.14±0.00	4.7±0.6 [34±4]	4.8±0.4 [25±3]	4.0±0.7 pentanol	10.8±0.1	1.8±0.6	5.9±0.0
Caproate	0.09±0.01	3.2±0.3 [23±2]	1.7±0.7 [10±4]	2.1±0.5 hexanol	9.8±0.6	0.5±0.1	6.2±0.1

5

After 9 days of incubation, CO was depleted in the control cultures and in those with propionate or butyrate. Conversely, in the incubations containing valerate or caproate, CO consumption was only 34±4% and 23±2%, respectively, after 28 days. These cultures were ended at this point, as no further metabolic activity was expected. The presence of 20 mM propionate or butyrate did not affect the final cell density of the cultures (≈0.5 g_{CDW} L^{-1}; p value > 0.05 compared to the control), suggesting no growth inhibition under these conditions. A similar behaviour was seen in *C. ljungdalii* when cultivated with 15 mM of either carboxylic acid (Perez et al., 2013). In addition, only a small fraction of electrons derived from CO are used in the reduction of carboxylic acids, therefore there is a negligible effect of this conversion on biomass formation. In contrast, growth inhibition was reported in syngas-fermenting cultures of *A. bacchi* at pH 7.5 with both propionate (20 mM) and butyrate (17 mM) (Liu et al., 2014b), which suggests a higher sensitivity of this strain. In our study, valerate and caproate (20 mM) did significantly inhibit growth of *A. wieringae* JM (final density of ≈0.1 g_{CDW} L^{-1}), consistent with a higher toxicity of carboxylic acids as carbon chain increases (Herrero et al., 1985).

A. wieringae JM reduced all the C3 - C6 carboxylic acids to alcohols, albeit to varying degrees (Table 5.1). The highest consumption was that of propionate (9.1±1.4 mM), yet about half of the carboxylate remained unused. Incomplete conversion of carboxylic acids could be due CO depletion, combined with the low final pH (≈5) that was likely detrimental to strain JM. The consumption of butyrate and valerate was similar (≈5 mM) despite the significant differences in biomass formation and CO utilisation between the two conditions. This indicates that the reduction of carboxylic acids occurred uncoupled to growth, probably just as a means of the cell to dispose of reducing equivalents derived from substrate (CO) oxidation. The lowest conversion was obtained for caproate, along with limited growth in these cultures.

Compared to the control, the final concentration of acetate was higher with propionate or butyrate present, in detriment of ethanol formation (Table 5.1). This could hint to a higher demand of ATP (produced via acetate kinase) in these cultures due to energy-consuming mechanisms dealing with the accumulation of intracellular protons. If that were the case, however, biomass formation would have been compromised, which was not observed. Instead, it is more likely that the cultures without carboxylate supplementation required a higher production of ethanol to halt acidification of the environment. It can be speculated that, in the experimental conditions, the production of higher alcohols preceded ethanol formation due to higher availability of the corresponding carboxylates (propionate and butyrate) vs. acetate at the start of cultivation (Perez et al., 2013). Thus, less ethanol would need to be produced in these cultures to stop acidification. This hypothesis is supported by the fact that the final pH in the control cultures was 4.8±0.0, the lowest of all the conditions tested, while higher final pH values were obtained with propionate and butyrate (5.1±0.2 and 5.0±0.0, respectively).

In general terms, the solventogenic ability of *A. wieringae* JM seems to be like that of other acetogens; the outcomes differ depending on the specific capabilities of each strain and the applied cultivation strategy. For example, *A. bacchi* reduced ≈37% of propionate or butyrate supplied (17 mM) into the corresponding alcohols at pH 7.5 (Liu et al., 2014b), a similar conversion efficiency to *A. wieringae* JM (Table 5.1). However, the authors also reported growth inhibition and low CO utilisation (≈30%), which we did not observe with strain JM. In another study, high conversion

(>70%) of C3 – C6 carboxylates (15 mM) were obtained with C. *ljungdahlii* (Perez et al., 2013), likely facilitated by the continuous syngas feed applied, which was not done in our study.

5.3.3   Effect of co-cultivation with *C. kluyveri* or *A. neopropionicum* on the physiology of *A. wieringae* JM in chemostat CO fermentation

The physiology of *A. wieringae* JM during CO fermentation and the induced changes during co-cultivation with *A. neopropionicum* or *C. kluyveri* were studied in CO-limited chemostats. Two bioreactors, R1 and R2, were operated in parallel, and cultivation in each system was divided in two phases with respective steady states: first, monoculture of *A. wieringae* JM (in R1 and R2; duplicates) and second, bi-culture of the acetogen with *C. kluyveri* (in R1) or with *A. neopropionicum* (in R2) (Fig. 5.2). Several technical issues (the stirring spiked, and the system turned off) occurred during operation of the bioreactors that altered biomass and product concentrations at different time points. Therefore, establishment of steady states of each phase took quite some time, and the total cultivation time was rather long (140 days) despite the relatively short HRT (48 h).

   Upon start of the continuous mode, increasing the stirring speed from 500 to 700 rpm (on day 23.7) led to an increase of the cell density and acetate levels (Fig. 5.2), accordingly with a CO-limited system. Agitation was maintained at 700 rpm for the rest of the cultivation; while higher stirring speeds could have been applied to enhance CO consumption, we wanted to avoid CO accumulation in the liquid, which might hamper growth of C. kluyveri during the co-cultivation phase. We assumed that the system remained CO-limited during the rest of the cultivation given the relatively low flowrate (0.01 vvm) and because, during co-cultivation, we did not observe inhibition of *C. kluyveri*. Steady-state parameters of the two bioreactors (mono- and bi-culture phases) are summarised in Table 5.2. During monoculture of *A. wieringae* JM, the main product of CO fermentation was acetate ($\approx$60 mM). Ethanol was detected in traces (<0.2 mM) except for transient accumulation (<3 mM) when system failures occurred. Inoculation of *C. kluyveri* (R1) and *A. neopropionicum* (R2) was done at the end of the monoculture steady states (day 60), and it was followed by the accumulation of products of the respective strains (butyrate, caproate and propionate) (Fig. 5.2c-d). These products could have only been formed by *C. kluyveri* and *A. neopropionicum* from ethanol as electron donor. Thus, while in monoculture the metabolism of *A. wieringae* JM was entirely acetogenic, co-cultivation of the acetogen with ethanol-consuming species immediately triggered ethanol production. This metabolic shift (from acetogenesis to solventogenesis) was also observed in *C. autoethanogenum* co-cultured with *C. kluyveri* (Diender et al., 2016b; Diender et al., 2019). Several studies have postulated that the acetogenic/solventogenic shift in acetogens under nutrient-limited growth is controlled by thermodynamics rather than by transcriptomic or translational regulation (Diender et al., 2019; Moreira et al., 2021; Richter et al., 2016b; Valgepea et al., 2018). In accordance with this, we hypothesise that, in the bi-cultures of our study, *C. kluyveri* and *A. neopropionicum* kept ethanol levels in the system very low (<0.1 mM), thus favouring the thermodynamics of ethanol production by the acetogen. Enzymes involved in ethanol production are always abundant (even during acetogenesis) in *A. wieringae* JM (Moreira et al., 2021), therefore ethanol can be produced immediately when the conversion is rendered favourable.
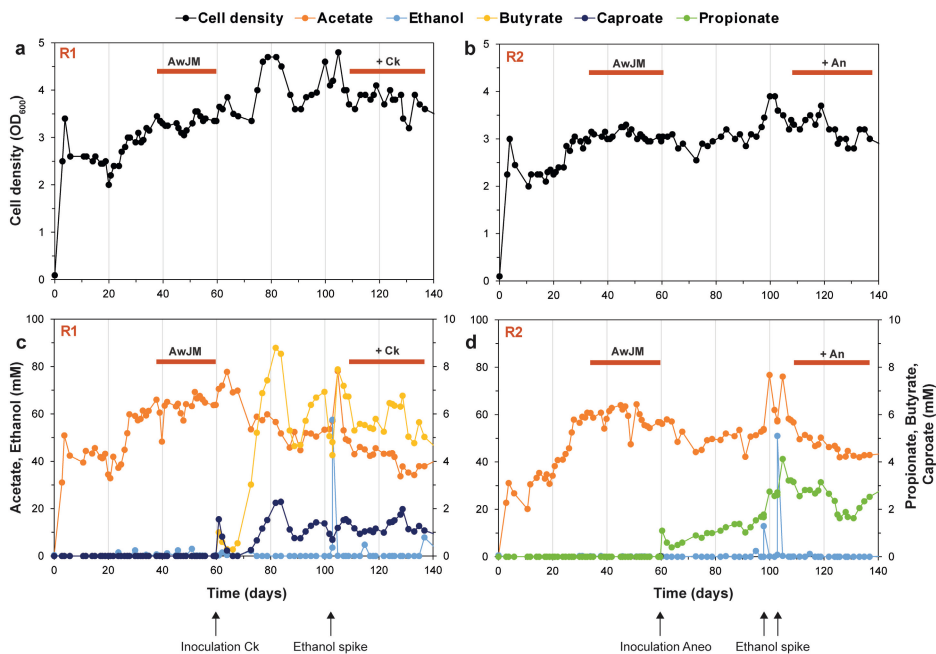
Figure 5.2 Cell density and products formed during cultivation of *A. wieringae* JM (AwJM) in monoculture and in bi-culture with *C. kluyveri* (R1; **a**, **c**) or *A. neopropionicum* (R2; **b**, **d**) in CO-limited chemostat bioreactors. Two phases can be distinguished in each bioreactor: monoculture of the acetogen (days 0 – 60), and co-culture with *C. kluyveri* (Ck) or *A. neopropionicum* (An) (days 60 – 140). Orange bars indicate the monoculture and bi-culture steady states.

In monoculture, consumption of CO by *A. wieringae* JM was significantly lower than observed in CO-limited chemostat cultivation of *C. autoethanogenum* (90% vs. ≈46% in this study) (Diender et al., 2019). Yet, a lower volumetric CO feeding rate was provided in that system (155 mmol L^{-1} d^{-1} vs. ≈430 mmol L^{-1} d^{-1} in this study). The volumetric CO uptake rate was therefore higher with *A. wieringae* JM (180 – 200 mmol L^{-1} d^{-1}; Table 5.2) than with *C. autoethanogenum* (147 mmol L^{-1} d^{-1}; Diender et al., 2019). This suggests a higher growth efficiency of strain JM, a trait that could be the result of metabolic adaptation to CO during the long-term enrichment previous to isolation (Arantes et al., 2020).

Bi-culture steady states were reached, after a period of sporadic technical issues, a few weeks later (day 109; Fig. 5.2). Compared to the monocultures, the cell density increased only slightly (by 5–10%) in both bi-cultures (Table 5.2), and the predominance of acetogenic cells was confirmed via microscopic observation. Consumption rate of CO during co-cultivation was the same as in the monoculture phase (Table 5.2), as observed in co-cultivation of *C. autoethanogenum* with *C. kluyveri* (Diender et al., 2019). This indicates that, in both the mono- and bi-culture phases, kinetics of the process were dictated by the limited mass transfer rate of CO into the liquid.

Table 5.2 Steady-state parameters[a] of *A. wieringae* JM monocultures (R1 and R2; duplicates) and subsequent bi-cultures with *C. kluyveri* (Ck; R1) or with *A. neopropionicum* (An; R2) in CO-limited chemostat bioreactors.

Parameter	R1		R2	
	Monoculture	Bi-culture Ck	Monoculture	Bi-culture An
CO volumetric inflow rate (mmol $L^{-1} d^{-1}$)	424		434	
HRT (h)	48.1		46.6	
D (h^{-1})	0.021		0.021	
Steady-state period (days)	**38 - 60**	**109 – 137**	**34 - 60**	**109 – 137**
Headspace pCO (kPa)	51.7±1.3	47.7±2.2	53.4± 2	52.4±2.7
Headspace pH$_2$ (kPa)	0.07±0.01	0.06±0.01	0.06±0.01	0.04±0.01
Headspace pCO$_2$ (kPa)	12.4±1.2	14.5±2.2	11.5±1.3	11.1±2.1
CO vol. uptake rate (mmol $L^{-1} d^{-1}$)	202±12	215±16	188±23	188±16
CO utilisation (%)	48±3	51±4	44±5	43±4
Biomass (g L^{-1})	0.80±0.06	0.89±0.03	0.79±0.11	0.85±0.03
Acetate (mM)	63.2±4.6	41.7±4.5	58.7±4.2	47.1±4.3
Ethanol (mM)	0.51±0.87 [b]	ND	<0.02	<0.01
Propionate (mM)	ND	ND	ND	2.4±0.5
Butyrate (mM)	ND	5.8±0.7	ND	<0.01
Caproate (mM)	ND	1.3±0.3	ND	ND
Acetate vol. production rate (mmol $L^{-1} d^{-1}$)	31.1±2.3	20.5±2.2	29.9±2.1	24.0±2.2
Ethanol vol. production rate (mmol $L^{-1} d^{-1}$)	0.25±0.43 [b]	0.6±0.1	<0.09	<0.02

[a]Average values with standard deviations correspond to values obtained in the steady-state periods indicated in Fig. 5.2. A steady-state was considered when biomass and acetate concentrations were stable (± 5-7%) for a period longer than 3x-times the HRT. This was the case with few exceptions (deviation up to 14%) due to the technical issues encountered during operation. [b]The large standard deviations are due to transient ethanol accumulation (<3 mM) upon sporadic system failures. HRT: hydraulic retention time; D: dilution rate; ND: not detected.

Compared to the monoculture phase, the steady-state acetate concentration was significantly lower in the bi-cultures, in favour of butyrate (5.8±0.7 mM) and caproate (1.3±0.3 mM) in R1, and propionate (2.4±0.5 mM) in R2. The low accumulation of these products compared to acetate (≈45 mM) can be attributed to limited availability of ethanol in the system. This was evident when the concentration of both propionate and acetate increased upon spiking with 10 mM ethanol and, later, 50 mM in R2 (on days 98 and 103, respectively; Fig. 5.2d). The same response was observed upon spiking 50 mM ethanol in R1 (on day 103; Fig. 5.2c). Interestingly, most ethanol upon the spike was oxidised to acetate (Fig. 5.2c-d), presumably by *A. wieringae* JM. Ethanol is an overflow product of acetogenic metabolism, and it is thought to serve as energy storage under conditions

of substrate scarcity (Allaart et al., 2023). Thus, *A. wieringae* JM likely used ethanol as additional electron donor due to CO limiting in the system, as previously observed in cultures of *C. autoethanogenum* upon depletion of CO (Diender et al., 2016b). Ethanol oxidation metabolism has also been described in *A. woodii* (Bertsch et al., 2015) and *C. ljungdahlii* (Liu et al., 2020b), and it is probably a common acetogenic trait.

5.3.4 Genome-scale metabolic modelling predicts *A. wieringae* JM phenotype and steady-state production rates

As first step to establish the community model of the tri-culture, we constructed the genome-scale metabolic model (GEM) of *A. wieringae* JM, iAWJM_SB617. This is the first GEM of this strain and, to our knowledge, the first of the species *A. wieringae*. The model comprises 617 genes, 1065 metabolites and 1081 reactions (Suppl. material § 5.6.2: Table S5.1). The final model obtained a score of 73% in MEMOTE. The annotation of metabolites and reactions received a very high score (≈82%). However, the annotation of genes scored only 33%, since neither KBase nor MEMOTE recognized the protein IDs (TYCXXXXX) or locus tags (FXB42_XXXXX) associated to *A. wieringae* JM. Qualitative validation of the model was done by assessing growth on several carbon sources and comparing the model output with experimental data generated in this study and from literature (Arantes et al., 2020; Ross et al., 2020) (Fig. 5.3).
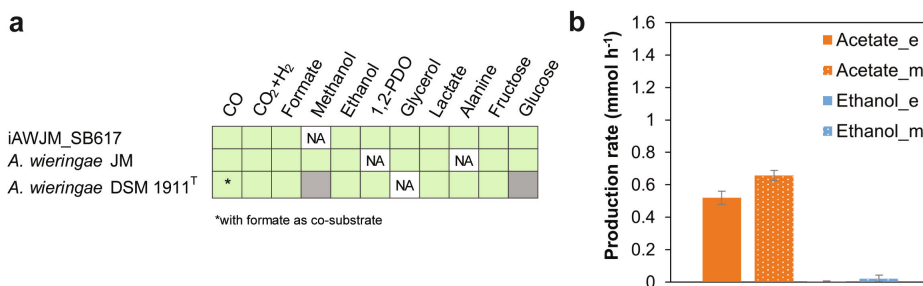
Figure 5.3 a) Growth phenotypes of *A. wieringae* JM predicted by the GEM constructed in this study, iAWJM_SB617, and reported in experimental studies (this work, and Arantes et al., 2020). Growth phenotypes of the type strain, *A. wieringae* DSM 1911[T] (Ross et al., 2020), are also included. Green: growth; grey: no growth; ND: no data available. **b**) Steady-state production rates of acetate and ethanol by A. *wieringae* JM during growth on CO observed in bioreactors ('_e') and predicted by the model ('_m'). Error bars indicate the standard deviation of two biological replicates (for experimental data) or 5000 samples (for model predictions).

The model correctly predicted growth of *A. wieringae* JM on all the C1 feedstocks tested except for methanol (Fig. 5.3a), due to incompleteness of the methanol assimilation pathway in the genome annotation. Growth on glucose seems to be a trait of strain JM but not of the type strain, as shown by our model and by cultivation experiments (Arantes et al., 2020; Braun & Gottschalk, 1982). This divergence could be due to different selective pressures in the original habitat of these strains, or merely to the use of different cultivation medium, as reports in literature are often contradictory (Ross et al., 2020). Our model also predicted growth on 1,2-PDO and the amino acid alanine,

both of which had not been tested before on strain JM but are predicted substrates of the genus *Acetobacterium* (Ross et al., 2020).

Accordingly with experimental observations, the model predicted growth of *A. wieringae* JM on CO as sole substrate (Fig. 5.3a). In contrast, the type strain of the species can only grow on CO in the presence of formate (Arantes et al., 2020), similarly to the close relative *A. woodii* (Bertsch & Müller, 2015b). The distinctive ability of strain JM to grow on CO is likely an evolutionary trait developed during long-term exposure to this substrate (Arantes et al., 2020). A hypothesis was formulated on the origin of such adaptation. Both *A. wieringae* type strain and *A. woodii* use the hydrogen-dependent CO_2 reductase (HDCR) for the reduction of CO_2 to formate in the methyl branch of the Wood-Ljungdahl pathway (Arantes et al., 2020; Schuchmann & Müller, 2013). According to our genome annotation, *A. wieringae* JM also harbours an HDCR composed of a formate dehydrogenase (TYC86388; *fdh*) and an Fe-hydrogenase (TYC85752; *hydA*). The HDCR is sensitive to high concentrations of CO; thus, a priori, growth on CO by acetogens harbouring the HDCR would be restricted to the presence of formate or H_2+CO_2, as observed in *A. woodii* and *A. wieringae* type strain (Arantes et al., 2020; Bertsch & Müller, 2015b). However, CO inhibition of the HDCR has been shown to be fully reversible (Ceccaldi et al., 2017). As hypothesised by Arantes et al. (2020), it is plausible that prolonged exposure to CO limited inhibition of the HDCR in strain JM, enabling use of CO as sole substrate. A similar case is that of the acetogen *Thermoanaerobacter kivui,* which also employs the HDCR and has been adapted to growth on CO (Weghoff & Müller, 2016).

Besides the growth phenotypes, model simulations also fitted the experimental values of steady-state acetate and ethanol production rates with good approximation (Fig. 5.3b). In bioreactor cultivation under steady-state, *A. wieringae* JM produced mostly acetate (0.51±0.01 mmol h⁻¹) and traces of ethanol (<0.01 mmol h⁻¹) (average of duplicates R1 and R2; Table 5.2). The higher production rates of acetate (0.66±0.03 mmol h⁻¹) and ethanol (0.02±0.02 mmol h⁻¹) resulting from the simulation could be due to a slightly higher predicted CO uptake rate (3.5±0.02 mmol h⁻¹) compared to the experimental value (3.3±0.2 mmol h⁻¹), or different ATP maintenance costs (non-growth associated maintenance; NGAM). The latter reaction ('rxn00062_aw') was fitted in the model using experimental values of the two replicate monoculture chemostats, however a better fitting could be obtained by calculating the NGAM and the growth-associated with maintenance (GAM) using data from chemostat cultivation at different growth rates, which was not available here. Overall, the predictions and simulations demonstrate the validity and reliability of the newly constructed GEM of *A. wieringae* JM, which we used to construct the multi-species model of the tri-culture.

5.3.5   The tri-culture of *A. wieringae* JM - *A. neopropionicum* - *C. kluyveri* is predicted to be feasible in a narrow range of species ratios and dilution rates

Simulations using cFBA were run to assess the feasibility of the tri-culture in a wide range of biomass species ratios and growth rates (or, dilution rates) during continuous growth on CO (Suppl. material § 5.6.2: Fig. S5.3). At the lowest growth rate tested, 0.005 h⁻¹ (HRT = 200 h), the tri-culture was predicted to be feasible at all biomass species ratios, which ranged from 1/1/8 to 8/1/1 (*A. wieringae* JM/*A. neopropionicum*/*C. kluyveri*). At growth rates between 0.01 – 0.025 h⁻¹ (HRT = 100 – 40 h), very low or very high abundance of any of the species was unfavourable to

the feasibility of the tri-culture. In other words, a balanced community resulted in a wider solution space in this range. Despite the three species having maximum growth rates of 0.1 – 0.2 h^{-1} (Candry et al., 2018; Parera Olm & Sousa, 2023), our simulations predicted the tri-culture to be unfeasible at growth rates higher than 0.03 h^{-1} (HRT < 33.3 h). In the model, the CO uptake rate is constrained based on experimental values, eventually limiting the minimum retention time required to allow for cross-feeding of shared metabolites in the tri-culture. We expect that simulations at higher CO uptake rates (which were not tested here) would have led to a feasible tri-culture also at higher growth rates due to increased overflow metabolism, i.e., higher ethanol production.

According to the simulations, abundances of the acetogen above 50% led to a feasible tri-culture only at growth rates below 0.02 h^{-1} (Suppl. material § 5.6.2: Fig. S5.3f-h), that is, with HRT > 50 h. In the chemostat experiment we performed, with an HRT of 48 h, *A. wieringae* JM largely dominated both bi-cultures, as indicated by the high proportion of acetate (Table 5.2) and by microscopic observations (not shown). Thus, the tri-culture would have likely not been established in these conditions. We hypothesise that, with the acetogen being the dominant species, longer HRTs would be required to yield a high enough concentration of acetate that would favour the production of ethanol, key intermediate in the tri-culture. In contrast, model simulations predicted a wider range of feasibility when *A. wieringae* JM was slightly less dominant in the community (i.e., 30 - 50%) (Suppl. material § 5.6.2: Fig. S5.3c-e). In this scenario, a higher abundance of the ethanol-consuming strains might favour the thermodynamics of ethanol production sufficiently even at shorter HRTs.

Next, we looked at predicted production rates at the range of biomass species ratios that led to a feasible tri-culture at a growth rate of 0.02 h^{-1} (HRT = 50 h) (Fig. 5.4). Valerate was the predominant product with a rather balanced community and with dominant chain-elongating activity, i.e., a biomass species ratio of 3/3/4 (*A. wieringae* JM/*A. neopropionicum*/*C. kluyveri*). Production of heptanoate was not predicted by the model, probably due to insufficient accumulation of the precursor (valerate) at the specified dilution rate. Low abundance of *A. neopropionicum* (20%; ratio 4/2/4) resulted in the highest production of caproate, yet valerate was still the main product in this condition. This scenario also resulted in the lowest acetate production rate, perhaps due to low contribution to acetate by *A. neopropionicum* and to enhanced chain-elongating activity. Thus, when *A. neopropionicum* was slightly more dominant (ratio 4/3/3), acetate production was higher, in detriment of the chain-elongated products. Overall, these results suggest that maintaining a strong chain-elongating activity and balanced carboxydotrophy and propionigenesis favours the production of valerate by the tri-culture.
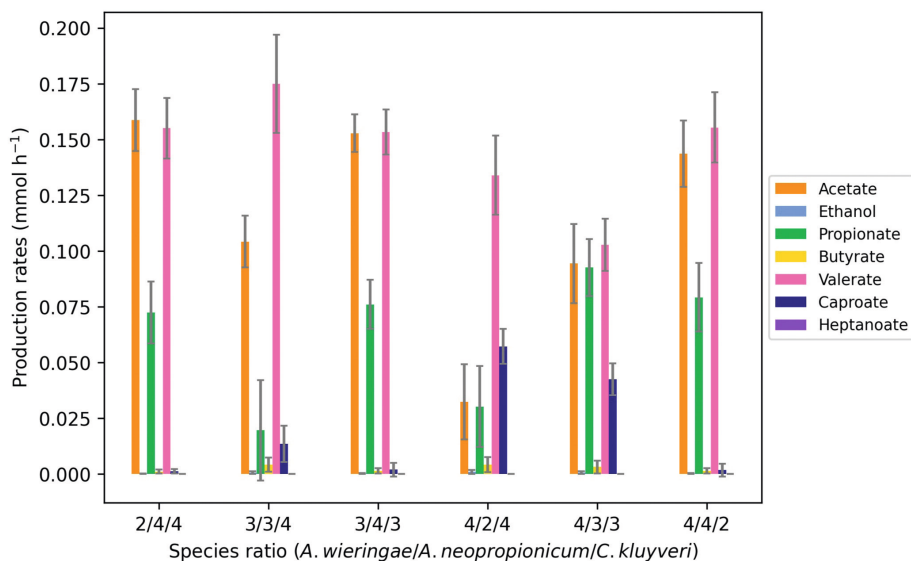
Figure 5.4 Production rates from CO fermentation by the tri-culture A. wieringae JM - A. neopropionicum - C. kluyveri, predicted by the model using FBA at the feasible biomass species ratios at a fixed growth rate of 0.02 h^{-1}.

5.3.6 cFBA simulations predict enhanced ethanol and chain-elongated products by the tri-culture with the addition of H$_2$

Syngas typically contains H$_2$ in a similar proportion as CO (Couto et al., 2013). Acetogens can use H$_2$ as additional electron donor to enable the fixation of CO$_2$, increasing the yield of carbon fixation in the fermentation (Redl et al., 2017). Here, we performed cFBA simulations with Flux Sampling to study the effect of H$_2$ addition on the production of acetate and ethanol by *A. wieringae* JM, and on the product spectrum of the tri-culture under steady-state. To this end, we varied the ratio of CO:H$_2$ uptake rates, with constrained CO uptake rate (1.5 - 3.5 mmol h^{-1}) and growth rate (0.02 h^{-1}; HRT = 50 h).

In simulations of *A. wieringae* JM monoculture, we tested CO:H$_2$ ratios ranging from 3.5 to 0.5 (Fig. 5.5a). The model simulations supported by data obtained in the chemostat experiment showed that, under the conditions tested, acetate was virtually the only product of CO fermentation (model prediction: 0.66±0.03 mmol h^{-1}) (Fig. 5.3b). Our results indicate that H$_2$ supplementation would increase acetate production as long as CO is present in a higher proportion, that is, up to a CO/H$_2$ ratio of 1 (Fig. 5.5a). At this ratio, the predicted acetate production was the highest (1.36±0.09 mmol h^{-1}), and ethanol production remained very low (<0.1 mmol h^{-1}). With CO/H$_2$ uptake rate ratios <1, solventogenesis was significantly enhanced. With a CO/H$_2$ ratio of 0.5 (i.e., with double the uptake rate of H$_2$ than CO), acetate production was negligible compared to an ethanol production of 1.56±0.01 mmol h^{-1}, the highest we obtained in our simulations.
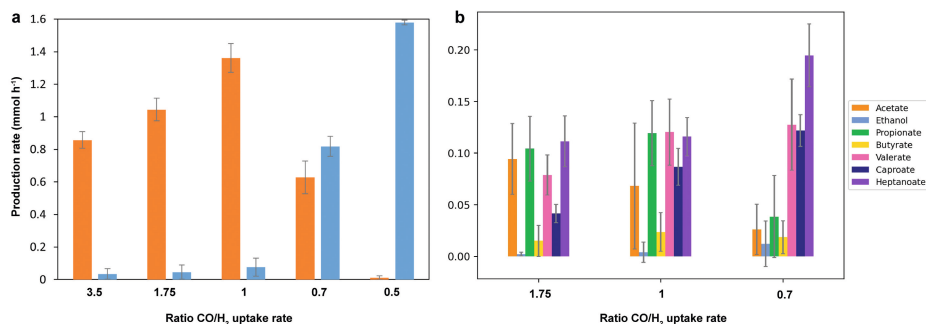
Figure 5.5 Production rates at different CO/H_2 uptake rate ratios by the monoculture of *A. wieringae* JM (**a**) and by the tri-culture of *A. wieringae* JM, *A. neopropionicum* and *C. kluyveri* (**b**) predicted by model simulations using FBA. Tri-culture model simulations were done at a fixed biomass species ratio of 4/3/3. The growth rate was fixed at 0.02 h^{-1} (HRT = 50 h).

Simulations of the effect of H_2 on the tri-culture model were done at a fixed biomass species ratio of 4/3/3 (*A. wieringae* JM/*A. neopropionicum*/*C. kluyveri*). This ratio was chosen as it resulted in a feasible tri-culture in previous simulations (Suppl. material § 5.6.2: Fig. S5.3), and it reflected predominance of the acetogen, matching our observations in the bioreactor experiments. We tested the CO/H_2 uptake rate ratios of 1.75, 1 and 0.7. Our results showed that the addition of H_2 gradually increased the production of chain-elongated products (Fig. 5.5b). Interestingly, the lowest presence of H_2 (ratio CO/H_2 of 1.75) already resulted in the production of heptanoate, which was not detected in simulations with only CO (Fig. 5.4). With the highest H_2 supplementation (ratio of 0.7), the predicted production rates of odd-chain products (C5+C7) reached 0.35 mmol h^{-1}, the highest obtained in our simulations. Heptanoate was predicted to be the main end product in this scenario, followed by similar proportions of valerate and caproate, and low accumulation of short-chain carboxylates. We hypothesise that, with H_2 as additional electron donor, propionigenesis (by *A. neopropionicum*) and subsequent chain elongation (by *C. kluyveri*) were enhanced due to increased production of ethanol by the acetogen (up to 0.78 mmol h^{-1} in our simulations; see git repository). As expected, the production of CO_2 decreased (to < 0.1 mmol h^{-1}) with increased presence of H_2, accordingly with a higher carbon fixation through the Wood-Ljungdahl pathway.

5.4   Conclusions

This study demonstrates the ability of a novel synthetic microbial tri-culture to produce odd- and even-chain carboxylic acids (C4-C7) from solely CO as substrate. The tri-culture is composed of *A. wieringae* JM, an acetogen that grows optimally at neutral pH; A. *neopropionicum*, a propionigenic bacterium that grows on ethanol; and *C. kluyveri*, well-studied for its chain-elongating metabolism. Co-cultivation of the three strains in a bioreactor with continuous supply of CO resulted in the production of C4-C7 carboxylic acids followed by the reduction of some of the acids into the corresponding higher alcohols (max. 14% mol/mol). Our work showed that *A. wieringae* JM shares particular traits observed in other acetogens, namely the thermodynamic regulation of the acetogenic/solventogenic metabolism, and the CO-driven reduction of carboxylic acids, which

can occur at neutral pH in this strain. In addition, genome-scale metabolic modelling combined with FBA predicted that, under steady-state, the tri-culture would be feasible in a narrow range of biomass species ratios that, generally, represent an overall balanced community. Low growth rates (or dilution rates) of < 0.03 h^{-1} were also essential for the viability of the tri-culture, presumably to enable sufficient production ethanol, key intermediate. Model simulations also showed that H$_2$ as additional electron donor to CO would increase ethanol production by the acetogen, ultimately enhancing the production of odd-chain carboxylates by the tri-culture. Future work may address improving the constructed GEM of *A. wieringae* JM with additional experimental data, as well as model-driven assessment of the tri-culture performance during continuous fermentation of CO.

5.5 Availability of data and materials

The constructed models and the data generated by the models in this study are available in the following Gitlab repository: \\https://gitlab.com/wurssb/Modelling/triculture_aw_an_ck/-/tree/master/.

Supplementary information is provided hereafter, in § 5.6.

5

5.6   Supplementary material

5.6.1   Supplementary Materials & Methods

Reconstruction of the GEM of *A. wieringae* JM, iAWJM_SB617

The genome-scale metabolic model (GEM) of *Acetobacterium wieringae* JM was reconstructed using as scaffold the GEM of the acetogen *Clostridium autoethanogenum* — iCLAU786 (Valgepea et al., 2017) —, and adapted according to the genomic features of *A. wieringae* JM. An orthology-based approach was followed. First, the genomic sequence of *A. wieringae* JM (GCA_008107585.1) and the reference annotation were retrieved (in GFF format) from the National Center for Biotechnology Information (NCBI) under accession number VSLA00000000 (Arantes et al., 2020). The genome was functionally annotated using eggNOG-mapper 2.1.7 (Huerta-Cepas et al., 2017) and structurally annotated using the reference annotation. The annotation can be found in the public GitLab repository: https://gitlab.com/wurssb/Modelling/triculture_aw_an_ck/-/tree/master/. The genomic sequence of *C. autoethanogenum* DSM 10061^{T} (GCA_001484725.1) was retrieved (in FASTA format) from NCBI (Humphreys et al., 2015) and orthologous genes of the two were identified using OrthoFinder 2.5.4. (Emms & Kelly, 2019). The scaffold model of *C. autoethanogenum* was adapted for *A. wieringae* JM. Reactions with a gene-protein-reaction (GPR) association of genes with predicted orthologs in *A. wieringae* JM were kept. A new GPR was associated to these reactions by replacing the *C. autoethanogenum* locus tag ('CAETGH_RSXXXXX') by the corresponding *A. wieringae* JM protein ID 'TYCXXXXX'. Reactions for which no homologous genes were identified were further inspected. Enzyme Commission (EC) numbers describing these reactions were retrieved from the template model, and gene(s) associated to these EC numbers in *A. wieringae* JM were retrieved either from the genome annotation file or from the PATRIC (Davis et al., 2019) or UniProt (Apweiler et al., 2004) databases. Reactions without an annotated EC number in the template model were searched by their ModelSEED (Henry et al., 2010), KEGG (Ogata et al., 1999), MetaCyc (Karp et al., 2002), or BIGG identifier (Schellenberger et al., 2010) in the corresponding databases. The EC numbers obtained were used to retrieve the genes from either the genome annotation file, PATRIC or UniProt databases. The stoichiometry and mass balances of the reactions was also verified in the aforementioned databases. The biomass reaction was kept the same as in the model of *C. autoethanogenum*. Finally, the draft model was transformed into SBML (xml) format using Python and COBRApy (Ebrahim et al., 2013).

Next, growth on CO and on H_2/CO_2 was maximised using flux balance analysis (FBA) in COBRApy. The uptake rates of CO, H_2 and CO_2 were fixed at 30 mmol g_{CDW}^{-1} h^{-1}, 40 mmol g_{CDW}^{-1} h^{-1} and 20 mmol g_{CDW}^{-1} h^{-1}, respectively. Then, reactions with non-associated GPR (orphan reactions) were removed, except for extracellular and transport reactions. We also checked whether the growth rate and the production rate of acetate were affected if each reaction belonging to the template model of *C. autoethanogenum* was removed. Reactions from the template model that led to the same rates when removed (under both CO and H_2/CO_2 growth) were excluded from the model as they were considered not essential and/or not present in *A. wieringae* JM. To eliminate these reactions, the function single_reaction_deletionReactions of COBRApy was used. Metabolites involved exclusively in the removed reactions were also eliminated. The model was amended with

reactions and metabolites whose associated proteins were annotated in the genome of *A. wieringae* JM and reported to be present in other *Acetobacterium* species (Ross et al., 2020) but not in *Clostridium*. Additionally, the GEM of the close relative *Acetobacterium woodii* ('CNA_AW') (Bertsch & Müller, 2015b; Koch et al., 2019) was used to refine the model. Reactions were added by keeping the same information and namespace of the scaffold model using ModelSEED. Once new reactions were added, the previous procedure was repeated to identify possible non-essential orphan reactions. The final model in format xml was translated into SBML Level 3 Version 1 using KBase (Arkin et al., 2018). The model was validated using MEMOTE (Lieven et al., 2020) and SBML Validator (Hucka et al., 2015). The final GEM of *A. wieringae* JM, iAWJM_SB617, can be found in the git repository in Table format, json and SBML L3V1 standardization, together with a MEMOTE report of quality assessment.

Qualitative validation of the GEM iAWJM_617 using FBA

The iAWJM_617 model was qualitatively validated by assessing growth phenotypes on carbon sources previously tested in or predicted for *A. wieringae* type strain and other *Acetobacterium* species (Ross et al., 2020). Model simulations were done through FBA in COBRApy version 0.24.0, and Python 3.9. For each carbon source, the lower bound of the substrate uptake rate per time point was constrained to -30 mmol g_{CDW}^{-1} h^{-1} when assessing growth on a single carbon source, and to -30 mmol g_{CDW}^{-1} h^{-1} in total when assessing growth on more than one carbon source, unless specified otherwise. The biomass synthesis reaction was used as the objective function. Growth was considered positive when the growth rate was higher than 0.0001 h^{-1}.

Quantitative validation of the GEM iAWJM_617 with chemostat cultivation data

Quantitative validation of the iAWJM_617 model was done by comparing production rates (of acetate and ethanol) predicted by the model with those measured in this study in the duplicate chemostat bioreactors of *A. wieringae* JM growing on CO. The hydraulic retention time (HRT) of the bioreactor determined the growth rate of the culture in steady-state, defined as the inverse of HRT (1/HRT). Fluxes were expressed as environmental fluxes (mmol h^{-1}) instead of specific fluxes (mmol g_{CDW} h^{-1}), as previously shown (Khandelwal et al., 2013). The biomass reaction was constrained by the growth rate multiplied by the average amount of biomass measured in the bioreactor. The lower bound of the CO uptake rate reaction was constrained between -3.5 mmol h^{-1} and -1 mmol h^{-1}. The *non-growth*-associated maintenance (NGAM) value of the ATP maintenance reaction ('rxn00062_aw') was adjusted based on the CO consumed in the cultivation experiment and it was used to constrain the lower bound of this reaction. The solution space and the set of fluxes compatible with the measured constraints were sampled using the sample function in the flux_analysis submodule of COBRApy. The results shown are the average and standard deviation of 10000 iterations.

## Construction of the community model of *A. wieringae* JM – *C. kluyveri* – *A. neopropionicum*

The tri-culture model of *A. wieringae* JM, *Anaerotignum neopropionicum* and *Clostridium kluyveri* was generated by combining the single species models of each strain: iAWJM_617 (this work),

iANEO_607 (Benito-Vaquerizo et al., 2022b) and iCKL708 (Zou et al., 2018), respectively. The methodology followed was the same as reported in our previous studies (Benito-Vaquerizo et al., 2020; Benito-Vaquerizo et al., 2022a). In short, each species was associated to an intracellular compartment: 'Cytosol_AW', 'Cytosol_AN' and 'Cytosol_CK', with 'aw', 'an' and 'ck' as their respective identifiers (id). The extracellular compartment, whose identifier is 'e', was shared by the three species. Intracellular metabolites were labelled with the id of the metabolite and the corresponding compartment id (e.g., acetate_aw). Reactions and metabolites that were defined as extracellular ('_e') in the single species models were also defined as extracellular in the tri-culture model. Extracellular reactions and metabolites originally present in more than one species were given the same nomenclature in the three-species model. Similarly, repeated reactions across the individual models were unified to be unique in the tri-culture model. Biomass of each species was represented by its own biomass synthesis reaction, denoted by the following id: 'Biomass_aw', 'Biomass_an' and 'Biomass_ck'. An additional reaction was created to represent the community biomass ('EX_Biomass_e'), which combined the three biomass contributions represented by metabolites 'cpd11416_aw', 'cpd11416_an' and 'Biomass_ck'. Lastly, the tri-culture model was transformed into SBML level 3 version 1 (git repository).

Tri-culture model simulations

FBA was used to evaluate the feasibility of the tri-culture in a range of combinations of species ratios and growth rates (dilution rates) during growth on CO. We tested growth rates from 0.005 to 0.05 h-1, and biomass species ratios between 0.1 and 0.9. The cell density of the community was estimated based on biomass measurements done in monoculture experiments of *A. wieringae* (0.32 g). For each community biomass, we assessed growth with all the combinations of growth rates and species ratios. The biomass of each species was calculated based on the indicated species ratio and the community biomass. The biomass of each species was multiplied by the pertinent growth rate, and the value was used to constrain the flux through the biomass synthesis reaction of each species. Species growth rates were set to be equal and equal to the community growth rate. The lower bound of the CO uptake reaction was constrained between -3.5 mmol h^{-1} and -1 mmol h^{-1}, based on CO inflow rates measured in chemostat cultivation of *A. wieringae* JM (this study). The community biomass reaction was defined as the objective function for maximization. We also explored the metabolite profile of CO fermentation at a fix growth rate (0.02 h^{-1}) and at the biomass species ratios that led to feasible solutions. The solution space and the set of fluxes compatible with the measured constraints were sampled using the sample function in the flux_analysis submodule of COBRApy. Finally, we simulated the effect of H_2 as additional energy source on the production of medium-chain carboxylic acids by the tri-culture. Several H_2 uptake rates were tested, under a fixed 4:3:3 species ratio (*A. wieringae* JM/*A. neopropionicum*/*C. kluyveri*) and growth rate of 0.02 h^{-1}. The total biomass was fixed to 0.32 g. The lower bound of the CO uptake rate was constrained to -3.5 mmol h^{-1}, and the upper bound to -1.5 mmol h^{-1}. H_2 uptake rates were varied from -5 to -2 mmol h^1. Presented results are the average and standard deviation based of 5000 iterations generated for each condition (git repository).

5.6.2   Supplementary Figures and Tables

a

b
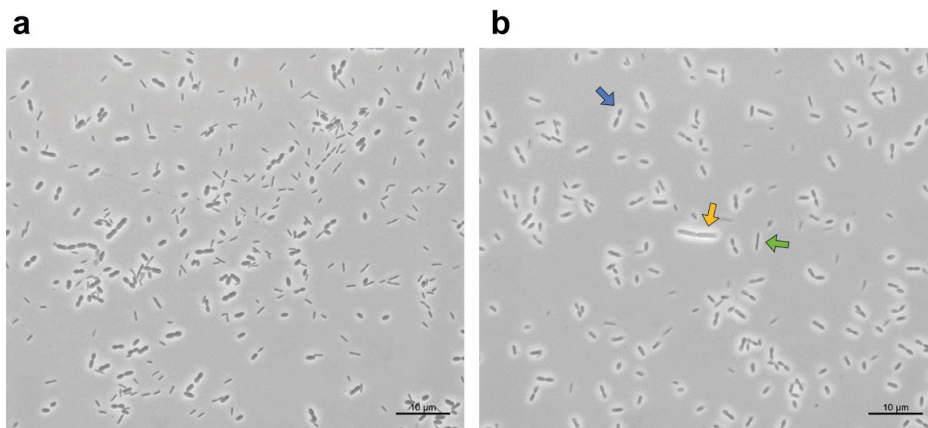
Figure S5.1 Phase-contrast microscopy pictures of the tri-culture in batch cultivation in a bioreactor with continuous gas supply ($CO/N_2/CO_2$). Samples were taken during the growth phase at **a**) 2.1 days, and **b**) 2.8 days. The arrows point to cells of *Acetobacterium wieringae* JM (blue), *Clostridium kluyveri* (orange) and *Anaerotignum neopropionicum* (green).
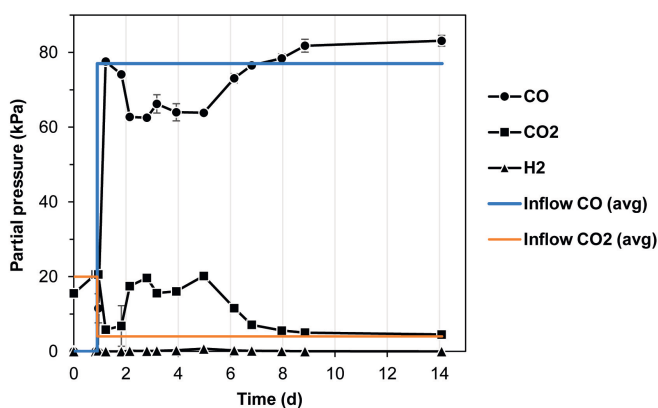
Figure S5.2 Composition of the gas inflow (average of technical replicate measurements) and headspace during batch cultivation of the tri-culture in a bioreactor with continuous gas supply ($CO/N_2/CO_2$). Error bars indicate the standard deviation of triplicate measurements.

Table S5.2 Composition of the model iAWJM_SB617. Three types of reactions are distinguished; conversion, transport and exchange reactions. Transport reactions represent the translocation of metabolites between the intracellular compartment (id:'aw') and the extracellular compartment (id:'e'). Exchange reactions represent the uptake of substrates or production of metabolites, into and outside the cell. Reactions non-associated with genes correspond mostly to: i) enzyme-independent transport reactions (e.g., diffusion reactions); and ii) exchange reactions that are artificial representations and, thus, without enzymes.

Features	Abundance
Genes	617
Metabolites	1065
Intracellular metabolites	915
Extracellular metabolites	152
Reactions	1081
Conversion reactions	832
Transport reactions	159
Exchange reactions	76
Reactions associated with genes	775 (71.7%)
Reactions non-associated with genes	306 (28.9%)

Figure S5.3 Predicted feasible solution space of the tri-culture of *A. wieringae* JM (AwJM), *A. neopropionicum* (Aneo) and *C. kluyveri* (Ck) in steady-state during growth on CO, obtained by FBA model simulations. Each panel corresponds to a fixed abundance of *A. wieringae* JM (10–80%).

5

Exploring pH effects on co-cultures of acetogens and *Clostridium kluyveri* for syngas fermentation

—

Siebe Peek*, Ivette Parera Olm*, Martijn Diender, Diana Z. Sousa

*Authors contributed equally.

Abstract

Clostridium autoethanogenum has been co-cultivated with *Clostridium kluyveri* to expand the product spectrum of syngas fermentation via chain elongation. However, a significant challenge observed in this co-culture is the discrepancy between the optimal pH requirements of the two microorganisms. Sustained production of ethanol by the acetogen —optimal at mildly acidic conditions in *C. autoethanogenum*— is key to maintain chain-elongation activity by *C. kluyveri*, which grows best at neutral pH. In this work, we explored the effect of pH on co-cultures using different acetogens with *C. kluyveri*. The selected acetogens, namely *C. autoethanogenum, Clostridium carboxidivorans, Acetobacterium wieringae* strain JM and *Alkalibaculum bacchi*, were chosen based on their different optimal pH for growth varying in a range from 6 to 8. Our goal was to identify the combinations of acetogen–*C. kluyveri* and pH that result in maximum CO and H_2 conversion, and produce the highest titres of medium-chain carboxylic acids (butyrate and caproate). *A. wieringae* JM and *C. autoethanogenum* were the best-performing strains in co-cultures with *C. kluyveri* to produce butyrate and caproate at pH values 7–7.5 and 6, respectively. In contrast, *A. bacchi* and *C. carboxidivorans* showed slow growth and poor H_2 utilisation (<15%). With repeated refilling of the headspace, the *A. wieringae* J–*C. kluyveri* co-cultures at pH 7.5 almost exclusively butanol (17 mM) and hexanol (15 mM), highlighting the solventogenic potential of this co-culture. This study contributes with the first acetogen–pH screening for optimal co-cultivation with *C. kluyveri* for the revalorisation of syngas (CO/H_2). To further enhance productivity and titres, future work should involve bioreactor experiments with controlled, continuous CO load using the most promising co-cultures. The findings of this study also contribute with insights into the physiology of different acetogens.

6.1 Introduction

Synthesis gas (syngas; $CO/H_2/CO_2$) fermentation has emerged as a promising biotechnological platform for the revalorisation of waste streams into chemicals (Köpke & Simpson, 2020). Besides biomass-derived syngas obtained through gasification, other sources of CO-rich streams are off-gases from steel-mills. The primary components of syngas can be metabolised by acetogens. These are strictly anaerobic bacteria that employ the reductive acetyl-CoA pathway to fix CO_2 while harvesting energy from CO and H_2, among other substrates (Schuchmann & Müller, 2014; Schuchmann & Müller, 2016). Acetate is the main product of acetogenic metabolism, and some species can also produce ethanol when sufficient reductive power is available. In acetogens, ethanol production is normally favoured in acidic environments and/or limiting certain nutrients (e.g., phosphate, metals or some B-vitamins) (Köpke et al., 2011). Due to the energy-constrained metabolism of acetogens (Schuchmann & Müller, 2014), the range of native products beyond acetate and ethanol is limited. Only a few species of acetogens are reported to produce other compounds, such as 2,3-butanediol or butyrate, albeit to a lesser amount (Liew et al., 2016; Molitor et al., 2017). Thus, in syngas fermentation, monocultures of wild-type acetogens have been almost exclusively exploited for their ability to produce ethanol. Metabolic and genetic engineering have recently advanced in model acetogens, such as *Clostridium autoethanogenum*, *Clostridium ljungdahlii* and in *Acetobacerium* species (Arslan et al., 2022; Bourgade et al., 2021; Lauer et al., 2022; Liew et al., 2022; Moreira et al., 2023). However, despite considerable progress, engineering of acetogens is still in early stages of development, as the efficient integration of foreign genetic material in these non-standard microorganisms is challenging (Bourgade et al., 2021; Charubin et al., 2018).

An alternative to broaden the product spectrum of syngas fermentation is to rely on microbial communities, either open mixed cultures (undefined) or synthetic co-cultures (defined) (Baleeiro et al., 2019; Parera Olm & Sousa, 2021). In these networks, the products of acetogenic metabolism can be converted into more complex, higher-value end products by other partners in the community. A well-known case is the co-cultivation of acetogens with chain-elongating bacteria, in which medium-chain carboxylic acids (MCCAs; e.g., caproate) can be produced from syngas, a process facilitated by cross-feeding of ethanol and acetate (Diender et al., 2016b; Richter et al., 2016a). *Clostridium kluyveri* is the model organism for ethanol-based chain elongation; its physiology has been extensively studied (Barker & Taha, 1942; Bornstein & Barker, 1948; Candry et al., 2020b; Kenealy & Waselefsky, 1985; Parera Olm & Sousa, 2023; Yin et al., 2017), its genome has been fully sequenced (Seedorf et al., 2008), and kinetic and metabolic models have been recently made available (Candry et al., 2018; Zou et al., 2018). In this microorganism, chain elongation takes place via the reverse β-oxidation pathway, a cyclic pathway that elongates a carboxylate two carbons at a time by adding an acetyl-CoA molecule derived from ethanol (Seedorf et al., 2008).

Co-cultures of acetogens and *C. kluyveri* are highly influenced by environmental pH, which has a direct impact on: i) the cell growth rate, ii) the product spectrum, iii) the equilibrium shift towards undissociated carboxylic acids that negatively affect cell growth, and iv) product recovery. In an earlier work, a synthetic co-culture of *C. autoethanogenum* and *C. kluyveri* was established that successfully produced butyrate (C4), caproate (C6) and their respective alcohols from solely CO (Diender et al., 2016b). *C. autoethanogenum* is a mild acidophile that grows at pH 4.5–6.5, with an

optimum of 5.8–6.0 (Abrini et al., 1994). In contrast, the optimum pH for *C. kluyveri* is 6.8, with growth observed between pH 6.0 and 7.5 (Barker & Taha, 1942). Due to the disparity between the optimal pH for growth of these microorganisms, the *C. autoethanogenum* – *C. kluyveri* co-culture was only functional within the narrow pH range of 5.5–6.5 (Diender et al., 2016b). Additionally, the pH influences the product spectrum of syngas-fermenting chain-elongating cultures. Mildly acidic conditions favour solventogenesis by acetogens, while pH values around neutrality are required to maintain chain elongation activity (Diender et al., 2016b; Ganigué et al., 2015; Ganigué et al., 2016; Richter et al., 2016a; San-Valero et al., 2020). Since ethanol availability is a requisite for chain elongation, the functionality of such co-cultures is conditioned by the balanced co-occurrence of acetogenic and chain-elongating metabolism. At the same time, acidic environments favour the accumulation of the undissociated form of carboxylic acids (with pKa values ≈4.8) that, due to their hydrophobic nature, pass freely across the cell membrane and inhibit cell growth (Kamp & Hamilton, 2006). On the other hand, acidic environments enhance *in situ* product recovery (e.g., via pertraction) since the driving force of such methods is the concentration gradient of the undissociated species of carboxylates (Gehring et al., 2020).

In addition to *C. autoethanogenum*, other acetogens have been used in co-cultivation with *C. kluyveri* for the fermentation of syngas. Examples are *C. ljungdahlii* (Richter et al., 2016a), a strain physiologically very similar to *C. autoethanogenum* (Bengelsdorf et al., 2016; Tanner et al., 1993), *Clostridium carboxidivorans* (Bäumler et al., 2021)*,* which grows optimally at pH 6.2 (Liou et al., 2005), and *Clostridium aceticum* (Fernández-Blanco et al., 2022) that has an optimum pH of 8.3 (Braun et al., 1981). Each of these acetogens has been isolated from a different environment, conferring each strain not only adaptation to distinct environmental factors such as pH, but also metabolic differences that influence substrate utilisation, product formation and cell growth (Bengelsdorf et al., 2016; Bertsch & Müller, 2015a; Diender et al., 2015; Shin et al., 2016). In this study, we screened a selection of acetogens in co-cultivation with *C. kluyveri* under different pH values in order to ascertain the combinations of species and pH yielding maximum CO and H_2 conversion rates and product titres of MCCAs (butyrate and caproate). We tested the following acetogenic strains at pH values from 6 to 8: *C. autoethanogenum*, *C. carboxidivorans*, *Acetobacterium wieringae* strain JM and *Alkalibaculum bacchi*. Our study highlights the importance of exploring diverse acetogenic strains and pH conditions in co-cultivation approaches for syngas fermentation.

6.2   Materials and Methods

6.2.1   Microbial strains and cultivation medium

All strains were obtained from the German Collection of Microorganisms and Cell Cultures (Leibniz Institute DSMZ, Braunschweig, Germany), with the exception of *A. wieringae* strain JM, which was isolated in our lab (Arantes et al., 2020). Medium preparation was done as described hereafter. The following components were combined to a final composition of (per litre): 1.0 g NH_4Cl, 0.8 g NaCl, 0.2 g $MgSO_4$·$7H_2O$, 0.1 g KCl, 0.1 g KH_2PO_4, 20 mg $CaCl_2$·$2H_2O$, 20 mM acetate, 10 mL of trace element solution from medium ATCC 1754, and 0.5 mg resazurin as redox indicator. 2-(N-Morpholino)ethanesulfonic acid (MES monohydrate) (20 g L^{-1}) or 4-(2-hydroxyethyl)-1-piperazineethanesulfonic acid (HEPES) (12 g L^{-1}) were added as buffering agents depending

on the experiment and initial pH of the medium, as indicated in the next section. After boiling the medium, 0.75 g L^{-1} of L-cysteine-HCl was added as reducing agent. The pH was adjusted to 6 (for *C. autoethanogenum*) or 7 (for all other strains) using NaOH. The reduced medium was then cooled down under a continuous N$_2$ flow, and dispensed into bottles that were sealed with butyl rubber stoppers and aluminium caps. The headspace was filled with the desired gas and according pressure after which the bottles were autoclaved. Yeast extract (final concentration of 0.5 g L^{-1}) and vitamins were added after autoclavation from anaerobic, sterile stock solutions. The final composition of vitamins was (per litre): 0.5 mg pyridoxine, 0.2 mg thiamin, 0.2 mg nicotinic acid, 0.1 mg p-aminobenzoic acid, 0.1 mg riboflavin, 0.1 mg D-Ca-pantothenate, 0.1 mg cobalamin, 0.05 mg folic acid, 0.05 mg lipoic acid, and 0.02 mg biotin. Cultures of all acetogens were grown in 250 mL anaerobic bottles filled with 50 mL medium with a CO/H$_2$ headspace (66:34%, v/v; 170 kPa). All acetogens were incubated shaking (100 rpm) at 37°C, with the exception of *A. wieringae* strain JM which was incubated at 30°C. Cultures of *C. kluyveri* were grown in 250 mL anaerobic bottles with 50 mL medium and a N$_2$/CO$_2$ headspace (80:20%, v/v; 150 kPa), with 20 mM acetate plus 80 mM ethanol as substrates. *C. kluyveri* cultures were incubated statically at 37°C.

6.2.2 Co-cultivation experiments in serum bottles

Co-cultures of *C. kluyveri* with either of six different acetogens were established in 250 mL serum bottles (batch) containing 50 mL medium as described above. The headspace of all bottles was filled with CO/H$_2$ (66:34%, v/v; 170 kPa). Inoculation was done with 1 mL of actively growing acetogen plus 1 mL of actively growing *C. kluyveri*. Table 6.1 shows the list of the strains studied in the co-cultures (six acetogens plus *C. kluyveri*), their pH for growth and the pH tested in co-culture experiments. For each acetogen-*C. kluyveri* pair, co-cultivation was done at different initial pH values from 6 to 8, with increments of 0.5. Two subsequent sets of experiments (A and B) were performed that differed in the strains tested, the buffer used, the shaking conditions and the headspace refilling. In both experiments, each condition was tested in triplicate. Specific details of each experiment are given below.

Table 6.1 Strains of acetogens and *C. kluyveri* tested in this study and their pH range for growth. The pH range tested in syngas-fermenting co-cultures of each acetogen with *C. kluyveri* is also included.

Strain	pH range	pH opt.	Ref.	Tested pH range in co-culture with *C. kluyveri* (this study)
Clostridium autoethanogenum DSM 10061	4.5–6.5	5.8–6.0	Abrini et al., 1994	6–6.5
Clostridium carboxidivorans DSM 15243	4.4–7.6	6.2	Liou et al., 2005	6–7
Acetobacterium wieringae strain JM	7[a]	NA	Arantes et al., 2020	6–7.5
Alkalibaculum bacchi DSM 22112	6.5–10.5	8–8.5	Allen et al., 2010	7.5–8
Clostridium kluyveri DSM 555	6–7.5	6.8	Barker & Taha, 1942	-

NA: data not available. [a]Strain JM is reported to grow at pH 7, but the pH range for growth has not been yet defined.

In experiment A, we tested the co-cultures of *C. kluyveri* with *C. autoethanogenum*, *C. carboxidiv-orans*, A. *wieringae* JM, and *A. bacchi*. Upon inoculation, bottles were incubated at 30°C statically and were placed shaking (150 rpm) when CO consumption was observed. The buffer used for cultivations with an initial pH of 6 and 6.5 was MES (86 mM), while for cultivations starting at pH 7 or higher the buffer was HEPES (50 mM). Liquid and gas sampling were performed regularly for analysis of cell density, headspace and soluble products composition.

In experiment B, *C. kluyveri* was co-cultivated with *C. autoethanogenum* or *A. wieringae* JM. Due to poor growth observed in the first experimental set (see Results: § 6.3.1), *C. carboxidivorans* and *A. bacchi* were left out of this part of the study. All incubations were performed with MES buffer (86 mM) as it sustained a more favourable environment for *C. kluyveri* than HEPES. Bottles were initially incubated at 30°C statically, and were put shaking (150 rpm) when at least one bottle of the three replicates consumed at least 15% of the initial CO. Additionally, the headspace was refilled when less than 15% of H_2 was left in at least one bottle of the three replicates. Refilling of the headspace was done multiple times (see Results), until no metabolic activity was observed in the cultures. Before the first refill of the headspace, liquid and gas sampling were performed regularly. Afterwards, liquid samples were only taken every time the headspace was refilled, while gas samples were still taken regularly.

6.2.3   Analytical techniques

Gaseous compounds (CO, CO_2, and H_2) were analyzed in a gas chromatograph (GC; Compact GC 4.0, Global Analyser Solutions, The Netherlands) with argon as carrier gas. The gas chromatograph comprised two channels with a thermal conductivity detector (TCD). CO and H_2 were separated using a Carboxen 1010 pre-column followed by a Molsieve 5A column operated at 140°C. Separation of CO_2 was performed on a Rt-Q-BOND column set at 60°C. Analysis of soluble compounds (acetate, ethanol, and butyrate) was performed by high-performance liquid chromatography (HPLC; LC-2030C, Shimadzu, Japan). The HPLC was equipped with a Shodex SH1821 column operated at 65 °C. Arabinose (10 mM) was used as internal standard and 0.01 N H_2SO_4 was used as eluent. The flowrate was set at 1 mL/min. The concentration of volatiles (butanol, hexanol, and caproate) was measured on a gas chromatograph (GC-2010, Shimadzu, Japan) equipped with a headspace autosampler (HS-20). The column employed was a DB-WAX Ultra Inert (Agilent, USA), operated at a gradient from 50 to 200 °C, and nitrogen was used as carrier gas. Sample preparation was performed in 10 mL headspace vials with 100 µL of clear liquid sample plus 100 µL 10 mM methanol in 1% (w/v) formic acid to acidify acids in the sample. The vial was transferred to the oven of the autosampler (60 °C) where it was held for five minutes before a headspace sample was taken that was brought on the column. Detection of compounds was done with a FID detector. Data analysis of both HPLC and GC peaks was performed with Chromeleon™ data analysis software (Thermo Fisher Scientific), version 7.2.10. The microbial growth was estimated using an optical density measurement at 600 nm (OD600) using a spectrophotometer (UV-1800, Shimadzu, Japan).

6.2.4 Calculation of the theoretical ethanol production

Ethanol is a key intermediate in the co-cultures, as it sustains growth of *C. kluyveri*. Ethanol is used in the production of butyrate and caproate via chain elongation. Subsequently, these carboxylic acids may be reduced to butanol and hexanol. Where indicated, the theoretical ethanol production by the acetogenic partner in co-cultures was calculated based on the stoichiometry of chain elongation and alcohol production (Table 6.2).

Table 6.2 Theoretical stoichiometry of chain elongation and CO-driven alcohol production, used to calculate the theoretical ethanol (in bold) produced in co-cultures.

Product	Reaction
Butyrate	$6\,\mathbf{C_2H_5OH} + 4\,CH_3COO^- \rightarrow 5\,C_3H_7COO^- + H^+ + 4\,H_2O + 2\,H_2$
Caproate	$6\,\mathbf{C_2H_5OH} + 5\,C_3H_7COO^- \rightarrow 5\,C_5H_{11}COO^- + CH_3COO^- + H^+ + 4\,H_2O + 2\,H_2$
Alcohols	$2\,CO + H_2O + Xn-COO^- + H^+ \rightarrow Xn-CH_2OH + 2\,CO_2$
(butanol and hexanol)	

6.3 Results and Discussion

6.3.1 Co-cultures without refilling of the headspace at pH 6–8 (experiment A)

In experiment A, we compared the performance of co-cultures of *C. kluyveri* with either *C. autoethanogenum*, *C. carboxidivorans*, *A. wieringae* JM or *A. bacchi*. These four species were selected for a first screening as they are representative acetogens of optimal growth at different pH: mildly acidic (*C. autoethanogenum* and *C. carboxidivorans*), neutral (*A. wieringae* JM) and slightly alkaline (*A. bacchi*) (Table 6.1). Serum bottles containing 20 mM acetate were incubated with CO/H$_2$ in the headspace (66:34%, v/v; 170 kPa) at pH values ranging from 6 to 8 (increments of 0.5) depending on the acetogen present in the culture (Table 6.1). Incubations were terminated when CO and H$_2$ were depleted or when cell growth (measured as OD$_{600}$) ceased. Consumption of CO/H$_2$, products formed, theoretical ethanol production (see § 6.2.4), and final pH of incubations are presented in Table 6.3.

Overall, a higher ethanol production in the system ("theoretical ethanol production") correlated with a higher formation of chain-elongated products —particularly, caproate— and/or of higher alcohols (butanol and hexanol). The highest production of butyrate (10.5 ± 0.4 mM) and caproate (4.46 ± 1.38 mM) were obtained with *C. autoethanogenum*–*C. kluyveri* co-cultures at pH 6. Both co-cultures *C. autoethanogenum*–*C. kluyveri* and *A. wieringae* JM–*C. kluyveri* showed the highest CO/H$_2$ consumption (75–100%, at all initial pH tested). In contrast, co-cultures with *A. bacchi* were characterized by slow and poor growth (Suppl. material § 6.5: Fig. S6.1) and incomplete consumption of H$_2$, similarly to *C. carboxidivorans* (Table 6.3). Interestingly, though, *A. bacchi*–*C. kluyveri* co-cultures produced the highest amounts of butanol ($\approx$4 mM) and hexanol ($\approx$4 mM). Co-cultures of *C. kluyveri* with *C. autoethanogenum* at pH 7, and with *A. bacchi* at pH 6.5–7 showed weak growth and low metabolic activity (Suppl. material § 6.5: Table S6.1).

Table 6.3 Experiment A: Consumption of CO/H_2, products formed, and final pH of co-cultures of *C. autoethanogenum*, *C. carboxidivorans*, *A. wieringae* strain JM or *A. bacchi* with *C. kluyveri* at varying starting pH (6–8). Values are the average and standard deviations of biological triplicates. In bold, the highest concentrations of ethanol and end produts (C4/C6) obtained with each acetogen are indicated. Underlined, the highest concentrations of ethanol and end produts (C4/C6) obtained in the experiment are indicated.

C. kluyveri in co-culture with	Gas consumption, mmol (%)		Products formed, mmol (mM)						Theoretical ethanol production[a], mmol	Final pH
	CO	H_2	Acetate	Ethanol	Butyrate	Caproate	Butanol	Hexanol		
C. autoethanogenum										
pH 6	9.31±0.40 (100±0.0)	4.62±0.11 (96.9±0.0)	1.55±0.23 (37.9±5.7)	0.04±0.0 (1.08±0,10)	**0.43±0.01** **(10.5±0.4)**	0.18±0.05 **(4.46±1.38)**	<0.03 **(0.51±0.25)**	- (traces)	**1.04**	5.4±0.0
pH 6.5	8.76±0.32 (97.7±0.0)	3.44±0.71 (74.9±0.2)	2.09±0.10 (50.0±2.6)	0.13±0.03 (3.28±0.73)	0.22±0.02 (5.46±0.51)	0.06±0.0 (1.61±0.14)	<0.01 (0.26±0.05)	- (traces)	0.60	5.8±0.1
C. carboxidivorans										
pH 6	9.3±0.2 (100±0.0)	0.7±0.1 (14.0±0.0)	1.26±0.07 (28.0±1.5)	0.08±0 (1.7±0.1)	0.35±0.02 **(7.7±0.4)**	0.12±0.0 **(2.8±0.0)**	<0.02 (0.3±0)	- (traces)	**0.82**	5.6±0
pH 6.5	9.3±0.2 (99.3±0.0)	0.7±0.6 (14.6±0.1)	1.08±0.17 (25.2±3.9)	0.12±0.01 (2.7±0.3)	0.32±0.08 (7.5±1.9)	0.11±0.05 (2.4±1.1)	<0.02 (0.4±0.1)	- (traces)	0.78	6.2±0
pH 7	3.3±0.2 (35.5±0.0)	0.1±0.1 (2.6±0.0)	0.45±0.03 (10.0±0.6)	0.26±0.02 (5.8±0.3)	0.15±0.01 (3.3±0.2)	0.05±0.0 (1.1±0.1)	0.07±0.02 **(1.6±0.5)**	<0.03 **(0.5±0.2)**	0.70	6.8±0.1
A. wieringae JM										
pH 6.5	8.69±0.43 (96.4±0.1)	4.54±0.29 (99.8±0.0)	1.98±0.16 (44.1±3.7)	0.04±0.03 (0.98±0.82)	0.29±0.05 (6.52±1.3)	0.06±0.01 (1.43±0.43)	- (traces)	- (traces)	0.55	5.9±0.0
pH 7	8.70±0.52 (97.6±0.0)	4.37±0.14 (97.5±0.0)	1.19±0.10 (27.1±2.3)	0.09±0.04 (2.07±1.02)	0.29±0.07 (6.79±1.75)	0.08±0.04 **(1.99±0.91)**	0.04±0.0 **(0.93±0.13)**	- (traces)	**0.72**	5.0±0.1
pH 7.5	9.00±0.27 (100±0.0)	4.50±0.20 (99.4±0.0)	1.81±0.05 (41.2±1.3)	<0.03 (0.64±0.45)	0.34±0.02 **(7.84±0.47)**	0.07±0.01 (1.70±0.26)	<0.01 (0.28±0.12)	- (traces)	0.64	5.1±0.1

C. kluyveri in co-culture with	Gas consumption, mmol (%)		Products formed, mmol (mM)						Theoretical ethanol production[a], mmol	Final pH
	CO	H$_2$	Acetate	Ethanol	Butyrate	Caproate	Butanol	Hexanol		
A. bacchi										
pH 7.5	6.10±1.17	0.35±0.26	0.08±0.05	0.22±0.08	0.07±0.01	0.04±0.04	0.17±0.04	0.17±0,02	**1.04**	6.9±0.0
	(67.6±0.1)	(7.4±0.1)	(1.86±1.32)	(5.06±1.90)	(1.66±0.42)	(**1.01±1.01**)	(3.90±0.95)	(**3.99±0.51**)		
pH 8	4.36±0.13	0.37±0.25	0.01±0.0	0.22±0.06	0.07±0.0	-	0.18±0	0.16±0.01	0.95	6.9±0.0
	(47.6±0.0)	(8.0±0.1)	(0.38±0.18)	(4.94±1.35)	(**1.70±0.09**)	(traces)	(**4.07±0.21**)	(3.52±0.25)		

Traces are concentrations <0.2 mM. [a]Total ethanol produced in the system by the acetogen, calculated taking into account its conversion to C4-C6 products, as described in the Materials and methods (§ 6.2.4).

6

In the next sections, we analyse and compare the performance of co-cultures based on two factors: the type of acetogen and the initial pH.

Effect of the acetogen

The performance of different acetogens can be evaluated by comparing co-cultures with *C. kluyveri* at the same pH. The *C. autoethanogenum–C. kluyveri* co-culture at pH 6 was the most efficient, as it depleted both gaseous substrates and produced the highest titres of butyrate (10.5±0.4 mM) and caproate (4.46±1.38 mM) of experiment A. The other co-culture at pH 6 was with *C. carboxidivorans*; this strain consumed all the available CO but consumed only 14% of the H_2 after 27 days of incubation, and produced lower amounts of C4/C6 products (Table 6.3). It is worth to not that these products could have originated solely from *C. carboxidivorans* without any significant contribution from *C. kluyveri* in the fermentation process (Phillips et al., 2015).

A second comparison can be made between co-cultures with *C. autoethanogenum*, *A. wieringae* JM or *C. carboxidivorans* at pH 6.5. A main difference was the incomplete utilisation of H_2 by *C. autoethanogenum* (74.9%) and *C. carboxidivorans* (14.6%) compared to its depletion by strain JM. In spite of this, the three co-cultures produced similar amounts of butyrate (≈6 mM) and caproate (≈2 mM) (Table 6.3), indicating different dynamics taking place in these co-cultures. Unexpectedly, co-cultures with *A. wieringae* JM did not yield significantly higher titres of chain-elongated products despite complete utilisation of CO/H_2. Our preliminary hypothesis is that this species assimilates more substrate into biomass, as suggested by high final cell densities (up to $OD_{600} = 2.6$) with this acetogen in all co-cultures (Suppl. material § 6.5: Fig. S6.1).

At pH 7, the co-culture of *A. wieringae* JM also performed best, as denoted by complete substrate utilisation and significant accumulation of C4/C6 products. In contrast, *C. carboxidivorans* consumed low CO/H_2 (<40% in total) and produced minimal amounts of products (Table 6.3).

At pH 7.5, two co-cultures were tested: *C. kluyveri* with either *A. wieringae* JM and with *A. bacchi*. Co-cultures with strain JM performed the best, both in terms of CO/H_2 utilisation (nearing 100%) and production of butyrate and caproate. In contrast, *A. bacchi* did not consume all the CO (67.6%, respectively) and H_2 (<10%). Poor substrate consumption by *A. bacchi* could be due to the suboptimal pH for this strain (Table 6.1). This would also explain the accumulation of ethanol (5.06±1.90 mM), butanol (3.90±0.95 mM) and hexanol (3.99±0.51 mM; the highest in experiment A) in these incubations. Likely, *A. bacchi* reduced the C4-C6 carboxylic acids produced in the system (Liu et al., 2014b) in order to reverse acidification of the environment.

Effect of pH

C. autoethanogenum consumed all the available CO in the two conditions tested (pH 6 and 6.5). The highest accumulation of chain-elongated products was obtained with the co-culture at pH 6, in which the H_2 was also depleted. In contrast, significantly lower amounts of C4/C6 products were obtained at pH 6.5, condition that resulted in the highest acetate concentration (50.0±2.6 mM) of experiment A. The lower productivity of this co-culture could be attributed to the slower growth of *C. autoethanogenum* at pH valus above 6 (Abrini et al., 1994; Table 6.1), resulting in a limited supply of ethanol/acetate for utilization by *C. kluyveri*.

Co-cultures with *A. wieringae* JM at initial pH values 6.5–7.5 behaved rather similarly. CO and H$_2$ were fully consumed in the three conditions, and the product spectrum was comparable, with a few exceptions. As in the co-cultures with *C. autoethanogenum*, acetate was the main product followed by butyrate in one order of magnitude lower (Table 6.3). Butyrate concentration did not differ strongly within the three conditions, with the highest value (7.84±0.47 mM) obtained at pH 7.5. The highest concentrations of caproate (1.99±0.91 mM) and butanol (0.93±0.13 mM) were observed at pH 7, presumably stimulated by the higher theoretical ethanol production in this condition (Table 6.3). The rather low production of caproate (compared to co-cultures with *C. autoethanogenum*) could be attributed to limited ethanol production in the system (Table 6.3).

A. bacchi co-cultures at pH 7.5 and 8 exhibited incomplete utilisation of CO ($\approx$50–70%) and H$_2$ ($\approx$8%). This was after 19 days of incubation, a longer period compared to growth of the two other acetogens (7 – 13 days; Suppl. material § 6.5: Fig. S6.1). *A. bacchi* co-cultures produced little acetate (<2 mM) and accumulated the highest amounts of ethanol ($\approx$5 mM) and higher alcohols ($\approx$4 mM), likely as a response to suboptimal pH conditions as mentioned above. A low preference of this train for CO, as observed before (Liu et al., 2014a), could have also triggered a detoxification mechanism, resulting in overflow metabolism towards the production of alcohols (Allaart et al., 2023).

C. carboxidivorans showed rather poor performance in the three conditions tested (pH 6–7). This was mainly due to low H$_2$ use (max. 14%) and slow growth (not shown), as described above.

Best acetogen/pH combinations for co-cultivation with *C. kluyveri*

Based on substrate utilisation and final titres of C4/C6 carboxylates, *C. autoethanogenum* and *A. wieringae* JM and are the best candidates for co-cultivation with *C. kluyveri*. The highest concentrations of butyrate and caproate were obtained with *C. autoethanogenum* at pH 6 (Table 6.3). While higher pH values are likely detrimental to *C. autoethanogenum*, a lower pH of 5.5 has been reported to support this co-culture (Diender et al., 2016b). At pH 6.5, the two acetogens appear as comparable choices; depending on the conditions, *C. autoethanogenum* could potentially sustain higher ethanol production. *A. wieringae* JM is an equally good candidate at pH 7 and 7.5.

An interesting observation was the higher cell density of co-cultures with *A. wieringae* JM (final OD$_{600}$ = 1.2–2.2) compared to co-cultures with *C. autoethanogenum* (OD$_{600}$ = 1.2–1.6) (Suppl. material § 6.5: Fig. S6.1). Experiments with pure cultures of the acetogens should be conducted to get more insight into this apparent divergence biomass yield, and to investigate the underlying physiological reasons.

The clear differential use of H$_2$ by the different acetogens does not come as a surprise, given their phylogenetic and physiological versatility. A recent study determined the H$_2$ thresholds of different acetogens; that is, the H$_2$ partial pressure at which acetogenesis becomes thermodynamically unfavourable (Laura & Jo, 2023). This threshold varies across acetogens due to their different bioenergetic mechanisms (e.g., the cation involved in chemiosmotic gradient, or the use of electron-bifurcating hydrogenases), which would explain the differences observed here.

6.3.2 Co-cultures with repeated refilling of the headspace (experiment B)

In experiment B, we compared co-cultures of *C. kluyveri* with the acetogens *C. autoethanogenum* and *A. wieringae* JM at different initial pH values (6–7.5). Due to poor substrate use of co-cultures

with *C. carboxidivorans* and *A. bacchi* in the previous experiment, these strains were not included here. In this experiment, the headspace was refilled upon CO/H$_2$ depletion. With this, we aimed to lower acetate accumulation and stimulate the production of the more reduced products (butyrate, caproate, and alcohols). In addition, MES buffer was used for all the incubations, as we considered that HEPES did not yield enough buffering capacity before. Table 6.4 summarizes the CO/H$_2$ consumption, product formation, theoretical ethanol production, and final pH in these incubations.

Co-cultures with *C. autoethanogenum* (pH 6–6.5) and *A. wieringae* JM (pH 6–7.5) consumed two and three CO/H$_2$ headspaces, respectively. Incubations with *A. wieringae* JM at pH 6 grew slower, and therefore only one headspace was sampled. Cumulative CO consumption was overall high (>90%) (Table 6.4). Conversely, H$_2$ consumption varied from 60 to 90%, being higher at pH 6 for both strains.

Effect of the acetogen

At pH 6.5, *A. wieringae* JM–*C. kluyveri* co-cultures exhibited the shortest lag phase (not shown), the highest amount of CO/H$_2$ consumed, and the highest combined titres of C4/C6 products (Table 6.4). At pH 6, *C. autoethanogneum* was a better acetogenic partner, since incubations with *A. wieringae* JM grew much slower. Since the latter were fed with only one headspace, an additional comparison can be made with results from experiment A. Co-cultures with *C. autoethanogenum* at pH 6 accumulated the highest amounts of C4/C6 carboxylic acids (Table 6.3), whereas *A. wieringae* JM produced more alcohols, indicating perhaps a suboptimal pH for this strain, an aspect that has not been yet determined.

Effect of the pH

C. autoethanogenum–*C. kluyveri* co-cultures at pH 6 and 6.5 exhibited similar gas consumption and product formation (Table 6.4). Accumulation of C4/C6 products was low in contrast to high production of acetate (50–70 mM) and ethanol (≈20 mM). Remarkably, the highest accumulation of C4/C6 products was observed in the co-culture at pH 6 in experiment A (without headspace refilling; Table 6.3). In contrast, the other three co-cultures (*C. autoethanogenum* at pH 6.5 in experiment A, and a at pH 6–6.5 in experiment B) have similar amounts of accumulated products. To explain this, an essential aspect to consider is the timing of initiating shaking conditions during the incubation. The incubations at pH 6 in experiment A were placed shaking when 30% of the CO was consumed, while the other three cultures were placed shaking when about 15% of the CO was consumed. Presumably, the establishment of *C. kluyveri* in the co-culture depends on the toxicity of dissolved CO and, consequently, the capacity of *C. autoethanogenum* to effectively detoxify the medium from CO. The timing of when shaking conditions are applied therefore played a crucial role in this dynamic, as seen previously (Diender et al., 2016b).

Table 6.4 Experiment B: Consumption of CO/H_2, products formed, and final pH of co-cultures of *C. autoethanogenum* and *A. wieringae* strain JM with *C. kluyveri* at varying starting pH (6–7.5), with refilling of the headspace upon substrate depletion. Values are the average and standard deviations of biological triplicates. In bold, the highest concentrations of ethanol and end produts (C4-C6) obtained with each acetogen are indicated. Underlined, the highest concentrations of ethanol end produts (C4-C6) obtained in the experiment are indicated.

| C. kluyveri in co-culture with	Gas consumption (cumulative), mmol (%)		Products formed, mmol (mM)						Theoretical ethanol production[a], mmol	Final pH
	CO	H₂	Acetate	Ethanol	Butyrate	Caproate	Butanol	Hexanol		
C. autoethanogenum										
pH 6	18.1±0.3 (95.9±2.2)	8.7±0.1 (91.6±2.1)	3.24±0.67 (70.5±14.6)	1.00±0.18 (21.8±4.0)	0.20±0.01 (4.4±0.3)	0.05±0.01 (1.2±0.1)	0.07±0.02 (1.6±0.5)	0.03±0.01 (0.6±0.2)	1.53	4.9±0.3
pH 6.5	18.7±0.9 (98.0±1.4)	7.1±0.6 (75.4±4.8)	2.2±0.51 (47.9±11.1)	1.08±0.09 (23.4±2.0)	0.19±0.07 (4.2±1.4)	0.04±0.01 (0.9±0.3)	0.15±0.09 (**3.2±1.9**)	0.05±0.02 (**1.0±0.4**)	**1.70**	6.0±0.1
A. wieringae JM										
pH 6[b]	9.1±0.1 (100±0.0)	4.4±0.1 (94.0±0.0)	0.94±0.02 (20.0±0.4)	0.66±0.06 (14.1±1.3)	0.21±0.02 (4.6±0.4)	0.05±0.0 (1.1±0.1)	0.14±0.0 (2.9±0.0)	0.04±0.0 (0.9±0.0)	1.3	5.8±0
pH 6.5	25.8±0.5 (90.3±1.7)	9.1±0.3 (64.2±1.7)	0.22±0.02 (4.8±0.5)	1.15±0.16 (24.9±3.4)	0.11±0.0 (2.4±0.1)	0.03±0.01 (0.7±0.1)	0.63±0.01 (13.7±0.3)	0.31±0.03 (6.7±0.7)	2.85	6.5±0
pH 7	27.5±0.8 (99.3±0.0)	9.5±0.2 (69.1±1.7)	0.35±0.13 (7.6±2.7)	0.12±0.03 (2.6±0.6)	0.41±0.06 (**8.8±1.3**)	0.48±0.07 (**10.5±1.5**)	0.49±0.05 (10.7±1.1)	0.23±0.03 (4.9±0.6)	**2.90**	6.3±0.1
pH 7.5	27.2±0.2 (95.5±0.2)	8.7±0.2 (61.2±1.1)	0.04±0.01 (0.9±0.2)	0.18±0.02 (3.8±0.4)	0.07±0.0 (1.4±0.0)	- (traces)	0.78±0.03 (**16.9±0.8**)	0.68±0.03 (**14.8±0.6**)	2.84	6.6±0.5

Traces are concentrations <0.2 mM. [a]Total ethanol produced in the system by the acetogen, calculated taking into account its conversion to C4-C6 products, as described in the Materials and methods (§ 6.2.4). [b]The headspace in these incubations was not refilled.

6

A. wieringae JM–*C. kluyveri* co-cultures at pH from 6.5 to 7.5 showed notable differences in the types of products formed. At pH 6.5, high amounts of ethanol (24.9±3.4 mM) accumulated, as well as significant amounts of C4/C6 alcohols (13.7±0.3/6.7±0.7 mM). Instead, at pH 7 higher concentrations of butyrate (8.8±1.3 mM) and caproate (10.5±1.5 mM) were observed, and butanol (10.7±1.1 mM) and hexanol (4.9±0.6 mM) were also produced. Remarkably, the *A. wieringae* JM–*C. kluyveri* co-culture at pH 7.5 produced the highest titres of butanol (16.9±0.8 mM or 1.3 g L^{-1}) and hexanol (14.8±0.6 mM or 1.5 g L^{-1}) with minimal carboxylic acid and ethanol accumulation. These are notably high concentrations and product specificities of higher alcohols for syngas fermentation, close those obtained with specialised solventogenic strains like *C. carboxidivorans* (Fernández-Blanco et al., 2023).

Solventogenesis by the *A. wieringae* JM–*C. kluyveri* co-culture

The *A. wieringae* JM–*C. kluyveri* co-cultures at initial pH 6.5 to 7.5 showed high solventogenic potential (Table 6.4). In these cultures, butyrate and caproate were first produced, and were subsequently reduced to their corresponding alcohols upon refilling of the headspace with CO/H$_2$ (Fig. 6.1). The switch to solventogenesis can be observed after the second headspace refill. Solventogenesis was most prominent in the co-cultures starting at pH 6.5 and 7.5, in which almost all the butyrate and caproate present were reduced. The co-culture starting at pH 7, however, did not completely convert all butyrate and caproate in butanol and hexanol. We hypothesize this could be due to enhanced activity of *C. kluyveri* (i.e., enhanced chain elongation) at the start of incubations, since the initial pH was closest to the optimum for this species (Table 6.1).

The exact reason for the solventogenic switch of *A. wieringae* JM remains to be clarified. We noted different phenomena taking place around the time of the switch. First, the pH of the cultivations (initially 6.5–7.5) dropped to 5.8–6.0, which has been reported to trigger alcohol but it hinders chain elongation production (Ganigué et al., 2016; Richter et al., 2016a). Second, the concentration of undissociated acids reached inhibitory levels, partially due to the drop in pH. The levels of undissociated acetic, butyric, and caproic acids were approximately 3, 1.4, and 0.85 mM, respectively, at t = 6.8 days. For caproic acid, this concentration falls in the same range as previously reported inhibitory to *C. kluyveri* (Diender et al., 2016b; Weimer & Stevenson, 2012). High concentrations of undissociated acids impair microbial growth by passing through the cell membrane, acidifying the cytoplasm, and releasing anions that interfere with microbial growth (Herrero et al., 1985). Third, it is possible that essential growth factors were depleted from the medium after seven days of exponential growth; at that point, the cell density of the co-cultures had reached its highest point at OD$_{600}$ 3.1 (data not shown). Notably, H$_2$ consumption by the co-cultures stopped around the same time of the switch to solventogenesis. This most likely is a direct consequence of the impaired growth of the co-culture. Solventogenesis is considered a non-growth associated, energy-inefficient overflow metabolism for acetogens (Allaart et al., 2023; Isom et al., 2015; Zahn & Saxena, 2012). Complying with this, we observed that 70–80% of the CO present in the third headspace refill was oxidised to CO$_2$, a higher amount than in both the first and second headspace refills.
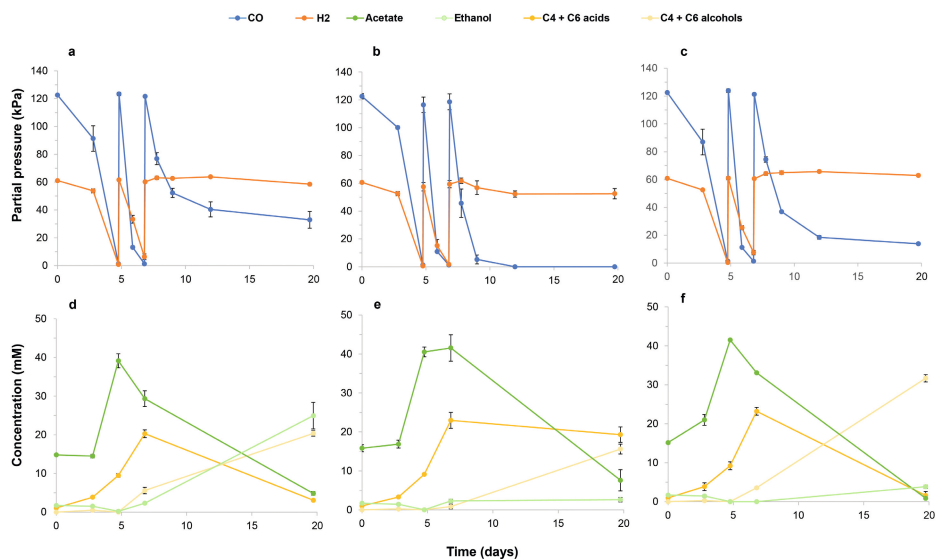
Figure 6.1 Experiment B: CO and H_2 consumption (a-c) and product profiles (d-f) over time of the co-cultures of *A. wieringae* JM–*C. kluyveri* at initial pH values of (a,b) 6.5, (b,e) 7.0, and (c,f) 7.5. Error bars indicate the standard deviation of biological triplicates.

6.4   Conclusions

This work provided a comprehensive comparison of the performance of well-known acetogenic species in co-cultivation with *C. kluyveri* for the fermentation of syngas (CO/H_2). In addition, we investigated the effect of the initial pH, a parameter that has a strong impact on the cell growth and behaviour of the species involved. Our results showed that *C. autoethanogenum* and *A. wieringae* JM were the best-performing strains for the production of C4/C6 carboxylates at pH values of 6 and 7–7.5, respectively. In contrast, *A. bacchi* and *C. carboxidivorans* showed rather slow growth and incomplete utilisation of H_2, which could be due to different bioenergetic mechanism in these species. Notably, *A. wieringae* JM-*C. kluyveri* co-cultures at initial pH of 7.5 produced high amounts of butanol and hexanol with high specificity when refilling of the headspace was applied. This finding sets the ground for future investigation on the production of higher alcohols from syngas by this co-culture. The results presented in this study emphasize the significance of strain- and pH-specific effects on the viability, performance, and product spectrum of syngas-fermenting co-cultures. Understanding the metabolic variations and environmental adaptations of different acetogens should enable the selection of suitable pH/strain combinations that yield high substrate utilization and target product formation. Moreover, the findings in this study contribute to the understanding of the physiology of acetogens and open new line of research. Further work shall include the cultivation of the most promising co-cultures in bioreactor with continuous supply of CO, to better study the effects of pH and evaluate the performance of the cultures in producing MCCAs or higher alcohols.

6.5 Supplementary material

Table S6.1 Preliminary experiment: Consumption of CO/H_2, products formed, and final pH of co-cultures of *C. autoethanogenum* or *A. bacchi* with *C. kluyveri* at varying starting pH 6.5 and 7. Incubation was performed non-shaking at 35°C. Values are the average and standard deviations of biological triplicates.

C. kluyveri in co-culture with	Gas consumption, mmol (%)		Products formed, mmol (mM)						Theoretical ethanol production[a], mmol	Final pH
	CO	H$_2$	Acetate	Ethanol	Butyrate	Caproate	Butanol	Hexanol		
C. autoethanogenum										
pH 7	1.52±0.41 (16.7±0.0)	0.96±0.33 (21.0±0.1)	0.86±0.02 (17.9±0.5)	0.20±0.0 (4.16±0.25)	0.17±0.0 (3.64±0.08)	<0.03 (0.69±0.03)	- ND	- ND	0,50	6.5±0
A. bacchi										
pH 6.5	1.80±1.53 (17.4±0.1)	0.81±0.87 (15.8±0.2)	1.65±0.01 (34.3±5.3)	<0.04 (0.72±0.05)	0.10±0.0 (2.14±0.08)	<0.02 (0.39±0.01)	- ND	- ND	0,21	6.5±0
pH 7	1.69±0.60 (18.0±0.1)	0.07±0.32 (1.4±0.1)	0.94±0.05 (19.9±0.2)	0.10±.00 (2.03±0.05)	0.15±0.01 (3.27±0.17)	<0.02 (0.72±0.07)	- ND	- ND	0,37	6.4±0

ND: not detected. [a]Total ethanol produced in the system by the acetogen, calculated taking into account its conversion to C4-C6 products, as described in the Materials and methods (§ 6.2.4).
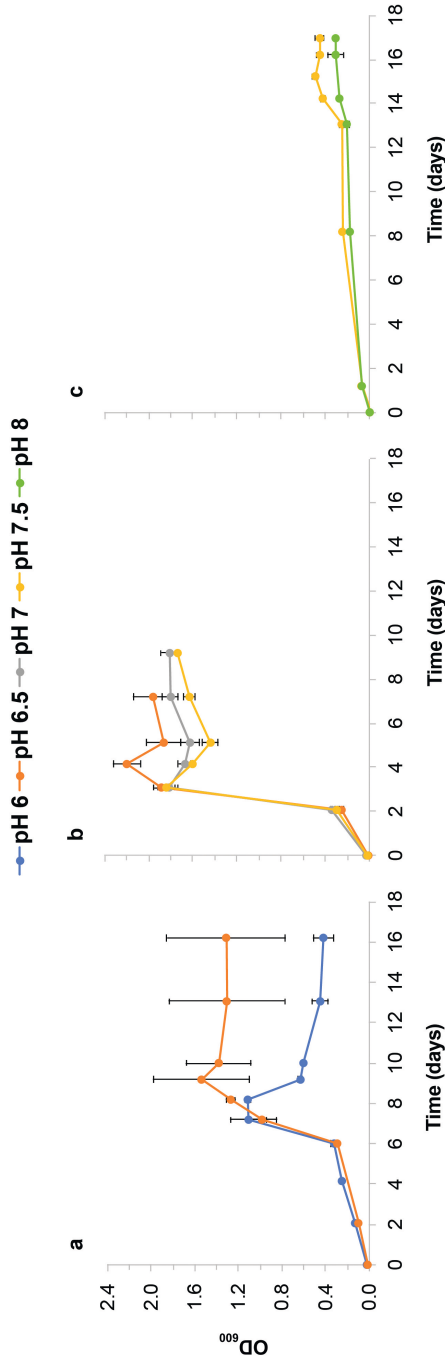
Figure S6.1 Experiment A: Cell density (measured as OD$_{600}$) over time of CO/H$_2$-fermenting co-cultures of *C. kluyveri* with (a) *C. autoethanogenum*, (b) *A. wieringae* JM, and (c) *A. bacch*, at varying initial pH values.

General discussion

—

GENERAL DISCUSSION

This thesis aimed at studying the potential of synthetic microbial consortia as innovative biotechnological platforms in syngas fermentation processes. While doing so, we focused on attaining the production of odd-chain products (carboxylic acids and alcohols) via chain elongation, thereby addressing a recognised gap in the field (Strik et al., 2022). The experimental findings from our work contribute particularly to the knowledge of chain elongation and microbial production of propionate from ethanol, an unconventional yet sustainable feedstock choice (Blank et al., 2020). The use of genome-scale metabolic modelling has played a pivotal role in uncovering novel insights into the species metabolism that were previously unexplored, and in evaluating the feasibility of the synthetic communities studied. Over the course of this study, we have witnessed a surge of interest regarding the use of microbial communities for the revalorisation of syngas, with numerous research contributions to the matter. In the following discussion, the key findings, challenges, and prospects arising from this thesis are examined in light of the current state of research in the field.

7.1 Microbial networks to expand the product range of syngas fermentation

Syngas/CO fermentation is an established industrial platform for the sustainable production of ethanol. At the forefront is the New-Zealand-founded LanzaTech, a company that, since its foundation in 2005, has been dedicated to advancing the CO fermentation platform and is now pushing the boundaries of applications beyond the production of ethanol (Karlson et al., 2021; Köpke & Simpson, 2020). Recently, LanzaTech's research team achieved an outstanding milestone by genetically engineering *Clostridium autoethanogenum* to realise the production of acetone and isopropanol from syngas with industrially relevant production rates (3 g L^{-1} h^{-1}), a remarkable accomplishment result of interdisciplinary efforts over years (Liew et al., 2022).

However, the inherent challenges associated with engineering acetogens cannot be overlooked. The fact that these microorganisms operate at the thermodynamic edge of life (Schuchmann & Müller, 2014) makes it a difficult task to achieve successful genetic modifications while sustaining robust growth on C1 feedstocks. Additionally, genetic tools for non-model microorganisms like acetogens are still in the developmental stage and face important challenges (Bourgade et al., 2021; Charubin et al., 2018). Examples are the evasion of host restriction-modification systems, successful DNA transformation protocols, or the development of high-throughput screening tools. In addition, genetic features of acetogens vary across strains, and some genetic tools are strain-specific (Bengelsdorf et al., 2016; Bourgade et al., 2021). Yet, significant advances are being made at a rapid pace (Lee et al., 2022), for example the development of a novel, efficient transformation system and molecular toolkit for *Acetobacterium*, reported recently by Moreira et al. (2023). Genome-scale metabolic modelling ha also proven useful as a tool to predict and guide genetic manipulation of acetogens (Benito-Vaquerizo et al., 2020; Kabimoldayev et al., 2018). It can be expected that further breakthroughs will be achieved in the years to come.

In light of the energetic restrictions of acetogens, alternative approaches are sought to expand the metabolic scenario of syngas fermentation. Nature provides a solution in the form of microbial communities, where synergistic interactions among different microorganisms enable complex pathways to occur. In the last decade, extensive research has focused on establishing principles and tools for the engineering of microbial communities for biotechnology and ecology studies, employing both experimental and computational approaches (Ben Said & Or, 2017; Brenner et al., 2008; Cao et al., 2017; Lawson et al., 2019; McCarty & Ledesma-Amaro, 2019; Roell et al., 2019; Zerfaß et al., 2018; Zhang & Wang, 2016).

As we expose in **Chapter 2**, both open mixed cultures and synthetic co-cultures are promising strategies for syngas fermentation, as they leverage the metabolic capabilities of diverse microorganisms to achieve a broader product spectrum (Diender et al., 2021). Microbial communities from environments treating heterogeneous wastes (i.e., activated sludge, anaerobic digesters) have shown carboxydotrophic ability while not being originally used or described for that, highlighting the omnipresence of acetogens and other carboxydotrophic microorganisms in nature. Undefined microbial communities might be particularly well suited for syngas biomethanation, as relevant methane production rates, with high selectivity and conversion efficiency, have been obtained in semi-pilot scale process (Table 2.1; Asimakopoulos et al., 2021b). Furthermore, despite the acknowledged low tolerance of methanogens to CO (Diender et al., 2016a; Parera Olm & Sousa, 2021), recent findings have demonstrated the remarkable adaptability of carboxydotrophic, methanogenic communities, eliminating CO inhibition as an obstacle in this process (Figueras et al., 2023). Due to its low operational costs, biomethanation of syngas could be particularly suited to increase the flexibility of small-scale gasification plants by exploiting syngas for heat and electricity production (Grimalt-Alemany et al., 2018b).

The production of chemicals of higher value via syngas fermentation is more attainable with the use of synthetic co-cultures, given the higher product specificities that can be obtained (**Chapter 2**; Diender et al., 2021). Since ethanol and acetate are the major native products of syngas fermentation, and the factors influencing their production have been well established, integration of syngas fermentation with the chain elongation platform has been a popular approach in this regard. Ganigué and colleagues demonstrated that sludge from an anaerobic digester was suitable to convert syngas into C4 and C6 products (Ganigué et al., 2015). Diender et al. (2016b) simplified this approach with a pioneering work of a carboxydotrophic synthetic co-culture of *C. autoethanogenum* with *C. kluyveri*, which was later tested for industrial implementation (Haas et al., 2018). Since then, many other synthetic co-cultures have been tested (Table 2.1), which also provided insights on the metabolic interactions involved.

7.2 Beating the odds with syngas-driven chain elongation

7.2.1 Solventogenesis vs. chain elongation: more than a pH issue

Perhaps the most critical aspect when combining syngas fermentation with chain elongation is the fermentation pH. Chain elongation by *C. kluyveri* is favoured at pH around 6.8 (Barker & Taha, 1942). On the other hand, it has been reported that alcohol production by acetogens is triggered at mildly acidic pH upon the accumulation of carboxylic acids (Diender et al., 2016b; Ganigué et

al., 2016; Richter et al., 2016a). This implies that chain elongation and solventogenesis (of ethanol or other alcohols) can hardly take place at the same time, which is a hurdle to productivity since ethanol production is essential to chain elongation. However, in our study with *Acetobacterium wieringae* JM in **Chapter 5**, we observed alcohol production (both ethanol and higher alcohols) at pH 7 or higher and concurrent with chain-elongating activity (§ 5.3.2). Additionally, striking differences in ethanol production across acetogens cultivated at pH values from 6 to 8 were observed in **Chapter 6**.

   This suggests that an acidic pH is not a fixed requisite to trigger solventogenic metabolism in acetogens. Instead, more important factors are: i) the thermodynamics of alcohol formation, as observed in co-cultivation with ethanol-consuming species (§ 5.3.3) and supported by literature (Diender et al., 2019; Mock et al., 2015; Richter et al., 2016b). And: ii) the accumulation of (un-dissociated) carboxylic acids to a threshold concentration that becomes inhibitory to cell growth. That is, in both cases, in the presence of excess reductant. This applies to acetogens but to other bacteria, too: in pure culture experiments, we observed that both Anaerotignum neopropionicum and C. kluyveri reduced propionate to propanol under conditions of reduced growth (low pH) and abundance of substrate (Chapter 3: § 3.3.1 and § 3.3.2). Other scenarios that restrict growth have also been shown to trigger solventogenesis, for example reducing the availability of yeast extract, certain metals or B-vitamins (Abubackar et al., 2019; Gaddy, 2007; Saxena & Tanner, 2011; Simpson et al., 2010; Zahn & Saxena, 2012). In essence, a lower pH (be it acidic or not) imposes a growth limitation, since it is a suboptimal pH that likely causes some disturbance to the cell. Achieving a high product specificity of acids or of alcohols in one-pot syngas fermentation is a challenge because acetate and longer carboxylic acids are products of active, exponential growth, while alcohols are the result of limited growth and overflow metabolism (Allaart et al., 2023; Zahn & Saxena, 2012), opposite scenarios. Synthetic co-cultures fermenting syngas and producing MCCAs operate somewhere in the middle of this dichotomy (Fig. 7.1).
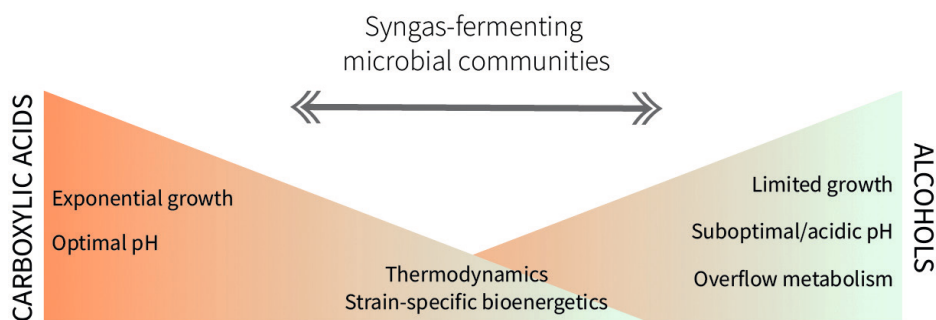
Figure 7.1 Dichotomy between carboxylic acid production and alcohol production in syngas fermentation: Opposing factors favour each type of metabolism, with thermodynamic and strain-specific bioenergetic factors strongly influencing both. Syngas-driven chain-elongating microbial communities operate somewhere in the middle.

Ensuring ethanol availability is a key challenge, as we observed in the tri-culture of *A. wieringae* JM, *A. neopropionicum* and *C. kluyveri*. In this tri-culture, despite the evident chain-elongating

activity, acetate accumulation was predominant (**Chapter 5**: § 5.3.1 and § 5.3.3). Strategies should be sought to address this problem in order to increase the productivity and potential of these cultures. The straight-forward approach would be to increase mass transfer of CO into the liquid by increasing agitation or employing different bioreactor configurations (Abubackar et al., 2019). However, care should be taken not to inhibit growth of the other species in the co-culture due to CO toxicity. Besides nutrient limitation as mentioned before, another option would be to supply ethanol, as it is done in chain-elongation studies (Grootscholten et al., 2013; Kucek et al., 2016). However, there is a potential drawback since the acetogenic partner may oxidise ethanol back to acetate when reducing equivalents become limiting, as reported for *C. autoethanogenum* (Diender et al., 2016b) and observed with *A. wieringae* JM in CO-limited chemostats (§ 5.3.3, Fig 5.2). Another potentially more suitable strategy to increase ethanol production is the addition of H_2, as demonstrated by our model simulations using flux balance analysis (Fig. 5.5) and reported in the literature (Steinbusch et al., 2011).

Furthermore, the choice of the acetogenic partner also influences the solventogenic/acetogenic behaviour of the synthetic co-culture. The screening study in **Chapter 6** revealed that *A. wieringae* JM and *C. autoethanogenum* were the most efficient in utilizing CO/H2, whereas *Alkalibaculum bacchi* and *Clostridium carboxidivorans* exhibited low H_2 utilization (Table 6.3). Among the first two, *C. autoethanogenum* appeared to be a more suitable partner for *C. kluyveri* in producing medium-chain carboxylic acids. Interestingly, *A. wieringae* JM showed great promise as candidate for solventogenesis through carboxylate reduction, producing significant titres of butanol and hexanol with high specificity (Table 6.4). Future research should focus on further understanding these metabolic variations among acetogens and leveraging them to enhance production yields and rates of end products. Investigating metabolic redundancy (i.e., different acetogens in the same co-culture) and robustness could also enhance the performance of synthetic co-cultures.

7.2.2 Synthetic co-cultivation for odd-chain products

Since only even-chain intermediates are produced via syngas fermentation (i.e., acetate and ethanol), the production of odd-chain compounds requires the presence of microorganisms specialised in the production of odd-chain intermediates (i.e., propionate) from syngas or their products. As proof-of-concept, in this thesis we relied on the ethanol-consuming bacterium *A. neopropionicum* as propionate-producer in the system. First, we demonstrated the continuous production of up to C7 carboxylates from ethanol and CO_2 by the bi-culture of *A. neopropionicum* and *C. kluyveri* (**Chapter 3**: § 3.3.4). We showed that C5–C7 carboxylic acids can be produced with high ethanol conversion efficiency (99%) and significant product specificity (≈25% for valerate; Table 3.4). This indicated the self-regulation of the species ratio in chemostat cultivation to sustain an interaction based on cross-feeding of acetate and propionate (Fig. 3.4). Such co-culture could be used to upgrade syngas fermentation effluent, a strategy tested before (Gildemyn et al., 2017; Vasudevan et al., 2014). Two-stage processes in which syngas fermentation to ethanol is separated from chain elongation would allow to establish optimal conditions for each conversion, potentially realising higher production rates of the end products.

We also tested the one-pot strategy by cultivating *A. wieringae* JM, *A. neopropionicum* and *C. kluyveri* in a batch bioreactor with continuous supply of CO (**Chapter 5**). Due to the nature of the

cultivation, the tri-culture produced first a mixture of C4-C6 carboxylic acids that were later reduced to the corresponding alcohols by the acetogen. In the later stage of cultivation, solventogenesis took place at the same time as chain-elongation and at pH around 7, a rather unusual observation as discussed earlier (§ 7.4.1). The tri-culture produced valerate (≈10 mM), but the main chain-elongated product was butyrate (≈24 mM), in line with favoured even-chain elongation by *C. kluyveri*, as seen in Chapter 3 (§ 3.3.4) and discussed later on (§ 7.6.3). Among the higher alcohols, we observed production of pentanol (up to 4.2 mM), which is rarely reported in syngas-fermenting studies with microbial communities. Certainly, this was facilitated by the presence of only a few (three, in this case) specialised strains in the consortia, in contrast to the very diversified types of metabolism and interactions generally converging in open mixed cultures that hinder product specificities.

Time constraints did not permit the establishment of the tri-culture in continuous cultivation. However, genome-scale metabolic modelling combined with community flux balance analysis (cFBA) resulted valuable in predicting and learning about the functionality of the co-culture (§ 5.3.5). The fact that the tri-culture was predicted most feasible at balanced biomass species ratios might stem from the fact that the three species (*A. wieringae* JM, *A. neopropionicum* and *C. kluyveri*) have similar growth rates. Presumably, the enhanced presence of either of the strains would either take over the culture or impede its feasibility. Model simulations also predicted that H_2 addition would enhance ethanol production and, consequently, the production of longer-chain carboxylates, including that of heptanoate. The use of H_2 as co-electron donor has proven successful in previous studies (Baleeiro et al., 2021; Steinbusch et al., 2011), and it would be worth to test also here.

While the tri-culture proved the proof-of-concept of combining syngas fermentation with propionigenesis and chain elongation to produce odd-chain products in one-pot, the titres obtained are far to be considered industrially relevant (>1 g L^{-1}). An alternative that might improve titres and productivity is to separate the production of ethanol from syngas, and odd-chain elongation in two bioreactors, as proposed in Chapter 3.

7.3   Genome-scale metabolic modelling: a double-edged sword for the study of microbial metabolism

Genome-scale metabolic modelling is a powerful tool for studying microbial metabolism, offering insights into the complex network of biochemical reactions within a cell (Almaas et al., 2004; Covert et al., 2004). By integrating genomic and biochemical information in genome-scale metabolic models (GEMs), this approach allows to explain and predict the metabolic capabilities of microorganisms and understand how they respond to their environment (Kim et al., 2018). In recent years, metabolic modelling has advanced to study model microbial communities, and many tools have been developed for this purpose (Ibrahim et al., 2021; McCarty & Ledesma-Amaro, 2019). Community modelling tools can aid in understanding the underlying interactions of microbial ecosystems (Goyal et al., 2014; Hanemaaijer et al., 2015; Hanemaaijer et al., 2017; Stolyar et al., 2007), as well as in the prediction, design and optimization of engineered communities for biotechnological applications (Benito-Vaquerizo et al., 2020; Benito-Vaquerizo et al., 2022a; Li & Henson, 2019; Moreno-Paz et al., 2022).

However, while certainly being a revolutionary approach, genome-scale metabolic modelling also presents limitations. Major hurdles are the availability of accurate experimental data for model reconstruction, and the difficulty to incorporate certain physiological or environmental variables (e.g., the effect of pH, enzyme affinity, or adaptation to stress factors) (Kim et al., 2018). For example, co-factor use by many enzymes is unclear [e.g., NAD(H) vs. NADP(H)], as well as H^+/Na^+ use by the Rnf complex. The model may also suggest phenotypes that are not observed empirically, as exemplified in the next section. These hurdles force the use of assumptions during the reconstruction and simulation processes, affecting the predictive accuracy of GEMs. Therefore, while metabolic modelling provides valuable insights, it must be handled thoughtfully, acknowledging it can be a double-edged sword in the study of microbial metabolism.

Our research emphasized the significance of validating GEMs with experimental data. This validation process played a key role in ensuring the accuracy of the model's predictions and establishing its credibility as a research tool. An example was the production and use of H_2 by *A. neopropionicum*, which was predicted by the preliminary model given the presence of a hydrogenase in the genome annotation of the species (**Chapter 4**). However, in cultivation experiments and previous studies (Ato et al., 2014; Tholozan et al., 1992), H_2 was never consumed or produced. Therefore, this reaction was blocked in the final GEM. Without this validation step, the inclusion of H_2 as product of the metabolism of *A. neopropionicum* would have resulted in erroneous predictions due to changes in the redox balance of the cell. This affectation would have also been reflected in the tri-culture model (**Chapter 5**) since H_2 can be used by the acetogen as additional electron donor to CO. While there are some gaps of information and likely incorrect assumptions in the first GEM of *A. neopropionicum*, we incorporated sufficient genomic and experimental data to elucidate key pathways and most relevant phenotypes (**Chapter 4**: Table 4.2, § 4.3.6).

The positive aspect of computational approaches was evident in this work. Through *in silico* analysis, we revealed the presence of two previously unidentified enzymatic complexes in *A. neopropionicum:* the acryloyl-CoA reductase–EtfAB (Acr-EtfAB), and the NADH-dependent reduced ferredoxin:NADP$^+$ oxidoreductase complex (Nfn) (**Chapter 4**). These complexes play crucial roles in the metabolism of this species. The Acr-EtfAB is an electron-bifurcating enzyme that catalyses the reduction or acryloyl-CoA to propionyl-CoA in the acrylate pathway. On the other hand, the Nfn generates NADPH, an essential reductant to anabolic redox reactions. By employing model simulations with the reconstructed GEM of *A. neopropionicum*, we successfully confirmed the functionality and significance of these enzymes. However, this was only possible by incorporating information from literature documenting the biochemistry and physiology of these enzymes. For example, theoretically, the Acr-EtfAB could drive the reduction of ferredoxin with NADH due to the high redox potential of the acryloyl-CoA/propionyl-CoA pair (E_0' = +70 mV), potentially driving a proton-motive force. Yet, this was disproved in experimental studies with the close relative *A. propionicum* that showed that the enzyme is found in the cytoplasm and that it is not involved in anaerobic respiration (Hetzel et al., 2003). Following a similar approach, we confirmed the presence in *A. wieringae* JM of the H_2-dependent CO_2-reductase (HDCR), the enzyme catalysing the reduction of CO_2 to formate in the WLP (**Chapter 5**). The presence of the HDCR in a CO-utilising acetogen is of significance due to the fact that this enzyme is inhibited by CO (Ceccaldi et al., 2017;

Schuchmann & Müller, 2013), as is the case for many hydrogenases. In the upcoming section, I further elaborate on this topic.

As highlighted previously, one inherent risk of genome-scale metabolic modelling is the making of incorrect assumptions that still result in a feasible solution space. While the model can offer some utility, it may incorporate information that is ultimately inaccurate or misleading. This likely happened here. In **Chapter 4**, we postulated that, in *A. neopropionicum*, formation of butyrate (a minor by-product) occurs via the circular variant of the acetyl-CoA route, as described for *C. kluyveri* (Seedorf et al., 2008). We identified candidate enzymes to catalyse all except for one of the reactions of the pathway (§ 4.3.7, Fig. 4.6). This included two enzymes usually involved in the acrylate pathway: i) the acryloyl-CoA reductase–EtfAB (Acr-EtfAB), which we hypothesised could also catalyse the reduction of crotonyl-CoA to butyryl-CoA due to similarity with butyryl-CoA dehydrogenase (Bcd) of *C. kluyveri*; and ii) the propionate-CoA:lactoyl-CoA transferase (Pct), which we assigned to the generation of butyrate from butyryl-CoA based on its broad substrate specificity (Selmer et al., 2002). The enzyme acetoacetyl-CoA thiolase (reaction 3 in Fig. 4.6) was not found in the genome but was added to the model during the gap-filling step. However, in a study published this year, Baur & Dürre (2023) fairly disclaimed our hypothesis of the butyrate pathway in *A. neopropionicum* and provided a more fitting alternative. According to the authors, the only possible way butyrate could be produced is via the degradation of L-threonine (present in low amounts in yeast extract), through the activity of enzymes that are all present in the genome of this strain. The proposed pathway makes use of one of the analogues we identified for the Bcd activity, as well as the Pct of the acrylate pathway. The theory of Baur & Dürre (2023) fit with our observations: the low concentrations of butyrate in the cultures could be attributed to the likely presence of threonine in yeast extract, a constituent of our medium.

In brief, GEMs and related computational approaches should be viewed as tools, not as a primary means, to study microbial interactions and metabolism. The statistician George Box said: "Remember that all models are wrong; the practical question is how wrong do they have to be to not be useful" (Box & Draper, 1987). Metabolic models are useful, as they reduce the vast complexity of metabolism and allow to derive the key principles of it. Yet, to exploit their potential, it is crucial to incorporate validation steps and to increase the availability of experimental data. This shall include not only phenotypical and physiological data, but also proteomics and/or transcriptomics datasets, as well as kinetic parameters. Such comprehensive models can aid not only in resolving fundamental questions and improving phenotype predictions (Großeholz et al., 2016; Zhou et al., 2021), but also in guiding strain engineering and bioprocess optimisation efforts (Domenzain et al., 2022).

7.4 Insights into the physiology and metabolism

7.4.1 Ethanol fermentation by *Anaerotignum neopropionicum*

Through this thesis, we have uncovered aspects of the physiology of the bacterial species studied. Perhaps the most extensive contribution in this regard has been elucidating the complete route for ethanol fermentation to propionate (via the acrylate pathway) in *A. neopropionicum* (**Chapter 4**: Fig. 4.5). The computational approach allowed us to shed light into the physiology of this species, which would have been challenging to achieve solely through empirical observations. Among other

contributions, we rejected the former assumption that reduced ferredoxin (Fd^{2-}) required for the synthesis of pyruvate from acetyl-CoA (via PFOR) was obtained during the oxidation of ethanol (Tholozan et al., 1992). This hypothesis did not hold true because ethanol oxidation yields NADH as electron carrier. Instead, with supporting evidence by Moreira et al. (2021), we postulated that Fd^{2-} is obtained in the Rnf complex through transfer of electrons from NADH in an ATP-driven manner. Operation of the Rnf complex in this way is usually referred to as the "reverse" direction since, in acetogenic bacteria, it functions most often to produce NADH from Fd^{2-}, ultimately driving ATP synthesis (Schuchmann & Müller, 2014). As our model simulations in *A. neopropionicum* demonstrated, the Rnf complex is essential during growth on ethanol as there is no other way to reduce ferredoxin from NADH. This is true for *A. neopropionicum* but it is also the case for acetogens that can grow on low-energy substrates (e.g., ethanol or lactate), such as *A. woodii* (Bertsch et al., 2015; Westphal et al., 2018). Importantly, our findings imply that substrate level phosphorylation via acetyl phosphate (i.e., via acetate production) remains the only mode of energy conservation in *A. neopropionicum*, at least during growth on ethanol.

The presence of a putative ferredoxin hydrogenase in *A. neopropionicum* was intriguing, yet its role remains to be elucidated. While hydrogenotrophic or hydrogenogenic activity was neither observed in our cultures nor reported in literature during growth on ethanol or sugars (**Chapter 4**; Baur & Dürre, 2023; Tholozan et al., 1992), it was suggested that the degradation of leucine or valine could result in the production of H_2 (Moreira et al., 2021). However, H_2 was not detected in cultures of *A. neopropionicum* that utilised these amino acids (Ato et al., 2014). Production of H_2 by the close relative species *A. propionicum* (formerly, *Clostridium propionicum*) has also not been reported except for in few reports where H_2 production was either very low (Chartrain & Zeikus, 1986) or it was not quantified (Ueki et al., 2017).

7.4.2   A putative HDCR in *Acetobacterium wieringae* JM

A. wieringae strain JM is able to grow on carbon monoxide as sole substrate, contrary to the type strain of the species and to the close relative *Acetobacterium woodii* (Arantes et al., 2020; Bertsch & Müller, 2015b). The presence in the two latter strains of the CO-sensitive H_2-dependent CO_2-reductase (HDCR) is hypothesised as the reason for this inability. HDCR catalyses the reduction of CO_2 to formate with H_2 or reduced ferredoxin (Schuchmann & Müller, 2013), the first step in the methyl branch of the WLP (Fig. 1.3) and, therefore, essential to acetogenesis. The hydrogenase module of this enzymatic complex is inhibited by CO, as is the case for other hydrogenases (Bertsch & Müller, 2015b; Ceccaldi et al., 2017; Schuchmann & Müller, 2013). Our *in silico* analysis of the GEM of *A. wieringae* strain JM corroborated the presence of an HDCR in *A. wieringae* JM —initially predicted by Arantes et al. (2022)—, as we identified the formate dehydrogenase (TYC86388; *fdh)* and an Fe-hydrogenase (TYC85752; *hydA*) subunits (**Chapter 5**: § 5.3.4). As set out above, the use of HDCR would be incompatible with growth on CO. However, inhibition of the HDCR by CO is reversible (Ceccaldi et al., 2017), and an adaptation period can enable growth on this substrate, as observed in *Thermoanaerobacter kivui* (Weghoff & Müller, 2016). Strain JM was isolated from a long-term carboxydotrophic enrichment exposed to CO (Arantes et al., 2020), a selective pressure that could have resulted in such adaptation in this microorganism as well.

The putative HDCR genes identified in our study were not found in a gene cluster, which would be expected for an enzymatic complex. Thus, alternatively, *A. wieringae* JM could harbour another variant of a formate dehydrogenase. Acetogens are phylogenetically very diverse and have been reported to use different enzymes for the reduction of CO_2 (Bertsch & Müller, 2015a; Schuchmann & Müller, 2014). Ferredoxin- or NAD(P)-dependent formate dehydrogenases, which are known not to be inhibited by CO, are typically used. Within the genus *Acetobacterium*, several types of clusters have been identified encoding for HDCR-related and formate dehydrogenase genes (Ross et al., 2020). Another case is that of *C. autoethanogenum*, which uses a formate dehydrogenase associated to an electron-bifurcating ferredoxin- and NADP-dependent hydrogenase (Wang et al., 2013). Despite the sensitivity of hydrogenases to CO, the CO steady-state concentrations in the cell would be lower than the apparent inhibition constant (Ki) of the enzyme, enabling the enzyme to function.

Further research is needed to verify the presence of an HDCR in *A. wieringae* JM. While this option aligns with the scenario observed in closely related strains, *A. wieringae* type strain and *A. woodii*, there is also a possibility that strain JM employs an alternative variant of a formate dehydrogenase, either in conjunction with a hydrogenase or independently. Such investigation will surely provide novel insights into the mechanisms and adaptations involved in the utilization of carbon monoxide by acetogens.

7.4.3   The cost of odd-chain elongation in *C. kluyveri*

In **Chapter 3**, we investigated aspects of the metabolism of odd-chain elongation by *C. kluyveri*, which has been generally less studied than the even-chain metabolism. A key finding was that ethanol-driven elongation of propionate had negative consequences in the cell growth and in the odd:even product ratio (§ 3.3.2; Table 3.3). We also found that the presence of acetate in propionate-fed cultures reversed the negative effects of growth, but that the theoretical odd:even product ratio was still altered (in batch cultivation experiments, 27% of odd-chain product were formed, while the theoretical proportion is 16.7%; Fig. 3.3). The question why excessive ethanol oxidation occurs during odd-chain elongation in *C. kluyveri* remains unanswered. As described in § 3.4.3, it is possible that this is a response to two factors: i) the toxicity of propionyl-CoA, and ii) a scarcity of acetyl-CoA, a major building block of the cell.

Excessive ethanol oxidation does not negate the possibility of a preference for either acetate or propionate. It is important to distinguish between these two phenomena. Both in pure culture experiments with *C. kluyveri* and co-cultures tested in this study, we observed a higher conversion of acetate (to even-chain products) compared to propionate (to odd-chain products), also when the availability of the two SCCAs was the same. These observations imply a distinct preference for the utilization of acetate, possibly due to higher enzyme affinity. Further research, including enzymatic assays and integration of recent studies (Candry et al., 2020b), is needed to understand the differential conversion of acetate and propionate in chain elongation of *C. kluyveri*. Understanding this can contribute to improving product specificity of odd-chain products in chain elongation processes.

7.5   Perspectives on the use of microbial communities for syngas fermentation

Medium-chain carboxylic acids, in particular butyrate and caproate, have been typically targeted as end products in syngas fermentation studies using microbial communities (Table 2.1 and Table 2.2). In this thesis, we have shown that the odd-chain counterparts (valerate and heptanoate) can also be produced by using a synthetic co-culture approach. However, the highest valerate titre obtained in this study (1.3 g L^{-1}; Table 3.4) and productivity (<0.1 g L^{-1} h^{-1}; Table 3.4) are still far from being industrially-relevant for their application as chemical building blocks (>5 g L^{-1}, >10 g L^{-1} h^{-1}) (Takors et al., 2018). In addition, the maximum product specificity of odd-chain products obtained is rather low (<50%), resulting in a mixture of C4-C7 carboxylates as end products. While further work can contribute to improving titres and product specificity, mixtures of MCCAs produced via fermentation also find applications, for example as animal feed (Ricci et al., 2018).

Additionally, the product spectrum of syngas fermentation can be further diversified. Recent interest has emerged in the production of higher alcohols through syngas fermentation as an alternative to conventional carbohydrate-based methods [i.e., acetone-butanol-ethanol (ABE) fermentation] (Fernández-Blanco et al., 2023; Pinto et al., 2021). Syngas-driven solventogenesis offers a cost-effective and flexible approach, bypassing food/feed competition concerns. While current butanol titres from syngas fermentation are an order of magnitude lower (2 g L^{-1}) than conventional methods (20 g L^{-1}), the ethical advantages of using syngas as feedstock make it an attractive platform for higher alcohol production. *C. carboxidivorans* has been most used for higher alcohol production from syngas, as there are hardly other species with the ability to produce such longer alcohols directly from autotrophic substrates. High production of hexanol (5 to 8 g L^{-1}) was recently achieved by this species with repeated addition of extractant and ethanol during CO fermentation (Oh et al., 2023).

Microbial consortia have also proven to be promising solventogenic platforms in this regard, in combination with process configurations aimed at improving productivity. For example, a co-culture of *Clostridium ljungdahlii* and *C. kluyveri* in a bioreactor with biomass retention and product extraction produced relevant titres of butanol (up to 4.2 g L^{-1}) and hexanol (up to 4.7 g L^{-1}) (Richter et al., 2016a). In another study, a two-stage process was employed, where carboxylates produced by a *C. carboxidivorans*–*C. kluyveri* co-culture in the first bioreactor (at pH 6) were subsequently reduced to alcohols by an acetogen in the second bioreactor (at pH 5), resulting in the accumulation of butanol, hexanol and octanol (Bäumler et al., 2023). In this thesis, a co-culture of *A. wieringae* JM with *C. kluyveri* produced up to 1.3 g L^{-1} butanol and 1.5 g L^{-1} hexanol (**Chapter 6**: Table 6.4). These are superior titres than obtained with *C. autoethanogenum* as acetogenic partner (Table 6.4; Diender et al., 2016b), revealing a higher solventogenic ability of strain JM that should be further explored. In addition, we also observed the production of pentanol (4.2 mM or 0.4 g L^{-1}) by the *A. wieringae* JM–*A. neopropionicum*–*C. kluyveri* tri-culture (**Chapter 5**: § 5.3.1). Pentanol accumulation had not been reported before by a syngas-fermenting microbial consortia; the presence of a propionigenic strain in the co-culture was essential to achieve this, highlighting the extended possibilities that can be attained through the use of synthetic co-cultures.

7

Incorporating genetically-engineered strains into synthetic co-cultures hold strong potential to increase the value of end products of syngas fermentation (Fig. 7.2). A successful example is the production of 3-hydroxypropionic acid and itaconic acid (< 50 mg L^{-1}) using genetically-modified *Escherichia coli* in co-cultivation with an acetogen (Cha et al., 2021). Acetate, generated through syngas fermentation, served as a key intermediate in this system. Although there were areas for improvement (e.g., achieving an efficient conversion of acetate to biochemicals by the engineered strain), this approach demonstrates that the combined use of genetic engineering and microbial community engineering magnifies the potential of syngas fermentation processes. As the introduction of genetic engineered strains in co-cultures starts to take place, the distinction between synthetic and artificial or engineered microbial communities may emerge, the former including genetically modified organisms (Cha et al., 2021; McCarty & Ledesma-Amaro, 2019; Roell et al., 2019).
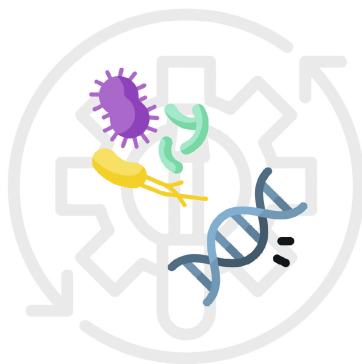
Figure 7.2 Combining microbial community engineering with genetic engineering can facilitate the efficient production of added-value products. In synergy, these two approaches offer a multifaceted solution to the challenges associated with syngas fermentation.

Ultimately, an interdisciplinary approach, combining expertise from different fields (including, among others, physiology, bacterial genetics and process engineering), is crucial to realise the highest potential of syngas fermentation as biotechnological manufacturing platform. Implementing process strategies such as two-stage processes, cascade reactors, and tightly controlling parameters like partial pressure of CO, stirring and pH are essential for optimizing productivity in production strategies. Downstream processing should also be considered in the early stages of bioprocess design; for example, in the case of medium-chain carboxylic acids, often in-line product extraction is applied that requires an acidic pH during fermentation (Ge et al., 2015; Gildemyn et al., 2017). Synthetic biology tools can help unravel the principles governing microbial communities (natural and synthetic), and guide their rational engineering (McCarty & Ledesma-Amaro, 2019). Regarding the use of community GEMs, being able to monitor different microbial populations and quantifying their relative ratios in the community can improve the quality and applicability of the models. Techniques like FISH (fluorescence in-situ hybridization), qPCR (quantitative PCR), FAST (fluorescence-activated cell sorting), microscopy, and others have been employed for monitoring cell populations, and have recently been applied in syngas fermentation and chain

elongation studies (Bäumler et al., 2023; Innard & Chong, 2022; Kim et al., 2013; Robles et al., 2023; Schneider et al., 2021).

7.6   Concluding remarks

Microbial communities are resilient systems, and their expanded metabolic networks make them a suitable platform for the production of chemicals. Synthetic co-cultures have proven to be particularly useful in this regard, as exemplified in this thesis. While this thesis has provided significant contributions, new questions have emerged, laying the foundation for exciting research directions. The study of microbial physiology, coupled with computational tools and bioprocess engineering, can help resolve these questions and advance syngas fermentation.

Syngas is meant to be a next-generation feedstock in biotechnology. As we look ahead, the continued collaboration and knowledge-sharing between industry, academia, and regulatory parties will be instrumental in unlocking the full potential of syngas fermentation. I strongly believe that harnessing the potential of this technology can contribute to addressing the pressing challenges of carbon CO_2 emissions, waste management, and sustainable chemical production.

REFERENCES

Abdoulmoumine, N., Adhikari, S., Kulkarni, A., & Chattanathan, S. (2015). A review on biomass gasification syngas cleanup. *Applied Energy*, *155*, 294–307. https://doi.org/10.1016/j.apenergy.2015.05.095

Abrini, J., Naveau, H., & Nyns, E.-J. J. (1994). *Clostridium autoethanogenum*, sp. Nov., an anaerobic bacterium that produces ethanol from carbon monoxide. *Archives of Microbiology*, *161*, 345–351. https://doi.org/10.1007/BF00303591

Abubackar, H. N., Veiga, M. C., & Kennes, C. (2011). Biological conversion of carbon monoxide: Rich syngas or waste gases to bioethanol. *Biofuels, Bioproducts and Biorefining*, *5*, 93–114. https://doi.org/10.1002/bbb.256

Abubackar, H. N., Veiga, M. C., & Kennes, C. (2019). Syngas fermentation for bioethanol and bioproducts. In M. J. Taherzadeh, J. Wong, & A. Pandey (Eds.), *Sustainable Resource Recovery and Zero Waste Approaches* (pp. 207–221). Elsevier. https://doi.org/10.1016/B978-0-444-64200-4.00015-3

Adams, M. W. W. (1990). The structure and mechanism of iron-hydrogenases. *Biochimica et Biophysica Acta (BBA) - Bioenergetics*, *1020*(2), 115–145. https://doi.org/10.1016/0005-2728(90)90044-5

Agler, M. T., Spirito, C. M., Usack, J. G., Werner, J. J., & Angenent, L. T. (2012). Chain elongation with reactor microbiomes: Upgrading dilute ethanol to medium-chain carboxylates. *Energy & Environmental Science*, *5*, 8189–8192. https://doi.org/10.1039/c2ee22101b

Agler, M. T., Wrenn, B. A., Zinder, S. H., & Angenent, L. T. (2011). Waste to bioproduct conversion with undefined mixed cultures: The carboxylate platform. *Trends in Biotechnology*, *29*(2), 70–78. https://doi.org/10.1016/j.tibtech.2010.11.006

Agnihotri, S., Yin, D. M., Mahboubi, A., Sapmaz, T., Varjani, S., Qiao, W., Koseoglu-Imer, D. Y., & Taherzadeh, M. J. (2022). A glimpse of the world of volatile fatty acids production and application: A review. *Bioengineered*, *13*(1), 1249–1275. https://doi.org/10.1080/21655979.2021.1996044

Allaart, M. T., Diender, M., Sousa, D. Z., & Kleerebezem, R. (2023). Overflow metabolism at the thermodynamic limit of life: How carboxydotrophic acetogens mitigate carbon monoxide toxicity. *Microbial Biotechnology*, *16*(4), 697–705. https://doi.org/10.1111/1751-7915.14212

Allen, T. D., Caldwell, M. E., Lawson, P. A., Huhnke, R. L., & Tanner, R. S. (2010). *Alkalibaculum bacchi* gen. Nov., sp. Nov., a CO-oxidizing, ethanol-producing acetogen isolated from livestock-impacted soil. *International Journal of Systematic and Evolutionary Microbiology*, *60*, 2483–2489. https://doi.org/10.1099/ijs.0.018507-0

Almaas, E., Kovács, B., Vicsek, T., Oltvai, Z. N., & Barabási, A.-L. (2004). Global organization of metabolic fluxes in the bacterium *Escherichia coli*. *Nature*, *427*, Article 6977. https://doi.org/10.1038/nature02289

Alves, J. I., Stams, A. J. M., Plugge, C. M., Madalena Alves, M., & Sousa, D. Z. (2013). Enrichment of anaerobic syngas-converting bacteria from thermophilic bioreactor sludge. *FEMS Microbiology Ecology*, *86*, 590–597. https://doi.org/10.1111/1574-6941.12185

Amani, T., Nosrati, M., & Sreekrishnan, T. R. (2010). Anaerobic digestion from the viewpoint of microbiological, chemical, and operational aspects—A review. *Environmental Reviews*, *18*, 255–278. https://doi.org/10.1139/A10-011

Anand, S., Kaur, H., & Mande, S. S. (2016). Comparative in silico analysis of butyrate production pathways in gut commensals and pathogens. *Frontiers in Microbiology*, *7*, Article 1945. https://doi.org/10.3389/fmicb.2016.01945

Angenent, L. T., Richter, H., Buckel, W., Spirito, C. M., Steinbusch, K. J. J., Plugge, C. M., Strik, D. P. B. T. B., Grootscholten, T. I. M., Buisman, C. J. N., & Hamelers, H. V. M. (2016). Chain elongation with reactor microbiomes: Open-culture biotechnology to produce biochemicals. *Environmental Science & Technology*, *50*, 2796–2810. https://doi.org/10.1021/acs.est.5b04847

Apweiler, R., Bairoch, A., Wu, C. H., Barker, W. C., Boeckmann, B., Ferro, S., Gasteiger, E., Huang, H., Lopez, R., Magrane, M., Martin, M. J., Natale, D. A., O'Donovan, C., Redaschi, N., & Yeh, L.-S. L. (2004). UniProt: The Universal Protein knowledgebase. *Nucleic Acids Research*, *32*(Database issue), D115–D119. https://doi.org/10.1093/nar/gkh131

Arantes, A. L., Alves, J. I., Stams, A. J. M., Alves, M. M., & Sousa, D. Z. (2018). Enrichment of syngas-converting communities from a multi-orifice baffled bioreactor. *Microbial Biotechnology*, *11*(4), 639–646. https://doi.org/10.1111/1751-7915.12864

Arantes, A. L., Moreira, J. P. C., Diender, M., Parshina, S. N., Stams, A. J. M., Alves, M. M., Alves, J. I., & Sousa, D. Z. (2020). Enrichment of anaerobic syngas-converting communities and isolation of a novel carboxydotrophic *Acetobacterium wieringae* strain JM. *Frontiers in Microbiology*, *11*, Article 58. https://doi.org/10.3389/fmicb.2020.00058

Arkin, A. P., Cottingham, R. W., Henry, C. S., Harris, N. L., Stevens, R. L., Maslov, S., Dehal, P., Ware, D., Perez, F., Canon, S., Sneddon, M. W., Henderson, M. L., Riehl, W. J., Murphy-Olson, D., Chan, S. Y., Kamimura, R. T., Kumari, S., Drake, M. M., Brettin, T. S., ... Yu, D. (2018). KBase: The United States Department of Energy Systems Biology Knowledgebase. *Nature Biotechnology*, *36*, 566–569. https://doi.org/10.1038/nbt.4163

Arslan, K., Bayar, B., Abubackar, H. N., Veiga, M. C., & Kennes, C. (2019). Solventogenesis in *Clostridium aceticum* producing high concentrations of ethanol from syngas. *Bioresource Technology*, *292*, Article 121941. https://doi.org/10.1016/j.biortech.2019.121941

Arslan, K., Schoch, T., Höfele, F., Herrschaft, S., Oberlies, C., Bengelsdorf, F., Veiga, M. C., Dürre, P., & Kennes, C. (2022). Engineering *Acetobacterium woodii* for the production of isopropanol and acetone from carbon dioxide and hydrogen. *Biotechnology Journal*, *17*, Article e2100515. https://doi.org/10.1002/biot.202100515

Asimakopoulos, K., Gavala, H. N., & Skiadas, I. V. (2018). Reactor systems for syngas fermentation processes: A review. *Chemical Engineering Journal*, *348*, 732–744. https://doi.org/10.1016/j.cej.2018.05.003

Asimakopoulos, K., Grimalt-Alemany, A., Lundholm-Høffner, C., Gavala, H. N., & Skiadas, I. V. (2021a). Carbon sequestration through syngas biomethanation coupled with H_2 supply for a clean production of natural gas grade biomethane. *Waste and Biomass Valorization*, *12*, 6005–6019. https://doi.org/10.1007/s12649-021-01393-2

Asimakopoulos, K., Kaufmann-Elfang, M., Lundholm-Høffner, C., Rasmussen, N. B. K., Grimalt-Alemany, A., Gavala, H. N., & Skiadas, I. V. (2021b). Scale up study of a thermophilic trickle bed reactor performing syngas biomethanation. *Applied Energy*, *290*, Article 116771. https://doi.org/10.1016/j.apenergy.2021.116771

Asimakopoulos, K., Łężyk, M., Grimalt-Alemany, A., Melas, A., Wen, Z., Gavala, H. N., & Skiadas, I. V. (2020). Temperature effects on syngas biomethanation performed in a trickle bed reactor. *Chemical Engineering Journal*, *393*, Article 124739. https://doi.org/10.1016/j.cej.2020.124739

Ato, M., Ishii, M., & Igarashi, Y. (2014). Enrichment of amino acid-oxidizing, acetate-reducing bacteria. *Journal of Bioscience and Bioengineering*, *118*, 160–165. https://doi.org/10.1016/j.jbiosc.2014.02.003

Aziz, R. K., Bartels, D., Best, A. A., DeJongh, M., Disz, T., Edwards, R. A., Formsma, K., Gerdes, S., Glass, E. M., Kubal, M., Meyer, F., Olsen, G. J., Olson, R., Osterman, A. L., Overbeek, R. A., McNeil, L. K., Paarmann, D., Paczian, T., Parrello, B., ... Zagnitko, O. (2008). The RAST Server: Rapid Annotations using Subsystems Technology. *BMC Genomics*, *9*, Article 75. https://doi.org/10.1186/1471-2164-9-75

Bader, J., Mast-Gerlach, E., Popović, M. K., Bajpai, R., & Stahl, U. (2010). Relevance of microbial coculture fermentations in biotechnology. *Journal of Applied Microbiology*, *109*(2), 371–387. https://doi.org/10.1111/j.1365-2672.2009.04659.x

Bae, J., Jin, S., Kang, S., Cho, B.-K., & Oh, M.-K. (2022). Recent progress in the engineering of C1-utilizing microbes. *Current Opinion in Biotechnology*, *78*, Article 102836. https://doi.org/10.1016/j.copbio.2022.102836

Baleeiro, F. C. F., Kleinsteuber, S., Neumann, A., & Sträuber, H. (2019). Syngas-aided anaerobic fermentation for medium-chain carboxylate and alcohol production: The case for microbial communities. *Applied Microbiology and Biotechnology*, *103*, 8689–8709. https://doi.org/10.1007/s00253-019-10086-9

Baleeiro, F. C. F., Kleinsteuber, S., & Sträuber, H. (2021). Hydrogen as a co-electron donor for chain elongation with complex communities. *Frontiers in Bioengineering and Biotechnology*, *9*, Article 650631. https://doi.org/10.3389/fbioe.2021.650631

R

REFERENCES

Baleeiro, F. C. F., Raab, J., Kleinsteuber, S., Neumann, A., & Sträuber, H. (2022). Mixotrophic chain elongation with syngas and lactate as electron donors. *Microbial Biotechnology*, *16*(2), 322–336. https://doi.org/10.1111/1751-7915.14163

Baleeiro, F. C. F., Varchmin, L., Kleinsteuber, S., Sträuber, H., & Neumann, A. (2023). Formate-induced CO tolerance and methanogenesis inhibition in fermentation of syngas and plant biomass for carboxylate production. *Biotechnology for Biofuels and Bioproducts*, *16*, Article 26. https://doi.org/10.1186/s13068-023-02271-w

Balk, M., Mehboob, F., van Gelder, A. H., Rijpstra, W. I. C., Damsté, J. S. S., & Stams, A. J. M. (2010). (Per)chlorate reduction by an acetogenic bacterium, *Sporomusa* sp., isolated from an underground gas storage. *Applied Microbiology and Biotechnology*, *88*, 595–603. https://doi.org/10.1007/s00253-010-2788-8

Balonek, C. M., Lillebø, A. H., Rane, S., Rytter, E., Schmidt, L. D., & Holmen, A. (2010). Effect of alkali metal impurities on Co–Re catalysts for Fischer–Tropsch synthesis from biomass-derived syngas. *Catalysis Letters*, *138*, 8–13. https://doi.org/10.1007/s10562-010-0366-4

Bambal, A. S., Guggilla, V. S., Kugler, E. L., Gardner, T. H., & Dadyburjor, D. B. (2014). Poisoning of a silica-supported cobalt catalyst due to presence of sulfur impurities in syngas during Fischer–Tropsch synthesis: Effects of chelating agent. *Industrial & Engineering Chemistry Research*, *53*, 5846–5857. https://doi.org/10.1021/ie500243h

Barker, H. A., & Taha, S. M. (1942). *Clostridium kluyverii*, an organism concerned in the formation of caproic acid from ethyl alcohol. *Journal of Bacteriology*, *43*, 347–363. https://doi.org/10.1128/JB.43.3.347-363.1942

Bäumler, M., Burgmaier, V., Herrmann, F., Mentges, J., Schneider, M., Ehrenreich, A., Liebl, W., & Weuster-Botz, D. (2023). Continuous production of ethanol, 1-butanol and 1-hexanol from CO with a synthetic co-culture of Clostridia applying a cascade of stirred-tank bioreactors. *Microorganisms*, *11*(4), Article 4. https://doi.org/10.3390/microorganisms11041003

Bäumler, M., Schneider, M., Ehrenreich, A., Liebl, W., & Weuster-Botz, D. (2021). Synthetic co-culture of autotrophic *Clostridium carboxidivorans* and chain elongating *Clostridium kluyveri* monitored by flow cytometry. *Microbial Biotechnology*, *15*(5), 1474–1485. https://doi.org/10.1111/1751-7915.13941

Baur, T., & Dürre, P. (2023). New insights into the physiology of the propionate producers *Anaerotignum propionicum* and *Anaerotignum neopropionicum* (formerly *Clostridium propionicum* and *Clostridium neopropionicum*). *Microorganisms*, *11*, Article 685. https://doi.org/10.3390/microorganisms11030685

Beck, M. H., Poehlein, A., Bengelsdorf, F. R., Schiel-Bengelsdorf, B., Daniel, R., & Dürre, P. (2016). Draft genome sequence of the strict anaerobe *Clostridium neopropionicum* X4 (DSM 3847[T]). *Genome Announcements*, *4*(2), Article e00209-16. https://doi.org/10.1128/genomeA.00209-16

Ben Said, S., & Or, D. (2017). Synthetic microbial ecology: Engineering habitats for modular consortia. *Frontiers in Microbiology*, *8*, Article 1125. https://doi.org/10.3389/fmicb.2017.01125

Bengelsdorf, F. R., Beck, M. H., Erz, C., Hoffmeister, S., Karl, M. M., Riegler, P., Wirth, S., Poehlein, A., Weuster-Botz, D., & Dürre, P. (2018). Bacterial anaerobic synthesis gas (syngas) and CO_2+H_2 fermentation. In S. Sariaslani & G. M. Gadd (Eds.), *Advances in Applied Microbiology* (Vol. 103, pp. 143–221). Academic Press. https://doi.org/10.1016/bs.aambs.2018.01.002

Bengelsdorf, F. R., Poehlein, A., Linder, S., Erz, C., Hummel, T., Hoffmeister, S., Daniel, R., & Dürre, P. (2016). Industrial acetogenic biocatalysts: A comparative metabolic and genomic analysis. *Frontiers in Microbiology*, *7*, Article 1036. https://doi.org/10.3389/fmicb.2016.01036

Benito-Vaquerizo, S., Diender, M., Parera Olm, I., Martins dos Santos, V. A. P., Schaap, P. J., Sousa, D. Z., & Suarez-Diez, M. (2020). Modeling a co-culture of *Clostridium autoethanogenum* and *Clostridium kluyveri* to increase syngas conversion to medium-chain fatty-acids. *Computational and Structural Biotechnology Journal*, *18*, 3255–3266. https://doi.org/10.1016/j.csbj.2020.10.003

Benito-Vaquerizo, S., Nouse, N., Schaap, P. J., Hugenholtz, J., Brul, S., López-Contreras, A. M., Martins Dos Santos, V. A. P., & Suarez-Diez, M. (2022a). Model-driven approach for the production of butyrate from CO_2/H_2 by a novel co-culture of *C. autoethanogenum* and *C. beijerinckii*. *Frontiers in Microbiology*, *13*, Article 1064013. https://doi.org/10.3389/fmicb.2022.1064013

Benito-Vaquerizo, S., Parera Olm, I., De Vroet, T., Schaap, P. J., Sousa, D. Z., Martins Dos Santos, V. A. P., & Suarez-Diez, M. (2022b). Genome-scale metabolic modelling enables deciphering ethanol metabolism via the acrylate pathway in the propionate-producer *Anaerotignum neopropionicum*. *Microbial Cell Factories*, *21*, Article 116. https://doi.org/10.1186/s12934-022-01841-1

Bergmann, F. T., Adams, R., Moodie, S., Cooper, J., Glont, M., Golebiewski, M., Hucka, M., Laibe, C., Miller, A. K., Nickerson, D. P., Olivier, B. G., Rodriguez, N., Sauro, H. M., Scharm, M., Soiland-Reyes, S., Waltemath, D., Yvon, F., & Le Novère, N. (2014). COMBINE archive and OMEX format: One file to share all information to reproduce a modeling project. *BMC Bioinformatics*, *15*, Article 369. https://doi.org/10.1186/s12859-014-0369-z

Bertsch, J., & Müller, V. (2015a). Bioenergetic constraints for conversion of syngas to biofuels in acetogenic bacteria. *Biotechnology for Biofuels*, *8*, Article 210. https://doi.org/10.1186/s13068-015-0393-x

Bertsch, J., & Müller, V. (2015b). CO metabolism in the acetogen *Acetobacterium woodii*. *Applied and Environmental Microbiology*, *81*(17), 5949–5956. https://doi.org/10.1128/AEM.01772-15

Bertsch, J., Siemund, A. L., Kremp, F., & Müller, V. (2015). A novel route for ethanol oxidation in the acetogenic bacterium *Acetobacterium woodii*: The AdhE pathway. *Environmental Microbiology*, *18*(9), 2913–2922. https://doi.org/10.1111/1462-2920.13082

Blank, L. M., Narancic, T., Mampel, J., Tiso, T., & O'Connor, K. (2020). Biotechnological upcycling of plastic waste and other non-conventional feedstocks in a circular economy. *Current Opinion in Biotechnology*, *62*, 212–219. https://doi.org/10.1016/j.copbio.2019.11.011

Bornstein, B. T., & Barker, H. A. (1948). The nutrition of *Clostridium kluyveri*. *Journal of Bacteriology*, *55*, 223–230. https://doi.org/10.1128/JB.55.2.223-230.1948

Bourgade, B., Minton, N. P., & Islam, M. A. (2021). Genetic and metabolic engineering challenges of C1-gas fermenting acetogenic chassis organisms. *FEMS Microbiology Reviews*, *45*(2), 1–20. https://doi.org/10.1093/femsre/fuab008

Box, G. E. P., & Draper, N. R. (1987). *Empirical model-building and response surfaces* (pp. xiv, 669). John Wiley & Sons.

Boyaval, P., & Corre, C. (1995). Production of propionic acid. *Le Lait*, *75*, 453–461. https://doi.org/10.1016/0023-7302(96)80128-X

Braun, M., & Gottschalk, G. (1982). *Acetobacterium wieringae* sp. Nov., a new species producing acetic acid from molecular hydrogen and carbon dioxide. *Zentralblatt Für Bakteriologie Mikrobiologie Und Hygiene: I. Abt. Originale C: Allgemeine, Angewandte Und Ökologische Mikrobiologie*, *3*(3), 368–376. https://doi.org/10.1016/S0721-9571(82)80017-3

Braun, M., Mayer, F., & Gottschalk, G. (1981). *Clostridium aceticum* (Wieringa), a microorganism producing acetic acid from molecular hydrogen and carbon dioxide. *Archives of Microbiology*, *128*(3), 288–293. https://doi.org/10.1007/BF00422532

Brenner, K., You, L., & Arnold, F. H. (2008). Engineering microbial consortia: A new frontier in synthetic biology. *Trends in Biotechnology*, *26*(9), 483–489. https://doi.org/10.1016/j.tibtech.2008.05.004

Buckel, W., & Thauer, R. K. (2013). Energy conservation via electron bifurcating ferredoxin reduction and proton/Na$^+$ translocating ferredoxin oxidation. *Biochimica et Biophysica Acta (BBA) - Bioenergetics*, *1827*(2), 94–113. https://doi.org/10.1016/j.bbabio.2012.07.002

Buckel, W., & Thauer, R. K. (2018a). Flavin-based electron bifurcation, a new mechanism of biological energy coupling. *Chemical Reviews*, *118*, 3862–3886. https://doi.org/10.1021/acs.chemrev.7b00707

Buckel, W., & Thauer, R. K. (2018b). Flavin-based electron bifurcation, ferredoxin, flavodoxin, and anaerobic respiration with protons (Ech) or NAD$^+$ (Rnf) as electron acceptors: A historical review. *Frontiers in Microbiology*, *9*, Article 401. https://doi.org/10.3389/fmicb.2018.00401

Butler, J. E., Young, N. D., & Lovley, D. R. (2009). Evolution from a respiratory ancestor to fill syntrophic and fermentative niches: Comparative genomics of six *Geobacteraceae* species. *BMC Genomics*, *10*, Article 103. https://doi.org/10.1186/1471-2164-10-103

Butler-Wu, S. M., Sengupta, D. J., Kittichotirat, W., Matsen, F. A., & Bumgarner, R. E. (2011). Genome sequence of a novel species, *Propionibacterium humerusii*. *Journal of Bacteriology*, *193*, 3678–3678. https://doi.org/10.1128/JB.05036-11

R

REFERENCES

Calvo-Flores, F. G., & Martin-Martinez, F. J. (2022). Biorefineries: Achievements and challenges for a bio-based economy. *Frontiers in Chemistry*, *10*, Article 973417. https://www.frontiersin.org/articles/10.3389/fchem.2022.973417

Candry, P., Huang, S., Carvajal-Arroyo, J. M., Rabaey, K., & Ganigué, R. (2020a). Enrichment and characterisation of ethanol chain elongating communities from natural and engineered environments. *Scientific Reports*, *10*, Article 3682. https://doi.org/10.1038/s41598-020-60052-z

Candry, P., Ulcar, B., Petrognani, C., Rabaey, K., & Ganigué, R. (2020b). Ethanol:propionate ratio drives product selectivity in odd-chain elongation with *Clostridium kluyveri* and mixed communities. *Bioresource Technology*, *313*, Article 123651. https://doi.org/10.1016/j.biortech.2020.123651

Candry, P., Van Daele, T., Denis, K., Amerlinck, Y., Andersen, S. J., Ganigué, R., Arends, J. B. A., Nopens, I., & Rabaey, K. (2018). A novel high-throughput method for kinetic characterisation of anaerobic bioproduction strains, applied to *Clostridium kluyveri*. *Scientific Reports*, *8*, Article 9724. https://doi.org/10.1038/s41598-018-27594-9

Cao, H., Wei, D., Yang, Y., Shang, Y., Li, G., Zhou, Y., Ma, Q., & Xu, Y. (2017). Systems-level understanding of ethanol-induced stresses and adaptation in *E. coli*. *Scientific Reports*, *7*, Article 44150. https://doi.org/10.1038/srep44150

Carlson, E. D., & Papoutsakis, E. T. (2017). Heterologous expression of the *Clostridium carboxidivorans* CO dehydrogenase alone or together with the acetyl Coenzyme A synthase enables both reduction of CO_2 and oxidation of CO by *Clostridium acetobutylicum*. *Applied and Environmental Microbiology*, *83*(16), Article e00829-17. https://doi.org/10.1128/AEM.00829-17

Cavalcante, W. de A., Leitão, R. C., Gehring, T. A., Angenent, L. T., & Santaella, S. T. (2017). Anaerobic fermentation for n-caproic acid production: A review. *Process Biochemistry*, *54*, 106–119. https://doi.org/10.1016/j.procbio.2016.12.024

Ceccaldi, P., Schuchmann, K., Müller, V., & Elliott, S. J. (2017). The hydrogen dependent CO_2 reductase: The first completely CO tolerant FeFe-hydrogenase. *Energy & Environmental Science*, *10*(2), 503–508. https://doi.org/10.1039/C6EE02494G

Cha, S., Lim, H. G., Kwon, S., Kim, D., Kang, C. W., & Jung, G. Y. (2021). Design of mutualistic microbial consortia for stable conversion of carbon monoxide to value-added chemicals. *Metabolic Engineering*, *64*, 146–153. https://doi.org/10.1016/j.ymben.2021.02.001

Chakraborty, S., Rene, E. R., Lens, P. N. L., Veiga, M. C., & Kennes, C. (2019). Enrichment of a solventogenic anaerobic sludge converting carbon monoxide and syngas into acids and alcohols. *Bioresource Technology*, *272*, 130–136. https://doi.org/10.1016/j.biortech.2018.10.002

Chandolias, K., Pekgenc, E., & Taherzadeh, M. (2019). Floating membrane bioreactors with high gas hold-up for syngas-to-biomethane conversion. *Energies*, *12*, 1046. https://doi.org/10.3390/en12061046

Chandolias, K., Richards, T., & Taherzadeh, M. J. (2018). Combined gasification-fermentation process in waste biorefinery. In T. Bhaskar, A. Pandey, S. V. Mohan, D.-J. Lee, & S. K. Khanal (Eds.), *Waste biorefinery* (pp. 157–200). Elsevier. https://doi.org/10.1016/B978-0-444-63992-9.00005-7

Chang, I. S., Kim, B. H., Lovitt, R. W., & Bang, J. S. (2001). Effect of CO partial pressure on cell-recycled continuous CO fermentation by *Eubacterium limosum* KIST612. *Process Biochemistry*, *37*, 411–421. https://doi.org/10.1016/S0032-9592(01)00227-8

Chartrain, M., & Zeikus, J. G. (1986). Microbial ecophysiology of whey biomethanation: Characterization of bacterial trophic populations and prevalent species in continuous culture. *Applied and Environmental Microbiology*, *51*(1), 188–196. https://doi.org/10.1128/aem.51.1.188-196.1986

Charubin, K., Bennett, R. K., Fast, A. G., & Papoutsakis, E. T. (2018). Engineering *Clostridium* organisms as microbial cell-factories: Challenges & opportunities. *Metabolic Engineering*, *50*, 173–191. https://doi.org/10.1016/j.ymben.2018.07.012

Chelliah, V., Juty, N., Ajmera, I., Ali, R., Dumousseau, M., Glont, M., Hucka, M., Jalowicki, G., Keating, S., Knight-Schrijver, V., Lloret-Villas, A., Natarajan, K. N., Pettit, J.-B., Rodriguez, N., Schubert, M., Wimalaratne, S. M., Zhao, Y., Hermjakob, H., Le Novère, N., & Laibe, C. (2015). BioModels: Ten-year anniversary. *Nucleic Acids Research*, *43*(Database issue), D542–D548. https://doi.org/10.1093/nar/gku1181

Chen, J.-S., & Blanchard, D. K. (1978). Isolation and properties of a unidirectional H_2-oxidizing hydrogenase from the strictly anaerobic N_2-fixing bacterium *Clostridium pasteurianum* W5. *Biochemical and Biophysical Research Communications*, *84*, 1144–1150. https://doi.org/10.1016/0006-291X(78)91703-5

Cherubini, F. (2010). The biorefinery concept: Using biomass instead of oil for producing energy and chemicals. *Energy Conversion and Management*, *51*, 1412–1421. https://doi.org/10.1016/j.enconman.2010.01.015

Cherubini, F., Jungmeier, G., Wellisch, M., Willke, T., Skiadas, I., Van Ree, R., & de Jong, E. (2009). Toward a common classification approach for biorefinery systems. *Biofuels, Bioproducts and Biorefining*, *3*(5), 534–546. https://doi.org/10.1002/bbb.172

Chiu, P. C., & Lee, M. (2001). 2-Bromoethanesulfonate affects bacteria in a trichloroethene-dechlorinating culture. *Applied and Environmental Microbiology*, *67*, 2371–2374. https://doi.org/10.1128/AEM.67.5.2371-2374.2001

Choi, S.-H., Kim, J.-S., Park, J.-E., Lee, K. C., Eom, M. K., Oh, B. S., Yu, S. Y., Kang, S. W., Han, K.-I., Suh, M. K., Lee, D. H., Yoon, H., Kim, B.-Y., Lee, J. H., Lee, J. H., Lee, J.-S., & Park, S.-H. (2019). *Anaerotignum faecicola* sp. Nov., isolated from human faeces. *Journal of Microbiology*, *57*, 1073–1078. https://doi.org/10.1007/s12275-019-9268-3

Christensen, J. M., Jensen, P. A., & Jensen, A. D. (2011). Effects of feed composition and feed impurities in the catalytic conversion of syngas to higher alcohols over alkali-promoted cobalt–molybdenum sulfide. *Industrial & Engineering Chemistry Research*, *50*, 7949–7963. https://doi.org/10.1021/ie200235e

Climate Target Update Tracker. (2023). Climate Action Tracker. https://climateactiontracker.org/climate-target-update-tracker-2022/

Coma, M., Vilchez-Vargas, R., Roume, H., Jauregui, R., Pieper, D. H., & Rabaey, K. (2016). Product diversity linked to substrate usage in chain elongation by mixed-culture fermentation. *Environmental Science & Technology*, *50*(12), 6467–6476. https://doi.org/10.1021/acs.est.5b06021

Couto, N., Rouboa, A., Silva, V., Monteiro, E., & Bouziane, K. (2013). Influence of the biomass gasification processes on the final composition of syngas. *Energy Procedia*, *36*, 596–606. https://doi.org/10.1016/j.egypro.2013.07.068

Covert, M. W., Knight, E. M., Reed, J. L., Herrgard, M. J., & Palsson, B. O. (2004). Integrating high-throughput and computational data elucidates bacterial networks. *Nature*, *429*, Article 6987. https://doi.org/10.1038/nature02456

Cui, Y., Yang, K.-L., & Zhou, K. (2020). Using co-culture to functionalize *Clostridium* fermentation. *Trends in Biotechnology*, *39*, 914–926. https://doi.org/10.1016/j.tibtech.2020.11.016

Dagle, R. A., Winkelman, A. D., Ramasamy, K. K., Lebarbier Dagle, V., & Weber, R. S. (2020). Ethanol as a renewable building block for fuels and chemicals. *Industrial & Engineering Chemistry Research*, *59*(11), 4843–4853. https://doi.org/10.1021/acs.iecr.9b05729

Dai, Z., Dong, H., Zhang, Y., & Li, Y. (2016). Elucidating the contributions of multiple aldehyde/alcohol dehydrogenases to butanol and ethanol production in *Clostridium acetobutylicum*. *Scientific Reports 2016 6:1*, *6*, Article 28189. https://doi.org/10.1038/srep28189

Daniell, J., Köpke, M., & Simpson, S. (2012). Commercial biomass syngas fermentation. *Energies*, *5*, 5372–5417. https://doi.org/10.3390/en5125372

Daniels, L., Fuchs, G., Thauer, R. K., & Zeikus, J. G. (1977). Carbon monoxide oxidation by methanogenic bacteria. *Journal of Bacteriology*, *132*, 118–126. https://doi.org/10.1128/JB.132.1.118-126.1977

Davis, J. J., Wattam, A. R., Aziz, R. K., Brettin, T., Butler, R., Butler, R. M., Chlenski, P., Conrad, N., Dickerman, A., Dietrich, E. M., Gabbard, J. L., Gerdes, S., Guard, A., Kenyon, R. W., Machi, D., Mao, C., Murphy-Olson, D., Nguyen, M., Nordberg, E. K., … Stevens, R. (2019). The PATRIC Bioinformatics Resource Center: Expanding data and analysis capabilities. *Nucleic Acids Research*, *48*(Database issue), D606–D612. https://doi.org/10.1093/nar/gkz943

de Leeuw, K. D., Ahrens, T., Buisman, C. J. N., & Strik, D. P. B. T. B. (2021). Open culture ethanol-based chain elongation to form medium chain branched carboxylates and alcohols. *Frontiers in Bioengineering and Biotechnology*, *9*, Article 697439. https://www.frontiersin.org/articles/10.3389/fbioe.2021.697439

De Ras, K., Van de Vijver, R., Galvita, V. V., Marin, G. B., & Van Geem, K. M. (2019). Carbon capture and utilization in the steel industry: Challenges and opportunities for chemical engineering. *Current Opinion in Chemical Engineering*, *26*, 81–87. https://doi.org/10.1016/j.coche.2019.09.001

De Vrieze, J., Christiaens, M. E. R., & Verstraete, W. (2017). The microbiome as engineering tool: Manufacturing and trading between microorganisms. *New Biotechnology*, *39*, 206–214. https://doi.org/10.1016/j.nbt.2017.07.001

Deodato, F., Boenzi, S., Santorelli, F. M., & Dionisi-Vici, C. (2006). Methylmalonic and propionic aciduria. *American Journal of Medical Genetics Part C: Seminars in Medical Genetics*, *142C*, 104–112. https://doi.org/10.1002/ajmg.c.30090

Diender, M., Parera Olm, I., Gelderloos, M., Koehorst, J., Schaap, P. J., Stams, A. J. M., & Sousa, D. Z. (2019). Metabolic shift induced by synthetic co-cultivation promotes high yield of chain elongated acids from syngas. *Scientific Reports*, *9*, Article 18081. https://doi.org/10.1038/s41598-019-54445-y

Diender, M., Parera Olm, I., & Sousa, D. Z. (2021). Synthetic co-cultures: Novel avenues for bio-based processes. *Current Opinion in Biotechnology*, *67*, 72–79. https://doi.org/10.1016/j.copbio.2021.01.006

Diender, M., Pereira, R., Wessels, H. J. C. T., Stams, A. J. M., & Sousa, D. Z. (2016a). Proteomic analysis of the hydrogen and carbon monoxide metabolism of *Methanothermobacter marburgensis*. *Frontiers in Microbiology*, *7*, Article 1049. https://doi.org/10.3389/fmicb.2016.01049

Diender, M., Stams, A. J. M., & Sousa, D. Z. (2015). Pathways and bioenergetics of anaerobic carbon monoxide fermentation. *Frontiers in Microbiology*, *6*, 1–18. https://doi.org/10.3389/fmicb.2015.01275

Diender, M., Stams, A. J. M., & Sousa, D. Z. (2016b). Production of medium-chain fatty acids and higher alcohols by a synthetic co-culture grown on carbon monoxide or syngas. *Biotechnology for Biofuels*, *9*, Article 82. https://doi.org/10.1186/s13068-016-0495-0

Diender, M., Uhl, P. S., Bitter, J. H., Stams, A. J. M. M., & Sousa, D. Z. (2018). High rate biomethanation of carbon monoxide-rich gases via a thermophilic synthetic co-culture. *ACS Sustainable Chemistry & Engineering*, *6*, 2169–2176. https://doi.org/10.1021/acssuschemeng.7b03601

Dolan, S. K., Wijaya, A., Geddis, S. M., Spring, D. R., Silva-Rocha, R., & Welch, M. (2018). Loving the poison: The methylcitrate cycle and bacterial pathogenesis. *Microbiology*, *164*(3), 251–259. https://doi.org/10.1099/mic.0.000604

Domenzain, I., Sánchez, B., Anton, M., Kerkhoven, E. J., Millán-Oropeza, A., Henry, C., Siewers, V., Morrissey, J. P., Sonnenschein, N., & Nielsen, J. (2022). Reconstruction of a catalogue of genome-scale metabolic models with enzymatic constraints using GECKO 2.0. *Nature Communications*, *13*, Article 3766. https://doi.org/10.1038/s41467-022-31421-1

Drake, H. L., Daniel, S. L., Küsel, K., Matthies, C., Kuhner, C., & Braus-Stromeyer, S. (1997). Acetogenic bacteria: What are the *in situ* consequences of their diverse metabolic versatilities? *BioFactors*, *6*(1), 13–24. https://doi.org/10.1002/biof.5520060103

Drake, H. L., Gössner, A. S., & Daniel, S. L. (2008). Old acetogens, new light. *Annals of the New York Academy of Sciences*, *1125*, 100–128. https://doi.org/10.1196/annals.1419.016

Du, Y., Zou, W., Zhang, K., Ye, G., & Yang, J. (2020). Advances and applications of *Clostridium* co-culture systems in biotechnology. *Frontiers in Microbiology*, *11*, Article 560223. https://doi.org/10.3389/fmicb.2020.560223

Duan, H., He, P., Shao, L., Lü, F., & Lu, F. (2021). Functional genome-centric view of the CO-driven anaerobic microbiome. *The ISME Journal*, *15*, 2906–2919. https://doi.org/10.1038/s41396-021-00983-1

Earth Overshoot Day. (2023). Global Footprint Network. https://www.footprintnetwork.org/our-work/earth-overshoot-day/

Ebrahim, A., Lerman, J. A., Palsson, B. O., & Hyduke, D. R. (2013). COBRApy: COnstraints-Based Reconstruction and Analysis for Python. *BMC Systems Biology*, *7*, Article 74. https://doi.org/10.1186/1752-0509-7-74

Emms, D. M., & Kelly, S. (2019). OrthoFinder: Phylogenetic orthology inference for comparative genomics. *Genome Biology*, *20*, Article 238. https://doi.org/10.1186/s13059-019-1832-y

Esquivel-Elizondo, S., Delgado, A. G., & Krajmalnik-Brown, R. (2017a). Evolution of microbial communities growing with carbon monoxide, hydrogen, and carbon dioxide. *FEMS Microbiology Ecology*, *93*(6), fix076. https://doi.org/10.1093/femsec/fix076

Esquivel-Elizondo, S., Delgado, A. G., Rittmann, B. E., & Krajmalnik-Brown, R. (2017b). The effects of CO_2 and H_2 on CO metabolism by pure and mixed microbial cultures. *Biotechnology for Biofuels*, *10*, Article 220. https://doi.org/10.1186/s13068-017-0910-1

European Commission. (2018). *A clean planet for all—A European long-term strategic vision for a prosperous, modern, competitive and climate neutral economy (COM(2018) 773).*

European Commission. (2019). *The European Green Deal (COM(2019) 640).*

Fernández-Blanco, C., Robles-Iglesias, R., Naveira-Pazos, C., Veiga, M. C., & Kennes, C. (2023). Production of biofuels from C1-gases with *Clostridium* and related bacteria—Recent advances. *Microbial Biotechnology*, *16*(4), 726–741. https://doi.org/10.1111/1751-7915.14220

Fernández-Blanco, C., Veiga, M. C., & Kennes, C. (2022). Efficient production of n-caproate from syngas by a co-culture of *Clostridium aceticum* and *Clostridium kluyveri*. *Journal of Environmental Management*, *302*(Part A), Article 113992. https://doi.org/10.1016/j.jenvman.2021.113992

Fernández-Naveira, Á., Veiga, M. C., & Kennes, C. (2017). H-B-E (hexanol-butanol-ethanol) fermentation for the production of higher alcohols from syngas/waste gas. *Journal of Chemical Technology & Biotechnology*, *92*, 712–731. https://doi.org/10.1002/JCTB.5194

Fernando, S., Adhikari, S., Chandrapal, C., & Murali, N. (2006). Biorefineries: Current status, challenges, and future direction. *Energy & Fuels*, *20*(4), 1727–1737. https://doi.org/10.1021/ef060097w

Figueras, J., Benbelkacem, H., Dumas, C., & Buffiere, P. (2023). Syngas biomethanation: In a transfer limited process, is CO inhibition an issue? *Waste Management*, *162*, 36–42. https://doi.org/10.1016/j.wasman.2023.03.011

Flamholz, A., Noor, E., Bar-Even, A., & Milo, R. (2012). eQuilibrator—The biochemical thermodynamics calculator. *Nucleic Acids Research*, *40*(Database issue), D770–D775. https://doi.org/10.1093/nar/gkr874

Foster, C., Charubin, K., Papoutsakis, E. T., & Maranas, C. D. (2021). Modeling growth kinetics, interspecies cell fusion, and metabolism of a *Clostridium acetobutylicum/Clostridium ljungdahlii* syntrophic co-culture. *mSystems*, *6*(1), Article e01325-20. https://doi.org/10.1128/mSystems.01325-20

Fox, J. D., Kerby, R. L., Roberts, G. P., & Ludden, P. W. (1996). Characterization of the CO-induced, CO-tolerant hydrogenase from *Rhodospirillum rubrum* and the gene encoding the large subunit of the enzyme. *Journal of Bacteriology*, *178*, 1515–1524. https://doi.org/10.1128/JB.178.6.1515-1524.1996

Gaddy, J. L. (2007). *Methods for increasing the production of ethanol from microbial fermentation* (Patent US7285402B2).

Ganigué, R., Naert, P., Candry, P., de Smedt, J., Stevens, C. V., & Rabaey, K. (2019). Fruity flavors from waste: A novel process to upgrade crude glycerol to ethyl valerate. *Bioresource Technology*, *289*, Article 121574. https://doi.org/10.1016/j.biortech.2019.121574

Ganigué, R., Ramió-Pujol, S., Sánchez, P., Bañeras, L., & Colprim, J. (2015). Conversion of sewage sludge to commodity chemicals via syngas fermentation. *Water Science and Technology*, *72*, 415–420. https://doi.org/10.2166/wst.2015.222

Ganigué, R., Sánchez-Paredes, P., Bañeras, L., & Colprim, J. (2016). Low fermentation pH is a trigger to alcohol production, but a killer to chain elongation. *Frontiers in Microbiology*, *7*, Article 702. https://doi.org/10.3389/fmicb.2016.00702

Garvie, E. I. (1980). Bacterial lactate dehydrogenases. *Microbiological Reviews*, *44*, 106–139.

Gavala, H. N., Grimalt-Alemany, A., Asimakopoulos, K., & Skiadas, I. V. (2021). Gas biological conversions: The potential of syngas and carbon dioxide as production platforms. *Waste and Biomass Valorization*, *12*, 5303–5328. https://doi.org/10.1007/s12649-020-01332-7

Ge, S., Usack, J. G., Spirito, C. M., & Angenent, L. T. (2015). Long-term n-caproic acid production from yeast-fermentation beer in an anaerobic bioreactor with continuous product extraction. *Environmental Science & Technology*, *49*(13), 8012–8021. https://doi.org/10.1021/acs.est.5b00238

R

REFERENCES

Gehring, T. A., Cavalcante, W. A., Colares, A. S., Angenent, L. T., Santaella, S. T., Lübken, M., & Leitão, R. C. (2020). Optimal pH set point for simultaneous production and pertraction of n-caproic acid: An experimental and simulation study. *Journal of Chemical Technology & Biotechnology*, *95*, 3105–3116. https://doi.org/10.1002/jctb.6486

Gildemyn, S., Molitor, B., Usack, J. G., Nguyen, M., Rabaey, K., & Angenent, L. T. (2017). Upgrading syngas fermentation effluent using *Clostridium kluyveri* in a continuous fermentation. *Biotechnology for Biofuels*, *10*. https://doi.org/10.1186/s13068-017-0764-6

Gleizer, S., Ben-Nissan, R., Bar-On, Y. M., Antonovsky, N., Noor, E., Zohar, Y., Jona, G., Krieger, E., Shamshoum, M., Bar-Even, A., & Milo, R. (2019). Conversion of *Escherichia coli* to generate all biomass carbon from CO_2. *Cell*, *179*, 1255-1263.e12. https://doi.org/10.1016/j.cell.2019.11.009

Goers, L., Freemont, P., & Polizzi, K. M. (2014). Co-culture systems and technologies: Taking synthetic biology to the next level. *Journal of The Royal Society Interface*, *11*, Article 20140065. https://doi.org/10.1098/rsif.2014.0065

Gonzalez-Garcia, R., McCubbin, T., Navone, L., Stowers, C., Nielsen, L., & Marcellin, E. (2017). Microbial propionic acid production. *Fermentation*, *3*, Article 21. https://doi.org/10.3390/fermentation3020021

Goyal, N., Widiastuti, H., Karimi, I. A., & Zhou, Z. (2014). A genome-scale metabolic model of *Methanococcus maripaludis* S2 for CO_2 capture and conversion to methane. *Molecular BioSystems*, *10*, 1043–1054. https://doi.org/10.1039/C3MB70421A

Griffin, D. W., & Schultz, M. A. (2012). Fuel and chemical products from biomass syngas: A comparison of gas fermentation to thermochemical conversion routes. *Environmental Progress & Sustainable Energy*, *31*, 219–224. https://doi.org/10.1002/ep.11613

Grimalt-Alemany, A., Łężyk, M., Asimakopoulos, K., Skiadas, I. V., & Gavala, H. N. (2020). Cryopreservation and fast recovery of enriched syngas-converting microbial communities. *Water Research*, *177*, Article 115747. https://doi.org/10.1016/j.watres.2020.115747

Grimalt-Alemany, A., Łężyk, M., Kennes-Veiga, D. M., Skiadas, I. V., & Gavala, H. N. (2019). Enrichment of mesophilic and thermophilic mixed microbial consortia for syngas biomethanation: The role of kinetic and thermodynamic competition. *Waste and Biomass Valorization*, *11*, 465–481. https://doi.org/10.1007/s12649-019-00595-z

Grimalt-Alemany, A., Łężyk, M., Lange, L., Skiadas, I. V., & Gavala, H. N. (2018a). Enrichment of syngas-converting mixed microbial consortia for ethanol production and thermodynamics-based design of enrichment strategies. *Biotechnology for Biofuels*, *11*, Article 198. https://doi.org/10.1186/s13068-018-1189-6

Grimalt-Alemany, A., Skiadas, I. V., & Gavala, H. N. (2018b). Syngas biomethanation: State-of-the-art review and perspectives. *Biofuels, Bioproducts and Biorefining*, *12*(1), 139–158. https://doi.org/10.1002/bbb.1826

Grootscholten, T. I. M., Steinbusch, K. J. J., Hamelers, H. V. M., & Buisman, C. J. N. (2013). High rate heptanoate production from propionate and ethanol using chain elongation. *Bioresource Technology*, *136*, 715–718. https://doi.org/10.1016/j.biortech.2013.02.085

Großeholz, R., Koh, C.-C., Veith, N., Fiedler, T., Strauss, M., Olivier, B., Collins, B. C., Schubert, O. T., Bergmann, F., Kreikemeyer, B., Aebersold, R., & Kummer, U. (2016). Integrating highly quantitative proteomics and genome-scale metabolic modeling to study pH adaptation in the human pathogen *Enterococcus faecalis*. *Npj Systems Biology and Applications*, *2*, Article 16017. https://doi.org/10.1038/npjsba.2016.17

Gu, C., Kim, G. B., Kim, W. J., Kim, H. U., & Lee, S. Y. (2019). Current status and applications of genome-scale metabolic models. *Genome Biology*, *20*, Article 212. https://doi.org/10.1186/s13059-019-1730-3

Guiot, S. R., Cimpoia, R., & Carayon, G. (2011). Potential of wastewater-treating anaerobic granules for biomethanation of synthesis gas. *Environmental Science & Technology*, *45*, 2006–2012. https://doi.org/10.1021/es102728m

Haas, T., Krause, R., Weber, R., Demler, M., & Schmid, G. (2018). Technical photosynthesis involving CO_2 electrolysis and fermentation. *Nature Catalysis*, *1*, 32–39. https://doi.org/10.1038/s41929-017-0005-1

Hanemaaijer, M., Olivier, B. G., Röling, W. F. M., Bruggeman, F. J., & Teusink, B. (2017). Model-based quantification of metabolic interactions from dynamic microbial-community data. *PLOS ONE*, *12*(3), Article e0173183. https://doi.org/10.1371/journal.pone.0173183

Hanemaaijer, M., Röling, W. F. M., Olivier, B. G., Khandelwal, R. A., Teusink, B., & Bruggeman, F. J. (2015). Systems modeling approaches for microbial community studies: From metagenomics to inference of the community structure. *Frontiers in Microbiology*, *6*, Article 213. https://doi.org/doi: 10.3389/fmicb.2015.00213

He, P., Han, W., Shao, L., & Lü, F. (2018). One-step production of C6–C8 carboxylates by mixed culture solely grown on CO. *Biotechnology for Biofuels*, *11*, Article 4. https://doi.org/10.1186/s13068-017-1005-8

Heffernan, J. K., Mahamkali, V., Valgepea, K., Marcellin, E., & Nielsen, L. K. (2022). Analytical tools for unravelling the metabolism of gas-fermenting Clostridia. *Current Opinion in Biotechnology*, *75*, Article 102700. https://doi.org/10.1016/j.copbio.2022.102700

Heffernan, J. K., Valgepea, K., de Souza Pinto Lemgruber, R., Casini, I., Plan, M., Tappel, R., Simpson, S. D., Köpke, M., Nielsen, L. K., & Marcellin, E. (2020). Enhancing CO_2-valorization using *Clostridium autoethanogenum* for sustainable fuel and chemicals production. *Frontiers in Bioengineering and Biotechnology*, *8*, Article 204. https://www.frontiersin.org/articles/10.3389/fbioe.2020.00204

Henry, C. S., DeJongh, M., Best, A. A., Frybarger, P. M., Linsay, B., & Stevens, R. L. (2010). High-throughput generation, optimization and analysis of genome-scale metabolic models. *Nature Biotechnology*, *28*(9), Article 9. https://doi.org/10.1038/nbt.1672

Herrero, A. A., Gomez, R. F., Snedecor, B., Tolman, C. J., & Roberts, M. F. (1985). Growth inhibition of *Clostridium thermocellum* by carboxylic acids: A mechanism based on uncoupling by weak acids. *Applied Microbiology and Biotechnology*, *22*(1), 53–62. https://doi.org/10.1007/BF00252157

Herrmann, H. A., Dyson, B. C., Vass, L., Johnson, G. N., & Schwartz, J.-M. (2019). Flux sampling is a powerful tool to study metabolism under changing environmental conditions. *Npj Systems Biology and Applications*, *5*(1), Article 1. https://doi.org/10.1038/s41540-019-0109-0

Hess, V., Oyrik, O., Trifunović, D., & Müller, V. (2015). 2,3-Butanediol metabolism in the acetogen *Acetobacterium woodii*. *Applied and Environmental Microbiology*, *81*(14), 4711–4719. https://doi.org/10.1128/AEM.00960-15

Hetzel, M., Brock, M., Selmer, T., Pierik, A. J., Golding, B. T., & Buckel, W. (2003). Acryloyl-CoA reductase from *Clostridium propionicum*: An enzyme complex of propionyl-CoA dehydrogenase and electron-transferring flavoprotein. *European Journal of Biochemistry*, *270*, 902–910. https://doi.org/10.1046/j.1432-1033.2003.03450.x

Holtzapple, M. T., & Granda, C. B. (2009). Carboxylate platform: The MixAlco process part 1: Comparison of three biomass conversion platforms. *Applied Biochemistry and Biotechnology*, *156*, 95–106. https://doi.org/10.1007/s12010-008-8466-y

Hoornweg, D., Bhada-Tata, P., & Kennedy, C. (2013). Environment: Waste production must peak this century. *Nature*, *502*(7473), 615–617. https://doi.org/10.1038/502615a

Hu, P., Chakraborty, S., Kumar, A., Woolston, B., Liu, H., Emerson, D., & Stephanopoulos, G. (2016). Integrated bioprocess for conversion of gaseous substrates to liquids. *Proceedings of the National Academy of Sciences*, *113*, 3773–3778. https://doi.org/10.1073/pnas.1516867113

Hucka, M., Bergmann, F. T., Hoops, S., Keating, S. M., Sahle, S., Schaff, J. C., Smith, L. P., & Wilkinson, D. J. (2015). The Systems Biology Markup Language (SBML): Language Specification for Level 3 Version 1 Core. *Journal of Integrative Bioinformatics*, *12*(2), 382–549. https://doi.org/10.1515/jib-2015-266

Huerta-Cepas, J., Forslund, K., Coelho, L. P., Szklarczyk, D., Jensen, L. J., von Mering, C., & Bork, P. (2017). Fast genome-wide functional annotation through orthology assignment by eggNOG-mapper. *Molecular Biology and Evolution*, *34*(8), 2115–2122. https://doi.org/10.1093/molbev/msx148

Humphreys, C. M., McLean, S., Schatschneider, S., Millat, T., Henstra, A. M., Annan, F. J., Breitkopf, R., Pander, B., Piatek, P., Rowe, P., Wichlacz, A. T., Woods, C., Norman, R., Blom, J., Goesman, A., Hodgman, C., Barrett, D., Thomas, N. R., Winzer, K., & Minton, N. P. (2015). Whole genome sequence and manual annotation of Clostridium autoethanogenum, an industrially relevant bacterium. *BMC Genomics*, *16*, Article 1085. https://doi.org/10.1186/s12864-015-2287-5

R

REFERENCES

Humphreys, C. M., & Minton, N. P. (2018). Advances in metabolic engineering in the microbial production of fuels and chemicals from C1 gas. *Current Opinion in Biotechnology*, *50*, 174–181. https://doi.org/10.1016/j.copbio.2017.12.023

Hwang, H. W., Yoon, J., Min, K., Kim, M.-S., Kim, S.-J., Cho, D. H., Susila, H., Na, J.-G., Oh, M.-K., & Kim, Y. H. (2020). Two-stage bioconversion of carbon monoxide to biopolymers via formate as an intermediate. *Chemical Engineering Journal*, *389*, Article 124394. https://doi.org/10.1016/j.cej.2020.124394

Ibrahim, M., Raajaraam, L., & Raman, K. (2021). Modelling microbial communities: Harnessing consortia for biotechnological applications. *Computational and Structural Biotechnology Journal*, *19*, 3892–3907. https://doi.org/10.1016/j.csbj.2021.06.048

Innard, N., & Chong, J. P. J. (2022). The challenges of monitoring and manipulating anaerobic microbial communities. *Bioresource Technology*, *344*, Article 126326. https://doi.org/10.1016/j.biortech.2021.126326

Intergovernmental Panel on Climate Change. (2018). *Global Warming of 1.5°C. An IPCC Special Report on the impacts of global warming of 1.5°C above pre-industrial levels and related global greenhouse gas emission pathways, in the context of strengthening the global response to the threat of climate change, sustainable development, and efforts to eradicate poverty.*

Intergovernmental Panel on Climate Change. (2023). *Summary for policymakers. In: Climate Change 2023: Synthesis report. A report of the Intergovernmental Panel on Climate Change. Contribution of working groups I, I and III to the Sixth Assessment report of the Intergovernmental Panel on Climate Change.* https://www.ipcc.ch/report/ar6/syr/downloads/report/IPCC_AR6_SYR_SPM.pdf

International Energy Agency. (2018). *The future of petrochemicals.* https://www.iea.org/reports/the-future-of-petrochemicals

International Energy Agency. (2023). *Chemicals.* https://www.iea.org/energy-system/industry/chemicals

Isom, C. E., Nanny, M. A., & Tanner, R. S. (2015). Improved conversion efficiencies for n-fatty acid reduction to primary alcohols by the solventogenic acetogen "*Clostridium ragsdalei*". *Journal of Industrial Microbiology and Biotechnology*, *42*(1), 29–38. https://doi.org/10.1007/s10295-014-1543-z

Johns, N. I., Blazejewski, T., Gomes, A. L., & Wang, H. H. (2016). Principles for designing synthetic microbial communities. *Current Opinion in Microbiology*, *31*, 146–153. https://doi.org/10.1016/j.mib.2016.03.010

Joseph, R. C., Kim, N. M., & Sandoval, N. R. (2018). Recent developments of the synthetic biology toolkit for *Clostridium*. *Frontiers in Microbiology*, *9*, Article 154. https://doi.org/10.3389/fmicb.2018.00154

Kabimoldayev, I., Nguyen, A. D., Yang, L., Park, S., Lee, E. Y., & Kim, D. (2018). Basics of genome-scale metabolic modeling and applications on C1-utilization. *FEMS Microbiology Letters*, *365*(20), Article fny241. https://doi.org/10.1093/femsle/fny241

Kamp, F., & Hamilton, J. A. (2006). How fatty acids of different chain length enter and leave cells by free diffusion. *Prostaglandins, Leukotrienes and Essential Fatty Acids*, *75*, 149–159. https://doi.org/10.1016/J.PLEFA.2006.05.003

Karlson, B., Bellavitis, C., & France, N. (2021). Commercializing LanzaTech, from waste to fuel: An effectuation case. *Journal of Management & Organization*, *27*(1), 175–196. https://doi.org/10.1017/jmo.2017.83

Karp, P. D., Riley, M., Paley, S. M., & Pellegrini-Toole, A. (2002). The MetaCyc database. *Nucleic Acids Research*, *30*(1), 59–61. https://doi.org/10.1093/nar/30.1.59

Kätelhön, A., Meys, R., Deutz, S., Suh, S., & Bardow, A. (2019). Climate change mitigation potential of carbon capture and utilization in the chemical industry. *PNAS*, *116*(23), 11187–11194. https://doi.org/10.1073/pnas.1821029116

Katsyv, A., & Müller, V. (2020). Overcoming energetic barriers in acetogenic C1 conversion. *Frontiers in Bioengineering and Biotechnology*, *8*, Article 621166. https://doi.org/10.3389/fbioe.2020.621166

Kawaguchi, H., Hasunuma, T., Ogino, C., & Kondo, A. (2016). Bioprocessing of bio-based chemicals produced from lignocellulosic feedstocks. *Current Opinion in Biotechnology*, *42*, 30–39. https://doi.org/10.1016/j.copbio.2016.02.031

Kenealy, W. R., & Waselefsky, D. M. (1985). Studies on the substrate range of *Clostridium kluyveri*; the use of propanol and succinate. *Archives of Microbiology*, *141*, 187–194. https://doi.org/10.1007/BF00408056

Khandelwal, R. A., Olivier, B. G., Röling, W. F. M., Teusink, B., & Bruggeman, F. J. (2013). Community flux balance analysis for microbial consortia at balanced growth. *PLOS ONE*, *8*(5), Article e64567. https://doi.org/10.1371/journal.pone.0064567

Kim, B. H., Bellows, P., Datta, R., & Zeikus, J. G. (1984). Control of carbon and electron flow in *Clostridium acetobutylicum* fermentations: Utilization of carbon monoxide to inhibit hydrogen production and to enhance butanol yields. *Applied and Environmental Microbiology*, *48*, 764–770. https://doi.org/10.1128/aem.48.4.764-770.1984

Kim, J., Lim, J., & Lee, C. (2013). Quantitative real-time PCR approaches for microbial community studies in wastewater treatment systems: Applications and considerations. *Biotechnology Advances*, *31*, 1358–1373. https://doi.org/10.1016/J.BIOTECHADV.2013.05.010

Kim, O. D., Rocha, M., & Maia, P. (2018). A review of dynamic modeling approaches and their application in computational strain optimization for metabolic engineering. *Frontiers in Microbiology*, *9*. https://www.frontiersin.org/articles/10.3389/fmicb.2018.01690

Kim, S. A., & Rhee, M. S. (2013). Marked synergistic bactericidal effects and mode of action of medium-chain fatty acids in combination with organic acids against *Escherichia coli* O157:H7. *Applied and Environmental Microbiology*, *79*, 6552–6560. https://doi.org/10.1128/AEM.02164-13

Kim, S., Lindner, S. N., Aslan, S., Yishai, O., Wenk, S., Schann, K., & Bar-Even, A. (2020). Growth of *E. coli* on formate and methanol via the reductive glycine pathway. *Nature Chemical Biology*, *16*, 538–545. https://doi.org/10.1038/s41589-020-0473-5

King, G. M., & Weber, C. F. (2007). Distribution, diversity and ecology of aerobic CO-oxidizing bacteria. *Nature Reviews Microbiology*, *5*, 107–118. https://doi.org/10.1038/nrmicro1595

Klasson, K. T., Cowger, J. P., Ko, C. W., Vega, J. L., Clausen, E. C., & Gaddy, J. L. (1990). Methane production from synthesis gas using a mixed culture of *R. rubrum*, *M. barkeri* and *M. formicicum*. *Applied Biochemistry and Biotechnology*, *24–25*, 317–328. https://doi.org/10.1007/BF02920256

Kliefoth, M., Langer, J. D., Matschiavelli, N., Oelgeschläger, E., & Rother, M. (2012). Genetic analysis of MA4079, an aldehyde dehydrogenase homolog, in *Methanosarcina acetivorans*. *Archives of Microbiology*, *194*, 75–85. https://doi.org/10.1007/s00203-011-0727-4

Koch, S., Kohrs, F., Lahmann, P., Bissinger, T., Wendschuh, S., Benndorf, D., Reichl, U., & Klamt, S. (2019). RedCom: A strategy for reduced metabolic modeling of complex microbial communities and its application for analyzing experimental datasets from anaerobic digestion. *PLOS Computational Biology*, *15*(2), e1006759. https://doi.org/10.1371/journal.pcbi.1006759

Kohlmayer, M., Huber, R., Brotsack, R., & Mayer, W. (2018). *Simultaneous CO_2 and CO methanation using microbes* (326561). Article 326561. https://doi.org/10.1101/326561

Köpke, M., Mihalcea, C., Bromley, J. C., & Simpson, S. D. (2011). Fermentative production of ethanol from carbon monoxide. *Current Opinion in Biotechnology*, *22*, 320–325. https://doi.org/10.1016/j.copbio.2011.01.005

Köpke, M., & Simpson, S. D. (2020). Pollution to products: Recycling of 'above ground' carbon by gas fermentation. *Current Opinion in Biotechnology*, *65*, 180–189. https://doi.org/10.1016/j.copbio.2020.02.017

Koskinen, P., Deptula, P., Smolander, O.-P., Tamene, F., Kammonen, J., Savijoki, K., Paulin, L., Piironen, V., Auvinen, P., & Varmanen, P. (2015). Complete genome sequence of *Propionibacterium freudenreichii* DSM 20271[T]. *Standards in Genomic Sciences*, *10*, Article 83. https://doi.org/10.1186/s40793-015-0082-1

Kucek, L. A., Spirito, C. M., & Angenent, L. T. (2016). High n-caprylate productivities and specificities from dilute ethanol and acetate: Chain elongation with microbiomes to upgrade products from syngas fermentation. *Energy & Environmental Science*, *9*, 3482–3494. https://doi.org/10.1039/c6ee01487a

Laanbroek, H. J., Abee, T., & Voogd, I. L. (1982). Alcohol conversion by *Desulfobulbus propionicus* Lindhorst in the presence and absence of sulfate and hydrogen. *Archives of Microbiology*, *133*, 178–184. https://doi.org/10.1007/BF00414998

Lagoa-Costa, B., Abubackar, H. N., Fernández-Romasanta, M., Kennes, C., & Veiga, M. C. (2017). Integrated bioconversion of syngas into bioethanol and biopolymers. *Bioresource Technology*, *239*, 244–249. https://doi.org/10.1016/j.biortech.2017.05.019

REFERENCES

Lauer, I., Philipps, G., & Jennewein, S. (2022). Metabolic engineering of *Clostridium ljungdahlii* for the production of hexanol and butanol from CO_2 and H_2. *Microbial Cell Factories*, *21*, Article 85. https://doi.org/10.1186/s12934-022-01802-8

Laura, M., & Jo, P. (2023). No acetogen is equal: Strongly different H_2 thresholds reflect diverse bioenergetics in acetogenic bacteria. *Environmental Microbiology*, 1–9. https://doi.org/10.1111/1462-2920.16429

Lawson, C. E., Harcombe, W. R., Hatzenpichler, R., Lindemann, S. R., Löffler, F. E., O'Malley, M. A., García Martín, H., Pfleger, B. F., Raskin, L., Venturelli, O. S., Weissbrodt, D. G., Noguera, D. R., & McMahon, K. D. (2019). Common principles and best practices for engineering microbiomes. *Nature Reviews Microbiology*, *17*, 725–741. https://doi.org/10.1038/s41579-019-0255-9

Lee, C. R., Kim, C., Song, Y. E., Im, H., Oh, Y.-K., Park, S., & Kim, J. R. (2018). Co-culture-based biological carbon monoxide conversion by *Citrobacter amalonaticus* Y19 and *Sporomusa ovata* via a reducing-equivalent transfer mediator. *Bioresource Technology*, *259*, 128–135. https://doi.org/10.1016/j.biortech.2018.02.129

Lee, H., Bae, J., Jin, S., Kang, S., & Cho, B.-K. (2022). Engineering acetogenic bacteria for efficient one-Carbon utilization. *Frontiers in Microbiology*, *13*, Article 865168. https://doi.org/10.3389/fmicb.2022.865168

Lee, J. (2021). Lessons from Clostridial genetics: Toward engineering acetogenic bacteria. *Biotechnology and Bioprocess Engineering*, *26*, 841–858. https://doi.org/10.1007/s12257-021-0062-9

Lee, J., Yun, H., Feist, A. M., Palsson, B. Ø., & Lee, S. Y. (2008). Genome-scale reconstruction and in silico analysis of the *Clostridium acetobutylicum* ATCC 824 metabolic network. *Applied Microbiology and Biotechnology*, *80*(5), 849–862. https://doi.org/10.1007/s00253-008-1654-4

Lee, R. A., & Lavoie, J. M. (2013). From first- to third-generation biofuels: Challenges of producing a commodity from a biomass of increasing complexity. *Animal Frontiers*, *3*(2), 6–11. https://doi.org/10.2527/af.2013-0010

Leng, L., Yang, P., Singh, S., Zhuang, H., Xu, L., Chen, W.-H., Dolfing, J., Li, D., Zhang, Y., Zeng, H., Chu, W., & Lee, P.-H. (2018). A review on the bioenergetics of anaerobic microbial metabolism close to the thermodynamic limits and its implications for digestion applications. *Bioresource Technology*, *247*, 1095–1106. https://doi.org/10.1016/j.biortech.2017.09.103

Li, C., Zhu, X., & Angelidaki, I. (2020). Carbon monoxide conversion and syngas biomethanation mediated by different microbial consortia. *Bioresource Technology*, *314*, Article 123739. https://doi.org/10.1016/j.biortech.2020.123739

Li, X., & Henson, M. A. (2019). Metabolic modeling of bacterial co-culture systems predicts enhanced carbon monoxide-to-butyrate conversion compared to monoculture systems. *Biochemical Engineering Journal*, *151*, Article 107338. https://doi.org/10.1016/j.bej.2019.107338

Li, X., & Henson, M. A. (2021). Dynamic metabolic modeling predicts efficient acetogen-gut bacterium cocultures for CO-to-butyrate conversion. *Journal of Applied Microbiology*, *131*(6), 2899–2917. https://doi.org/10.1111/jam.15155

Liang, J., Huang, H., & Wang, S. (2019). Distribution, evolution, catalytic mechanism, and physiological functions of the flavin-based electron-bifurcating NADH-dependent reduced ferredoxin: $NADP^+$ oxidoreductase. *Frontiers in Microbiology*, *10*, Article 373. https://doi.org/10.3389/fmicb.2019.00373

Liao, M. J., Din, M. O., Tsimring, L., & Hasty, J. (2019). Rock-paper-scissors: Engineered population dynamics increase genetic stability. *Science*, *365*, 1045–1049. https://doi.org/10.1126/science.aaw0542

Lieven, C., Beber, M. E., Olivier, B. G., Bergmann, F. T., Ataman, M., Babaei, P., Bartell, J. A., Blank, L. M., Chauhan, S., Correia, K., Diener, C., Dräger, A., Ebert, B. E., Edirisinghe, J. N., Faria, J. P., Feist, A. M., Fengos, G., Fleming, R. M. T., García-Jiménez, B., ... Zhang, C. (2020). MEMOTE for standardized genome-scale metabolic model testing. *Nature Biotechnology*, *38*(3), Article 3. https://doi.org/10.1038/s41587-020-0446-y

Liew, F. E., Martin, M. E., Tappel, R. C., Heijstra, B. D., Mihalcea, C., & Köpke, M. (2016). Gas fermentation—A flexible platform for commercial scale production of low-carbon-fuels and chemicals from waste and renewable feedstocks. *Frontiers in Microbiology*, *7*, Article 694. https://doi.org/10.3389/fmicb.2016.00694

Liew, F. E., Nogle, R., Abdalla, T., Rasor, B. J., Canter, C., Jensen, R. O., Wang, L., Strutz, J., Chirania, P., De Tissera, S., Mueller, A. P., Ruan, Z., Gao, A., Tran, L., Engle, N. L., Bromley, J. C., Daniell, J., Conrado, R., Tschaplinski, T. J., ... Köpke, M. (2022). Carbon-negative production of acetone and isopropanol by gas fermentation at industrial pilot scale. *Nature Biotechnology*, *40*(3), 335–344. https://doi.org/10.1038/s41587-021-01195-w

Liou, J. S.-C., Balkwill, D. L., Drake, G. R., & Tanner, R. S. (2005). *Clostridium carboxidivorans* sp. Nov., a solvent-producing clostridium isolated from an agricultural settling lagoon, and reclassification of the acetogen *Clostridium scatologenes* strain SL1 as *Clostridium drakei* sp. Nov. *International Journal of Systematic and Evolutionary Microbiology*, *55*(5), 2085–2091. https://doi.org/10.1099/ijs.0.63482-0

Liu, K., Atiyeh, H. K., Stevenson, B. S., Tanner, R. S., Wilkins, M. R., & Huhnke, R. L. (2014a). Continuous syngas fermentation for the production of ethanol, n-propanol and n-butanol. *Bioresource Technology*, *151*, 69–77. https://doi.org/10.1016/j.biortech.2013.10.059

Liu, K., Atiyeh, H. K., Stevenson, B. S., Tanner, R. S., Wilkins, M. R., & Huhnke, R. L. (2014b). Mixed culture syngas fermentation and conversion of carboxylic acids into alcohols. *Bioresource Technology*, *152*, 337–346. https://doi.org/10.1016/j.biortech.2013.11.015

Liu, Z., Wang, K., Chen, Y., Tan, T., & Nielsen, J. (2020a). Third-generation biorefineries as the means to produce fuels and chemicals from CO_2. *Nature Catalysis*, *3*(3), Article 3. https://doi.org/10.1038/s41929-019-0421-5

Liu, Z.-Y., Jia, D.-C., Zhang, K.-D., Zhu, H.-F., Zhang, Q., Jiang, W.-H., Gu, Y., & Li, F.-L. (2020b). Ethanol metabolism dynamics in *Clostridium ljungdahlii* grown on carbon monoxide. *Applied and Environmental Microbiology*, *86*(14), Article e00730-20. https://doi.org/10.1128/AEM.00730-20

Lo, J., Humphreys, J. R., Magnusson, L., Wachter, B., Urban, C., Hebdon, S. D., Xiong, W., Chou, K. J., & Ching Maness, P. (2022). Acetogenic production of 3-hydroxybutyrate using a native 3-hydroxybutyryl-CoA dehydrogenase. *Frontiers in Microbiology*, *13*, Article 948369. https://doi.org/10.3389/fmicb.2022.948369

Luo, G., Jing, Y., Lin, Y., Zhang, S., & An, D. (2018). A novel concept for syngas biomethanation by two-stage process: Focusing on the selective conversion of syngas to acetate. *Science of The Total Environment*, *645*, 1194–1200. https://doi.org/10.1016/j.scitotenv.2018.07.263

Luo, G., Wang, W., & Angelidaki, I. (2013). Anaerobic digestion for simultaneous sewage sludge treatment and CO biomethanation: Process performance and microbial ecology. *Environmental Science & Technology*, *47*(18), 10685–10693. https://doi.org/10.1021/es401018d

Ma, S., Luo, R., Gold, J. I., Yu, A. Z., Kim, B., & Kenis, P. J. A. (2016). Carbon nanotube containing Ag catalyst layers for efficient and selective reduction of carbon dioxide. *Journal of Materials Chemistry A*, *4*, 8573–8578. https://doi.org/10.1039/c6ta00427j

Maerker, C., Rohde, M., Brakhage, A. A., & Brock, M. (2005). Methylcitrate synthase from *Aspergillus fumigatus*. *The FEBS Journal*, *272*(14), 3615–3630. https://doi.org/10.1111/j.1742-4658.2005.04784.x

Martin, K. J., & Nerenberg, R. (2012). The membrane biofilm reactor (MBfR) for water and wastewater treatment: Principles, applications, and recent developments. *Bioresource Technology*, *122*, 83–94. https://doi.org/10.1016/j.biortech.2012.02.110

Martin, M. E., Richter, H., Saha, S., & Angenent, L. T. (2016). Traits of selected *Clostridium* strains for syngas fermentation to ethanol. *Biotechnology and Bioengineering*, *113*, 531–539. https://doi.org/10.1002/bit.25827

Maruyama, K., & Kitamura, H. (1985). Mechanisms of growth inhibition by propionate and restoration of the growth by sodium bicarbonate or acetate in *Rhodopseudomonas sphaeroides* S. *The Journal of Biochemistry*, *98*, 819–824. https://doi.org/10.1093/oxfordjournals.jbchem.a135340

McCarty, N. S., & Ledesma-Amaro, R. (2019). Synthetic biology tools to engineer microbial communities for biotechnology. *Trends in Biotechnology*, *37*(2), 181–197. https://doi.org/10.1016/j.tibtech.2018.11.002

McGlade, C., & Ekins, P. (2015). The geographical distribution of fossil fuels unused when limiting global warming to 2°C. *Nature*, *517*, 187–190. https://doi.org/10.1038/nature14016

R

REFERENCES

Messias, S., Sousa, M. M., Nunes da Ponte, M., Rangel, C. M., Pardal, T., & Reis Machado, A. S. (2019). Electrochemical production of syngas from CO_2 at pressures up to 30 bar in electrolytes containing ionic liquid. *Reaction Chemistry & Engineering*, *4*, 1982–1990. https://doi.org/10.1039/C9RE00271E

Milne, C. B., Eddy, J. A., Raju, R., Ardekani, S., Kim, P.-J., Senger, R. S., Jin, Y.-S., Blaschek, H. P., & Price, N. D. (2011). Metabolic network reconstruction and genome-scale model of butanol-producing strain *Clostridium beijerinckii* NCIMB 8052. *BMC Systems Biology*, *5*, Article 130. https://doi.org/10.1186/1752-0509-5-130

Moazeni, F., Zhang, G., & Sun, H. J. (2010). Imperfect asymmetry of life: Earth microbial communities prefer D-lactate but can use L-lactate also. *Astrobiology*, *10*, 397–402. https://doi.org/10.1089/ast.2009.0438

Mock, J., Zheng, Y., Mueller, A. P., Ly, S., Tran, L., Segovia, S., Nagaraju, S., Köpke, M., Dürre, P., & Thauer, R. K. (2015). Energy conservation associated with ethanol formation from H_2 and CO_2 in *Clostridium autoethanogenum* involving electron bifurcation. *Journal of Bacteriology*, *197*, 2965–2980. https://doi.org/10.1128/JB.00399-15

Molitor, B., Marcellin, E., & Angenent, L. T. (2017). Overcoming the energetic limitations of syngas fermentation. *Current Opinion in Chemical Biology*, *41*, 84–92. https://doi.org/10.1016/j.cbpa.2017.10.003

Molitor, B., Richter, H., Martin, M. E., Jensen, R. O., Juminaga, A., Mihalcea, C., & Angenent, L. T. (2016). Carbon recovery by fermentation of CO-rich off gases – Turning steel mills into biorefineries. *Bioresource Technology*, *215*, 386–396. https://doi.org/10.1016/j.biortech.2016.03.094

Moreira, J. P. C., Diender, M., Arantes, A. L., Boeren, S., Stams, A. J. M., Alves, M. M., Alves, J. I., & Sousa, D. Z. (2021). Propionate production from carbon monoxide by synthetic cocultures of *Acetobacterium wieringae* and propionigenic bacteria. *Applied and Environmental Microbiology*, *87*(14), Article e02839-20. https://doi.org/10.1128/AEM.02839-20

Moreira, J. P. C., Heap, J. T., Alves, J. I., & Domingues, L. (2023). Developing a genetic engineering method for *Acetobacterium wieringae* to expand one-carbon valorization pathways. *Biotechnology for Biofuels and Bioproducts*, *16*, Article 24. https://doi.org/10.1186/s13068-023-02259-6

Moreno-Gonzalez, M., Berger, A., Borsboom-Hanson, T., & Mérida, W. (2021). Carbon-neutral fuels and chemicals: Economic analysis of renewable syngas pathways via CO_2 electrolysis. *Energy Conversion and Management*, *244*, Article 114452. https://doi.org/10.1016/j.enconman.2021.114452

Moreno-Paz, S., Schmitz, J., Martins dos Santos, V. A. P., & Suarez-Diez, M. (2022). Enzyme-constrained models predict the dynamics of *Saccharomyces cerevisiae* growth in continuous, batch and fed-batch bioreactors. *Microbial Biotechnology*, *15*(5), 1434–1445. https://doi.org/10.1111/1751-7915.13995

Morris, J. J., Lenski, R. E., & Zinser, E. R. (2012). The Black Queen hypothesis: Evolution of dependencies through adaptive gene loss. *mBio*, *3*(2), Article e00036-12. https://doi.org/10.1128/mBio.00036-12

Moscoviz, R., Trably, E., Bernet, N., & Carrère, H. (2018). The environmental biorefinery: State-of-the-art on the production of hydrogen and value-added biomolecules in mixed-culture fermentation. *Green Chemistry*, *20*(14), 3159–3179. https://doi.org/10.1039/C8GC00572A

Nagarajan, H., Sahin, M., Nogales, J., Latif, H., Lovley, D. R., Ebrahim, A., & Zengler, K. (2013). Characterizing acetogenic metabolism using a genome-scale metabolic reconstruction of *Clostridium ljungdahlii*. *Microbial Cell Factories*, *12*, 1–13. https://doi.org/10.1186/1475-2859-12-118

Nam, C. W., Jung, K. A., & Park, J. M. (2016). Biological carbon monoxide conversion to acetate production by mixed culture. *Bioresource Technology*, *211*, 478–485. https://doi.org/10.1016/j.biortech.2016.03.100

Navone, L., McCubbin, T., Gonzalez-Garcia, R. A., Nielsen, L. K., & Marcellin, E. (2018). Genome-scale model guided design of *Propionibacterium* for enhanced propionic acid production. *Metabolic Engineering Communications*, *6*, 1–12. https://doi.org/10.1016/j.meteno.2017.11.001

Novaes, R. F. V. (1986). Microbiology of anaerobic digestion. *Water Science and Technology*, *18*, 1–14. https://doi.org/10.2166/wst.1986.0159

O'Brien, J. M., Wolkin, R. H., Moench, T. T., Morgan, J. B., & Zeikus, J. G. (1984). Association of hydrogen metabolism with unitrophic or mixotrophic growth of *Methanosarcina barkeri* on carbon monoxide. *Journal of Bacteriology*, *158*, 373–375. https://doi.org/10.1128/JB.158.1.373-375.1984

Ogata, H., Goto, S., Sato, K., Fujibuchi, W., Bono, H., & Kanehisa, M. (1999). KEGG: Kyoto Encyclopedia of Genes and Genomes. *Nucleic Acids Research*, *27*(1), 29–34. https://doi.org/10.1093/nar/27.1.29

Oh, H. J., Gong, G., Ahn, J. H., Ko, J. K., Lee, S.-M., & Um, Y. (2023). Effective hexanol production from carbon monoxide using extractive fermentation with *Clostridium carboxidivorans* P7. *Bioresource Technology*, *367*. https://doi.org/10.1016/j.biortech.2022.128201

Orth, J. D., Thiele, I., & Palsson, B. O. (2010). What is flux balance analysis? *Nature Biotechnology*, *28*, 245–248. https://doi.org/10.1038/nbt.1614

Oswald, F., Dörsam, S., Veith, N., Zwick, M., Neumann, A., Ochsenreither, K., & Syldatk, C. (2016). Sequential mixed cultures: From syngas to malic acid. *Frontiers in Microbiology*, *7*, Article 891. https://doi.org/10.3389/fmicb.2016.00891

Pacheco, A. R., Moel, M., & Segrè, D. (2019). Costless metabolic secretions as drivers of interspecies interactions in microbial ecosystems. *Nature Communications*, *10*, Article 103. https://doi.org/10.1038/s41467-018-07946-9

Pagani, I., Lapidus, A., Nolan, M., Lucas, S., Hammon, N., Desh-Pande, S., Cheng, J. F., Chertkov, O., Davenport, K., Tapia, R., Han, C., Goodwin, L., Pitluck, S., Liolios, K., Mavromatis, K., Ivanova, N., Mikhailova, N., Pati, A., Chen, A., ... Klenk, H. P. (2011). Complete genome sequence of *Desulfobulbus propionicus* type strain (1pr3T). *Standards in Genomic Sciences*, *4*, 100–110. https://doi.org/10.4056/sigs.1613929

Parera Olm, I., & Sousa, D. Z. (2021). Conversion of carbon monoxide to chemicals using microbial consortia. In A.-P. Zeng & N. J. Claassens (Eds.), *One-Carbon Feedstocks for Sustainable Bioproduction* (Vol. 180, pp. 373–407). Springer International Publishing. https://doi.org/10.1007/10_2021_180

Parera Olm, I., & Sousa, D. Z. (2023). Upgrading dilute ethanol to odd-chain carboxylic acids by a synthetic co-culture of *Anaerotignum neopropionicum* and *Clostridium kluyveri*. *Biotechnology for Biofuels and Bioproducts*, *16*, Article 83. https://doi.org/10.1186/s13068-023-02336-w

Parizzi, L. P., Grassi, M. C. B., Llerena, L. A., Carazzolle, M. F., Queiroz, V. L., Lunardi, I., Zeidler, A. F., Teixeira, P. J. P. L., Mieczkowski, P., Rincones, J., & Pereira, G. A. G. (2012). The genome sequence of *Propionibacterium acidipropionici* provides insights into its biotechnological and industrial potential. *BMC Genomics*, *13*, Article 562. https://doi.org/10.1186/1471-2164-13-562

Park, S., Yasin, M., Kim, D., Park, H.-D., Kang, C. M., Kim, D. J., & Chang, I. S. (2013). Rapid enrichment of (homo)acetogenic consortia from animal feces using a high mass-transfer gas-lift reactor fed with syngas. *Journal of Industrial Microbiology and Biotechnology*, *40*, 995–1003. https://doi.org/10.1007/s10295-013-1292-4

Pereira, F. M. (2014). *Intensified bioprocess for the anaerobic conversion of syngas to biofuels*. Universidade do Minho.

Perez, J. M., Richter, H., Loftus, S. E., & Angenent, L. T. (2013). Biocatalytic reduction of short-chain carboxylic acids into their corresponding alcohols with syngas fermentation. *Biotechnology and Bioengineering*, *110*, 1066–1077. https://doi.org/10.1002/bit.24786

Phillips, J. R., Atiyeh, H. K., Tanner, R. S., Torres, J. R., Saxena, J., Wilkins, M. R., & Huhnke, R. L. (2015). Butanol and hexanol production in *Clostridium carboxidivorans* syngas fermentation: Medium development and culture techniques. *Bioresource Technology*, *190*, 114–121. https://doi.org/10.1016/j.biortech.2015.04.043

Phillips, J. R., Klasson, K. T., Clausen, E. C., & Gaddy, J. L. (1993). Biological production of ethanol from coal synthesis gas. *Applied Biochemistry and Biotechnology*, *39–40*, 559–571. https://doi.org/10.1007/BF02919018

Pinto, T., Flores-Alsina, X., Gernaey, K. V., & Junicke, H. (2021). Alone or together? A review on pure and mixed microbial cultures for butanol production. *Renewable and Sustainable Energy Reviews*, *147*, Article 111244. https://doi.org/10.1016/j.rser.2021.111244

Piwowarek, K., Lipińska, E., Hać-Szymańczuk, E., Kieliszek, M., & Ścibisz, I. (2018). *Propionibacterium* spp.—Source of propionic acid, vitamin B12, and other metabolites important for the industry. *Applied Microbiology and Biotechnology*, *102*, 515–538. https://doi.org/10.1007/s00253-017-8616-7

Poehlein, A., Schlien, K., Chowdhury, N. P., Gottschalk, G., Buckel, W., & Daniel, R. (2016). Complete genome sequence of the amino acid-fermenting *Clostridium propionicum* X2 (DSM 1682). *Genome Announcements*, *4*(2), Article e00294-16. https://doi.org/10.1128/genomea.00294-16

R

REFERENCES

Popp, J., Lakner, Z., Harangi-Rákos, M., & Fári, M. (2014). The effect of bioenergy expansion: Food, energy, and environment. *Renewable and Sustainable Energy Reviews*, *32*, 559–578. https://doi.org/10.1016/j.rser.2014.01.056

Qiao, W., Xu, S., Liu, Z., Fu, X., Zhao, H., & Shi, S. (2022). Challenges and opportunities in C1-based biomanufacturing. *Bioresource Technology*, *364*, Article 128095. https://doi.org/10.1016/j.biortech.2022.128095

Ranaei, V., Pilevar, Z., Mousavi Khaneghah, A., & Hosseini, H. (2020). Propionic acid: Method of production, current state and perspectives. *Food Technology and Biotechnology*, *58*, 115–127. https://doi.org/10.17113/ftb.58.02.20.6356

Rangarajan, E. S., Li, Y., Ajamian, E., Iannuzzi, P., Kernaghan, S. D., Fraser, M. E., Cygler, M., & Matte, A. (2005). Crystallographic trapping of the glutamyl-CoA thioester intermediate of family I CoA transferases. *Journal of Biological Chemistry*, *280*(52), 42919–42928. https://doi.org/10.1074/JBC.M510522200

Ravikrishnan, A., & Raman, K. (2015). Critical assessment of genome-scale metabolic networks: The need for a unified standard. *Briefings in Bioinformatics*, *16*(6), 1057–1068. https://doi.org/10.1093/bib/bbv003

Redl, S., Diender, M., Jensen, T. Ø., Sousa, D. Z., & Nielsen, A. T. (2017). Exploiting the potential of gas fermentation. *Industrial Crops and Products*, *106*, 21–30. https://doi.org/10.1016/j.indcrop.2016.11.015

Reichardt, N., Duncan, S. H., Young, P., Belenguer, A., McWilliam Leitch, C., Scott, K. P., Flint, H. J., & Louis, P. (2014). Phylogenetic distribution of three pathways for propionate production within the human gut microbiota. *The ISME Journal*, *8*, 1323–1335. https://doi.org/10.1038/ismej.2014.14

Ricci, A., Allende, A., Bolton, D., Chemaly, M., Davies, R., Herman, L., Koutsoumanis, K., Lindqvist, R., Nørrung, B., Robertson, L., Ru, G., Sanaa, M., Simmons, M., Skandamis, P., Snary, E., Speybroeck, N., Kuile, B. T., Threlfall, J., Wahlström, H., … Fernández Escámez, P. (2018). Evaluation of the application for a new alternative processing method for animal by-products of Category 3 material (ChainCraft B.V.). *EFSA Journal*, *16*(6), Article 5281. https://doi.org/10.2903/j.efsa.2018.5281

Richter, H., Loftus, S. E., & Angenent, L. T. (2013). Integrating syngas fermentation with the carboxylate platform and yeast fermentation to reduce medium cost and improve biofuel productivity. *Environmental Technology (United Kingdom)*, *34*, 1983–1994. https://doi.org/10.1080/09593330.2013.826255

Richter, H., Molitor, B., Diender, M., Sousa, D. Z., & Angenent, L. T. (2016a). A narrow pH range supports butanol, hexanol, and octanol production from syngas in a continuous so-culture of *Clostridium ljungdahlii* and *Clostridium kluyveri* with in-line product extraction. *Frontiers in Microbiology*, *7*, Article 1773. https://doi.org/10.3389/fmicb.2016.01773

Richter, H., Molitor, B., Wei, H., Chen, W., Aristilde, L., & Angenent, L. T. (2016b). Ethanol production in syngas-fermenting *Clostridium ljungdahlii* is controlled by thermodynamics rather than by enzyme expression. *Energy & Environmental Science*, *9*(7), 2392–2399. https://doi.org/10.1039/C6EE01108J

Robles, A., Sundar, S. V., Mohana Rangan, S., & Delgado, A. G. (2023). Butanol as a major product during ethanol and acetate chain elongation. *Frontiers in Bioengineering and Biotechnology*, *11*, Article 1181983. https://www.frontiersin.org/articles/10.3389/fbioe.2023.1181983

Roell, G. W., Zha, J., Carr, R. R., Koffas, M. A., Fong, S. S., & Tang, Y. J. (2019). Engineering microbial consortia by division of labor. *Microbial Cell Factories*, *18*, Article 35. https://doi.org/10.1186/s12934-019-1083-3

Roghair, M., Hoogstad, T., Strik, D. P. B. T. B., Plugge, C. M., Timmers, P. H. A., Weusthuis, R. A., Bruins, M. E., & Buisman, C. J. N. (2018). Controlling ethanol use in chain elongation by CO_2 loading rate. *Environmental Science & Technology*, *52*, 1496–1505. https://doi.org/10.1021/acs.est.7b04904

Ross, D. E., Marshall, C. W., Gulliver, D., May, H. D., & Norman, R. S. (2020). Defining genomic and predicted metabolic features of the *Acetobacterium* genus. *mSystems*, *5*(5), Article e00277-20. https://doi.org/10.1128/MSYSTEMS.00277-20

Rother, M., & Metcalf, W. W. (2004). Anaerobic growth of *Methanosarcina acetivorans* C2A on carbon monoxide: An unusual way of life for a methanogenic archaeon. *Proceedings of the National Academy of Sciences*, *101*, 16929–16934. https://doi.org/10.1073/pnas.0407486101

Samain, E., Albagnac, G., Dubourguier, H. C., & Touzel, J. P. (1982). Characterization of a new propionic acid bacterium that ferments ethanol and displays a growth factor-dependent association with a gram-negative homoacetogen. *FEMS Microbiology Letters*, *15*, 69–74. https://doi.org/10.1111/j.1574-6968.1982.tb00040.x

Sancho Navarro, S., Cimpoia, R., Bruant, G., & Guiot, S. R. (2016). Biomethanation of syngas using anaerobic sludge: Shift in the catabolic routes with the CO partial pressure increase. *Frontiers in Microbiology*, *7*. https://doi.org/10.3389/fmicb.2016.01188

Santos, F., Boele, J., & Teusink, B. (2011). A practical guide to genome-scale metabolic models and their analysis. In D. Jameson, M. Verma, & H. V. Westerhoff (Eds.), *Methods in Enzymology* (Vol. 500, pp. 509–532). Elsevier. https://doi.org/10.1016/B978-0-12-385118-5.00024-4

San-Valero, P., Abubackar, H. N., Veiga, M. C., & Kennes, C. (2020). Effect of pH, yeast extract and inorganic carbon on chain elongation for hexanoic acid production. *Bioresource Technology*, *300*, Article 122659. https://doi.org/10.1016/j.biortech.2019.122659

Saxena, J., & Tanner, R. S. (2011). Effect of trace metals on ethanol production from synthesis gas by the ethanologenic acetogen, *Clostridium ragsdalei*. *Journal of Industrial Microbiology and Biotechnology*, *38*, 513–521. https://doi.org/10.1007/s10295-010-0794-6

Schellenberger, J., Park, J. O., Conrad, T. M., & Palsson, B. Ø. (2010). BiGG: A Biochemical Genetic and Genomic knowledgebase of large scale metabolic reconstructions. *BMC Bioinformatics*, *11*, Article 213. https://doi.org/10.1186/1471-2105-11-213

Schink, B., Kremer, D. R., & Hansen, T. A. (1987). Pathway of propionate formation from ethanol in *Pelobacter propionicus*. *Archives of Microbiology*, *147*, 321–327. https://doi.org/10.1007/BF00406127

Schneider, M., Bäumler, M., Lee, N. M., Weuster-Botz, D., Ehrenreich, A., & Liebl, W. (2021). Monitoring co-cultures of *Clostridium carboxidivorans* and *Clostridium kluyveri* by fluorescence in situ hybridization with specific 23S rRNA oligonucleotide probes. *Systematic and Applied Microbiology*, *44*(6), Article 126271. https://doi.org/10.1016/j.syapm.2021.126271

Schomburg, I., Chang, A., Hofmann, O., Ebeling, C., Ehrentreich, F., & Schomburg, D. (2002). BRENDA: A resource for enzyme data and metabolic information. *Trends in Biochemical Sciences*, *27*(1), 54–56. https://doi.org/10.1016/S0968-0004(01)02027-8

Schuchmann, K., & Müller, V. (2013). Direct and reversible hydrogenation of CO_2 to formate by a bacterial carbon dioxide reductase. *Science*, *342*(6164), 1382–1385. https://doi.org/10.1126/science.1244758

Schuchmann, K., & Müller, V. (2014). Autotrophy at the thermodynamic limit of life: A model for energy conservation in acetogenic bacteria. *Nature Reviews Microbiology*, *12*, 809–821. https://doi.org/10.1038/nrmicro3365

Schuchmann, K., & Müller, V. (2016). Energetics and application of heterotrophy in acetogenic bacteria. *Applied and Environmental Microbiology*, *82*, 4056–4069. https://doi.org/10.1128/AEM.00882-16

Seedorf, H., Fricke, W. F., Veith, B., Bruggemann, H., Liesegang, H., Strittmatter, A., Miethke, M., Buckel, W., Hinderberger, J., Li, F., Hagemeier, C., Thauer, R. K., & Gottschalk, G. (2008). The genome of *Clostridium kluyveri*, a strict anaerobe with unique metabolic features. *PNAS*, *105*, 2128–2133. https://doi.org/10.1073/pnas.0711093105

Seeliger, S. (2002). Energetics and kinetics of lactate fermentation to acetate and propionate via methylmalonyl-CoA or acrylyl-CoA. *FEMS Microbiology Letters*, *211*, 65–70. https://doi.org/10.1016/S0378-1097(02)00651-1

Selmer, T., Willanzheimer, A., & Hetzel, M. (2002). Propionate CoA-transferase from *Clostridium propionicum*. *European Journal of Biochemistry*, *269*, 372–380. https://doi.org/10.1046/j.0014-2956.2001.02659.x

Shen, N., Dai, K., Xia, X.-Y., Zeng, R. J., & Zhang, F. (2018). Conversion of syngas (CO and H_2) to biochemicals by mixed culture fermentation in mesophilic and thermophilic hollow-fiber membrane biofilm reactors. *Journal of Cleaner Production*, *202*, 536–542. https://doi.org/10.1016/j.jclepro.2018.08.162

Shen, Y., Brown, R., & Wen, Z. (2014). Syngas fermentation of *Clostridium carboxidivorans* P7 in a hollow fiber membrane biofilm reactor: Evaluating the mass transfer coefficient and ethanol production performance. *Biochemical Engineering Journal*, *85*, 21–29. https://doi.org/10.1016/j.bej.2014.01.010

R

Shin, J., Song, Y., Jeong, Y., & Cho, B.-K. (2016). Analysis of the core genome and pan-genome of autotrophic acetogenic bacteria. *Frontiers in Microbiology*, *7*, Article 1531. https://doi.org/10.3389/fmicb.2016.01531

Shortall, K., Djeghader, A., Magner, E., & Soulimane, T. (2021). Insights into aldehyde dehydrogenase enzymes: A structural perspective. *Frontiers in Molecular Biosciences*, *8*, Article 659550. https://doi.org/10.3389/fmolb.2021.659550

Shrestha, S., Xue, S., & Raskin, L. (2023). Competitive reactions during ethanol chain elongation were temporarily suppressed by increasing hydrogen partial pressure through methanogenesis inhibition. *Environmental Science & Technology*, *57*(8), 3369–3379. https://doi.org/10.1021/acs.est.2c09014

Simanshu, D. K., Savithri, H. S., & Murthy, M. R. N. (2005). Crystal structures of ADP and AMPPNP-bound propionate kinase (TdcD) from *Salmonella typhimurium*: Comparison with members of acetate and sugar kinase/heat shock cognate 70/actin superfamily. *Journal of Molecular Biology*, *352*, 876–892. https://doi.org/10.1016/j.jmb.2005.07.069

Simpson, S. D., Warner, I. L., Fung, J. M. Y., & Köpke, M. (2010). *Optimised fermentation media* (World Intellectual Property Organization Patent WO2010064932A1). https://patents.google.com/patent/WO2010064932A1/en

Sims, R. E. H., Mabee, W., Saddler, J. N., & Taylor, M. (2010). An overview of second generation biofuel technologies. *Bioresource Technology*, *101*, 1570–1580. https://doi.org/10.1016/j.biortech.2009.11.046

Singla, A., Verma, D., Lal, B., & Sarma, P. M. (2014). Enrichment and optimization of anaerobic bacterial mixed culture for conversion of syngas to ethanol. *Bioresource Technology*, *172*, 41–49. https://doi.org/10.1016/j.biortech.2014.08.083

Sipma, J., Henstra, A. M., Parshina, S. N., Lens, P. N. L., Lettinga, G., & Stams, A. J. M. (2006). Microbial CO conversions with applications in synthesis gas purification and bio-desulfurization. *Critical Reviews in Biotechnology*, *26*, 41–65. https://doi.org/10.1080/07388550500513974

Sipma, J., Lens, P. N. L., Stams, A. J. M., & Lettinga, G. (2003). Carbon monoxide conversion by anaerobic bioreactor sludges. *FEMS Microbiology Ecology*, *44*, 271–277. https://doi.org/10.1016/S0168-6496(03)00033-3

Slepova, T. V., Sokolova, T. G., Lysenko, A. M., Tourova, T. P., Kolganova, T. V., Kamzolkina, O. V., Karpov, G. A., & Bonch-Osmolovskaya, E. A. (2006). *Carboxydocella sporoproducens* sp. Nov., a novel anaerobic CO-utilizing/H_2-producing thermophilic bacterium from a Kamchatka hot spring. *International Journal of Systematic and Evolutionary Microbiology*, *56*, 797–800. https://doi.org/10.1099/ijs.0.63961-0

Soboh, B., Linder, D., & Hedderich, R. (2002). Purification and catalytic properties of a CO-oxidizing:H_2-evolving enzyme complex from *Carboxydothermus hydrogenoformans*: CO-oxidizing:H_2-evolving enzyme complex. *European Journal of Biochemistry*, *269*(22), 5712–5721. https://doi.org/10.1046/j.1432-1033.2002.03282.x

Sokolova, T. G. (2002). Carboxydocella thermautotrophica gen. Nov., sp. Nov., a novel anaerobic, CO-utilizing thermophile from a Kamchatkan hot spring. *International Journal of Systematic and Evolutionary Microbiology*, *52*, 1961–1967. https://doi.org/10.1099/ijs.0.02173-0

Sorokin, D. Y., Diender, M., Merkel, A. Y., Koenen, M., Bale, N. J., Pabst, M., Sinninghe Damsté, J. S., & Sousa, D. Z. (2020). *Natranaerofaba carboxydovora* gen. Nov., sp. Nov., an extremely haloalkaliphilic CO-utilizing acetogen from a hypersaline soda lake representing a novel deep phylogenetic lineage in the class 'Natranaerobiia'. *Environmental Microbiology*, *23*(7), 3460–3476. https://doi.org/10.1111/1462-2920.15241

Spirito, C. M., Richter, H., Rabaey, K., Stams, A. J., & Angenent, L. T. (2014). Chain elongation in anaerobic reactor microbiomes to recover resources from waste. *Current Opinion in Biotechnology*, *27*, 115–122. https://doi.org/10.1016/j.copbio.2014.01.003

Stamatopoulou, P., Malkowski, J., Conrado, L., Brown, K., & Scarborough, M. (2020). Fermentation of organic residues to beneficial chemicals: A review of medium-chain fatty acid production. *Processes*, *8*(12), Article 12. https://doi.org/10.3390/pr8121571

Stams, A. J. M., Kremer, D. R., Nicolay, K., Weenk, G. H., & Hansen, T. A. (1985). Pathway of propionate formation in *Desulfobulbus propionicus*. *Archives of Microbiology*, *140*, Article 298. https://doi.org/10.1007/BF00446965

Steinbusch, K. J. J., Arvaniti, E., Hamelers, H. V. M. H. V. M., & Buisman, C. J. N. C. J. N. (2009). Selective inhibition of methanogenesis to enhance ethanol and n-butyrate production through acetate reduction in mixed culture fermentation. *Bioresource Technology*, *100*, 3261–3267. https://doi.org/10.1016/j.biortech.2009.01.049

Steinbusch, K. J. J., Hamelers, H. V. M., Plugge, C. M., & Buisman, C. J. N. (2011). Biological formation of caproate and caprylate from acetate: Fuel and chemical production from low grade biomass. *Energy & Environmental Science*, *4*, 216–224. https://doi.org/10.1039/C0EE00282H

Stoll, I. K., Boukis, N., & Sauer, J. (2020). Syngas fermentation to alcohols: Reactor technology and application perspective. *Chemie-Ingenieur-Technik*, *92*(1–2), 125–136. https://doi.org/10.1002/CITE.201900118

Stolyar, S., Van Dien, S., Hillesland, K. L., Pinel, N., Lie, T. J., Leigh, J. A., & Stahl, D. A. (2007). Metabolic modeling of a mutualistic microbial community. *Molecular Systems Biology*, *3*, Article 92. https://doi.org/10.1038/msb4100131

Straathof, A. J. J., Wahl, S. A., Benjamin, K. R., Takors, R., Wierckx, N., & Noorman, H. J. (2019). Grand research challenges for sustainable industrial biotechnology. *Trends in Biotechnology*, *37*, 1042–1050. https://doi.org/10.1016/j.tibtech.2019.04.002

Strik, D. P. B. T. B., Ganigué, R., & Angenent, L. T. (2022). Editorial: Microbial chain elongation- close the carbon loop by connecting-communities. *Frontiers in Bioengineering and Biotechnology*, *10*, Article 894490. https://www.frontiersin.org/articles/10.3389/fbioe.2022.894490

Strous, M., & Sharp, C. (2018). Designer microbiomes for environmental, energy and health biotechnology. *Current Opinion in Microbiology*, *43*, 117–123. https://doi.org/10.1016/j.mib.2017.12.007

Sullivan, L., Cates, M. S., & Bennett, G. N. (2010). Structural correlations of activity of *Clostridium acetobutylicum* ATCC 824 butyrate kinase isozymes. *Enzyme and Microbial Technology*, *46*, 118–124. https://doi.org/10.1016/j.enzmictec.2009.10.001

Sun, J., Haveman, S. A., Bui, O., Fahland, T. R., & Lovley, D. R. (2010). Constraint-based modeling analysis of the metabolism of two *Pelobacter* species. *BMC Systems Biology*, *4*, Article 174. https://doi.org/10.1186/1752-0509-4-174

Sun, X., Atiyeh, H. K., Huhnke, R. L., & Tanner, R. S. (2019). Syngas fermentation process development for production of biofuels and chemicals: A review. *Bioresource Technology Reports*, *7*, Article 100279. https://doi.org/10.1016/j.biteb.2019.100279

Sunfire. (2020). *Renewable syngas (SynLink)*. https://www.sunfire.de/en/syngas

Takkellapati, S., Li, T., & Gonzalez, M. A. (2018). An overview of biorefinery-derived platform chemicals from a cellulose and hemicellulose biorefinery. *Clean Technologies and Environmental Policy*, *20*(7), 1615–1630. https://doi.org/10.1007/s10098-018-1568-5

Takors, R., Kopf, M., Mampel, J., Bluemke, W., Blombach, B., Eikmanns, B., Bengelsdorf, F. R., Weuster-Botz, D., & Dürre, P. (2018). Using gas mixtures of CO, CO_2 and H_2 as microbial substrates: The do's and don'ts of successful technology transfer from laboratory to production scale. *Microbial Biotechnology*, *11*(4), 606–625. https://doi.org/10.1111/1751-7915.13270

Tang, Y., Huang, Y., Gan, W., Xia, A., Liao, Q., & Zhu, X. (2021). Ethanol production from gas fermentation: Rapid enrichment and domestication of bacterial community with continuous CO/CO_2 gas. *Renewable Energy*, *175*, 337–344. https://doi.org/10.1016/j.renene.2021.04.134

Tanner, R. S., Miller, L. M., & Yang, D. (1993). *Clostridium ljungdahlii* sp. Nov., an acetogenic species in Clostridial rRNA homology group I. *International Journal of Systematic and Evolutionary Microbiology*, *43*(2), 232–236. https://doi.org/10.1099/00207713-43-2-232

Teixeira, L. V., Moutinho, L. F., & Romão-Dumaresq, A. S. (2018). Gas fermentation of C1 feedstocks: Commercialization status and future prospects. *Biofuels, Bioproducts and Biorefining*, *12*, 1103–1117. https://doi.org/10.1002/bbb.1912

Thauer, R. K., Jungermann, K., & Decker, K. (1977). Energy conservation in chemotrophic anaerobic bacteria. *Bacteriological Reviews*, *41*, 100–180. https://doi.org/10.1128/br.41.1.100-180.1977

Thiele, I., & Palsson, B. Ø. (2010). A protocol for generating a high-quality genome-scale metabolic reconstruction. *Nature Protocols*, *5*, 93–121. https://doi.org/10.1038/nprot.2009.203

R

REFERENCES

Tholozan, J. L., Touzel, J. P., Samain, E., Grivet, J. P., Prensier, G., & Albagnac, G. (1992). *Clostridium neopropionicum* sp. Nov., a strict anaerobic bacterium fermenting ethanol to propionate through acrylate pathway. *Archives of Microbiology*, *157*, 249–257. https://doi.org/10.1007/BF00245158

Tripathi, N., Hills, C. D., Singh, R. S., & Atkinson, C. J. (2019). Biomass waste utilisation in low-carbon products: Harnessing a major potential resource. *Npj Climate and Atmospheric Science*, *2*, Article 35. https://doi.org/10.1038/s41612-019-0093-5

Ueki, A., Goto, K., Ohtaki, Y., Kaku, N., & Ueki, K. (2017). Description of *Anaerotignum aminivorans* gen. Nov., sp. Nov., a strictly anaerobic, amino-acid-decomposing bacterium isolated from a methanogenic reactor, and reclassification of *Clostridium propionicum*, *Clostridium neopropionicum* and *Clostridium lactatifermentans* as species of the genus *Anaerotignum*. *International Journal of Systematic and Evolutionary Microbiology*, *67*(10), 4146–4153. https://doi.org/10.1099/ijsem.0.002268

United Nations Department of Economic and Social Affairs, Population Division. (2022). *World population prospects 2022: Summary of results.* (UN DESA/POP/2022/TR/NO. 3.). https://www.un.org/development/desa/pd/sites/www.un.org.development.desa.pd/files/wpp2022_summary_of_results.pdf

United Nations Framework Convention on Climate Change. (2015). *Paris Agreement to the United Nations Framework Convention on Climate Change*. https://unfccc.int/files/meetings/paris_nov_2015/application/pdf/paris_agreement_english_.pdf

Valgepea, K., de Souza Pinto Lemgruber, R., Abdalla, T., Binos, S., Takemori, N., Takemori, A., Tanaka, Y., Tappel, R., Köpke, M., Simpson, S. D., Nielsen, L. K., & Marcellin, E. (2018). H_2 drives metabolic rearrangements in gas-fermenting *Clostridium autoethanogenum*. *Biotechnology for Biofuels*, *11*, Article 55. https://doi.org/10.1186/s13068-018-1052-9

Valgepea, K., Loi, K. Q., Behrendorff, J. B., Lemgruber, R. de S. P., Plan, M., Hodson, M. P., Köpke, M., Nielsen, L. K., & Marcellin, E. (2017). Arginine deiminase pathway provides ATP and boosts growth of the gas-fermenting acetogen *Clostridium autoethanogenum*. *Metabolic Engineering*, *41*, 202–211. https://doi.org/10.1016/j.ymben.2017.04.007

van der Wielen, Pwjj. (2002). *Clostridium lactatifermentans* sp. Nov., a lactate-fermenting anaerobe isolated from the caeca of a chicken. *International Journal of Systematic and Evolutionary Microbiology*, *52*(3), 921–925. https://doi.org/10.1099/ijs.0.02048-0

Vasudevan, D., Richter, H., & Angenent, L. T. (2014). Upgrading dilute ethanol from syngas fermentation to n-caproate with reactor microbiomes. *Bioresource Technology*, *151*, 378–382. https://doi.org/10.1016/j.biortech.2013.09.105

Verma, S., Hamasaki, Y., Kim, C., Huang, W., Lu, S., Jhong, H.-R. M., Gewirth, A. A., Fujigaya, T., Nakashima, N., & Kenis, P. J. A. (2018). Insights into the low overpotential electroreduction of CO_2 to CO on a supported gold catalyst in an alkaline flow electrolyzer. *ACS Energy Letters*, *3*, 193–198. https://doi.org/10.1021/acsenergylett.7b01096

Vital, M., Howe, A. C., & Tiedje, J. M. (2014). Revealing the bacterial butyrate synthesis pathways by analyzing (meta)genomic data. *mBio*, *5*(2), Article e00889. https://doi.org/10.1128/mBio.00889-14

Wainaina, S., Horváth, I. S., & Taherzadeh, M. J. (2018). Biochemicals from food waste and recalcitrant biomass via syngas fermentation: A review. *Bioresource Technology*, *248*, 113–121. https://doi.org/10.1016/j.biortech.2017.06.075

Walter, K. A., Nair, R. V., Cary, J. W., Bennett, G. N., & Papoutsakis, E. T. (1993). Sequence and arrangement of two genes of the butyrate-synthesis pathway of *Clostridium acetobutylicum* ATCC 824. *Gene*, *134*, 107–111. https://doi.org/10.1016/0378-1119(93)90182-3

Walther, T., & François, J. M. (2016). Microbial production of propanol. *Biotechnology Advances*, *34*, 984–996. https://doi.org/10.1016/j.biotechadv.2016.05.011

Wang, H.-J., Dai, K., Wang, Y.-Q., Wang, H.-F., Zhang, F., & Zeng, R. J. (2018a). Mixed culture fermentation of synthesis gas in the microfiltration and ultrafiltration hollow-fiber membrane biofilm reactors. *Bioresource Technology*, *267*, 650–656. https://doi.org/10.1016/j.biortech.2018.07.098

Wang, H.-J., Dai, K., Xia, X.-Y., Wang, Y.-Q., Zeng, R. J., & Zhang, F. (2018b). Tunable production of ethanol and acetate from synthesis gas by mesophilic mixed culture fermentation in a hollow fiber membrane biofilm reactor. *Journal of Cleaner Production*, *187*, 165–170. https://doi.org/10.1016/j.jclepro.2018.03.193

Wang, P., Wang, H., Qiu, Y., Ren, L., & Jiang, B. (2018c). Microbial characteristics in anaerobic digestion process of food waste for methane production–A review. *Bioresource Technology*, *248*, 29–36. https://doi.org/10.1016/j.biortech.2017.06.152

Wang, S., Huang, H., Kahnt, J., Mueller, A. P., Köpke, M., & Thauer, R. K. (2013). NADP-Specific electron-bifurcating [FeFe]-hydrogenase in a functional complex with formate dehydrogenase in *Clostridium autoethanogenum* grown on CO. *Journal of Bacteriology*, *195*, 4373–4386. https://doi.org/10.1128/JB.00678-13

Wang, S., Huang, H., Moll, J., & Thauer, R. K. (2010). NADP$^+$ reduction with reduced ferredoxin and NADP$^+$ reduction with NADH are coupled via an electron-bifurcating enzyme complex in *Clostridium kluyveri*. *Journal of Bacteriology*, *192*, 5115–5123. https://doi.org/10.1128/JB.00612-10/FORMAT/EPUB

Weghoff, M. C., & Müller, V. (2016). CO metabolism in the thermophilic acetogen *Thermoanaerobacter kivui*. *Applied and Environmental Microbiology*, *82*, 2312–2319. https://doi.org/10.1128/AEM.00122-16

Wei, L., Pordesimo, L. O., Igathinathane, C., & Batchelor, W. D. (2009). Process engineering evaluation of ethanol production from wood through bioprocessing and chemical catalysis. *Biomass and Bioenergy*, *33*, 255–266. https://doi.org/10.1016/j.biombioe.2008.05.017

Weimer, P. J., & Stevenson, D. M. (2012). Isolation, characterization, and quantification of *Clostridium kluyveri* from the bovine rumen. *Applied Microbiology and Biotechnology*, *94*, 461–466. https://doi.org/10.1007/s00253-011-3751-z

Wen, Z., Minton, N. P., Zhang, Y., Li, Q., Liu, J., Jiang, Y., & Yang, S. (2017). Enhanced solvent production by metabolic engineering of a twin-clostridial consortium. *Metabolic Engineering*, *39*, 38–48. https://doi.org/10.1016/j.ymben.2016.10.013

Wen, Z., Wu, M., Lin, Y., Yang, L., Lin, J., & Cen, P. (2014). Artificial symbiosis for acetone-butanol-ethanol (ABE) fermentation from alkali extracted deshelled corn cobs by co-culture of *Clostridium beijerinckii* and *Clostridium cellulovorans*. *Microbial Cell Factories*, *13*, Article 92. https://doi.org/10.1186/s12934-014-0092-5

West, S. A., Diggle, S. P., Buckling, A., Gardner, A., & Griffin, A. S. (2007). The social lives of microbes. *Annual Review of Ecology, Evolution, and Systematics*, *38*, 53–77. https://doi.org/10.1146/annurev.ecolsys.38.091206.095740

Westman, S., Chandolias, K., & Taherzadeh, M. (2016). Syngas biomethanation in a semi-continuous reverse membrane bioreactor (RMBR). *Fermentation*, *2*(2), Article 8. https://doi.org/10.3390/fermentation2020008

Westphal, L., Wiechmann, A., Baker, J., Minton, N. P., & Müller, V. (2018). The Rnf complex is an energy-coupled transhydrogenase essential to reversibly link cellular NADH and ferredoxin pools in the acetogen *Acetobacterium woodii*. *Journal of Bacteriology*, *200*(21), Article e00357-18. https://doi.org/10.1128/JB.00357-18

Wood, D. A., Nwaoha, C., & Towler, B. F. (2012). Gas-to-liquids (GTL): A review of an industry offering several routes for monetizing natural gas. *Journal of Natural Gas Science and Engineering*, *9*, 196–208. https://doi.org/10.1016/j.jngse.2012.07.001

Woolston, B. M., Emerson, D. F., Currie, D. H., & Stephanopoulos, G. (2018). Rediverting carbon flux in *Clostridium ljungdahli* using CRISPR interference (CRISPRi). *Metabolic Engineering*, *48*, 243–253. https://doi.org/10.1016/j.ymben.2018.06.006

World Steel Association. (2022). *Sustainability performance of the steel industry 2003-2021*.

Xu, D., Tree, D. R., & Lewis, R. S. (2011). The effects of syngas impurities on syngas fermentation to liquid fuels. *Biomass and Bioenergy*, *35*, 2690–2696. https://doi.org/10.1016/j.biombioe.2011.03.005

Xu, S., Fu, B., Zhang, L., & Liu, H. (2015). Bioconversion of H$_2$/CO$_2$ by acetogen enriched cultures for acetate and ethanol production: The impact of pH. *World Journal of Microbiology and Biotechnology*, *31*, 941–950. https://doi.org/10.1007/s11274-015-1848-8

R

REFERENCES

Xue, X., Gu, D., Xia, X., Qin, Y., Wu, H., Jiang, H., Jiang, T., & Wang, B. (2022). Solar bipolar cell facilitating carbon dioxide for efficient coproduction of electricity and syngas. *Journal of Power Sources*, *521*, Article 230985. https://doi.org/10.1016/j.jpowsour.2022.230985

Yeol Jung, G., Rae Kim, J., Ok Jung, H., Park, J.-Y., & Park, S. (1999). A new chemoheterotrophic bacterium catalyzing water-gas shift reaction. *Biotechnology Letters*, *21*, 869–873. https://doi.org/10.1023/a:1005599600510

Yin, Y., Zhang, Y., Karakashev, D. B., Wang, J., & Angelidaki, I. (2017). Biological caproate production by *Clostridium kluyveri* from ethanol and acetate as carbon sources. *Bioresource Technology*, *241*, 638–644. https://doi.org/10.1016/j.biortech.2017.05.184

Zahn, J. A., & Saxena, J. (2012). *Novel ethanologenic Clostridium species, Clostridium coskatii* (U.S. Patent and Trademark Office Patent US20120156747A1).

Zengler, K., & Zaramela, L. S. (2018). The social network of microorganisms—How auxotrophies shape complex communities. *Nature Reviews Microbiology*, *16*, 383–390. https://doi.org/10.1038/s41579-018-0004-5

Zerfaß, C., Chen, J., & Soyer, O. S. (2018). Engineering microbial communities using thermodynamic principles and electrical interfaces. *Current Opinion in Biotechnology*, *50*, 121–127. https://doi.org/10.1016/j.copbio.2017.12.004

Zhang, F., Ding, J., Shen, N., Zhang, Y., Ding, Z., Dai, K., & Zeng, R. J. (2013). In situ hydrogen utilization for high fraction acetate production in mixed culture hollow-fiber membrane biofilm reactor. *Applied Microbiology and Biotechnology*, *97*, 10233–10240. https://doi.org/10.1007/s00253-013-5281-3

Zhang, H., Li, Z., Pereira, B., & Stephanopoulos, G. (2015). Engineering *E. coli–E. coli* cocultures for production of muconic acid from glycerol. *Microbial Cell Factories*, *14*, Article 134. https://doi.org/10.1186/s12934-015-0319-0

Zhang, H., & Wang, X. (2016). Modular co-culture engineering, a new approach for metabolic engineering. *Metabolic Engineering*, *37*, 114–121. https://doi.org/10.1016/J.YMBEN.2016.05.007

Zhou, J., Zhuang, Y., & Xia, J. (2021). Integration of enzyme constraints in a genome-scale metabolic model of *Aspergillus niger* improves phenotype predictions. *Microbial Cell Factories*, *20*, Article 125. https://doi.org/10.1186/s12934-021-01614-2

Zhu, L., Xu, X., Wang, L., Dong, H., Yu, B., & Ma, Y. (2015). NADP$^+$-Preferring D-lactate sehydrogenase from *Sporolactobacillus inulinus*. *Applied and Environmental Microbiology*, *81*, 6294–6301. https://doi.org/10.1128/AEM.01871-15

Zinder, S. H., Anguish, T., & Cardwell, S. C. (1984). Selective inhibition by 2-bromoethanesulfonate of methanogenesis from acetate in a thermophilic anaerobic digestor. *Applied and Environmental Microbiology*, *47*, 1343–1345. https://doi.org/10.1128/AEM.47.6.1343-1345.1984

Zou, W., Ye, G., Zhang, J., Zhao, C., Zhao, X., & Zhang, K. (2018). Genome-scale metabolic reconstruction and analysis for *Clostridium kluyveri*. *Genome*, *61*, 605–613. https://doi.org/10.1139/gen-2017-0177

R

APPENDICES

Summary

List of publications

Acknowlegdements

About the author

SENSE Research School Diploma

—

SUMMARY

The transition towards sustainable chemical production is crucial for long-term environmental sustainability and the reduction of CO_2 emissions. By shifting away from finite fossil resources and adopting renewable feedstocks and biobased processes, we can mitigate the environmental impact and promote the development of a low-carbon, circular economy. In this context, this thesis takes part in the growing interest on the revalorisation of C1 feedstocks, and explores the potential of microbial communities as biocatalytic platforms. I focused on investigating syngas-driven chain elongation to produce odd-chain carboxylic acids and alcohols using synthetic microbial consortia. A combination of experimental work and genome-scale metabolic modelling demonstrated the advantages of an interdisciplinary approach in advancing our understanding of microbial metabolism and interactions.

Through a comprehensive review, **Chapter 2** delved into the potential of microbial communities for producing fuels and chemicals from carbon monoxide. The characteristics of open mixed cultures and synthetic co-cultures were examined, and contrasted with those of monocultures of acetogens. Whereas open mixed cultures have promising potential for syngas biomethanation, products of higher complexity, such as medium-chain carboxylates or higher alcohols, are better produced using synthetic co-cultivation approaches due to higher product specificities. Genetic engineering may expand the possibilities of synthetic co-cultures by facilitating the production of non-native compounds. Looking ahead, we recommended the application of genome-scale metabolic modelling for studying microbial interactions and predicting co-culture behaviour.

In **Chapter 3**, we tested the performance of a synthetic co-culture composed of two anaerobic, ethanol-consuming species, *Anaerotignum neopropionicum* and *Clostridium kluyveri*. This co-culture produced a mixture of odd- and even-chain carboxylic acids (up to C7) from ethanol and CO_2. Within a syngas platform, ethanol and CO_2 can be produced via syngas fermentation with acetogens. In the co-culture, *A. neopropionicum* generated propionate and acetate, which *C. kluyveri* used for chain elongation. Continuous cultivation in a bioreactor showed the viability of the co-culture at ethanol loading rates up to 6.7 g L^{-1} d^{-1}. Approximately 37% odd-chain products were obtained, indicating the co-culture's potential for odd-chain elongation in addition to even-chain elongation. Experiments with *C. kluyveri* revealed the excessive oxidation of ethanol to acetate in the presence of propionate, a behaviour that we further discussed. In addition, we determined the tolerance of *A. neopropionicum* to ethanol (≈300 mM) and the maximum growth rate on this substrate (0.103±0.003 h^{-1}), extending the knowledge on the physiology of this strain.

In **Chapter 4**, the first genome-scale metabolic model (GEM) of *A. neopropionicum* was constructed and validated, by combining an in silico analysis of the genome with experimental data. We identified all the enzymes involved in the fermentation of ethanol to propionate (via the acrylate pathway) in this microorganism, as well as important aspects of the energetic metabolism. Key findings include the identification of three important complexes: the acryloyl-CoA reductase–electron-transferring flavoprotein (Acr-EtfAB), the membrane-associated reduced ferredoxin:NAD$^+$ oxidoreductase (Rnf), and the NADH-dependent reduced ferredoxin:NADP$^+$ oxidoreductase (Nfn). Our GEM shows that, in this species, the Rnf complex operates "in reverse", catalysing the ATP-driven reduction of ferredoxin, crucial for pyruvate synthesis during growth on ethanol.

Growth phenotypes and product profiles during batch cultivation were predicted by model simulations using dynamic flux balance analysis (dFBA) with high accuracy, supporting the reliability of the model. This model was used in a follow-up study to construct a multi-species GEM of a syngas-fermenting tri-culture (Chapter 5).

In **Chapter 5**, we integrated the knowledge gained in the previous works by studying a tri-culture of the acetogen *Acetobacterium wieringae* JM with *A. neopropionicum* and *C. kluyveri*, using experimental and computational approaches. On the one hand, we showed that, in batch cultivation with continuous supply of CO as sole substrate, the tri-culture produced medium-chain carboxylates (C4–C7) and, subsequently, higher alcohols, among them pentanol that had not been reported before for syngas-fermenting microbial consortia. The fermentation was done at neutral pH, which was a key factor to maintain the activity of the three strains in co-cultivation. We also demonstrated that the acetogen switches from acetogenesis to ethanol production (partly) when in the presence of the ethanol-consuming species, under conditions that would otherwise not favour such metabolism. On the other hand, we constructed the first GEM of *A. wieringae* JM and we used it in the construction of a multi-species GEM of the tri-culture. Model simulations using community flux balance analysis (cFBA) predicted that a balanced presence of the three strains is key for the feasibility of the tri-culture in steady-state conditions. The effect of H_2 addition on the product spectrum of the co-culture was also simulated. In addition, we identified the H_2-dependant CO_2-reductase (HDCR) in *A. wieringae* JM, and theorised how this strain is able to grow solely on CO despite the reported CO inhibitory effect on this enzyme.

Chapter 6 aimed at consolidating knowledge on the diverse metabolic capabilities of acetogens in co-cultivation with *C. kluyveri*. Co-cultures of *C. kluyveri* with various relevant acetogens were established at pH values from 6 to 8, and tested for their ability to consume CO/H_2 and produce chain-elongated products (i.e., butyrate and caproate). Results indicated varying CO and H_2 utilization among the acetogens tested. Based on substrate utilization and final titres of C4/C6 carboxylates, *C. autoethanogenum* and *A. wieringae* JM were identified as the best co-cultivation candidates with *C. kluyveri* at pH 6–7.5. In addition, the *A. wieringae* JM–*C. kluyveri* co-culture demonstrated promising potential as a solventogenic platform, producing mainly butanol and hexanol upon refilling of the headspace.

A general discussion is given in **Chapter 7**, highlighting the strengths and limitations of the use of synthetic co-cultures in syngas fermentation, and placing them in context of the current developments in the field. Novel aspects of the microbial physiology that were uncovered in this research are also discussed, and new lines of investigation are proposed. Suggestions are given for future work, that emphasize the need for an interdisciplinary approach in realising the full potential of syngas fermentation.

A

LIST OF PUBLICATIONS

Diender, M., Dykstra, J. C., **Parera Olm, I.**, Kengen, S. W. M., Stams, A. J. M., & Sousa, D. Z. (2023). The role of ethanol oxidation during carboxydotrophic growth of *Clostridium autoethanogenum*. *Microbial Biotechnology*. [In Press] https://doi.org/10.1111/1751-7915.14338

Parera Olm, I., & Sousa, D. Z. (2023). Upgrading dilute ethanol to odd-chain carboxylic acids by a synthetic co-culture of *Anaerotignum neopropionicum* and *Clostridium kluyveri*. *Biotechnology for Biofuels and Bioproducts*, 16, Article 83. https://doi.org/10.1186/s13068-023-02336-w

Benito-Vaquerizo, S., **Parera Olm, I.**, De Vroet, T., Schaap, P. J., Sousa, D. Z., Martins dos Santos, V. A. P., & Suarez-Diez, M. (2022). Genome-scale metabolic modelling enables deciphering ethanol metabolism via the acrylate pathway in the propionate-producer *Anaerotignum neopropionicum*. *Microbial Cell Factories*, *21*, Article 116. https://doi.org/10.1186/s12934-022-01841-1

Parera Olm, I., & Sousa, D. Z. (2021). Conversion of carbon monoxide to chemicals using microbial consortia. In A.-P. Zeng & N. J. Claassens (Eds.), *One-Carbon Feedstocks for Sustainable Bioproduction* (Vol. 180, pp. 373–407). Springer International Publishing. https://doi.org/10.1007/10_2021_180

Diender, M., **Parera Olm, I.**, & Sousa, D. Z. (2021). Synthetic co-cultures: novel avenues for bio-based processes. *Current Opinion in Biotechnology*, 67, 72–79. https://doi.org/10.1016/j.copbio.2021.01.006

Benito-Vaquerizo, S., Diender, M., **Parera Olm, I.**, Martins dos Santos, V. A. P., Schaap, P. J., Sousa, D. Z., & Suarez-Diez, M. (2020). Modeling a co-culture of *Clostridium autoethanogenum* and *Clostridium kluyveri* to increase syngas conversion to medium-chain fatty-acids. *Computational and Structural Biotechnology Journal*, 18, 3255–3266. https://doi.org/10.1016/j.csbj.2020.10.003

Diender, M., **Parera Olm, I.**, Gelderloos, M., Koehorst, J., Schaap, P. J., Stams, A. J. M., & Sousa, D. Z. (2019). Metabolic shift induced by synthetic co-cultivation promotes high yield of chain elongated acids from syngas. *Scientific Reports*, 9, Article 18081. https://doi.org/10.1038/s41598-019-54445-y

In preparation:
Parera Olm, I., Benito-Vaquerizo, S., Dubaere, C., Martins dos Santos, V.A.P., Suarez-Diez, M., Sousa, D.Z. (2023). Carbon monoxide conversion to medium-chain carboxylic acids and higher alcohols using a Clostridial tri-culture.

Peek, S., **Parera Olm, I.**, Diender, M., Sousa, D.Z. (2023). Exploring pH effects on co-cultures of acetogens and *Clostridium kluyveri* for syngas fermentation.

A

ACKNOWLEDGEMENTS

To me, this journey has been about the people I have met, and the experiences we have shared together. I feel immensely fortunate for having crossed paths with you, and for the lessons and memories I take with me forever.

Diana, thank you for your caring guidance and support. You always believed in me more than I did, and gave me the courage I needed when I did not feel capable. You are down-to-earth and see the person before the scientist, and this is something I value in you. Thank you for recognising my strengths and helping me improve my weaknesses. I really enjoyed working with you these years, and I am very glad we can continue doing research together for a little longer.

Maria, me alegro mucho de que hayas formado parte de mi tesis. Agradezco mucho tu dedicación, tus valiosos comentarios y buenos consejos, que siempre han servido para mejorar mi trabajo. Gracias por estar siempre presente y por transmitirme confianza. Ha sido un verdadero placer trabajar contigo, y he aprendido mucho de ti.

Fons, thank you for granting me this opportunity in the first place. I appreciate the noble work you have done and your guidance. Whenever there was the chance, I enjoyed our conversations.

I could not have conquered this thesis without the constant support of a very special person. **Sara**, no sé por dónde empezar a agradecerte lo mucho que has hecho por mí; tu perseverancia me ha ayudado tanto a seguir hacia delante en los momentos más difíciles. Juntas hemos formado un gran equipo, he disfrutado muchísimo abriendo y cerrando nuestros melones, y me he empapado de tu asidua manera de trabajar y tu risueña filosofía de vida. Ojalá nuestros caminos se vuelvan a cruzar. Te quiero un melón!

Niels, I am very happy that you were part of this project, too. Your kind and hard-working attitude have been encouraging, and I am grateful that we have helped each other with our obstacles along the way. Thanks for always listening, and for the positive energy you bring about.

I am also very grateful for the dedication of the other members of the SynValue project. **Ana**, **Peter**, **Vitor**, **Jeroen**: your constructive feedback has moved my project forward, and I deeply appreciate the diverse expertise and points of view you brought to the table. Thanks also to **Henk** (Paques), for your genuine interest and valuable comments; and to **René** (Paques) and **Robin** (Torrgas) for your feedback and insight, and for welcoming us at the industrial facilities.

My gratitude also goes to the committee members for taking an interest and evaluating my thesis: **Annemiek ter Heijne**, **Joana Alves**, **Bastian Molitor** and **Djordje Bajić**.

I would probably not be writing these pages if it wasn't for the person who took me in back in 2016 when I was still a student in my twenties, and who has guided me since then. **Martijn**, I had this

feeling when I first met you that I would learn a lot *from* you, but what I could not have imagined is that one day I would also learn *with* you. You are truly one of a kind; a great scientist and, more importantly, a good-hearted person. Super Martijn, isn't it? ;) I enjoyed every challenge we embarked on together, and today still I feel honoured and grateful for working with you. Thank you, for the guidance, feedback, teaching and patience you had with me. Thanks for believing in me and for your encouragement.

To my dear paranymphs, who've kept me grounded when things got hectic, and who've been my partners in crime in countless adventures. **Cata**, gracias por tanto. Tú me conoces mejor que nadie, y me siento muy afortunada de haberte encontrado en este camino. Me enseñaste que lo importante está más allá de nuestros logros, y ésta sea quizás sea la lección más valiosa que me llevo de esta experiencia. Tu valentía y tu alegría se contagian, y hacen que hasta la tarde más tonta contigo sea medicina para el alma. Gracias por ayudarme a llegar hasta aquí con el corazón contento. Te quiero mucho. **Nico**, gracias por estar ahí siempre, por ser un amigo de los buenos, por tu radical honestidad, por escucharme y por la palty! Contigo he aprendido a expresarme sin miedo, y es que eres de las pocas personas que me conocen y me aceptan tal y como soy, con mis locuras y absurdeces. Gracias por estar ahí para pasarlo bien y para dejar de pasarlo mal. Te quiero un montón! Little **Siebe**, as much as I like to mess around with you, I am glad to have found in you a friend I can count on. It meant the world to me that you ~~forced~~ reminded me to smile during the last months of my thesis, when my good mood was fading away. And all the Kinder Bueno, of course ;) Your unhurried pace in life is as unnerving as it is inspiring, and it has thought me that steady, little steps can also get you very far. My heartful thank to you.

I feel so lucky to have landed in the Microbial Physiology group, for the friendly and supportive atmosphere we have created, and because I've found friends for life. **Daan**, what can I say that I don't tell you every time we go out. You are one of my most precious friends; caring, honest, FUN, open-minded and hopeless romantic. Yes, I like you for that, too ;) I really value the friendship we have built over the years. Thanks for being there on my best and worst days! You have made me better. **Sarita**, gracias por ser tan buena amiga, por ayudarme tanto y sacarme de los días malos con un abrazo y unas birras, y por las risas luego. Eres una curranta y una científica top, y he aprendido mucho de ti. Sobre todo, gracias por enseñarme a tomarme la vida con sentido del humor, y del amor. Te admiro y te quiero! **Peter**, there are not enough fancy words in the dictionary to describe how much I admire you. As a scientist, as a person and as a friend. Thank you for your kind support, for always teaching me a thing or two, and for all the fun we have together. I treasure our friendship and hope it lasts forever. **Lot**, you are as kind as you are strong. Thank you for being so caring, considerate, down-to-earth and fun to be with. I value your peaceful vibes and your determination, and I have learned so much from you. I love sharing productivity hacks, organisation tips and yoga poses with you :) You hold a special place in my heart. **James**, thanks for being.. well, princess James. Behind the well-dressed, hard-working and clever scientist there is this sweet and fun guy I was fortunate to meet. We have walked this journey together, and I am very proud of who you have become. I am very grateful for the time we have spent in the lab, playing boardgames, sharing confidences and messing around with each other. Thank you, from the bottom of my heart. **Iame**,

A

195

Iamesita, Iamazing; lo eres todo, amiga. Gracias por tu cariño, por preocuparte tanto por mí y por estar siempre, en las buenas y en las malas. Es genial cómo siempre logras transmitirme tu alegría y optimismo; ¡soy muy afortunada de tenerte! **Eva**, lo nuestro fue corto, ¡pero tan intenso! :) Eres la chica más buena, trabajadora y llena de energía positiva que conozco. Estoy muy feliz de haber compartido una parte de esta aventura contigo, y de haber ganado una amiga para siempre. Te quiero. **Nohemí**, gracias por el cariño que siempre me has dado. Tenerte aquí fue un regalo, y disfruté mucho del tiempo que estuviste viviendo en mi casa, volviendo las frutas picantes, y las tardes más amables. Gracias por tu dulzura. **Yuan**, thanks for your kind friendship, for our confidences and your good advice. I really enjoyed the time you were in Wageningen, and I'm so grateful for the extra chance we had last summer, it made me really happy to reunite with you.

Timon, thanks for your generosity, you have a solution at hand for almost every problem in life, except for HEL, of course (we don't talk about it). Thanks also for your kind friendship, I enjoy our good times in the lab and sharing a beer or two, or three. **Maaike**, I had a good feeling about you in that first interview for your PhD, and I was right! I appreciate how kind, helpful, and good scientist you are. Thank you for your cheerful presence. **Reinier**, you take humour in the office to the next level! I truly enjoy your company, and I try as much as I can to soak up this relentless positive energy of yours. Thanks also for bringing some variety to my processed sugar-based diet on those dark, writing days with pieces of fruit that I never ate. **Lukas**, thanks for bringing some proper German sense to the office. Sorry that we always make fun of you, though (or Siebe). Now, really, thanks for the good humour and always on-point advice. **Marten**, the Handyman! Thanks being such a great colleague; I really enjoyed thinking along you, and I admire your hands-on ability to craft anything from scratch. **Anna** (**D.**), thanks for being so sweet and mindful, for bearing with my constant sighs and swear words of desperation at the end of my thesis. You have been very supportive and I feel grateful. **Max**, my favourite hipster! I am really glad that I tricked you into coming to Wageningen and, even better, into becoming friends. Jokes aside, thanks for your good vibes that always cheer me up. **Anastasia**, I appreciate your kindness, your fun-loving nature, and your caring attitude. Your positive energy is contagious, and I always enjoy spending time with you! **Adrián**, gracias por tu apoyo y tus sabios consejos de doctor cuando estaba terminado y lo veía todo oscuro. Eres un buen amigo, aunque no siempre coincidamos en cuanto al sentido del humor ;) **Yehor**, I am very thankful for your kind help with my reactors and other technical stuff in the lab, and for your sense of humour. **Emilie**, thank you for sharing your kind and friendly essence with me, I truly enjoy the time we spend together over some beers or cake :) **Anca**, I admire your perseverance in the job, which never interferes with your kindness towards others. Thank you for being so considerate, and for your good advice when I needed it.

Ton, we owe Micfys to you, and not only because you keep everything up and running, but, most importantly, because you bring your spirit into it. Thanks for your kindness, generosity, your help on countless occasions, and for your stories. **Irene**, gracias por la fuerza y la alegría que siempre transmites, por tu honestidad y tus buenos consejos. ¡Te admiro como científica y como fiestera profesional! **Ben**, it was a blast having you around! I enjoyed the Ben vibes in an outside the lab. **Tom**, I am very glad that we have you in our team; thanks for making things run smoother, and for

your positive energy and sense of humour. **Çağlar**, I guess a part of you belongs to Micfys after all. Thanks for the support during our bioreactor battles, and for your kind friendship. **Jarrett**, Peter pronounced you an honorary member of Micfys, and who am I to contradict Dr. P. Q. Fischer. Thanks for being the greatest North-American of all times, not because of your superior literary skills, painfully good sense of humour or big heart, but because you are the only one I know. Now, seriously, ¡gracias por ser tan buen amigo! **Tarik**, I had so much fun with you in the lab! Thanks for your genuine friendship. **Luis**, tú también empezaste en Micfys. ¡Gracias por tu buena onda y por ser mi top DJ en las noches de Wageningen! **Caroline**, thanks for your kindness and for always being so open to help and share your knowledge. To **Anna** (**F.**), **Maryse**, **Nam**, **Guillermo, Cristina**, **Peer, Bruna**, **Francesca, Kejia**, **Octavio**, **Julia**, **Jasper**, all the students and others I might have missed: thanks for the good times in Micfys and for everything you taught me.

The Laboratory of Microbiology would not stand on its feet if it wasn't for the dedication of the greatest team of technicians: **Steven**, **Ton**, **Iame**, **Yehor**, **Tom**, **Phillipe**, **Merlijn**, **Hans**, **Ineke**, **Belén**, **Anna**, **Rob**, **Felix** and **Victor**. My deepest gratitude to you for making the lab run smoothly and safe, and for the nice atmosphere you create. **Phillipe**, **Minke**: thanks for your admirable dedication to teaching; I learn a lot from you. Thank you, **Anja**, **Heidi**, **Hannie** and **Sarash** for your making our lives easier with your administrative support. **Heidi**, thanks for your endless patience and efficient help with the finances of the PhD Trip.

Thijs, my sincere appreciation to you as Chair for making the Laboratory of Microbiology a wonderful place to work and to grow.

To my dear friends. **Dani**, vales oro; gracias por tu cercanía, tu genial sentido del humor, y por ser un buen amigo. Gracias por escucharme, por reírte conmigo y por el fireball. Eres un científico diez y un fiestero once. ¡Te adoro! **Max**, ets un amic gegant ;) Gràcies per ser-hi durant tots aquests anys, per escoltar-me sempre, per les risas i per la teva generositat. I miss our good old times with **Zak** and **Rodolfo**, when we were just playing to be microbiologists, enquiring into the deepness of the most trivial matters in life while excelling at having the time of our lives. I love you, guys! **Stephan**, your friendship arrived when I most needed it. You became one of my best confidents, and I am very grateful of the friendship we have. Thanks for always listening, and for bearing with my silliness, my drama and my serious party habits. I treasure you! My dear **Isi**, we have made it so far since that first chat in the electrophoresis room <3 Thanks for being such a caring, loving, supporting, honest and fierce friend. You put all your heart on everything you do, be it work, fun, or shots, and that is something I admire. I love you to the moon and back. **Ricardito**, gracias por tu tierna amistad, por escucharme y hacerme pensar, por estar ahí cuando estaba ausente, y por tener siempre media cerveza para ofrecerme :) Agradezco mucho tu apoyo al final de mi tesis. Te aprecio mucho. **Kassi**, you always cheer me up, and have this good energy that I love to have around. Thank you for your sweet support always, and for the fun we have together! **Enrique**, nos hemos visto crecer; estoy muy orgullosa de ti y muy feliz de poder seguir contando contigo. Gracias por tu apoyo incondicional, por transmitirme siempre esa vitalidad y buena energía y por tu corazón tan grande. **Belén**, gràcies per la teva generositat i bon rotllo durant tots aquests anys. T'aprecio molt! **Carrie**, thanks for being

A

the best president of the MIB drinking club! And for being so sweet and fun; I always enjoyed our time together. **Costas**, thanks for your caring, considerate and fun spirit. And, let's say it, for your bad jokes, too ;) I am grateful for the chance to get to know you better during the PhD trip, and for the good times together. **Jolanda**, thanks for being so kind and easy to be with. I truly appreciate your good vibes and your friendship. **Menia**, thanks for always lifting my mood with your kindness; I love your good energy and always have fun with you! **Nancy**, thanks for your sweet and cheerful friendship, I enjoy your company and our conversations. **Miguel**, gracias por tu buen rollo! Eres mi gamberro favorito. **Maria**, gracias por tu dulce cercanía y tu energía siempre positiva. **Lyon**, you are the king of the dancing floor, thank you for the good vibes you bring about!

To many others of the labs of Microbiology and Systems and Synthetic Biology: **Prokopis**, **Jannie**, **Sharon**, **Christos**, **Jeroen**, **Eva**, **Laureen**, **Burak**, **Yassin**, **Gerben**, **Christian**, **Despoina**, **Janneke**, **Wen**, **Carina**, **Isma**, **Thomas**, **Lorenzo**, **Catarina**, **Patrick**, **Emmy**, **Taojun**, **Chen**, **Joep**, **Thijs**, **Evgenios**, **Panos**, **Patricia**, **Guillaume**, **Jennah**, **Marie-Luise** and more I might be missing. Thank you for the good times, you are truly wonderful people and I cherish our memories. And to those of the generation before me: **Basti**, **Sven**, **Kal**, **Javi**, **Rob**, **Benoit**, thank you for taking me in to your gatherings and grown-up parties when I was still a young master student. I had, and still have, so much fun with you!

To the organising committee of the PhD trip 2019: **Giannis**, **Ran**, **Costas**, **Lot**, **Enrique**, **Catarina**, **Caifang** and **Nong**, it was a great experience to organise the trip with you. I learned a lot, got to know you better, and had a lot of fun.

To my wonderful students, **Philipp**, **Siemen**, **Gerben**, **Charles** and **Bastiaan**; thank you for dedication, and for teaching me more than I taught you.

My sincere gratitude to the PIs of the Microbiology lab for the valuable feedback and lessons during the many research meetings and conversations, and for stimulating such a positive working and learning atmosphere.

Maxim, it is wonderful that we graduate with only two days of difference! You are a kind, smart, hard-working scientist, and I am grateful to having shared some adventures with you. I tried.. but you always got the better awards! You are exceptional; gracias por tu bonita amistad :)

To **Tibo** and my Pomona girls: **Diana**, **Vera**, **Sofi**, **Iris**, **Varsha**, **Domi**, **Jin**. You made our house a home, and I am really grateful for that. Thanks for withstanding my stressful days, my hangovers, my terrible cooking skills and my pineapple pizza. You hold a very special place in my heart!

Chris, thanks for teaching me to not worry, be happy. I am very glad that I can count on you to bring peace to my soul, and to have the best fun with. Thanks for being a colourful friend, for your music, and for the Mexican name jokes. ¡Te adoro, amigo! **Alberto**, gracias por las mil aventuras,

por tu buen rollo y tu sentido del humor murciano. Me lo he pasado genial contigo, charlando de la vida, bailando y riendo. Nuestro accidente de bicis estará para siempre grabado en mi corazón.

And to the many others that made of Wageningen the special place that it is: thank you!

A la meva gentuza, per fer-me sentir que no ha passat el temps quan torno a casa, i per l'èxtasi que és quan ens veiem. Gràcies per ser-hi sempre; us estimo infinit! **Miri** i **Agnès**, gràcies per venir fins aquí a celebrar amb mi aquest dia, i fer que sigui encara més especial.

Eric, meeting you was the sweetest gift of this journey. Thank you for your incessant love and support. You put up with my worst days and helped me get through them with kindness and compassion. Thank you for taking care of me when I was reaching the finish line; for debating my ideas, for the patience, for the food and the soothing hugs. I am very lucky to have you. I love you.

A vosaltres, **familia**, estimats **tiets** i **tietes**, **cosins** i **cosinetes**, **Isaac** i **Roser**, per fer que tornar a casa sigui realment això: tornar a casa. Per la comprensió quan no hi he pogut ser, i per rebre'm sempre amb tant de carinyo. **Toni**, **Maria**, sou els millors germans que podria tenir; gràcies per pensar sempre en mi i per fer-me sentir tan a prop tot i estar lluny.

Mama, **Papa**, gràcies per donar-me les ales per volar.

A

ABOUT THE AUTHOR

Ivette was born on the 1st of May of 1992 in Viladecavalls (Barcelona, Spain). In 2014, she obtained her bachelor's degree in Biotechnology from the Universitat Autònoma de Barcelona, having developed a keen interest in microbial processes for biotechnological applications. As part of these studies, she did an Erasmus traineeship in the Bioprocess Engineering chairgroup at Wageningen University & Research (WUR) in the Netherlands, where she learned about microalgae cultivation processes. This experience encouraged her to continue her education abroad, so she pursued the master's degree in Biotechnology at WUR, specialising in Process Technology. She did her master's thesis at the Laboratory of Microbiology of the same university, where she studied syngas fermentation with Clostridial co-cultures, under the supervision of Dr Martijn Diender and Prof. Diana Z. Sousa. Ivette completed her degree with another Erasmus traineeship at the microbial research company Organobalance (Novozymes Berlin) in Berlin, Germany, where she worked on yeast fermentation.

In 2018, Ivette returned to the Laboratory of Microbiology at WUR to begin her PhD project, supervised by Prof. Diana Z. Sousa (promotor). Her work focused on the study and application of synthetic microbial co-cultures for the production of carboxylic acids through syngas fermentation and chain elongation, the results of which are presented in this thesis. Currently, Ivette continues to work at the Laboratory of Microbiology at WUR, where she advances her research on anaerobic microbial processes for syngas fermentation.

Netherlands Research School for the
Socio-Economic and Natural Sciences of the Environment

D I P L O M A

for specialised PhD training

The Netherlands research school for the
Socio-Economic and Natural Sciences of the Environment
(SENSE) declares that

Ivette Parera Olm

born on the 1st of May 1992 in Viladecavalls, Spain

has successfully fulfilled all requirements of the
educational PhD programme of SENSE.

Wageningen, 27th of October 2023

Chair of the SENSE board   The SENSE Director

Prof. dr. Martin Wassen   Prof. Philipp Pattberg

The SENSE Research School has been accredited by the Royal Netherlands Academy of Arts and Sciences (KNAW)

K O N I N K L I J K E   N E D E R L A N D S E
A K A D E M I E   V A N   W E T E N S C H A P P E N

The SENSE Research School declares that **Ivette Parera Olm** has successfully fulfilled all requirements of the educational PhD programme of SENSE with a work load of 36.5 EC, including the following activities:

SENSE PhD Courses

o   Environmental research in context (2018)
o   Research in context activity: 'Organisation of the PhD trip MIB-SSB 2019' (2018-2019)

Other PhD and Advanced MSc Courses

o   Microbial Physiology and Fermentation Technology, TU Delft (2019)
o   Critical Thinking and Argumentation, Wageningen Graduate Schools (2022)

External Training

o   Gas chromatography–mass spectrometry (GC–MS), IS-X Academy – Expert center for chromatography (2022)

Management and Didactic Skills Training

o   Supervising two MSc and three BSc students with thesis (2019-2023)
o   Teaching in the BSc course "Microbial Physiology" (2018-2022) and "Microbiology and Biochemistry" (2019)
o   Teaching in the Summer School Anaerobic Microbiology (EMBO) (2019)

Oral Presentations

o   *Synthetic co-cultures for syngas fermentation to odd-chain fatty acids,* Environmental Technology for Impact conference (ETEI), 3-4 June 2020, Online
o   *Synthetic microbial co-cultures for syngas fermentation to odd-chain carboxylic acids*, 4th International Conference on Biogas Microbiology (ICBM), 9-11 May 2022, Braga, Portugal
o   *Synthetic microbial co-cultures for syngas fermentation to odd-chain carboxylic acids*, 1st Emerging Microbial Technologies conference (EMT), 27 May 2022, Delft, The Netherlands
Ethanol-based chain elongation via syngas fermentation using synthetic microbial co-cultures, 2nd International Chain Elongation Conference (ICEC), 2-4 November 2022, Bad Boll, Germany

SENSE coordinator PhD education

Dr. ir. Peter Vermeulen

A